ISSPIC XVII
Fukuoka, 2014

17th International Symposium on Small Particles and Inorganic Clusters

Program and Abstracts

7-12 September 2014,
Fukuoka, Japan

Edited by Atsushi Nakajima, Tatsuya Tsukuda, and Akira Terasaki.

Preface

This book bundles program and abstracts for the 17th International Symposium on Small Particles and Inorganic Clusters (ISSPIC-17) held in Fukuoka, Japan, on 7-12 September 2014. The central subject of the symposia is fundamental science of finite-size effects and control of material properties at the nanometer scale.

The ISSPIC conference started as an international symposium on small particles and inorganic clusters in 1976, and has since evolved into an international conference leading the cluster- and nano-science fields. The symposia topics present a balanced overview of new results, emerging trends and perspectives in the science of atomic and molecular clusters, nanoparticles and nanostructures. The conference provides an interdisciplinary forum for presentation and discussion of fundamental and technological developments in these fields. It is expected that the interdisciplinary approach stimulates emergence of new research topics, enabling innovative applications of nanoscience.

The ISSPIC-17 contents cover the areas of atomic and molecular clusters and nanoparticles in various environments; free, supported, embedded, ligated, assembled, etc. For these wide variety of clusters and nanoparticles, the physical and chemical properties and functionalities have been extensively investigated both by theoretical and by experimental approaches. They include structure and thermodynamics, electronic structure and quantum effects, spectroscopy and dynamics, reactivity and catalysis, electron correlation for magnetism and superconductivity, optical properties and plasmonics, carbon-based nanomaterials, biotechnological and medical applications (imaging and sensors), environmental studies, device-oriented topics, and energy-related topics.

The presentations, consisting of invited talks, hot topic oral contributions, and poster contributions, clearly show the width and breadth of the scientific topics listed above, underlining that the field and scientific community of ISSPIC is thriving, exciting, and challenging.

Finally, we would like to appreciate your continuous concern about the appalling disaster in the extremely destructive earthquake which hit the northeastern area of Japan in March 2011. Your understandings and continuous supports have encouraged us to hold this ISSPIC-17 in Japan.

Atsushi Nakajima (chair) and Akira Terasaki (co-chair)
On behalf of the local organizing committee

International Advisory Committee

Julio A. Alonso	University of Valladolid, Spain
Vlasta Bonačić-Koutecký	Humboldt University, Berlin, Germany
Kit Bowen	Johns Hopkins University, USA
Cathérine Bréchignac	CNRS, Orsay, France
Michel Broyer	Université Claude Bernard, Lyon, France
A.W. Castleman, Jr.	Pennsylvania State University, USA
Ori Chesnovsky	Tel-Aviv University, Israel
Ignacio L. Garzón	Universidad Nacional Autónoma de México, Mexico
Hannu Häkkinen	University of Jyväskylä, Finland
Min Han	Nanjing University, China
Ulrich Heiz	Technische Universität Munich, Germany
Claude Henry	University of Marseille, France
Manfred Kappes	Karlsruhe Institute of Technology, Germany
Uzi Landman	Georgia Institute of Technology, Atlanta, USA
Peter Lievens	KU Leuven, Belgium
Karl-Heinz Meiwes-Broer	University of Rostock, Germany
Paolo Milani	University of Milano, Italy
Atsushi Nakajima	Keio University, Japan
Richard E. Palmer	University of Birmingham, UK
Paul Scheier	University of Innsbruck, Austria
Akira Terasaki	Kyushu University, Japan
Tatsuya Tsukuda	University of Tokyo, Japan
Fabrice Vallée	Université Claude Bernard, Lyon, France
Lai-Sheng Wang	Brown University, Providence, USA
Robert L. Whetten	University of Texas in San Antonio, USA
Ludger Wöste	Free University Berlin, Germany

Emeritus members

R.S. Berry	University of Chicago, USA
J. Friedel	University Paris-Sud, France
M.F. Gillet	University Paul Cezanne, Aix Marseille, France
Helmut Haberland	Albert-Ludwigs University, Freiburg, Germany
F. Hensel	Phillips University, Marburg, Germany
Joshua Jortner	Tel Aviv University, Israel
Koji Kaya	RIKEN, Saitama, Japan
T. Patrick Martin	Max Planck Institute Stuttgart, Germany
Rene Monot	Ecole Polytechnique Federale, Lausanne
Arne Rosen	University of Gothenburg, Sweden
Guanghou Wang	Nanjing University, China

Local Organizing Committee

Atsushi Nakajima	Keio University (Chair)
Akira Terasaki	Kyushu University (Co-chair)
Shinji Hayashi	Kobe University
Hideo Higuchi	The University of Tokyo
Koji Kaya	RIKEN
Yoshiyuki Kawazoe	Tohoku University
Shigeo Maruyama	The University of Tokyo
Hiroyuki Noji	The University of Tokyo
Susumu Saito	Tokyo Institute of Technology
Jun'ichi Sone	National Institute for Materials Science
Testuya Taketsugu	Hokkaido University
Katsumi Tanigaki	Tohoku University
Toshiharu Teranishi	Kyoto University
Makoto Tokunaga	Kyushu University
Masaharu Tsuji	Kyushu University
Tatsuya Tsukuda	The University of Tokyo

Advisory Committee

Kazuhiko Ishihara	The University of Tokyo
Toyoki Kunitake	Kitakyushu Foundation for the Advancement of Industry, Science and Technology
Keiji Morokuma	Kyoto University & Emory University
Hisanori Shinohara	Nagoya University
Toshio Yanagida	Osaka University & RIKEN

Local Steering Committee

Akira Terasaki	Kyushu University (Chair)
Masashi Arakawa	Kyushu University
Kenji Furuya	Kyushu University
Tamao Ishida	Tokyo Metropolitan University
Haruyuki Nakano	Kyushu University
Yasuro Niidome	Kagoshima University
Kazuhiko Ohashi	Kyushu University
Takashi Ohshima	Kyushu University
Kenji Sakota	Kyushu University
Hiroshi Sekiya	Kyushu University
Makoto Tokunaga	Kyushu University
Masaharu Tsuji	Kyushu University
Takeshi Tsuji	Shimane University
Sunao Yamada	Kyushu University
Norio Yoshida	Kyushu University
Kazunari Yoshizawa	Kyushu University

September 8th, Monday

9:00	Opening Atsushi Nakajima / Sunao Yamada (Dean, School of Engineering, Kyushu University)
9:20	Resolving the atomic structure and meta-stability of size-selected gold clusters Richard Palmer (Invited)
10:00	Quantum chemical molecular dynamics (QM/MD) simulations of nucleation, growth and healing processes of fullerenes, carbon nanotubes and graphenes Keiji Morokuma (Invited)
10:40	Coffee break
11:10	Total structures of atomically precise gold nanoclusters and beyond Rongchao Jin (Invited)
11:50	Nanoparticles by design: $Fe_{75}Pt_{72}$ Vijay Kumar
12:10	Gold-oxide nanoparticles - what is the oxidation state in gold? Maxim Tchaplyguine
12:30	Lunch
14:00	Water clusters: thermal behavior and electron solvation Bernd von Issendorff (Invited)
14:40	Nanoparticles and clusters from doped He nanodroplets Paul Scheier (Invited)
15:20	Observation of phase transitions between finite temperature polymorphs of gallium clusters: from β to γ to δ from first-principles Nicola Gaston
15:40	Unusual temperature-dependent structure in the ionization yield of an aluminum cluster: possible superconducting electron pairing at T>100 K Vitaly Kresin
16:00	Coffee break
16:30	Meteoric smoke nanoparticles and clouds in upper planetary atmospheres Thomas Leisner (Invited)
17:10	Infrared photodissociation spectroscopy of carbon species of astrophysical relevance E. Cristina Stanca-Kaposta
17:30	Vibrational and low-temperature thermal properties of metal nanoparticles Ignacio L. Garzón
17:50	Industry (National Instruments Japan and TOYAMA Co., Ltd.)
18:30	

Resolving the atomic structure and meta-stability of size-selected gold clusters

Richard E Palmer

Nanoscale Physics Research Laboratory, University of Birmingham, U.K.
r.e.palmer@bham.ac.uk; www.nprl.bham.ac.uk

The controlled deposition of size-selected nanoclusters, assembled from atoms in the gas phase, is a novel [1] but increasingly popular route to the fabrication of functional surfaces structured on the sub-10nm scale, with applications in catalysis, coatings, biochips [2], etc. Efforts to scale-up the rate of cluster generation thus promise significant future impact. However fundamental questions remain over the equilibrium atomic structures of the clusters themselves, since direct gas phase structural studies have been limited and new techniques like aberration-corrected scanning transmission electron microscopy (ac-STEM) are only now being applied to soft-landed, size-selected clusters. I will survey our recently published [2-6] and latest systematic ac-STEM experiments which address the atomic structure of size-selected "magic number" gold clusters - Au_{20}, Au_{55}, Au_{309}, Au_{561}, and Au_{923} – including dynamical manipulation experiments [6], which probe the transformation of metastable isomers into more stable configurations, and reaction-exposure experiments, which probe the stability of the cluster structures under real catalytic conditions. The results distinguish the predominant, competing isomers as a function of cluster size, expose concepts such as templated-growth, provide a body of date to stimulate and constrain computational models and are readily extendable to other sizes and cluster materials including binary systems.

Reference(s)

[1] R.E. Palmer, S. Pratontep and H.-G. Boyen, Nature Materials **2** 443 (2003).
[2] R.E. Palmer and C. Leung, Trends in Biotechnology **25** 48 (2007).
[3] Z.W. Wang and R.E. Palmer, Nano Lett. **12** 91 (2012).
[4] Z.W. Wang and R.E. Palmer, Nanoscale **4** 4947 (2012) [*Cover*].
[5] Z.W. Wang and R.E. Palmer, Nano Lett. **12** 5510 (2012).
[6] Z.W. Wang and R.E. Palmer, Phys. Rev. Lett. **108** 245502 (2012).

Quantum chemical molecular dynamics (QM/MD) simulations of nucleation, growth and healing processes of fullerenes, carbon nanotubes and graphenes

Keiji Morokuma

Fukui Institute for Fundamental Chemistry, Kyoto University, Kyoto 606-8103, Japan

Nucleation, growth and healing of carbon nanostructures (fullerenes, carbon nanotubes and graphenes, respectively, without catalyst, with metal cluster catalysts and on metal surfaces) are self-assembly processes from a chaotic pool of small carbon clusters to ordered nanostructures. Although some “theories” exist that advocate well-defined pathways for construction of ordered structures, high-temperature nature of these processes strongly suggests that the dynamics is the key.

In order to explicitly consider the quantum nature of these sp^2 carbon systems and follow dynamics for up to nano second, we have been using quantum chemical molecular dynamics (QM/MD) simulation techniques with a semi-empirical density functional tight-binding theory called DFTB. For all these fullerenes (0 dimensional or 0D), carbon nanotubes (1D) and graphenes (2D), the self-assembly process takes place in a surprising similar fashion. At first, small carbon species (such as C_2 and C_4) assembles in chains, and a Y-shaped carbon chain junction closes and forms the first ring that is always five-membered. “Nucleation”, formation of several five and six-membered aromatic rings takes places by entanglement of carbon chains around this five-membered ring. The “growth” of sp^2 carbon network is continued by addition of more carbon species into the system. The growth produces five-membered as well as six-membered rings and thus the chirality of growing structures is not maintained. During the growth process, a slow healing process takes place at the same time. In the healing process defects consisting mainly of five- (and seven-) membered rings are converted via a variety of processes (such as addition of one carbon atom) into six-membered rings. Usually the chirality of the original cap of the nanotube is lost during the growth process and the healing does not restore the original chirality. Depending on the support that retains an open end of growing structure, different products are obtained; without support, all open ends close to form a fullerene structure; with metal cluster support, the 1D nano tube is formed; and with metal surface support, the 2D graphene is formed. The lecture will illustrate examples and principles of these carbon nanostructure self-assembly.

Reference(s)

[1] S. Irle, A. J. Page, B. Saha, Y. Wang, K. R. S. Chandrakumar, Y. Nishimoto, H.-J. Qian, K. Morokuma, in eds. J. Leszczynski and M. Shukla, “Practical Aspects of Computational Chemistry: An Overview of the Last Two Decades and Current Trends”, 103-172 (2012): Springer-European Academy of Sciences. ISBN 978-94-007-0922-5

[2] A. J. Page, F. Ding, S. Irle and K. Morokuma, Rep. Prog. Phys. In press.

[3] H-B. Li, A. J. Page, C. Hettich, B. Aradi, C. Köhler, T. Frauenheim, S. Irle and K. Morokuma, Chem. Sci. doi:10.1039/c4sc00491d

Total Structures of Atomically Precise Gold Nanoclusters and Beyond

Rongchao Jin

Department of Chemistry, Carnegie Mellon University, Pittsburgh, Pennsylvania, USA

Determining the total structures of nanoclusters constitutes a major goal in nanoscience research. Gold nanoclusters are particularly attractive due to their extraordinary stability and elegant optical properties. A prerequisite to total structure determination is to obtain atomically precise nanoclusters, which had been a major challenge in the past research and thus hampered the pursuit of fundamental science of nanoclusters. We have recently developed successful methodologies for synthesizing a series of atomically precise gold nanoclusters protected by thiolates (denoted as $Au_n(SR)_m$, with n ranging from a few dozens to several hundreds). Such ultrasmall particles (ca. 1–3 nm) exhibit distinct quantum size effects and interesting electronic/optical properties, which are fundamentally different from the properties of larger counterparts—*plasmonic* nanoparticles. New types of atom-packing structures have been discovered in $Au_n(SR)_m$ nanoclusters through X-ray crystallographic analysis. These well-defined nanoclusters hold potential in catalysis as new model catalysts, and atomic level structure-reactivity correlation will ultimately offer fundamental understanding on nanocatalysis.

References

[1] H. Qian, M. Zhu, Z. Wu, and R. Jin, Acc. Chem. Res. 45 (2012) 1470.
[2] C. Zeng, T. Li, A. Das, N. L. Rosi, and R. Jin, J. Am. Chem. Soc. 135 (2013) 10011.
[3] C. Zeng, Y. Chen, G. Li, and R. Jin, Chem. Mater. 26 (2014) 2635.
[4] H. Kawasaki, S. Kumar, G. Li, C. Zeng, D. R. Kauffman, J. Yoshimoto, Y. Iwasaki, and R. Jin, Chem. Mater. 26 (2014) 2777.
[5] G. Li, C. Zeng, and R. Jin, J. Am. Chem. Soc. 136 (2014) 3673.
[6] A. Das, T. Li, K. Nobusada, C. Zeng, N. L. Rosi, and R. Jin, J. Am. Chem. Soc. 135 (2013) 18264.
[7] H. Qian, D.-e. Jiang, G. Li, C. Gayathri, A. Das, R. R. Gil, and R. Jin, J. Am. Chem. Soc. 134 (2012) 16159.
[8] D. R. Kauffman, D. Alfonso, C. Matranga, H. Qian, and R. Jin, J. Am. Chem. Soc. 134 (2012) 10237.
[9] G. Li and R. Jin, Acc. Chem. Res. 46 (2013) 1749.

Nanoparticles by Design: $Fe_{75}Pt_{72}$

Bheema Lingam Chittari[1] and Vijay Kumar,[1,2]

[1]*Dr. Vijay Kumar Foundation(VKF), 1969 Sector 4, Gurgaon 122001, Haryana, India*
[2]*Center for Informatics, School of Natural Sciences, Shiv Nadar University, Chithera, Gautam Budh Nagar - 203207, U.P., India*

The development of size specific nanoparticles of materials is important for their applications to take advantage of their specific properties. Core-shell nanoparticles of a variety of materials have been studied. In particular Pt nanoparticles with a core of another transition metal have been found to improve dramatically their catalytic activity. Moreover, FePt nanoparticles are important for high density magnetic recording as well as for the development of strong magnets together with soft magnets. We have systematically investigated Fe-Pt nanoparticles of different sizes and with different initial structures including bulk fragments, decahedral, and icosahedral structures. In one such study it is found that a bulk fragment of $Fe_{51}Pt_{12}$ instantaneously transforms to icosahedral structure with a few Pt atoms inside and eight atoms attached to icosahedral structure on the surface. We removed the eight atoms on the surface and subsequently moved the Pt atoms from inside to the surface. This lowered the energy of the 55-atom nanoparticle suggesting segregation of Pt to be favorable on the surface. Also it indicates that at this size range the icosahedral structure is preferred. Further calculations on several compositions of small size nanoalloys showed Fe-Pt ordering or maximizing the unlike bonds to be most favorable. Using these considerations we found a unique combination of 147 atom icosahedral Fe-Pt nanoparticle in which 55 atom core is made of Fe atoms and 72 Pt atoms are on the outer shell of Maykay icosahedron. 20 Fe atoms are on the centers of the Pt hexagons giving the stoichiometry $Fe_{75}Pt_{72}$. This has 231 μ_B magnetic moments. In this structure the magnetic moments on Fe and Pt atoms are higher compared with the values in bulk FePt. Note that Fe_{55} cluster has icosahedral structure to be most favorable with large magnetic moments. Also Pt likes to segregate at surface, and there is ordering of FePt on the surface which leads to this optimal nanoparticle. This is the finest model nanoparticle by design for magnetic as well as catalytic applications. The overall composition of this nanoparticle is FePt- like, but it decomposes in to a Fe core and Fe-Pt shell. We hope that such structures are likely to exist for even bigger nanoparticles before a transition to Fe-Pt like core. We anticipate that our studies will motivate experiments on synthesis of such nanoparticles for catalysis, ultrahigh density magnetic recording applications as well as for building strong magnets without using rare earths.

Gold-oxide nanoparticles – what is the oxidation state in gold?

M.Tchaplyguine[1], M.H.-Mikkelä[1], Ch. Zhang[2], T. Andersson[2], O. Björneholm[2]

[1] *MAX-lab, Lund University, P.O. Box 118, 22100 Lund, Sweden*
[2] *Department of Physics and Astronomy, Uppsala University, Box 530, 75121 Uppsala, Sweden*

Over the years it has been vividly discussed what made gold nanoparticles so drastically different to "bulk" gold in chemical activity- their size, their peculiar electronic structure, their interaction with a specific substrate, etc. [1,2,3,4]. The chemical reaction discussed most is the oxidation of carbon monoxide at gold surface in the presence of oxygen. This reaction proceeds via the formation of the surface oxide of the catalyst – gold. Among the main experimental obstacles to our understanding of gold reactivity enhancement in nanoparticles are the difficulty to oxidize gold at laboratory conditions and the instability of gold oxide. Using photoelectron spectroscopy the chemical state of gold in the oxide at "macroscale" has been established to be typically trivalent (Au_2O_3): Photoelectron spectroscopy detects well-separated responses of the oxide and metallic gold in the Au 4f-region spectrum, the oxide being 1.9 eV higher in electron binding energy than the signal from metallic gold. In the present work gold-oxide containing nanoparticles have been fabricated in the size regime known to be efficient for catalytic oxidation – below 10 nm. Our fabrication method is based on vapour aggregation, involving metal atoms sputtered off the solid - in the oxygen-containing magnetron-discharge plasma. The gold oxidation state/valency has been investigated by means of x-ray photoelectron spectroscopy- "on the fly" for the particles in the beam and after the deposition on SiO_2 substrate. In both cases the gold-oxide response occurs to be $\approx$1.5 eV above the metallic response what corresponds to lower oxidation states with valency +2 or +1 – in contrast to characteristic for the "bulk" value +3. Some earlier results suggest the formation of divalent gold oxide at our conditions. The gold valency in an oxide comes into the play when its interaction with CO molecules is about to take place. A CO molecule is a two-electron donor in a reaction with noble metals. If the substance to which CO has to bind is a *divalent* metal compound with dangling bonds at the surface the situation is optimal for the CO chemisorption. Our approach allowing to fabricate nanoparticles with lower gold oxides and to derive their oxidation degree may be relevant for the studies connected to nano-catalysis. Moreover, taking into account our recent results on silver-oxide containing nanoparticles [5], it may be seen as a method of producing catalytically active nanostructured systems with controlled properties.

References

[1] D. Widmann, R. J. Behm. Acc. Chem. Res. 47 (2014) 740.
[2] H. Häkkinen, M. Moseler, U. Landman, Phys. Rev. Lett. 89 (2002) 033401.
[3] B. Yoon, H. Häkkinen, U. Landman, et al, Science 307 (2005) 403.
[4] M.Haruta. Cat.Today 36 (1997) 153.
[5] M.Tchaplyguine, Ch.Zhang, T.Andersson, O.Björneholm. ChemPhys.Lett. 600 (2014) 96

Water clusters: thermal behavior and electron solvation

Bernd v. Issendorff

Physikalisches Institut, Universität Freiburg, 79104 Freiburg, Germany

Bulk water exhibits many unusual properties, which mirror the complexity of its hydrogen network structure. It is therefore not surprising that water clusters and nanoparticles are special in many aspects as well. We have recently shown that negatively charged water clusters exhibit a melting-like transition at surprisingly low temperatures (at about 120 K for $H_20_{118}^-$) [1] . Further studies have shown that this behavior depends only weakly on the charge state of the cluster or on the type of impurity incorporated. Furthermore the size dependence indicates that the transition does not extrapolate to the melting transition of normal ice, but rather to the glass transition of amorphous ice, which occurs at about 136 K. This can be rationalized by the fact that water clusters with few hundred molecules do not form a crystalline network like bulk ice, but exhibit structures much closer to that of the amorphous forms of solid water.

Another phenomenon closely related to the hydrogen network structure of water is the solvation of a free electron. Since the first observation of negatively charged water clusters [2] the question has been discussed at what size the attached electron gets truly solvated, that is resides inside the cluster. We could recently show that apart from the already known three isomer classes of water cluster anions (in all of which the electron is bound to the cluster surface), another isomer class exists, which becomes dominant at about size 46 and most probably is the one with an internal electron [3]. Extending the photoelectron spectroscopy studies to cluster anions with up to 1600 water molecules we could now obtain a reliable extrapolation of the electron binding energy for the bulk. This yields a value of about 3.6 eV, which is slightly larger than commonly assumed.

Reference(s)

[1] C. Hock, M. Schmidt, R. Kuhnen, C. Bartels, L. Ma, H. Haberland, and B. v.Issendorff, Phys. Rev. Lett. 103, 073401 (2009).

[2] M. Armbruster, H. Haberland, and H.-G. Schindler, Phys. Rev. Lett. 47, 323 (1981).

[3] L. Ma, K. Majer, F. Chirot, and B. v. Issendorff, J. Chem. Phys. 131, 144303 (2009).

Nanoparticles and clusters from doped He nanodroplets

Michael Renzler[1], Johannes Postler[1], Alexander Kaiser[1], Matthias Daxner[1], Diethard K. Böhme[2], David Stock[1], Martin Kuhn[1], Stefan Ralser[1], Stephan Denifl[1], Olof Echt[2] and Paul Scheier[1]

[1] *Institut für Ionenphysik und Angewandte Physik, Universität Innsbruck, Austria*
[2] *Department of Chemistry,York University, Toronto, ON, Canada M3J 1P3*
[3] *Department of Physics, University of New Hampshire, Durham, NH 03824, United States*

Pickup of atoms and molecules into superfluid He nanodroplets (HND) is a powerful technique to form clusters and nanoparticles at low (0.38K) temperatures. The resulting dopant complexes are mostly analyzed utilizing mass spectrometry after ionization [1,2]. In the present contribution the influence of charge on the physisorption of CO_2 on fullerenes is investigated. The linear shape of CO_2 molecule and its response to a positive surface charge, due to the slightly negative terminal O atoms, can lead to “packing” consequences and increased surface adsorption.

Recently several groups deposited neutral metal and semiconductor nanoparticles grown in large HND and analyzed them by transmission electron microscopy [3-5]. Both spherical nanoparticles and nanometer wide fibers have been reported. However, the typical log-normal size distribution of the neutral HND and the Poissonian pickup statistics leads to a substantial size spread of the dopant clusters. Here we report on a novel approach that reduces the size distribution of the HND, simply by ionization. The yield of the resulting singly charged HND is very high and enables the efficient formation of mono-dispersed clusters via subsequent pickup.

This work was supported by the FWF, Wien (P23657, I978 and P26635)

Reference(s)

[1] J.P. Toennies, and A.F. Vilesov, Angew. Chemie Int. Ed. 43 (2004) 2622-2648.
[2] O. Echt, A. Kaiser, S. Zöttl, A. Mauracher, S. Denifl, P. Scheier, ChemPlusChem 78 (2013) 910-920
[3] L. Gomez, E. Loginov, and A.F. Vilesov, Phys. Rev. Lett. 108 (2012) 155302.
[4] A. Volk, P. Thaler, M. Koch, E. Fisslthaler, W. Grogger, and W.E. Ernst, J. Chem. Phys. 138 (2013) 214312.
[5] SF. Yang, A.M. Ellis, D. Spence, C. Feng, A. Boatwright, E. Latimer, and C. Binns, Nanoscale 5 (2013) 11545-11553

Observation of phase transitions between finite temperature polymorphs of gallium clusters: from β to γ to δ from first-principles

N. Gaston[1], K. G. Steenbergen[2]

[1] *MacDiarmid Institute for Advanced Materials and Nanotechnology, School of Chemical and Physical Sciences, Victoria University of Wellington, New Zealand*
[2] *Department of Chemistry, The University of Kansas, USA*

Gallium is a highly polymorphic element with a rich phase diagram, which poses a real challenge to first-principles theory. The experimental discovery of superheating in gallium clusters [1] contradicted the clear and well-demonstrated paradigm that the melting temperature of a particle should decrease with its size [2]. In addition, the extremely sensitive dependence of melting temperature on size also goes to the heart of nanoscience, and the interplay between the effects of electronic and geometric structure.

We have performed extensive first-principles molecular dynamics calculations, incorporating parallel tempering for an efficient exploration of configurational phase space [3]. In the nanoparticles, melting is preceded by transitions between phases. A structural feature is identified that systematically increases with the latent heat and appears throughout the observed phase changes of this curious metal. We will present our detailed analysis of the solid-state isomers, performed using extensive statistical sampling of the trajectory data for the assignment of cluster structures to known phases of gallium [4].

Finally, we offer a first explanation of the greater-than-bulk melting temperatures, through analysis of the factors that stabilise the liquid structures.

Reference(s)

[1] G. A. Breaux, R. C. Benirschke, T. Sugai, B. S. Kinnear, and M. F. Jarrold, Phys. Rev. Lett. **91**, 215508 (2003)
[2] P. Pawlow, Z. Phys. Chem. **65**, 1 (1909)
[3] K.G. Steenbergen, N. Gaston, Physical Review B **88**, 161402 (2013)
[4] K.G. Steenbergen, N. Gaston, J. Chem. Phys., **140**, 064102 (2014)

Unusual temperature-dependent structure in the ionization yield of an aluminum cluster: Possible superconducting electron pairing at T>100 K

Avik Halder, Anthony Liang, and Vitaly V. Kresin

Department of Physics and Astronomy, University of Southern California, Los Angeles, CA

A number of theoretical papers (see, e.g., [1-4]) have predicted that free metal clusters with shell structure exhibit superconducting-type electron pairing. This should occur only for certain individual sizes and materials, but when it does, it is expected to be greatly enhanced relative to bulk samples, with a corresponding increase in the critical temperature. This is a unique consequence of the high electron state degeneracy associated with shell structure.

Superconducting pair correlations should have spectroscopic manifestations. To search for the first observation of such an effect, we have carried out a series of accurate measurements of the photoionization yield curves of Al_n clusters for several temperatures in the range of 70 K – 230 K. The clusters' internal temperatures were controlled by a newly designed thermalizing tube attached to a magnetron-sputtering condensation cluster source.

The experiment revealed that while the majority of yield curves show no significant temperature variation, a few clusters are exceptional: a noticeable feature appears in the near-threshold region and grows substantially as the temperature decreases to ≈100 K. For example, this is prominent in the closed-shell cluster Al_{66} (198 valence electrons), which had in fact been identified by theory as one of the candidates for high-T_c pairing. This behavior has not been reported for cluster previously, but is reminiscent of temperature effects in threshold photoemission from high-T_c superconductors [5]. It is a consequence of the increase in the effective density of states due to electron pairing. We suggest that the data represent a signature of superconducting transition in a "magic" metal cluster with T_c >100 K.

This work is supported by the U.S. National Science Foundation.

dY/dE (Y=ionization yield)

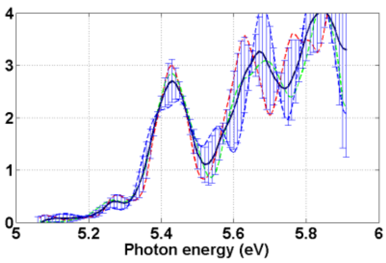

Relative height of near-threshold peak as a function of temperature

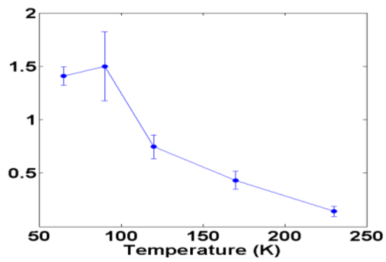

Reference(s)
[1] V. Z. Kresin, and Yu. N. Ovchinnikov, Phys. Rev. B **74**, 024514 (2006).
[2] M. Groitory *et al.*, Phys. Rev. B **83**, 214509 (2011).
[3] Z. Lindenfeld *et al.*, Phys. Rev. B **84** 064532 (2011).
[4] M. Hopjan and P. Lipavský, Phys. Rev. B **89**, 094507 (2014).
[5] S. A. Nepijko *et al.*, Physica C **288**, 173 (1997).

Meteoric smoke nanoparticles and clouds in upper planetary atmospheres

Denis Duft[1], Mario Nachbar[2], Jan Meinen[1], Markus Eritt[2] and Thomas Leisner[1,2]

[1] *Institute for Meteorology and Climate Research, Karlsruhe Institute of Technology, Karlsruhe, Germany*
[2] *Institut für Umweltphysik, University of Heidelberg, Heidelberg, Germany*

Most planets, including the earth feature a pronounced global minimum of temperature at the mesopause, i.e. at the transition into the thermosphere. This region is prone to form clouds whenever condensable gases exist in the atmosphere. These outermost cloud layers may determine largely the planetary appearance to remote sensing instruments.
On earth, these clouds are ubiquitous in the polar summer mesopause and are known as noctilucent clouds. As the mesopause is generally far above the ground (on the earth ~85 km), the cloud condensation nuclei are not primary aerosol particles that are transported up from ground, but are constituted by nanoparticles formed by the recondensation of meteoric material. These are the only type of aerosol in the atmosphhere that remain of nanometer- size due to the low temperature and pressure in the mesosphere.

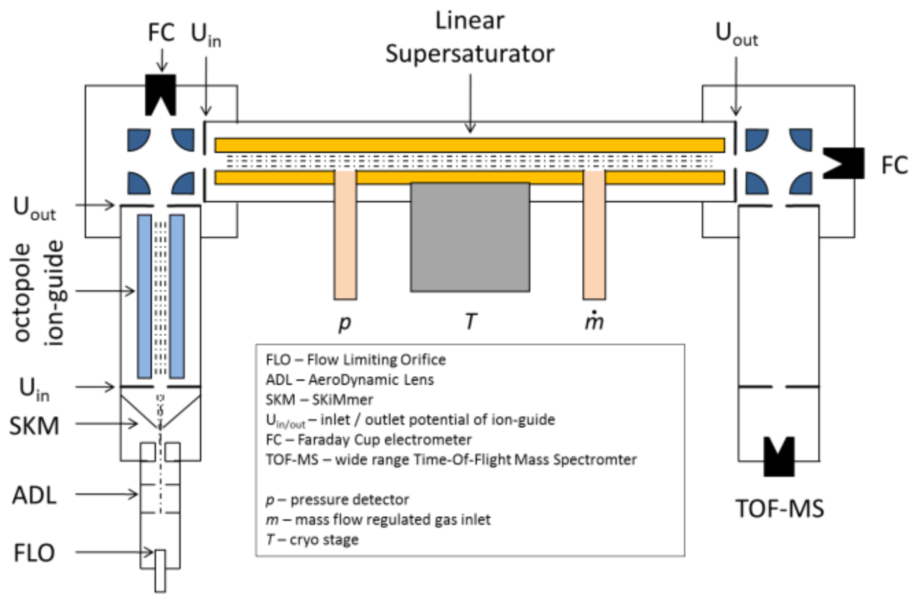

Fig.1 *Scheme of the experimental setup for hetero-geneous chemistry on atmospheric nanoparticles. "TRAPS": Trapped Reactive Atmospheric Particles Spectrometer*

In this contribution, we present a novel laboratory experiment TRAPS (Fig.1) that allows to prepare and analyze meteoric dust nanoparticles in an electrodynamic trap under conditions of planetary mesospheres [1]. We present first results of the nucleation and growth of ice on these particles and compare the results to classical nucleation theory.

Reference(s)

[1] Meinen, J., Khasminskaya, S., Ruehl, E., Baumann, W. and Leisner, T. (2010), Aerosol Science and Technology 44(4): 316-328.

Infrared Photodissociation Spectroscopy of Carbon Species of Astrophysical Relevance

E. Cristina Stanca-Kaposta,[1] Falko Schwaneberg,[1] Xiaowei Song,[2] Matthieu Lalanne,[1] Matias R. Fagiani,[2] Ludger Wöste[1] and Knut R. Asmis[2,3]

[1] *Institut für Experimentalphysik, Freie Universität Berlin, Germany*

[2] *Fritz-Haber-Institut der Max-Planck-Gesellschaft, Berlin, Germany*

[3] *Wilhelm-Ostwald-Institut, Universität Leipzig, Germany*

It is well known that the interstellar medium is rich in different carbon species including long linear carbon chains, polyacetylanic radicals as well as more complex systems such as C_2H_5OCHO and C_3H_7CN. [1] Besides neutral and cationic molecules, more recently and unexpectedly, molecular anions like $C_{2n}H^-$ (n = 2 - 4) as well as C_3N^- and C_5N^- have been detected and identified based on comparison with laboratory experiments.

Here, we present the gas phase vibrational spectroscopy of cryogenically-cooled carbon anion species of the type C_nN^-, C_nH^- and C_nO^- by way of infrared photodissociation (IRPD) spectroscopy of messenger-tagged $C_nM^-\cdot m(D_2)$ (M = N, H ,O) complexes.[2] The experiments are performed in a tandem mass spectrometer consisting of a quadrupole mass filter, a temperature adjustable (8 - 350K) linear ring-electrode radio-frequency ion trap and a linear time-of-flight (TOF) mass filter. The anions of interest are generated by reactive sputtering of a graphite target within a magnetron sputter source. $C_nM^-\cdot m(D_2)$ (M = N, H ,O) complexes are formed via three-body collisions in the ion trap which is held at 15-20 K and is filled with D_2 as buffer gas. Irradiation of the anions with a tunable infrared OPO/OPA laser occurs in the center of the extraction region of the TOF mass filter. The vibrational action spectra are measured by monitoring the IR-photoinduced loss of D_2 molecules from the $C_nM^-\cdot m(D_2)$ complexes as a function of photon energy.

The IRPD spectra are assigned based on a comparison to *ab initio* [3] and DFT vibrational frequencies and intensities. Experimentally measured vibrational transitions are in good agreement with the predicted anharmonic as well as, where not available, scaled harmonic frequencies. The influence of the D_2-messenger molecules on the structure and the IRPD spectrum is found to be small. Compared to the results of previous IR matrix isolation studies additional, in particular weaker, IR-active transitions are identified.

References

[1] Ramya Nagarajan and John P. Maier, Int. Rev. Phys. Chem. 29 (2010) 521

[2] E. Cristina Stanca-Kaposta, Falko Schwaneberg, Matias R. Fagiani, Torsten Wende, Franz Hagemann, Annett Wünschmann, Ludger Wöste, and Knut R. Asmis, Z. Phys. Chem 228 (2014) 351.

[3] P. Botschwina and R. Oswald, J. Chem. Phys. 129 (2008) 044305.

Vibrational and Low-Temperature Thermal Properties of Metal Nanoparticles

Huziel E. Sauceda,[1] J. Jesús Pelayo,[1] Fernando Salazar,[2] Luis A. Pérez,[1] Ignacio L. Garzón[1]

[1]*Universidad Nacional Autónoma de México, Instituto de Física, 01000 México, D. F., México*
[2]*Instituto Politécnico Nacional, ESIME Culhuacán, 04430 México, D. F., México*

We report the vibrational spectra and density of states of Au, Pt, and Ag nanoparticles in the size range of 0.5 - 4 nm. The vibrational spectra were calculated through atomistic simulations using the many-body Gupta potential. Linear relations with the nanoparticle diameter were obtained for the periods of two characteristic oscillations: the quasi-breathing and the lowest frequency (acoustic gap) modes. These results are consistent with the calculation of the periods corresponding to the breathing and acoustic gap modes of an isotropic, homogeneous metallic nanosphere, performed with continuous elastic theory using bulk properties. Additionally, experimental results on the period of isotropic volume oscillations of Au nanoparticles measured by time-resolved pump-probe spectroscopy are presented, indicating a linear variation with the mean diameter in the size range of 2 - 4 nm. These, and similar results previously obtained for Pt nanoparticles with size between 1.3 – 3 nm, are in good agreement with the calculated quasi-breathing mode periods of the metal nanoparticles, independently of their morphologies. [1]

We also report the vibrational spectrum and density of states (VDOS) of the cationic sodium cluster Na_{139}^{+} using DFT. The calculated vibrational frequencies were used to evaluate the cluster caloric curve and heat capacity at low temperatures. An excellent agreement was obtained between the calculated caloric curve and experimental data recently reported down to 6 K. A further analysis shows that the calculated heat capacity of the 139-atom cationic sodium cluster does not follow the bulk Debye T^3 law at very low temperatures, due to the discreteness of the cluster frequency spectrum, and to the finite value of its acoustic gap (lowest frequency value). [2]

The size and shape dependence of the specific heat at low temperatures as well as its evolution towards the bulk limit for Au nanoparticles in the size range of 0.5-4 nm is also reported. The results indicate that the acoustic gap is responsible of a slight reduction in the specific heat with respect to bulk in the temperature range, 0 < T <Tr , (Tr ≈ 5 K for Au nanoparticles with size 1.4 nm). [3] Also, the well-known increment in the specific heat of metal nanoparticles with respect to the bulk value, caused by the enhancement of the VDOS at low frequencies, is recovered for Tr < T < Ts (Ts ≈ 35–45 K). [3]

Reference(s)

[1] H. E. Sauceda, D. Mongin, P. Maioli, A. Crut, M. Pellarin, N. del Fatti, F. Vallée, and I. L. Garzón, J. Phys. Chem. C 116 (2012) 25147.
[2] H. E. Sauceda, J. J. Pelayo, F. Salazar, L. A. Pérez, and I. L. Garzón, J. Phys. Chem. C 117 (2013) 11393.
[3] H. E. Sauceda, F. Salazar, L. A. Pérez, and I. L. Garzón, J. Phys. Chem. C 117 (2013) 25160.

September 9th, Tuesday

ISSPIC XVII
Fukuoka, 2014

9:00	Cluster assemblies as novel nanoscale materials with tunable properties Shiv Khanna (Invited)
9:40	Mass spectrometric investigations of nanoparticles: from small liganded metal nanoclusters to large nanoparticles assemblies Rodolphe Antoine (Invited)
10:20	Far-infrared spectroscopy of clusters of the platinum metals: evidence for cubic structures of Ru and Ir clusters André Fielicke
10:40	Conference photo Coffee break
11:10	Professor Satoru Sugano Memorial
11:30	Energetics, edge geometries, and electronic properties of silicene Susumu Saito
11:50	One-dimensional uneven structured exotic-nanocarbon: geometric curvature effects at nanoscale Jun Onoe
12:10	The formation of supported carbon clusters during graphene chemical vapor deposition (CVD) growth Feng Ding
12:30	Lunch
14:00	Effects of electronic and geometric structure on the activity of size-selected model catalysts and electrocatalysts Scott Anderson (Invited)
14:40	Plasmonic property of multidimensional self-assembled metallic nanoparticles Kaoru Tamada (Invited)
15:20	Surface plasmons in quantum-sized noble-metal clusters: quantum calculations and the classical picture of charge oscillations Hans-Christian Weissker
15:40	Clusters for photocatalysis Gunther Andersson
16:00	Coffee break
16:30	Poster Session A
18:30	Cultural event

Cluster Assemblies As Novel Nanoscale Materials With Tunable Properties

S. N. Khanna

Department of Physics, Virginia Commonwealth University, Richmond, VA 23284-2000, USA

An exciting development in nanoscience is the formation of materials whereby atomic clusters serve as the building blocks. Since the properties of clusters change with size, composition and the charged state, cluster assemblies offer the attractive proposition of forming materials with novel combination of properties. Cluster solids can be stabilized either by using counter ions or via ligands to passivate the reacting species. The resulting assemblies allow the integration of multiple length scales into a hierarchical material and the emergent properties depend on the nature of the building blocks as well as the architecture of the assembled material as the solids combine intra-cluster, inter-cluster, linker-cluster, and ligand-cluster interactions, unavailable in conventional atomic solids.

The talk will first review our efforts in synthesizing cluster-based solids where the primitive motifs are the multiply-charged polyatomic anions, called Zintl anions. New building blocks can be formed by covalently linking multiple anions and the nature of the assemblies can be further controlled by extending the countercations to include cryptated ions. Through variations of the anionic motifs and alkali/cryptated ions, it becomes possible to assemble the resulting solids in various architectures including zero, one, two, and three dimensional solids. In particular, I will present our results on the cluster-assembled materials derived from anionic As_7^{3-} combined with countercations including alkali metals and cryptated K^+ ions, and building motifs that also involve Zintl ions covalently linked with Hg, Zn, Cd, Pd, etc. The talk will highlight how different cluster assemblies can be synthesized by using covalent linkers and assembling them with countercations in various proportions. The talk will also review two recent developments. The first involves ligated cluster assemblies involving metallic cores. In particular, I will present our results on assemblies with a bi-metallic core and the properties of the resulting material. The second involves our effort in developing air stable nano-materials. I will describe our recent success in synthesizing and characterizing new alkaline earth Metal Organic-Frameworks (MOFs). Taking the band gap energy of the resulting material as the property of choice, I will show that the energy bands in these cluster solids exhibit far less dispersion than in atomic solids and that the band gap energy can be controlled over a wide range.

The talk will also review our recent efforts in designing novel rare earth free magnets that could rival the current rare earth based permanent magnets. I will show that the materials consist of nanoparticles with ultra high magnetic anisotropies offering potential for memory storage and other applications.

Mass Spectrometric Investigations of Nanoparticles : from small liganded metal nanoclusters to large nanoparticles assemblies

Rodolphe Antoine

Institut Lumière Matière, UMR5306 Université Lyon 1-CNRS,Université de Lyon 69622 Villeurbanne cedex, France

Metal nanoparticles (NPs) are fascinating due to their unique optical and electronic properties, which are size and structure dependent. The recent progress in the synthesis of functionalized NPs (in particular with biomolecules) challenges the understanding of their electronic, spectroscopic, and chemical properties at the molecular level. Gas phase studies offer the opportunity to produce and study hybrid systems under well-defined conditions.

The present work aims at characterizing nanoparticles with mass spectrometric investigations. In a first part of my presentation, I will present results on structural and optical characterization of small protected metal clusters by high-resolution mass spectrometry and coupling with action spectroscopy.[1, 2] Then I will move to a new instrumental set-up to study large nanoparticles in the gas phase, by determining accurately their mass and charge.[3] A charge detection mass spectrometry technique combined to ESI technique is used to "weighing" large DNAs, nanoparticles and nanoparticles assemblies in the megadalton range of molecular weight. I will show how the simultaneous measure of mass and charge can be used to fathom structural properties of nanoparticles assemblies. I will also present the implementation of tandem mass spectrometry for experiments on single nanoobjects, using two charge detection devices. Single ions can be stored for several dozen milliseconds. During the trapping time, single ions can be irradiated by a continuous wavelength CO_2 laser. Illustration of infrared multiphoton dissociation tandem mass spectrometry will be given for single megadalton ions of DNAs.[4, 5]

References

[1] R. Hamouda, B. Bellina, F. Bertorelle, I. Compagnon, R. Antoine, M. Broyer, D. Rayane, P. Dugourd, Journal of Physical Chemistry Letters, 1 (2010) 3189-3194.
[2] F. Bertorelle, R. Hamouda, D. Rayane, M. Broyer, R. Antoine, P. Dugourd, L. Gell, A. Kulesza, R. Mitric, V. Bonacic-Koutecky, Nanoscale, 5 (2013) 5637-5643.
[3] T. Doussineau, C.Y. Bao, C. Clavier, X. Dagany, M. Kerleroux, R. Antoine, P. Dugourd, Review of Scientific Instruments, 82 (2011) 084104.
[4] R. Antoine, T. Doussineau, P. Dugourd, F. Calvo, Physical Review A, 87 (2013) 013435.
[5] T. Doussineau, R. Antoine, M. Santacreu, P. Dugourd, Journal of Physical Chemistry Letters, 3 (2012) 2141-2145.

Far-infrared spectroscopy of clusters of the platinum metals: Evidence for cubic structures of Ru and Ir clusters

Christian Kerpal,[1] Jonathan T. Lyon,[2] John Bowlan,[1] Dan J. Harding,[1] and André Fielicke[1,3]

[1] *Fritz-Haber-Institut der Max-Planck-Gesellschaft, Berlin, Germany*
[2] *Department of Natural Sciences, Clayton State University, Morrow, Georgia, United States*
[3] *Institut für Optik und Atomare Physik, Technische Universität Berlin, Germany*

Transition metal clusters are frequently used as model systems for low coordinated sites of extended surfaces and their study can provide valuable insights into the mechanisms of surface reactions. In many cases, however, there is a lack of information on their structures and the relationship between structure and chemical behavior. Present developments of computational electronic structure methods often still have difficulties with a reliable prediction of cluster structures, and their properties, from first principles. This holds in particular for metals with only partially filled d (transition metals) or f (lanthanides, actinides) shells or for heavy elements, like gold, where relativistic effects become more pronounced. Experimental data can help for testing the validity of these predictions and in motivating methodological developments. Cluster size specific far-infrared spectra as obtained via infrared multiple photon dissociation of messenger complex are structural fingerprints and allow via comparison to spectra predicted, i.e. from DFT calculations, for structural assignments.
Clusters of the platinum group metals (4d: Ru, Rh, Pd; 5d: Os, Ir, Pt) are of particular interest [1], due to the importance of the metals in catalytic applications, but also due to the surprising prediction of uncommon simple cubic structural motifs [2,3]. However, for Rh the stability of cubic geometries seems to be an artifact of the GGA-DFT method and experimentally polytetrahedral structures are identified that are also found as most stable isomers when using hybrid functionals in DFT [4]. While also Pt clusters show polytetrahedral structures similar to many other transition metals [5], Ru and Ir indeed appear to follow the cubic growth motif for small cluster sizes (n=6-9).

References

[1] D.J. Harding, A. Fielicke, Chem. Eur. J. 20 (2014) 3258.
[2] Y.-C. Bae, V. Kumar, H. Osanai, Y. Kawazoe, Phys. Rev. B 72 (2005) 125427.
[3] Y.-C. Bae, H. Osanai, V. Kumar, Y. Kawazoe, Mater. Trans. 46 (2005) 159.
[4] D.J. Harding, T.R. Walsh, S.M. Hamilton, W.S. Hopkins, S.R. Mackenzie, P. Gruene, M. Haertelt, G. Meijer, A. Fielicke, J. Chem. Phys. 132 (2010) 011101.
[5] D.J. Harding, C. Kerpal, D.M. Rayner, A. Fielicke, J. Chem. Phys. 136 (2012) 211103.

Energetics, edge geometries, and electronic properties of silicene

Susumu Saito[1-3] and Takashi Koretsune[1,4]

[1] *Department of Physics, Tokyo Institute of Technology, Tokyo, Japan*
[2] *International Research Center for Nanoscience and Quantum Physics, Tokyo Institute of Technology, Tokyo, Japan*
[3] *Materials Research Center for Element Strategy, Tokyo Institute of Technology,Yokohama, Japan*
[4] *Center for Emergent Matter Science, RIKEN, Wako, Saitama, Japan*

Ever since graphene was successfully produced in 2004, atomic-layer materials have been attracting much attention due partly to their interesting electronic properties and partly to their potential importance as future device materials. In this regard, silicene, the Si atomic-layer material, is of great scientific and technological importance. Electronically silicene is expected to possess massless Dirac electrons as in the case of graphene while its geometry is different from graphene because the silicene plane is to be buckled. Theoretically, electronic properties of free-standing silicene have been studied well while experimentally silicene has been produced only with substrates. In the framework of the density-functional theory we study silicene and its composite atomic-layer materials in order to clarify their energetics and electronic properties. We also study the edge geometries of not only the free-standing silicene but also the silicene on substrates. It is found that silicene shows much larger reconstruction of edge atoms than graphene, and buckling is strongly enhanced around the edge (Figure 1). Finally, we also discuss the relative stabilities of three-dimensional Si clusters and silicene flakes to clarify the preferable conditions to produce silicene.

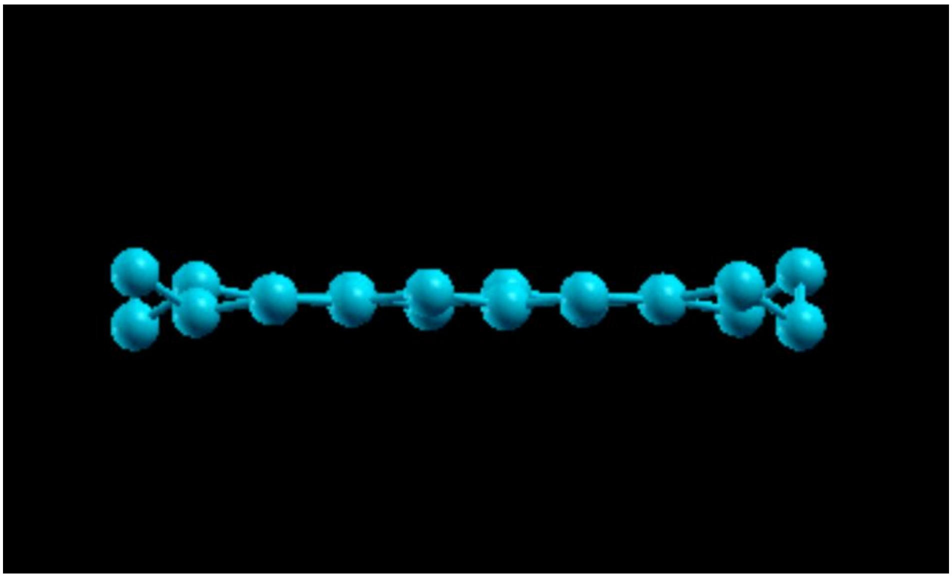

Figure 1. Geometry of silicene nanoribbon

One-dimensional uneven structured exotic-nanocarbon : Geometric curvature effects at nanoscale

Jun Onoe

Department of Physical Science and Engineering, Nagoya University, Nagoya, Japan

In 1916, A. Einstein first applied Riemannian geometry to physics for developing the general theory of relativity and predicted the time-space strained by gravitational field. Four years later, his prediction was demonstrated by the observation of a gravitational lens. This can be regarded as geometric curvature effects on photonic properties.

It is of great interest to examine whether or not the geometric curvature effects affects the electronic properties of condensed matters that are extremely smaller than the universe. Although Riemannian geometry has been applied to quantum mechanics since 1950s for considering the electron behaviors on curved spaces, nobody could have hitherto answered this question, because the electronic properties of materials with geometric curvature shapes have never been examined experimentally.

We have fabricated a new form of nanocarbon from electron-beam (EB) irradiation of C_{60} films [1–11], and found the formation of a one-dimensional (1D) peanut-shaped C_{60} polymer exhibiting the electronic, optical, and phonon properties of 1D metal [12–16]. Since the peanut-shaped C_{60} polymer has both positively and negatively Gaussian curvatures (k), it can be regarded as a new nanocarbon allotrope (exotic-nanocarbon) that differs from graphene (k = 0), fullerenes (k > 0), nanotubes (k = 0 in body, k > 0 at cap edge), and the hypothetical Mackay crystal (k < 0). Thus, the exotic-nanocarbon can be expected to exhibit novel properties different from those of the nanocarbon allotropes.

In this talk, we will demonstrate the geometric curvature effects on the electronic properties based on Tomononaga-Luttinger Liquids [15], which has been predicted by our group [16], by examining *in situ* high-resolution photoemission spectra of the 1D metallic uneven peanut-shaped C_{60} polymer film.

References

[1] J. Onoe et al., *Appl. Phys. Lett.* **82**, 595 (2003)
[2] J. Onoe et al., *Appl. Phys. Lett.* **85**, 2741 (2004)
[3] T.A. Beu, J. Onoe, and A. Hida, *Phys. Rev. B* **72**, 155416 (2005)
[4] S. Ueda, Y. Noguchi, T. Ishii, J. Onoe, and K. Ohno, *J. Phys. Chem. B* **110**, 22374 (2006)
[5] T.A. Beu and J. Onoe, *Phys. Rev. B* **74**, 195426 (2006)
[6] J. Onoe et al., *Phys. Rev. B* **75**, 233410 (2007)
[7] Y. Toda, S. Ryuzaki, and J. Onoe, *Appl. Phys. Lett.* **92**, 094102 (2008)
[8] J. Onoe et al., *J. Appl. Phys.* **104**, 103706 (2008)
[9] A. Takashima, T. Nishii, and J. Onoe, *J. Phys. D* : *Appl. Phys.* **45**, 485302 (2012)
[10] S. Ryuzaki, M. Nishiyama, and J. Onoe, *Diamond & Relat. Mater.* **33**, 12 (2013)
[11] A. Takashima,J. Onoe, and T. Nishii, *J. Appl. Phys.* **108**, 033514 (2010)
[12] J. Onoe et al., *Appl. Phys. Lett.* **97**, 241911 (2010)
[13] J. Onoe et al., *J. Phys.: Condens. Matter* **24**, 175405 (2012)
[14] S. Ryuzaki and J. Onoe, *Appl. Phys. Lett.* **104**, 113301 (2014)
[15] J. Onoe et al., *Europhys. Lett.* **97**, 27001 (2012)
[16] H. Shima, H. Yoshioka, and J. Onoe, *Phys. Rev. B* **79**, 201401 (R) (2009)

The Formation of Supported Carbon Clusters During Graphene Chemical Vapor Deposition (CVD) Growth

Feng Ding, Qinghong Yuan, Junfeng Gao, Haibo Shu, Xiuyun Zhang, Ziwei Xu

Institute of Textile and Clothing, Hong Kong Polytechnic University, Hong Kong, PR China

The epitaxial CVD growth on catalyst surface is the most promising method of synthesizing high quality, large area graphene. A complete growth process includes (i) the nucleation of graphene domains, (ii) the expansion the domain and (iii) the coalescence of the graphene domains into a macroscopic graphene layer. I'm going to present our recent theoretical studies on (i) in detail and (ii) in brief:

During the nucleation stage on most catalyst surface, C chains that have up to 8-13 C atoms are found very stable and a transition from sp^1 one dimensional (1D) C chain to sp^2 two dimensional (2D) graphene island is necessary to initiate the graphene nucleation.[1-2] The metal step was found to be the preferred site of graphene nucleation on catalyst surface and the medium sized C cluster, C_{21}, showed exceptional stability on the catalyst surface; [3-4]

Edge construction is crucial for graphene in vacuum, while graphene edge on catalyst prefers to maintain its pristine form. [5] While the naked graphene edge on Cu(111) surface tends to be terminated by Cu add atoms and the special passivation contribute to the fast growth rate of graphene armchair edge; [6]

Three modes of graphene CVD growth, on terrace, near metal step, and the embedded growth are proposed and the graphene epitaxy growth or the determination of graphene's orientation on various catalyst are carefully studied; [7-8]

References:

[1] J. F. Gao, et. al., *J. Phys. Chem. C, 115 (36), 17695, (2011)*

[2] J. F. Gao, et. al., *J. Am. Chem. Soc., 133(13), 5009, (2011)*

[3] Q. H. Yuan, et. al., *J. Am. Chem. Soc., 133(40), 16072, (2011)*

[4] Q. H. Yuan, et. al., *J. Am. Chem. Soc., 134, 2970-2975, (2012)*

[5] J. F. Gao, et. al., *J. Am. Chem. Soc, 134, 6204-6209, (2012)*

[6] H. Shu, et. al., *ACS Nano, 6, 3243-3250 (2012)*

[7] X. Y. Zhang, et. al., *J. Phys. Chem. Lett., 3, 2822, (2012)*

[8] Q. H. Yuan, et. al., submitted

Effects of electronic and geometric structure on the activity of size-selected model catalysts and electrocatalysts

Alexander von Weber, Eric Baxter, Matthew Kane, Sloan Roberts, and Scott Anderson

Department of Chemistry, University of Utah, Salt Lake City, UT, USA

Mass-selected cluster deposition is used to prepare model catalysts and electrodes for *in situ* studies of both chemical and physical properties. The goal, in addition to looking for cluster/support combinations with interesting catalytic activity, is to use size-dependent correlations of activity with various physical or spectroscopy properties, to identify which properties of the samples are responsible for controlling activity. Electronic structure is probed by a combination of X-ray and UV photoelectron spectroscopies. Sample morphology, including the nature of reactant binding sites, is probed by low energy He^+ scattering. Reactivity is probed using either mass spectrometry, for gas-surface reactions, or by electrochemical measurements, in the case of size-selected electrodes.

Results will be presented for CO oxidation and ethylene dehydrogenation over Pd_n and Pt_n clusters on several different oxide supports, where strong support thickness- and size-dependent correlations are seen between activity and both electronic structure and the availability of specific sites for oxygen activation. Results for the electrochemical ethanol oxidation, hydrogen evolution, and oxygen reduction reactions over Pt_n on ITO and glassy carbon will also be discussed. Here too, there appear to be strong correlations between the electronic properties of the supported clusters, and their activity as oxidation catalysts.

Plasmonic Property of Multidimensional Self-assembled Metallic Nanoparticles

Kaoru Tamada*

Institute for Materials and Engineering (IMCE), Kyushu University, Fukuoka, Japan

In this paper, we report a fundamental optical property of self-assembled multidimensional metallic nanoparticle sheets fabricated by Langmuir-Schaefer method at air-water interface. The 2D and 3D Ag self-assembled nanoparticle sheets exhibit a unique optical property due to the collective excitation of localized surface plasmon resonance (LSPR). The homogeneously coupled LSPR in 2D sheet results in not only a significant red-shift and sharpened LSPR band but also an additional amplification of electric field at the interface [1]. We also found that the multilayered Ag and Au particle films on metal substrates exhibit a drastic reflection color change due to the number of deposited layers [2, 3], where a unique light confinement takes place together with 3D LSPR coupling. We have also studied the characteristics of gold and silver (AuNP/AgNP) mixed nanoparticle film fabricated by spreading AuNP/AgNP mixed solutions. The UV-vis absorption spectra and the FDTD simulation revealed that the LSPR of AuNP and AgNP were not coupled each other even when their resonance wavelength was overlapped by their domain size control.

Recently we also confirmed that the nanoparticle sheet provides highly confined and enhanced fluorescence signals (LSPR field-enhanced fluorescence) [4]. The Ag nanoparticle sheet enabled to provide 4 times enhanced fluorescence image with 160 nm spatial resolution in 30 msec/frame shot under the total internal reflection fluorescence (TIRF) microscope. In the presentation, nano-patterning of the sheets by use of local oxidation nanolithography (LON) and their surface potential change are also discussed.

References

[1] M. Toma, K. Toma, K. Michioka, Y. Ikezoe, D. Obara, K. Okamoto, K. Tamada, Phys. Chem. Chem. Phys. 12, (2012) 14749.

[2] K. Okamoto, B. Lin, K. Imazu, A. Yoshida, K. Toma, M. Toma, K. Tamada, Plasmonics, 8, (2013) 581,

[3] A. Yoshida, K. Imazu, X. Li, K. Okamoto, K. Tamada, Langmuir, 28, (2012) 17153.

[4] E. Usukura, S. Shinohara, K. Okamoto, J. Lim, K. Char, K. Tamada, Appl. Phys. Lett., 104, (2014)121906.

Surface Plasmons in Quantum-Sized Noble-Metal Clusters: Quantum Calculations and the Classical Picture of Charge Oscillations

Hans-Christian Weissker[1,2] and Xóchitl López-Lozano[3]

[1] *CINaM-CNRS & Aix-Marseille Univ., 13288 Marseille, France.*

[2] *European Theoretical Spectroscopy Facility, France; www.etsf.eu.*

[3] *Department of Physics and Astronomy, The University of Texas at San Antonio. One UTSA Circle, San Antonio, Texas 78249, USA*

The localized surface-plasmon resonance (LSPR) in metal clusters corresponds to a collective charge oscillation of the quasi-free electrons of the metal. In the present work, we use the real-time formulation [1] of time-dependent density-functional theory (TDDFT) with pseudopotentials to study the correspondence and differences of the quantum calculations with the classical picture.

By means of animations, we discuss the real-time evolution of the electronic density for different geometries. While there is a clear correspondence between the overall picture of a charge oscillation and the actual dynamics in quantum-sized clusters, the situation is much more intricate owing to quantum effects and the inhomogeneity of the cluster due to the presence of the d electrons. A fine pattern is present over the volume of the cluster even at moments of zero overall polarization. The difference between Ag and Au is clearly visible. Finally, we discuss the question of collective vs. molecular-like transitions, showing that even in the case of single transitions, the dynamics of the total density can be similar to the picture of a charge oscillation.

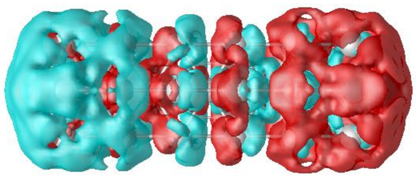

Figure: Snapshot of the density dynamics showing the longitudinal charge oscillation in a 37-atom Ag nanorod.

References

[1] Yabana, K.; Bertsch, G. F., Phys. Rev. B **54**, 4484 (1996).

[2] Weissker, H.-Ch., Whetten, R.L., and López-Lozano, X.; PCCP **16**, 12495 (2014).

[3] López-Lozano, X.; Barron, H.; Mottet, C.; Weissker, H.-Ch., PCCP **16**, 1820 (2014).

Clusters for Photocatalysis

Gunther Andersson,[1] Gregory Metha,[2] Vladimir Golovko,[3] Tomonobu Nakayama,[4] Koji Kimoto,[4] Hassan Al Qahtani,[1, 4] Jason Alvino,[2] Trystan Bennett,[2] Jan-Yves Ruzicka,[3] David P. Anderson,[3] Rantej Kler,[1, 2] and Rohul Adnan [3]

[1] *Flinders Centre for NanoScale Science and Technology, Flinders University, Adelaide, Australia*
[2] *School of Chemistry and Physics, The University of Adelaide, Adelaide, Australia*
[3] *Department of Chemistry, University of Canterbury, Christchurch, New Zealand*
[4] *National Institute for Material Science, Tsukuba, Japan*

Gold clusters with a size < 1.5 - 2 nm deposited and immobilized onto inert supports are known to be catalytically active with the size threshold often coinciding with the loss of metallic properties of Au nanoparticles. The size threshold has been established for both naked clusters prepared under UHV conditions [1] and chemically-synthesised well-defined metal nanoparticles [2]. Clusters can be deposited from the gas phase as size selected clusters [3] or from the liquid phase when using chemically synthesised nanoparticles [4] with the latter route offering the benefit of easy scale-up.

A few challenges need to be solved regarding the deposition process of chemically made clusters onto inert supports. First, it must be investigated whether removal of the ligands is required to make the chemically made clusters catalytic active. The presence of ligands might hinder gas molecules from accessing the catalytically active sites of the clusters. We have found that removal of phosphorous ligands can be achieved by heating to around 200ºC in vacuum [4]. Second, the agglomeration of the clusters must be avoided in order to keep the cluster size small. In particular heating for ligand removal could lead to agglomeration. We have deposited $Au_n(PPh_3)_y$ (n = 8, 9 and 101, y depending on the cluster size) on titania and found that treatment of the titania prior to deposition influences the agglomeration during ligand removal. Treatments applied include basic and acidic treatment, calcination under H_2 and O_2 and UV/ozone treatment. Electron spectroscopy techniques (X-ray photoelectron spectroscopy (XPS)), scanning techniques (atomic force microscopy (AFM)) and microscopy ((scanning) transmission electron microscopy (STEM and TEM) have been used to investigate the deposition process. Subsequent to deposition, the electronic and conformational structure must also be determined as these two properties are believed to play a crucial role in catalysis. Metastable induced electron spectroscopy (MIES) has been used to determine the electronic structure of deposited clusters.

References

[1] M. Valden, X. Lai, and D. W. Goodman, Science 281(1998) 1647.
[2] M. Turner, V. B. Golovko, O. P. H. Vaughan, P. Abdulkin, A. Berenguer-Murcia, M. S. Tikhov, B. F. G. Johnson, and R. M. Lambert, Nature 454(2008) 981.
[3] M. Büttner and P. Oelhafen, Surface Science 600, 1170 (2006).
[4] D. P. Anderson, J. F. Alvino, A. Gentleman, H. A. Qahtani, L. Thomsen, M. I. J. Polson, G. F. Metha, V. B. Golovko, and G. G. Andersson, PCCP 15, 3917 (2013).

September 10th, Wednesday

9:00 Gold and silver in nanoscale, dispersed by ligands to molecular precision
Hannu Häkkinen (Invited)

9:40 Density functional theory investigations of gold and silver nanoparticle properties
Christine Aikens (Invited)

10:20 Electronic communication between metallic moiety and organic functionalities in ultrasmall organic-modified gold clusters
Katsuaki Konishi

10:40 Coffee break

11:10 Motions of individual biomolecular motors probed by gold nanoparticle and nanorod
Ryota Iino (Invited)

11:50 Tracking photo-emitted electrons from gold nanoparticles by femtosecond laser-driven confocal microscopy
Marcel Di Vece

12:10 Functionalization of boron nitride nanosheets by a metal support for the oxygen reduction reaction
Andrey Lyalin

12:30 Excursion

19:00 Conference dinner

Gold and silver in nanoscale, dispersed by ligands to molecular precision

Hannu Häkkinen[1,2,3]

[1] *Department of Chemistry,*
[2] *Department of Physics, and*
[3] *Nanoscience Center, University of Jyväskylä, FI-40014 Jyväskylä, Finland*

Nanometer-scale, ligand-stabilized noble metal clusters have emerged in recent years as a novel form of nanoscale matter with potential applications in molecular electronics, optics, sensing, drug delivery and biolabeling. Tremendous advances have been achieved in understanding their stability and structure due to contributions from synthetic work, X-ray crystallography and density functional theory computations. Their electronic structure can be understood surprisingly well from the simple concepts that have been used in the related field of bare gas-phase metal clusters since 1980's, particularly from the so-called "superatom model" that accounts for the delocalized sp-electrons in the metal core.[1,2] Forming in most cases the frontier orbitals of the nanoparticle, these electrons are responsible for low-energy optical transitions and much of the chemistry. Recent progress in understanding the structure as well as physical and chemical properties of this class of "superatoms" is reviewed,[3-8] and a novel application of using atomically precise, functionalized thiol-stabilized gold nanoclusters for site-specific conjugation to enteroviruses for TEM imaging is discussed.[9]

References

[1] M. Walter et al., Proc. Natl. Acad. Sci (USA) **105**, 9157 (2008).
[2] H. Häkkinen, Chem. Soc. Rev. **37**, 1847 (2008).
[3] H. Häkkinen, Nature Chemistry **4**, 443 (2012).
[4] H. Yang et al., Nature Communications **4**, 2422 (2013).
[5] H. Yang et al., J. Am. Chem. Soc. **136**, 7197 (2014).
[6] S. Malola et al., J. Phys. Chem. Lett. **2**, 2316 (2011).
[7] S. Malola et al., ACS Nano **7**, 10263 (2013).
[8] M. Azubel et al., submitted (2014).
[9] V. Marjomäki et al., Proc. Natl. Acad. Sci (USA) **111**, 1277 (2014).

Density Functional Theory Investigations of Gold and Silver Nanoparticle Properties

Christine M. Aikens

Kansas State University, Manhattan, KS 66506, USA

Theoretical investigations of monolayer-protected noble metal nanoparticles play an important role in determining the origins of the unique chemical and physical properties of these systems that lead to applications in photonics, sensing, catalysis, etc. Density functional theory (DFT) and time-dependent DFT (TDDFT) have been employed to calculate chemical reactivity and physical properties for a number of gold and silver nanoparticles of experimental interest.

Small thiolate-stabilized nanoparticles are of interest for their catalytic, fluorescent, and sensing properties. TDDFT calculations have recently been employed to elucidate the excitation spectrum of $Au_{25}(SR)_{18}^{-}$ and related nanoparticles. This particle can be interpreted as a "superatom", in which a core of essentially free electrons is surrounded by gold-thiolate oligomeric ligands. The ligand field arising from the surrounding gold-thiolate oligomers is responsible for the splitting of the intraband transition. In addition, we will examine the “magic” $Au_{38}(SR)_{24}$ nanocluster. Using a combination of electronic structure calculations, XRD, and optical and CD spectra, this nanocluster is shown to be chiral with D_3 symmetry. $Au_{38}(SR)_{24}$ is found to have an elongated structure; the electronic structure of this elongated “nanorod” is similar to that previously determined for silver nanorods. As for $Au_{25}(SR)_{18}$, delocalized superatom-like orbitals are responsible for its properties.

Silver-DNA systems have been of interest for many years because these small systems are fluorescent and can be used as biotags. However, the structures of these systems are not yet known. In this work, we show that slightly bent, twisted nanowires could explain the optical absorption and circular dichroism (CD) spectra of these interesting experimental systems.

Electronic communication between metallic moiety and organic functionalities in ultrasmall organic-modified gold clusters

Katsuaki Konishi,[1,2] Naoki Kobayashi,[1] and Yukatsu Shichibu[1,2]

[1] *Graduate School of Environmental Science, Hokkaido University, Sapporo, Japan*
[2] *Faculty of Environmental Earth Science, Hokkaido University, Sapporo, Japan*

In the chemistry of ligand-protected metal clusters, the interaction between the metallic core and surround organic moieties has been of unexplored but important subjects. The interaction between π-system and a gold core is especially interesting because it potentially offers unique chemistry. During the course of study on diphosphine-ligated Au clusters [1-3], we have recently found [core+*exo*]-type clusters $[Au_8(dppp)_4X_2]^{2+}$ having organic ligands (X) appended on the terminal *exo* gold atoms of the Au_8 unit [1]. In this presentation we demonstrate a π-mediated electronic communication event between the gold unit and distal organic functionality in the acid-induced chromism of pyridylethynyl-modified Au8 clusters [4].

Au_8 clusters bearing two alkynyl ligands $[Au_8(dppp)_4(C{\equiv}CR)_2]^{2+}$ were synthesized by the reaction of the reduced form ($[Au_8(dppp)_4]^{2+}$) with alkynyl anions. Although the C≡C moieties directly attached to the Au_8 units did not affect the optical properties arising from intracluster transitions [3], the pyridylethynyl-bearing clusters exhibited reversible visible absorption and photoluminescence responses to protonation/deprotonation events of the terminal pyridyl moieties. The chromism behaviors were highly dependent on the relative position of the pyridine nitrogen atom, suggesting that the resonance-coupled movement of the positive charge upon protonation is involved in the optical responses. Thus the formation of extended charged resonance structures causes significant perturbation effects on the electronic properties of the Au_8 unit. These observations provide an example of resonance-coupled transmission of chemical information to a distal cluster unit through π-conjugated groups, and also demonstrate the utility of the combination with organic chemistry in the design of cluster-based responsive systems.

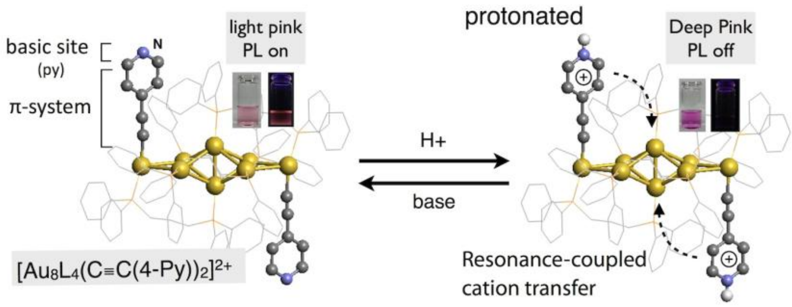

References

[1] Y. Kamei, Y. Shichibu, and K. Konishi, *Angew. Chem. Int. Ed*., 50, (2011) 7442.
[2] Y. Shichibu, Y. Kamei, and K. Konishi, *Chem. Commun.*, 48, (2012) 7559.
[3] Y. Shichibu and K. Konishi,, *Inorg. Chem*., 52, (2013) 6570.
[4] N. Kobayashi, Y. Kamei, Y. Shichibu, and K. Konishi, *J. Am. Chem. Soc*.,*135*, (2013) 16078; JACS spotlights, *J. Am. Chem. Soc*.,*135*, (2013) 17237.

Motions of individual biomolecular motors probed by gold nanoparticle and nanorod

Ryota Iino[1,2]

[1] *Okazaki Institute for Integrative Bioscience, Institute for Molecular Science, National Institutes of Natural Sciences, Aichi, Japan*
[2] *Department of Functional Molecular Science, School of Physical Sciences, The Graduate University for Advanced Studies (SOKENDAI), Kanagawa, Japan*

Advances in optical microscopy have made it possible to watch individual biological molecular machines in action. Just by watching and making the movies of single molecules, we can learn a lot about their dynamic properties. The most successful examples of this approach are rotary and linear molecular motors made of proteins [1, 2]. Molecular motors generate mechanical forces that drive their motions from the energy of chemical reaction. Molecular motors move fast, precisely, and efficiently. Our efforts have helped much to understand the operation mechanisms supporting sophisticated behaviors of molecular motors.

We have recently developed new laser dark-field microscopes [3]. Our new microscopes can determine the centroid position of single gold nanoparticle with microsecond temporal resolution and one-nanometer localization precision, or the three dimensional orientation of single gold nanorod with microsecond temporal resolution and one-degree angle precision. These methods can be applied to the high-speed single-molecule imaging of the molecular motors by using gold nanoparticle or nanorod as a probe. We can monitor not only the detail of motions such as mechanical steps generating force and pauses waiting for elementary steps of chemical reaction, but also conformational changes inside individual molecular motors. In my presentation, I will introduce our recent data on a rotary motor F_1-ATPase and a linear motor kinesin (Fig. 1).

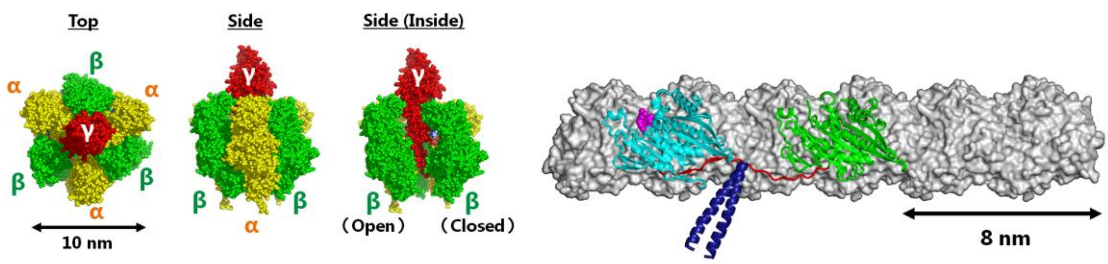

Fig. 1. (Left) a rotary motor F_1-ATPase. (Right) a linear motor kinesin.

References

[1] R. Iino, H. Noji, Curr. Opin. Struct. Biol. 23 (2013) 229-234.
[2] R. Iino, H. Noji, IUBMB Life. 65 (2013) 238-246.
[3] H. Ueno, S. Nishikawa, R. Iino, K.V. Tabata, S. Sakakihara, T. Yanagida, H. Noji, Biophys. J. 98 (2010) 2014-2023.

Tracking photo-emitted electrons from gold nanoparticles by femtosecond laser-driven confocal microscopy

Wiebke Albrecht[1], Wingjohn Tang[1], Alfons van Blaaderen[1], Marcel Di Vece[1 2]

[1] *Soft Condensed Matter, Debye Institute for Nanomaterials Science, Utrecht University*
[2] *Nanophotonics, Debye Institute for Nanomaterials Science, Utrecht University*

A wealth of fascinating phenomena are associated with the plasmonics of metal nanostructures. Local field enhancement and phased array antennas are examples of how interaction of metal nanostructures with light provides interesting physics with in addition technological relevance. Recent work showed that metallic nanostructures are able to emit photoelectrons, even when being excited with laser energies well below the work function of the metal [1,2]. The photoelectrons originating from the metal nanostructure are captured by the local (strong) plasmonic field and moreover, are accelerated strongly by the same field. The acceleration provides energies to the electron which are far above the laser excitation energy [3]. Eventually the propelled electron is emitted and can be detected by electron spectrometry which is sensitive to direction and energy. Not only would visualizing the electron trajectories be revealing, it would also make the study of how such accelerated electrons interact with their environment for instance by the detection of possible (intermediate) reactions much easier.

We present a study in which we imaged the electroluminescence trails of photoelectrons emitted from gold clusters by femto second laser confocal microscopy. As far as we know the emitted electron paths are visualized for the first time. The direction of the paths are governed by the scanning direction of the microscope but also by the laser polarization [4]. A complicated reaction chain with trapped electrons which are reaccelerated provides insight into the dynamics of this novel and complicated system. We analyzed several cluster densities to obtain the optimal condition for this process.

The gold clusters were prepared by a gas aggregation magnetron sputtering cluster source and deposited on glass in the soft landing regime. This ensures a spherical shape and the vacuum provides an ultra-clean surface. A state-of-the-art confocal microscope with an integrated high-intense Ti:Sapphire fs-laser (Leica SP8) was used to image the electron trails.

Better control and understanding of this intriguing fundamental process can lead to the creation of ultrafast electron sources on the nanoscale.

Reference(s)

[1] G. Herink, et al., *Nature*, **483** (2012) 190
[2] A. Grubisic et al., *Nano Lett.* **12**, (2012) 4823-4829
[3] P. Dombi et al., *Nano Lett.* **13**, (2013) 674-678
[4] Th. Fennel et al., *PRL* **98**, (2007) 143401

Functionalization of boron nitride nanosheets by a metal support for the oxygen reduction reaction

Andrey Lyalin,[1] Akira Nakayama,[1,2] Kohei Uosaki,[3] and Tetsuya Taketsugu[1,2]

[1] *Elements Strategy Initiative for Catalysts and Batteries (ESICB), Kyoto University, Kyoto, Japan*
[2] *Department of Chemistry, Faculty of Science, Hokkaido University, Sapporo, Japan*
[3] *Global Research Center for Environment and Energy based on Nanomaterials Science (GREEN), National Institute for Materials Science (NIMS), Tsukuba, Japan*

It is demonstrated that boron nitride (BN), which is catalytically inert insulator with a wide band gap, can be functionalized and act as an electrocatalyst for oxygen reduction reaction (ORR). Such functionalization can be achieved by the nitrogen doping [1] or deposition of the BN nanosheets on some transition metals, such as Ni(111) [2] or Au(111) [3]. Density-functional theory calculations show that interaction of BN nanosheets with the metal supports results in formation of the band states in the forbidden zone of BN, as it occurs in the case of Ni(111) support [2] or a slight protrusion of the unoccupied BN states toward the Fermi level as it observed for Au(111) support [3]. Modification of the BN band structure can be explained by the orbital mixing and electron sharing at the interface [4,5]. Analysis of the binding preference and adsorption energies of the ORR intermediates on functionalized BN nanosheets demonstrate possibility of ORR. It is experimentally proved that overpotential for ORR at the gold electrode is significantly reduced by depositing BN nanosheets (Fig. 1). The present study demonstrates the possibility to functionalize inert materials to become ORR catalysts, opening new ways to design effective Pt-free catalysts for fuel cells based on materials never before considered as catalysts.

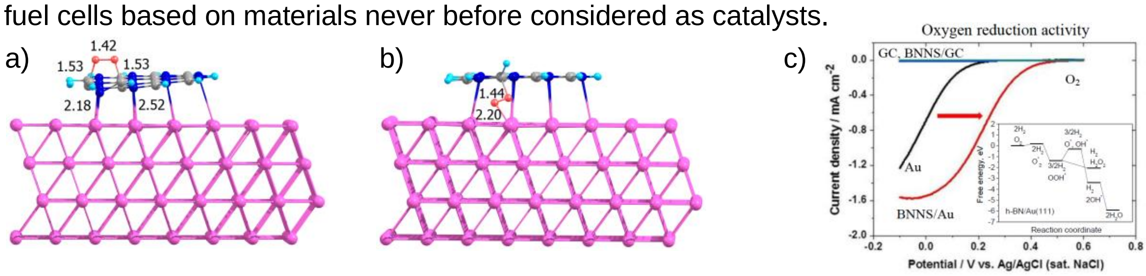

Figure 1. Optimized structures of O_2 adsorbed at the edge of the small h-BN island on the Au(111) surface (a) and (b). The linear sweep voltammograms of (i) bare Au, (ii) BNNS/Au, (iii) bare glassy carbon (GC), and (iv) BNNS/GC as well as free energy diagram for ORR on the h-BN/Au(111) (c).

References

[1] A. Lyalin, A. Nakayama, K. Uosaki, and T. Taketsugu, PCCP 15 (2013) 2809.
[2] A. Lyalin, A. Nakayama, K. Uosaki, and T. Taketsugu, J. Phys. Chem. C 117 (2013) 21359.
[3] K. Uosaki, G. Elumalai, H. Noguchi, T. Masuda, A. Lyalin, A. Nakayama, and T. Taketsugu, JACS 136 (2014) 6542.
[4] R. Laskowski, P. Blaha, K. Schwarz, Phys. Rev. B 78 (2008) 045409.
[5] A. B. Preobrajenski, S. A. Krasnikov, A. S. Vinogradov, M. L. Ng, T. Kaambre, A. A. Cafolla, and N. Martensson, Phys. Rev. B 77 (2008) 085421.

September 11th, Thursday

ISSPIC XVII
Fukuoka, 2014

9:00 Metal-polymer nanocomposites produced by supersonic cluster beam implantation with tunable electrical, optical and mechanical properties
Paolo Milani (Invited)

9:40 Switching, tunneling, and superconductivity in percolating cluster films
Simon Brown (Invited)

10:20 Nanoisland formation of small Ag_N-clusters on HOPG as determined by inner-shell photoionization spectroscopy
Matthias Neeb

10:40 Coffee break

11:10 Photophysical properties of supramolecular nanostructures in gas-phase
Manfred Kappes (Invited)

11:50 Channeling vibrational energy to probe the electronic density of states in metal clusters
Andrei Kirilyuk

12:10 Frontier orbital rule for electron transport in molecules
Kazunari Yoshizawa

12:30 Lunch

14:00 The 3D-architecture of individual free silver nanoparticles captured by X-ray scattering
Karl-Heinz Meiwes-Broer (Invited)

14:40 Hidden charge states in soft-X-ray laser-produced nanoplasmas revealed by fluorescence spectroscopy
Tim Laarmann

15:00 The role of metal doping on the reversible adsorption and storage of hydrogen in nanoporous carbons
Maria J. López

15:20 Photoelectron spectroscopy and density functional theory investigation of $V_xSi_{12}^-$ (x = 1-3) clusters: discovery of a silicon-based ferrimagnetic wheel structure
Xiaoming Huang

15:40 $Co\cdot Ar^+$ complexes: the smallest and most exotic bar magnets with giant magnetic anisotropy energy
Tobias Lau

16:00 Coffee break

16:30 Poster Session B

18:30 Cultural event

Metal-polymer nanocomposites produced by supersonic cluster beam implantation with tunable electrical, optical and mechanical properties

A. Bellacicca[1], F. Borghi[1], A. Podestà[1], C. Melis[2],
L. Colombo[2], C. Ghisleri[3], L. Ravagnan[3], P. Milani[1]

[1] CIMAINA, *Department of Physics, University of Milano, Milano, Italy*
[2] *Department of Physics, University of Cagliari, Cagliari, Italy*
[3] *WISE srl, Milano, Italy*

Stretchable functional materials are enabling ingredients for the fabrication of wearable electronics, smart prosthetics and soft robotics. These applications require the integration of electronic, optical and actuation capabilities on soft, conformable and biocompatible polymeric substrates [1].

Recently we demonstrated that neutral metallic nanoparticles produced in the gas phase and aerodynamically accelerated in a supersonic expansion can be implanted in a polymeric substrate to form a conductive nanocomposite with superior resilience and interesting structural and functional properties [2-4]. This approach is called supersonic cluster beam implantation (SCBI).

Here we present experimental and theoretical results about the production of devices based on metal/polymer nanocomposites with electrical, optical and mechanical properties that can be precisely tuned by controlling the fraction of metal clusters implanted in the polymeric matrix [5-6]. State of the art applications and devices for stretchable optics, neurostimulation and soft robotics will be shown and discussed.

References

[1] S. Bauer, et al., Adv. Mater. 26, 149 (2014)
[2] G. Corbelli, et al., Adv. Mater. 23, 4504 (2011)
[3] C. Ghisleri, et al., Laser & Photonics Rev. 7, 1020 (2013)
[4] C. Ghisleri, et al., Appl. Phys. Lett. 104, 061910 (2014)
[5] R. Cardia, et al., J. Appl. Phys. 113, 224307 (2013)
[6] C. Ghisleri, et al., J. Phys. D: Appl. Phys. 47, 015301 (2014)

Switching, Tunneling, and Superconductivity in Percolating Cluster Films

S. A. Brown[1], A. Nande[1], S. Fostner[1], R. Gazoni[1], A. Smith[1], A. Sattar[1], J. Grigg[1], S. Couet[2], K. Temst[2], M.J. Van Bael[3],

[1] *The MacDiarmid Institute for Advanced Materials and Nanotechnology, Dept. of Physics and Astronomy, University of Canterbury, 8140, Christchurch, New Zealand*
[2] *Instituut voor Kern- en Stralingsfysica, Celestijnenlaan 200 D, KU Leuven, Leuven B-3001, Belgium*
[3] *Laboratory of Solid State Physics and Magnetism, Celestijnenlaan 200 D, KU Leuven, Leuven B-3001, Belgium*

When clusters are randomly deposited on a surface they produce percolating films which have remarkable electrical properties.[1] Here we will focus on devices that contain percolating films of Sn and Pb clusters between a pair of electrical contacts, and especially those that are deliberately constructed so as to guarantee that the film is close to the percolation threshold (onset of conduction). In these devices quantum mechanical tunnelling is important[2], and several new and unexpected phenomena are observed. In particular we have recently demonstrated switching between well-defined, quantized, conductance values [multiples of the quantum of conductance ($2e^2/h$)], at room temperature.[3]

Recently we have begun exploring the superconducting properties of these films. We find that the percolating films have interesting characteristics that are intermediate between those of 1D and 2D systems. We will discuss phase slips[4,5], which appear to occur in the narrow necks between clusters, and the competition between percolation effects and the vortex unbinding associated with the Berenzinski-Kosterlitz-Thouless transition[6,7]. We will also discuss a superconductor to insulator transition which can be driven by the applied current.

Reference(s)

[1] J. Schmelzer jr, S. A. Brown, A. Wurl, M. Hyslop, and R. J. Blaikie, Phys. Rev. Lett. **88**, 226802 (2002).
[2] S. Fostner, R. Brown, J. Carr, and S. A. Brown, Phys. Rev. B **89**, 075402 (2014).
[3] A. Sattar, S. Fostner, and S. A. Brown, Phys. Rev. Lett. **111**, 136808 (2013).
[4] A. Nande et al, to be published.
[5] J. S. Langer and Vinay Ambegaokar, Physical Review **164**, 498 (1967); W. A. Little, Physical Review **156**, 396 (1967).
[6] V. L. Berezinskii, Sov. Phys. JETP **34**, 610 (1972); J. M. Kosterlitz and D. J. Thouless, J. Phys. C **6**, 1181 (1973).
[7] S. Fostner et al, to be published.

Nanoisland formation of small Ag_N-clusters on HOPG as determined by inner-shell photoionization spectroscopy

M. Neeb[1], M. Al-Hada[2], S. Peredkov[3], S. Peters[3], W. Eberhardt[3,4]

[1] *Helmholtz-Zentrum Berlin, BESSY II, Berlin, Germany*
[2] *Department of Physics, Amran University, Amran, Jemen*
[3] *IOAP, Technical-University Berlin, Berlin, Germany*
[4] *Center for Free Electron Laser Science cFEL, DESY, Hamburg, Germany*

Small Ag-clusters represent highly interesting particles for optoelectronic applications due to their quantum-sized electronic properties like tunable plasmon frequencies, fluorescence activity and metal-biomolecule hybrid formation [1,2,3]. Moreover Ag-particles dispersed on planar supports such as oxides and carbon represent an important type of heterogeneous catalysts [4,5] as well as nanocomposite material for tunable electronic and optical applications of e.g. graphene [6,7].

In general, element-specific X-ray photoionization studies have been demonstrated to be useful for the investigation of deposited clusters [8]. Here we show by the application of XPS and Auger spectroscopy that small Ag-clusters coalesce into bulk-like nanoislands upon deposition onto the surface of pristine HOPG, a few-layer model of graphene. In case of oxidation of the metallic islands a positive binding energy shift (XPS) is observed in distinct contrast to the negative chemical shift usually observed for oxidized silver compounds. This is interpreted by an electrostatic Coulomb shift of the oxidized Ag-islands from which the size of the nanoislands has been determined according to the electric potential of a charged disc.

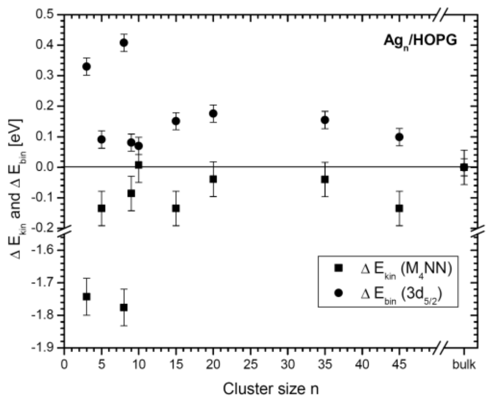

References

[1] L.A. Peyser, A.E. Vinson, A.P. Bartko, R.M. Dickson, Science **291**, 103 (2001).
[2] C. Félix, C. Sieber, W. Harbich, J. Buttet, I. Rabin, W. Schulze, G. Ertl, PRL **86**, 2992 (2001).
[3] T. Tabarin, A. Kulesza,R. Antoine, R. Mitric, M. Broyer, P. Dugourd, V. Bonacic-Koutecky, PRL **101**, 213001 (2008).
[4] D.V. Demidov. I.P. Prosvirin, A.M. Sorokin, V.I. Bukhtiyarov, Catal. Sci. Technol., **1**, 1432 (2011).
[5] V. I. Bukhtiyarov, M. Hävecker, V. V. Kaichev, A. Knop-Gericke, R. W. Mayer, R. Schlögl, Phys. Rev. B **67**, 235422 (2003).
[6] Z. Li, P. Zhang, K. Wang, Z. Xu, J. Wei, L. Fan, D. Wu, H. Zhu, J. Mater. Chem. **21**, 13241, (2011).
[7] G. Lu, S. Mao, S. Park, R.S. Ruoff, J. Chen, Nano Res. **2**, 192 (2009).
[8] S. Peters, S. Peredkov, M. Al-Hada, M. Neeb, W: Eberhardt, Surf. Sci. **608**, 129 (2013) and references therein.

Photophysical properties of supramolecular nanostructures in gas-phase

Manfred Kappes,[1,2] Patrick Weis,[1] Detlef Schooss, [2] Oliver Hampe, [2†] Jean-Francois Greisch, [2] Matthias Vonderach, [1] Ulrike Schwarz,[1] Patrick Jäger [2] and Marc-Oliver Winghart [1]

[1] *Institute of Physical Chemistry, KIT, Karlsruhe, Germany*
[2] *Institute of Nanotechnology, KIT, Karlsruhe, Germany*
[†] *deceased 23.4.14*

Electrospray ionization (ESI) can be used to isolate fragile, self-assembled supramolecular organometallic structures from solution. Additionally, clusters and further adducts of such species can be formed during the ESI process itself. Information on gas-phase structures and properties can be obtained using methods well known from research on elemental clusters: high resolution mass spectrometry, ion mobility (IMS), anion photoelectron spectroscopy (PES), photodissociation spectroscopy (PD) and trapped ion photoluminescence – sometimes in combination, e.g. IMS-PES [1] or IMS-PD. In this talk I will discuss applications to charged aggregates of strongly absorbing metalloporphyrins [2] (and azoporphyrins [3]) as well-as to photoluminescent lanthanide cluster complexes with organic antenna molecules [4].

References

[1] M. Vonderach, O. T. Ehrler, P. Weis and M. Kappes, Anal. Chem. 83 (2011), 1108; M. Vonderach, O. T. Ehrler, K. Matheis, P. Weis and M. Kappes, J. Am. Chem. Soc. 134 (2012) 7830.

[2] T. Karpuschkin, M. Kappes and O. Hampe, Angewandte Chemie Int. Ed. 52 (2013), 10374-10377; U. Schwarz, M. Vonderach, M. Kappes, R. Kelting, K. Brendle and P. Weis, Int. J. Mass Spec. 339 (2013), 24; U. Schwarz, M. Vonderach, M. Armbruster, K. Fink and M. Kappes, J. Phys. Chem A 118 (2014), 369.

[3] P. Weis, U. Schwarz, F. Hennrich, D. Wagner, S. Bräse and M. Kappes, Phys. Chem. Chem. Phys. 16 (2014), 6225.

[4] J.-F. Greisch, M. Harding, B. Schäfer, M. Rotter, M. Ruben, W. Klopper, M. Kappes and D. Schooss, J. Phys. Chem. A 118 (2014), 94; J.-F. Greisch, M. Harding, B. Schäfer, M. Ruben, W. Klopper, M. Kappes and D. Schooss, J. Phys. Chem. Lett., 5 (2014), 1727.

Channeling Vibrational Energy to Probe the Electronic Density of States in Metal Clusters

Jeroen Jalink[1], Joost M. Bakker[2], Theo Rasing[1], and Andrei Kirilyuk[1]

[1] *Radboud University Nijmegen, Institute for Molecules and Materials, Heyendaalseweg 135, 6525 AJ Nijmegen, The Netherlands*
[2] *Radboud University Nijmegen, Institute for Molecules and Materials, FELIX Facility, Toernooiveld 7, 6525 ED Nijmegen, The Netherlands*

Atomic clusters are the smallest pieces of matter where condensed matter properties gradually emerge with the number of constituent atoms [1]. The physical and chemical properties of each cluster vary strongly on an atom-by-atom level leading to intriguing magnetic [2], electric [3] and catalytic [4] properties. An important factor in these phenomena is the electronic structure of the particular cluster, which is thus of primary importance. The electronic structure of neutral clusters can be probed using photoelectron spectroscopy (PES) of mass selected anionic clusters [5]. However, such PES studies are usually limited to the geometry of the anion. Since the geometric structures of clusters can vary for different charge states, it is important to probe the electronic structure of the neutral species directly. Direct spectroscopic studies on neutral transition metal clusters such as laser-induced fluorescence and resonance-enhanced multiphoton ionization have only been reported for systems containing up to 3 atoms. It is likely that the large density of electronic states leads to a rapid electronic relaxation, precluding detection.

Here we demonstrate a method based on two-color IR-UV spectroscopy to probe the electronic density of states near the Fermi level in neutral metal clusters. Our method consists of measuring the UV ionization yield of clusters at different internal temperatures. The temperature is modulated by resonantly pumping cluster lattice vibrations. Such excitation is followed by two processes: (1) intramolecular vibrational redistribution of the energy within ps and (2) energy flow from the lattice into the electronic system. The time scale for the second process is determined by the electron-phonon (vibronic) coupling and for transition metals it is of the order of ps. Our approach thus ensures a thermal equilibrium within the experimental time scale (~μs). Fowler's model of surface photoemission is modified to incorporate the discrete nature of the electronic structure, which allows to validate electronic structure calculations. Intriguingly, the energy redistribution between vibrations and electrons could in principle be probed in a time-resolved experiment.

Reference(s)
[1] W.A. de Heer, Rev. Mod. Phys. 65 (1993) 611.
[2] X. Xu, S. Yin, R. Moro, A. Liang, J. Bowlan, W.A. de Heer, Phys. Rev. Lett. 107 (2011) 057203.
[3] R. Moro, X. Xu, S. Yin, W.A. de Heer, Science 300 (2003) 1265.
[4] S.M. Lang, T.M. Bernhardt, R.N. Barnett, U. Landman, Angew. Chem. Int. Ed. 2010, 49, 980.
[5] C. Bartels, C. Hock, J. Huwer, R. Kuhnen, J. Schwöbel, B. von Issendorff, Science 323 (2009) 1323.

Frontier Orbital Rule for Electron Transport in Molecules

Kazunari Yoshizawa

Institute for Materials Chemistry and Engineering, Kyushu University
Nishi-ku, Fukuoka 819-0395, JAPAN

Our orbital view studies about molecular conductance for 10 years is presented. We have developed a chemical way of thinking about electron transport in molecules in terms of frontier orbital theory [1-4]. The phase and amplitude of the HOMO and LUMO of π-conjugated molecules determine the essential properties of their electron transport. By considering a close relationship between Green’s function and the molecular orbitals, we derived an orbital rule that would help our chemical understanding of the phenomenon. First, the sign of the product of the orbital coefficients at sites *r* and *s* in the HOMO should be different from the sign of the product of the orbital coefficients at sites *r* and *s* in the LUMO for good electron transport, as indicated in the scheme. Secondly, sites *r* and *s* in which the amplitude of the HOMO and LUMO is large should be connected. We confirmed these theoretical predictions experimentally by using break junctions to measure the single-molecule conductance of naphthalene dithiol derivatives [5]. The measurement of the symmetry-allowed 1,4-naphthalene dithiol shows a conductance that exceeds that of the symmetry-forbidden 2,7-naphthalene dithiol by two orders of magnitude.

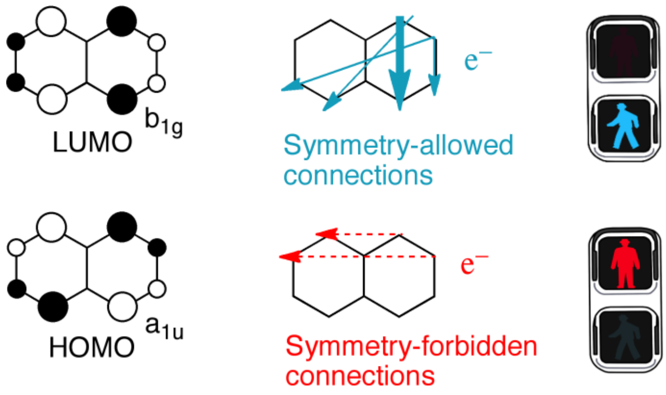

The intermolecular electronic coupling in π-stacked structures plays an important role in the electron conduction in extended systems. We studied a π-stacked benzene molecule [2,2]paracyclophane to investigate the effect of the intermolecular interactions in aromatic hydrocarbons on its electron-transport properties [6]. The qualitative but essential understanding in the orbital views would extend the application of the rule from a single molecule to a crystal structure for the development of high performance molecular devices.

References

[1] Yoshizawa, K. *Acc. Chem. Res.* **2012**, *45*, 1612.
[2] Tada, T.; Yoshizawa, K. *ChemPhysChem* **2002**, *3*, 1035.
[3] Yoshizawa, K.; Tada, T.; Staykov, A. *J. Am. Chem. Soc.* **2008**, *130,* 9406.
[4] Tsuji, Y.; Staykov, A.; Yoshizawa, K. *J. Am. Chem. Soc.* **2011**, *133*, 5955.
[5] Taniguchi, M.; Tsutsui, M.; Mogi, R.; Sugawara, T.; Tsuji, Y.; Yoshizawa, K.; Kawai, T. *J. Am. Chem. Soc.* **2011**, *133*, 11426.
[6] Li, X.; Staykov, A.; Yoshizawa, K. *Bull. Chem. Soc. Jpn.* **2012**, *85*, 181.

The 3D-architecture of individual free silver nanoparticles captured by X-ray scattering

I. Barke[1], D. Rupp[2], H. Hartmann[1], L. Flückiger[2], M. Saupe[3], M. Adolph[2], Ch. Peltz[1], S. Bartling[1], T. Fennel[1], T. Moeller[2], K.-H. Meiwes-Broer[1]

[1] *Institut of Physics, University of Rostock, Universitätsplatz 3, 18051 Rostock, Germany*
[2] *Technical University of Berlin, Straße des 17. Juni 135, 10623 Berlin, Germany*
[3] *SLAC National Acceleretor Laboratory 2575 Sand Hill Road, Menlo Park, CA 94025*

Identifying the morphology of free metal particles is one of the fundamental objectives in cluster science. In recent years the most favorable shapes of metal clusters consisting of a small number of atoms have been successfully solved based on a combination of theoretical and experimental methods. However, for large unsupported clusters the structure determination remained difficult. In this contribution we present single particle scattering images from free silver clusters obtained at the free-electron laser facility FLASH using XUV photons with ≈ 13.5 nm wavelength. Single-shot x-ray scattering enables 3D characterization of the particles, which can be considered fixed in space for the duration of photon exposure. In contrast to previous results from rare gas clusters [1], anisotropic features with high symmetry are observed, reflecting the regular shape of metal particles with radii larger than ≈ 40 nm. A fast and versatile algorithm for simulation of scattering images from arbitrarily shaped three-dimensional particles is used that is benchmarked against state-of-the-art finite difference time domain simulations for selected morphologies and sizes. A variety of cluster morphologies can be identified, including truncated octahedrons, decahedrons, twinned tetrahedrons, and icosahedrons. Excellent agreement is obtained between measured and simulated scattering images demonstrating the feasibility of reliable shape determination of particles in the free beam. Moreover, the role of photon absorption could be revealed.

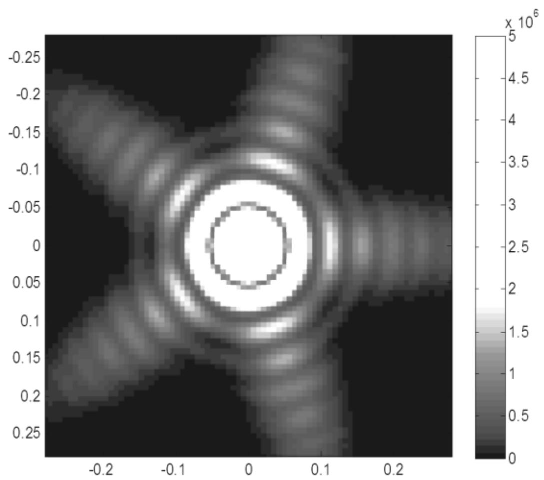

Scattering image from a 85 nm silver cluster of icosahedral shape, simulated with Finite Difference Time Domain (FDTD) calculations. Photon wavelength 13.5 nm

The observations show that energetically non-ideal morphologies continue to exist in the free beam even for sizes exceeding 200 nm in diameter. Considering that icosahedral Ag particles are reported to undergo a transition to fcc structure with increasing cluster size [2], our results shed new light on the growth of large particles in the gas phase.

References

[1] C. Bostedt, E. Eremina, D. Rupp, M. Adolph, H. Thomas, M. Hoener, A. R. B. de Castro, J. Tiggesbäumker, K.-H. Meiwes-Broer, T. Laarmann, H. Wabnitz, E. Plönjes, R. Treusch, J. R. Schneider, and T. Möller, Phys. Rev. Lett. 108, 093401 (2012)
[2] Baletto et al., J. Chem. Phys. 116 (2002)

Hidden Charge States in Soft-X-Ray Laser-Produced Nanoplasmas Revealed by Fluorescence Spectroscopy

L. Schroedter,[1] M. Müller,[2] A. Kickermann,[1] A. Przystawik,[1] S. Toleikis,[1] M. Adolph,[2] L. Flückiger,[2] T. Gorkhover,[2] L. Nösel,[2] M. Krikunova,[2] T. Oelze,[2] Y. Ovcharenko,[2] D. Rupp,[2] M. Sauppe,[2] D. Wolter,[2] S. Schorb,[3] C. Bostedt,[3] T. Möller,[2] and T. Laarmann[1,4]

[1] *Deutsches Elektronen-Synchrotron DESY, Hamburg, Germany*
[2] *Institut für Optik und Atomare Physik, Technische Universität Berlin, Berlin, Germany*
[3] *SLAC National Accelerator Laboratory, Stanford, USA*
[4] *The Hamburg Centre for Ultrafast Imaging CUI, Hamburg, Germany*

A fascinating application of X-Ray Free-Electron Lasers (XFEL) is coherent diffraction imaging of single particles in a single light pulse. However, a severe challenge is the damage done to the biopolymers by the light pulse. Besides elastic scattering by bound electrons, strong ionization takes place and the molecule is destroyed. It is an open question whether sufficient scattering signal can be detected before the molecule disintegrates. One possible way to alleviate this problem is adding a sacrificial tamper layer around the molecule which slows down the expansion. In the present contribution we discuss experiments on clusters as nanoscopic model systems to test the effect of tamper layers [1], as so-called core-shell clusters were generated, with a core consisting of one element surrounded by a shell consisting of another element. By detecting emitted fluorescence photons in the extreme ultraviolet spectral range we were able to derive information on the first few hundred femtoseconds of the FEL interaction with the composite clusters. The data recorded at the FLASH facility at DESY provide fingerprints of transient states of high energy density matter. The experiments give direct evidence that - in addition to the multiply charged cluster surface which Coulomb explodes and finally leads to fluorescence from individual ions - also the cluster ion core is initially highly charged. During the FEL interaction and before disintegration, highly charged ions that have lost more than 10 electrons each are generated and could clearly be identified by their characteristic radiative transitions. Therefore, fluorescence spectroscopy probes ultrafast radiative decay of highly charged ions in a time window which is not accessible by conventional mass spectrometry. In agreement with theory, the latter traces remnants of the interaction, where electron thermalization followed by nonradiative recombination has already produced significantly lower charge states. Thus, a sacrificial tamper layer provides an efficient electron source for partial neutralization of highly charged ions created in the center. The significant reduction of charge states increases the available time for recording a diffraction pattern in coherent imaging experiments elucidating the three-dimensional structure of biopolymers.

Reference

[1] L. Schroedter et al., Phy. Rev. Lett. 112 (2014) 183401.

The role of metal doping on the reversible adsorption and storage of hydrogen in nanoporous carbons

María J. López, Iván Cabria, and Julio A. Alonso

Departamento de Física Teórica, Atómica y Óptica, Universidad de Valladolid, Valladolid, Spain
maria.lopez@fta.uva.es

Storage is the main problem to use hydrogen as an alternative fuel to gasoline in cars. Nanoporous carbons, whose walls have an atomic structure formed of graphene-like ribbons with many defects, are among the best candidate materials as containers. However, under the mild conditions of technological interest (room temperature and moderate pressures) they exhibit a limited/poor storage capacity due to the weak adsorption of molecular hydrogen to the pore walls [1], below 0.1 eV per molecule. Experimental evidences suggest that doping the porous carbons with metals may enhance their storage capacity although the mechanism is not well understood. We have performed density functional calculations to investigate the reversible adsorption of hydrogen on palladium doped nanoporous carbons, paying special attention to the problems that arise in the desorption step. Our simulations on Pd atoms and clusters supported on graphene reveal that hydrogen binds directly to the Pd atoms and clusters following two different adsorption modes: molecular adsorption and dissociative atomic chemisorption [2]. The energies for molecular adsorption are in the range appropriate for achieving reversible adsorption/desorption at room temperature. However, desorption of the stored molecular hydrogen competes with other alternative processes: a) dissociative chemisorption of hydrogen, after passing through the activation barrier and b) desorption of Pd-H complexes. We have found that desorption of Pd-H complexes can be successfully avoided by anchoring the Pd atoms and clusters to defects present on the carbonaceous substrate [3]. In addition, we find that the presence of defects improves the dispersion of the metal on the carbon network with the consequent beneficial effect on the storage capacity of the material.

Reference(s)

[1] J.A. Alonso, I. Cabria, M.J. López , J. Mater. Res. Vol. 28 (2013) 589.
[2] I. Cabria, M.J. López, S. Fraile, J.A. Alonso, J Phys. Chem. C 116 (2012) 21179.
[3] M.J. López, I. Cabria, J.A. Alonso, J. Phys. Chem. C 118 (2014) 5081.

Acknowledgement: This work was supported by MICINN of Spain (Grant MAT2011-22781)

Photoelectron Spectroscopy and Density Functional Theory Investigation of $V_xSi_{12}^-$ (x = 1-3) clusters: Discovery of a Silicon-based Ferrimagnetic Wheel Structure

Jijun Zhao,[1] Xiaoming Huang,[1] Xiaoqing Liang,[1] Hong-Guang Xu,[2] Shengjie Lu,[2] Weijun Zheng [2]

[1] *Key Laboratory of Materials Modification by Laser, Ion and Electron Beams, Dalian University of Technology, Dalian 116024, China*

[2] *Institute of Chemistry, Chinese Academy of Sciences, Beijing 100190, China*

We combine anion photoelectron spectroscopy and density functional theory (DFT) to examine the structures as well as the electronic and magnetic properties of $V_xSi_{12}^-$ (x=1, 2, 3) clusters. Our studies show that VSi_{12}^- adopts a V-centered hexagonal prism with a singlet spin state. Addition of the second V atom leads to a capped hexagonal antiprism for $V_2Si_{12}^-$ in a doublet spin state. Most interestingly, $V_3Si_{12}^-$ exhibits a ferrimagnetic bicapped hexagonal antiprism wheel-like structure with a total spin of 4 μ_B and a HOMO-LUMO gap of 0.35 eV. The number of unpaired electrons in neutral and anionic V_3Si_{12} cluster can be understood by the Wade-Mingos rules for polyhedral clusters.

In addition, our combined study of photoelectron spectroscopy and DFT calculations show that $Fe_2Ge_n^-$ and $Cr_2Ge_n^-$ (n=3-12) clusters exhibit robust ferromagnetic and antiferromagnetic behaviors, respectively, which are nearly irrelevant to the cluster size and geometry. All these findings not only extend our understanding of doped silicon/germanium clusters but also provide novel building blocks for nanoscale spintronic devices.

Co·Ar$^+$ complexes: The smallest and most exotic bar magnets with giant magnetic anisotropy energy

Vicente Zamudio-Bayer,[1,2] Konstantin Hirsch,[1] Arkadiusz Ławicki,[1] Akira Terasaki,[3] Bernd von Issendorff,[2] and Tobias Lau[1]

[1] *Institut für Methoden und Instrumentierung der Forschung mit Synchrotronstrahlung, Helmholtz-Zentrum Berlin für Materialien und Energie GmbH, Berlin, Germany*
[2] *Physikalisches Institut, Universität Freiburg, Freiburg, Germany*
[3] *Department of Chemistry, Kyushu University, Fukuoka, Japan*

In macroscopic magnets, the magnetization direction is rigidly fixed with respect to the geometrical shape by the magnetic anisotropy energy. This is why a macroscopic bar magnet, like a compass needle, is aligned with an external magnetic field. The situation is usually different in small transition metal clusters, where the orientation of the magnetic moment can rotate freely against the cluster body, and superparamagnetic behavior is typically found [1-3].

We have for the first time observed evidence of the geometrical alignment of small Co·Ar$^+$ complexes with an external magnetic field, thus creating the smallest and most exotic bar magnets, consisting of only one magnetic ion bound to a rare gas atom. In these systems, the spin magnetic moment is coupled to the intramolecular axis by more than 5 meV of magnetic anisotropy energy.

The magnetic and spatial alignment was probed by the simultaneous detection of X-ray natural linear dichroism and X-ray magnetic circular dichroism of size-selected free Co·Ar$^+$ complexes at $T < 10$ K and $B = 5$ T in a linear radio-frequency ion trap [3,4]. This technique will allow us to explore the physical limits of the magnetic anisotropy energy in small transition metal clusters, molecules, and complexes [5].

References

[1] C. P. Bean and J. D. Livingston, J. Appl. Phys. 30 (1959) S120.
[2] P. Ballone, P. Milani, and W. A. de Heer, Phys. Rev. B 44 (1991) 10350.
[3] M. Niemeyer, K. Hirsch, V. Zamudio-Bayer, A. Langenberg, M. Vogel, M. Kossick, C. Ebrecht, K. Egashira, A. Terasaki, T. Möller, B. v. Issendorff, and J. T. Lau, Phys. Rev. Lett. 108 (2012) 057201.
[4] K. Hirsch, J. T. Lau, P Klar, A. Langenberg, J. Probst, J. Rittmann, M. Vogel, V. Zamudio-Bayer, T. Möller, and B. von Issendorff, B. J. Phys. B: At. Mol. Opt. Phys. 42 (2009) 154029.
[5] T. O. Strandberg, C. M. Canali, and A. H. MacDonald, Nat. Mater. 6 (2007) 648.

September 12th, Friday

9:00	Tuning cluster functionality by size and composition Peter Lievens (Invited)
9:40	Clusters as model systems for catalysis Thorsten Bernhardt (Invited)
10:20	Stable stoichiometry and chemical reactivity of cluster ions revealed by high temperature TPD experiments Fumitaka Mafuné
10:40	Coffee break
11:10	Extending the sizes and charge states of polyanionic metal clusters Steffi Bandelow
11:30	Characterization of single-molecule magnets in isolation Gereon Niedner-Schatteburg
11:50	Spin orientation in isolated magnetic nanoalloys - topology, dielectric and magnetic properties of manganese doped tin-clusters Mn/Sn_N Urban Rohrmann
12:10	ISSPIC 18
12:20	Concluding remarks and perspectives Vlasta Bonačić-Koutecký (Invited)
13:00	Closing Akira Terasaki

Tuning cluster functionality by size and composition

Peter Lievens and Ewald Janssens

Department of Physics & Astronomy, Faculty of Science, KU Leuven, Belgium

Tuning cluster properties by their size and composition has been a long standing challenge in cluster science, and has over the years been realized by the synthesis and study of a wide variety of bimetallic, binary, and also some ternary clusters. One specific asset of studying mixed clusters is the possibility to tailor independently the cluster geometry via the number of atoms and the cluster electronic properties determined by the number of (delocalized) electrons. From a fundamental point of view this interplay of geometry and electronic structure is ideal to challenge advanced quantum mechanical modeling as well as phenomenological descriptions of size and composition dependent properties. With respect to the role of nanoparticles and clusters in nanotechnology applications, the atom by atom control of physical and chemical properties is an important asset.

This talk will deal with growth, stability patterns, structure, electronic and optical properties and magnetism of small binary metal clusters, in particular composed of coinage, transition metal and group 14 elements. Experimental studies based on laser vaporization cluster production, mass spectrometry, laser spectroscopy, and photofragmentation will be discussed. Further insight in cluster functionality is obtained by comparisons with quantum chemical computations, mainly based on density functional theory.

Clusters as Model Systems for Catalysis

Thorsten M. Bernhardt

Institute of Surface Chemistry and Catalysis, University of Ulm,
Albert-Einstein-Allee 47, 89069 Ulm, Germany

Gas phase metal clusters represent ideal model systems to gain molecular level insight into the energetics and kinetics of metal-mediated catalytic reactions. In this contribution the idea of metal cluster model systems for catalysis will be illustrated with a particular emphasis put on the importance of a conceptual understanding gained through these well-defined studies [1].

Furthermore, specific examples from our laboratory will be presented that illustrate the potential of ion trap mass spectrometry (in combination with collaborative first principles calculations) to reveal pertinent molecular details of important catalytic processes. These examples will cover a wide variety of reaction systems ranging from the CO combustion catalyzed in car exhaust converters [2] over hydrogen feed gas purification catalysts important to advanced fuel cell technologies [3] to the water splitting reaction mediated by the manganese oxide cluster complex [4], which is the active catalytic center of the photosystem II in biological oxygen evolving systems.

Reference(s)

[1] S.M. Lang, T.M. Bernhardt, Phys. Chem. Chem. Phys. 14 (2012) 9255.
[2] S.M. Lang, I. Fleischer, T.M. Bernhardt, R.N. Barnett, U. Landman, J. Am. Chem. Soc. 134 (2012) 20654.
[3] S.M. Lang, T.M. Bernhardt, M. Krstić, V. Bonačić-Koutecký, Angew. Chem. Int. Ed. 53 (2014) 5467.
[4] S.M. Lang, I. Fleischer, T.M. Bernhardt, R.N. Barnett, U. Landman, Nano Lett. 13 (2013) 5549.

Stable stoichiometry and chemical reactivity of cluster ions revealed by high temperature TPD experiments

Fumitaka Mafuné,[1] Ken Miyajima,[2] and Toshiaki Nagata[3]

[1] *Department of Basic Science, School of Arts and Sciences, The University of Tokyo, Tokyo, Japan*

Temperature programmed desorption (TPD) is commonly used in a surface chemistry, which enables us to identify dissociating species from the surface as a function of a temperature. For gas phase clusters, challenging experiments have been performed by Bernhardt and his coworkers in a lower temperature than a room temperature for a variety of elements and novel reactions of clusters with small molecules have been proposed. In the present study, we focused on developing TPD for the gas phase clusters in a higher temperature, because practically, a considerable number of the catalytic reactions of bulk materials are known to proceed at high temperature.

Cerium oxide is commonly used in a practical catalyst as a catalytic support and a catalytic promoter as well. It is known that cerium takes both +3 and +4 charge states, so that it tends to adsorb oxygen in an oxygen rich environment, whereas it releases oxygen in an oxygen poor environment. The propensity relates to oxygen storage capacity of cerium oxide. In the present study, we examined thermally stable stoichiometry and chemical reactions of the gas phase cerium oxide clusters using TPD method. Cerium oxide cluster ions, $Ce_nO_{2n+x}^+$ (n = 3–10, x = −1 to +2), were prepared in the gas phase by laser ablation of a cerium oxide rod in the presence of oxygen diluted in He as the carrier gas. The stable stoichiometry of the cluster ions was investigated using a mass spectrometer in combination with TPD. Oxygen molecules were found to be released from the oxygen-rich clusters, $Ce_nO_{2n+x}^+$ (x = 1, 2), and stoichiometric $Ce_nO_{2n-1}^+$ and $Ce_nO_{2n}^+$ were exclusively formed by heating treatment at 573 K as,

$$Ce_nO_{2n+x}^+ \rightarrow Ce_nO_{2n+x-2}^+ + O_2\uparrow \rightarrow Ce_nO_{2n-4}^+ + O_2\uparrow \rightarrow \ldots. \rightarrow Ce_nO_{2n-1}^+ \text{ and } Ce_nO_{2n}^+ \quad (1)$$

$Ce_nO_{2n-1}^+$ and $Ce_nO_{2n}^+$ species were thus found to be thermally stable and the oxygen-rich clusters consisted of robust $Ce_nO_{2n-1}^+$ and $Ce_nO_{2n}^+$ and weakly bound oxygen atoms. When the stoichiometric clusters were heated further up to ~800 K, further oxygen-molecule release started to be observed. Thermal dissociation processes are size-dependent, which relate to geometrical and electronical structures of the clusters.

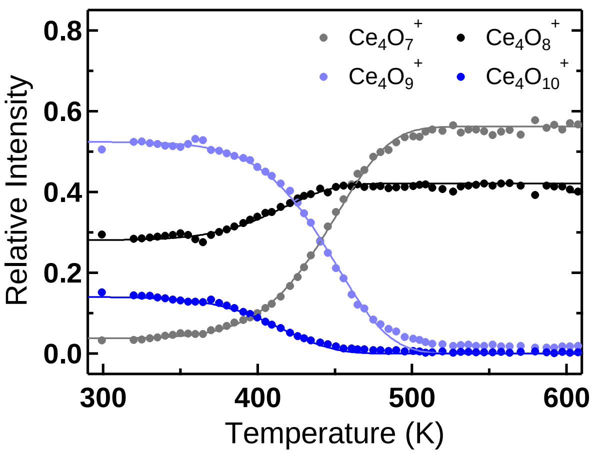

Figure 1. TPD plot for $Ce_4O_m^+$.

Extending the Sizes and Charge States of Polyanionic Metal Clusters

Steffi Bandelow,[1] Franklin Martinez,[1,2] Gerrit Marx,[1] Lutz Schweikhard,[1] and Albert Vass[1]

[1] *Institute of Physics, Ernst-Moritz-Arndt University Greifswald, Germany*
[2] *present address: Institute of Physics, University of Rostock, Germany*

The ClusterTrap setup [1] combines several ion-storage devices for a variety of experimental studies on metal clusters including collision-induced dissociation, (delayed) photodissociation, further ionization to higher positive or negative charge states by electron impact or electron attachment, respectively. All selection, preparation and interaction steps can be performed on extended time scales up to several seconds. The unique arrangement of two linear radiofrequency quadrupole (RFQ) ion traps (Paul traps) and an ion-cyclotron-resonance trap (ICR or Penning trap) allows one to dedicate them with respect to specific functions and optimizations.

In particular, one Paul trap is used for the accumulation of cluster ions from a pulsed laser-vaporization source and preselection of the cluster size. In the second Paul trap, electrons can be attached at well-defined energies by use of a “digital” (i.e. rectangular) RF trapping potential [2]. This allows one to study for the first time the energy dependence of electron attachment to polyanionic metal clusters and to determine the heights of their repulsive Coulomb barriers. With a recent replacement of the superconducting magnet, the field strength was increased from B = 5 T to 12 T. Thus, the electron attachment in the ICR trap was extended to (negative) charge states as high as z = -6 for gold and z = -10 for aluminum clusters, respectively. The yields of the charge states measured as a function of reaction time confirm a sequential electron-attachment process.

Next, we will study polyanion decay induced by laser light. The studies will be performed with respect to cluster size, charge state and chemical element as well as laser intensity and photon energy, and also regarding possible delays between photo-interaction and electron detachment or cluster dissociation. Furthermore, it is planned to use multi-reflection time-of-flight mass spectrometry, recently further developed by us for precision measurements in nuclear physics [3], for high-resolution separation of the (relatively large) polyanionic cluster, and to combine ion-trap techniques of polyanion production with their investigation by photo-electron spectroscopy.

[1] L. Schweikhard *et al.*, Eur. Phys. J. D 9 (1999) 15; F. Martinez *et al.*, Eur. Phys. J. D 63 (2011) 255; F. Martinez *et al.*, Int. J. Mass Spectrom. 365-366 (2014) 266.
[2] S. Bandelow *et al.*, Int. J. Mass Spectrom. 336 (2013) 47 and 353 (2013) 49.
[3] R.N. Wolf *et al.*, Int. J. Mass Spectrom. 349-350 (2013) 123; F. Wienholtz *et al.*, Nature 498 (2013) 346.

Characterization of Single-Molecule Magnets in Isolation

Joseph Fournier,[3] Maximilian Gaffga,[1] Joachim Hewer,[1] Bernd von Issendorff, [4]
Mark A. Johnson,[3] Johannes Lang,[1] Tobias Lau,[2] Arkadiusz Lawicki,[4] Jennifer Meyer,[1]
Gereon Niedner-Schatteburg,[1] Akira Terasaki,[5] Matthias Tombers,[1] Conrad Wolke,[3]
Vicente Zamudio-Bayer,[2,4]

[1] *Department of Chemistry, TU Kaiserslautern, Kaiserslautern, Germany*
[2] BESSY*, Helmholtz Center, Berlin, Germany*
[3] *Department of Chemistry, Yale University, New Haven, USA*
[4] *Department of Physics, University Freiburg, Freiburg, Germany*
[5] *Department of Chemistry, Kyushu University, Fukuoka, Japan*

X-ray induced Magnetic Circular Dichroism (XMCD) at the L-edge of transition metals has served to determine the individual spin- and orbital contributions to the magnetic moments of isolated and mass selected cluster ions [1,2]. Here, we present the results of recent XMCD experiments on ligand stabilized complexes, so called single-molecule magnets (SMMs), as e.g. $[Mn_{12}O_{12}(OAc)_{16}(H_2O)_4]$ ("Mn_{12}-acetate"). Isolation experiments confirm bulk findings and predicted couplings [3].

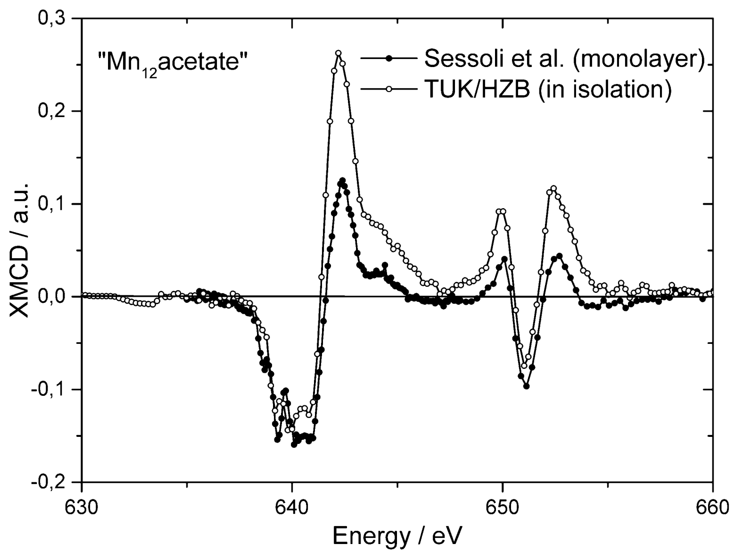

Infrared Multiple Photon Dissociation (IR-MPD) spectroscopy serves to obtain complementary information. Such investigations revealed weak and surprisingly strong metal effects alike, e.g. in the case of lanthanoid variation. These findings are to discuss in the light of ab initio DFT modelling.

Reference
[1] S. Peredkov, M. Neeb, W. Eberhardt, J. Meyer, M. Tombers, H. Kampschulte, GNS; Phys. Rev. Lett. **107**, (2011), 233401
[2] M. Niemeyer, K. Hirsch, V. Zamudio-Bayer, A. Langenberg, M. Vogel, M. Kossick, C. Ebrecht, K. Egashira, A. Terasaki, T. Moller, B. v. Issendorff, and J. T. Lau; Phys. Rev. Lett. **108**, (2012), 057201
[3] M. Mannini, P. Sainctavit, R. Sessoli, C. Cartier dit Moulin, F. Pineider, M.-A. Arrio, A. Cornia, and D. Gatteschi, Chem. Eur. J. **14**, (2008), 7530

Spin orientation in isolated magnetic nanoalloys – topology, dielectric and magnetic properties of manganese doped tin-clusters Mn/Sn_N

Urban Rohrmann,[1] Peter Schwerdtfeger[2] and Rolf Schäfer[1]

[1] *Department of Chemistry, Technical University of Darmstadt, Darmstadt, Germany*
[2] *Centre for Theoretical Chemistry and Physics, Massey University, Albany, New Zealand*

Molecular beam deflection experiments in inhomogeneous electric and magnetic fields (Stark- and Stern-Gerlach experiment, respectively) in combination with density functional theory (DFT) allow to study systematically the impact of molecular topology on the magnetic response of isolated nanoalloyed clusters. In Stark-experiments the dielectric response of the clusters is measured. The electric dipole moment and polarizability are sensitive probes for the topology of the clusters.[1] This allows to identify the molecular geometries by matching experimental observations with molecular dynamics simulations of the clusters, based on our DFT studies. The experimentally verified molecular structure (in general the lowest energy isomer in the computational studies) then is considered to investigate the correlation with the magnetic response measured in Stern-Gerlach experiments.
The clusters are generated in a laser ablation source with cryogenically cooled nozzle in order to study the influence of thermal excitations of the clusters on the magnetic response. The spatial distribution (beam profile) of the vibrationally excited clusters is exclusively shifted in the direction of the field gradient with vanishing broadening of the beam profile. This reflects a vibrationally induced spin orientation process.[2] The magnetic dipole moments are extracted from the shift of the beam profiles and compare very well to the spin-only magnetic dipole moment expected for the lowest energy spin isomers found computationally.
At very low nozzle temperature a large fraction of each cluster species is at the vibrational ground state and the magnetic response depends critically on the composition / topology of the cluster. $Mn@Sn_{12}$ has been identified as a true paramagnetic superatom, with spatially quantized spin angular momentum.[2] With one exception ($Mn@Sn_{14}$) the remaining clusters do not show such response due to the reduced symmetry molecular environment. This is interpreted in terms of adiabatic magnetization, induced by avoided crossings among Zeeman levels.[3]

Reference(s)
[1] S. Heiles, R. Schäfer, *Dielectric Properties of Isolated Clusters* (Springer, 2014).
[2] U. Rohrmann, R. Schäfer, *Phys. Rev. Lett.* 111, 133401 (2013).
[3] X. Xu, S. Yin, R. Moro, W. A. de Heer, *Phys. Rev. Lett.* 95, 237209 (2005).

ISSPIC XVII
Fukuoka, 2014

POSTER SESSION A

September 9th, Tuesday
16:30 - 18:30

Spectroscopy and dynamics	A1-A17
Electronic structure and quantum effects	A18-A36
Biotechnological and medical applications: imaging and sensors	A37-A41
Structure and thermodynamics	A42-A65
Reactivity and catalysis	A66-A88

A1 **First-Principles Study of Excited State Evolution in a Protected Gold Complex**
Olga Lopez-Acevedo, Ari Ojanperä, Martti Puska ; *Aalto University*

A2 **Optical properties and structures of isolated gold-silver nanoalloys from molecular beam photodissociation spectroscopy**
A. Shayeghi[1], D. A. Götz[1], R. L. Johnston[2], R. Schäfer[1] ; [1] *Technische Universität Darmstadt,* [2] *University of Birmingham*

A3 **Fluorescent oxidized Si nanoclusters and reversible interactions with solvent**
Hanieh Yazdanfar, Mike J. McNally, Gediminas Galini, Mark Watkins, Klaus von Haeften ; *University of Leicester*

A4 **Single-shot imaging of giant Xe clusters with X-ray free-electron laser**
T. Nishiyama[1], C. Bostedt[2], K. R. Ferguson[2], C. Hutchison[1], K. Nagaya[1,3], H. Fukuzawa[3,4], K. Motomura[4], S. Wada[3,5], T. Sakai[1], K. Matsuami[1], T. Tachibana[4], Y. Ito[4], W. Q. Xu[4], S. Mondal[4], T. Umemoto[5], C. Nicolas[6], C. Miron[6], T. Kameshima[7], Y. Joti[7], K. Tono[7], T. Hatsui[3], M. Yabashi[3], K. Ueda[3,4], M. Yao[1] ; [1] *Kyoto University,* [2] *SLAC National Accelerator Laboratory,* [3] *RIKEN SPring-8 Center,* [4] *Tohoku University,* [5] *Hiroshima University,* [6] *Synchrotron SOLEIL, L'Orme des Merisiers,* [7] *JASRI*

A5 **Ultrafast dynamics in single clusters captured with time-resolved x-ray imaging**
D. Rupp[1], M. Adolph[1], L. Flückiger[1], T. Gorkhover[1,2], M. Krikunova[1], J.-P. Müller[1], M. Müller[1], M. Sauppe[1], D. Wolter[1], S. Schorb[1,2], S. Düsterer[4], R. Treusch[4], C. Bostedt[2,3], T. Möller[1] ; [1] *IOAP, Technische Universität Berlin,* [2] *LCLS at SLAC National Accelerator Laboratory,* [3] *Stanford University and SLAC,* [4] *FLASH at DESY*

A6 **Momentum mapping of fragment ions generated upon Coulomb explosions of dichloroethylene isomers in intense laser fields**
Yoriko Wada[1], Hiroshi Akagi[2], Ryuji Itakura[2], Tomonari Wakabayashi[1], Takayuki Kumada[2] ; [1] *Kindai University,* [2] *Japan Atomic Energy Agency*

A7 **Vibrational Spectroscopy of Monolayer Protected Gold Clusters: A Close Look at the Au-S Interface**
Birte Varnholt, Patric Oulevey, Igor Dolamic, Thomas Bürgi ; *University of Geneva*

A8 **Vibrational spectroscopy of Au-nanocluster single crystals**
Jaakko Koivisto, Kirsi Salorinne, Satu Mustalahti, Tanja Lahtinen, Sami Malola, Hannu Häkkinen, Mika Pettersson ; *University of Jyväskylä*

A9 **Two-color IR-UV spectroscopy of Nb_nC_m clusters**
Valeriy Chernyy, Joost Bakker, Andrei Kirilyuk ; *Radboud University Nijmegen*

A10 **Comparative study of ultrafast relaxation dynamics of $Au_{144}(C_2H_4Ph)_{60}$ and $Au_{102}(pMBA)_{44}$ nanoclusters by using mid-IR transient absorption spectroscopy**
Satu Mustalahti, Pasi Myllyperkiö, Tanja Lahtinen, Sami Malola, Kirsi Salorinn, Jaakko Koivisto, Hannu Häkkinen, Mika Pettersson ; *University of Jyväskylä*

A11 **Characterization of counter ions in solutions using thiol molecules adsorbed on silver nanoparticles**
Saori Handa, Yingying Yu, Masayuki Futamata ; *Saitama University*

A12 **Highly-sensitive gap mode Raman spectroscopy on various substrates**
Maho Ishikura, Hiroki Suzuki, Masayuki Futamata ; *Saitama University*

A13 **In-situ produced BiO_x nanoparticles: Studied in a beam and as deposited by photoelectron spectroscopy**
Mikko-Heikki Mikkelä[1], Maxim Tchaplyguine[1], Chaofan Zhang[2], Tomas Andersson[2], Erik Mårsell[1], Olle Björneholm[2] ; [1] *Lund University,* [2] *Uppsala University*

A14 **Photofragment-ion imaging from mass-selected cluster ions using a linear-type tandem reflectron**
Kenichi Okutsu, Kenichiro Yamazaki, Keijiro Ohshimo, Fuminori Misaizu ; *Tohoku University*

A15 **Time Resolved Study of EUV-FEL Triggered Nano-Plasma of Rare-Gas Clusters**
K. Nagaya[1,2], T. Sakai[1], T. Nishiyama[1], K. Matsunami[1], S. Yase[1], M. Yao[1], H. Fukuzawa[2,3], K. Motomura[3], T. Tachibana[3], S. Mondal[3], K. Ueda[2,3], S. Wada[2,4], H. Hayashita[4], N. Saito[2,5], T. Togashi[2,6], M. Nagasono[2], M. Yabashi[2] ; [1] *Kyoto University,* [2] *RIKEN SPring-8 Center,* [3] *Tohoku University,* [4]*Hiroshima University,* [5] *NMIJ, AIST,* [6] *JASRI*

A16 **X-ray absorption spectroscopy of size-selected cerium oxide clusters**
Tetsuichiro Hayakawa[1], Masashi Arakawa[2], Shun Sarugaku[2], Kota Ando[2], Kenichiro Tobita[2], Tomonori Ito[2], Kazuhiro Egashira[1], Akira Terasaki[2,3] ; [1] *East Tokyo Laboratory, Genesis Research Institute, Inc.,* [2] *Kyushu University,* [3] *Toyota Technological Institute*

A17 **Photodepletion spectroscopy of silver cluster cations in a temperature-controlled ion trap**
Tomonori Ito, Kenichiro Tobita, Masashi Arakawa, Akira Terasaki ; *Kyushu University*

A18 **Geometry, Electronic, and Magnetic properties as well as selective O_2 and CO adsorption on Au_nRh_m clusters**
Marcela .R. Beltrán, Fernando. Buendía ; *Universidad Nacional Autónoma de México, Instituto de Investigaciones en Materiales*

A19 **AB INITIO STUDY OF CATIONIC, ANIONIC AND NEUTRAL Au_nRh_m CLUSTERS**
Fernando Buendía[1], Marcela R. Beltrán[1] ; [1]*Universidad Nacional Autónoma de México, Instituto de Investigaciones en Materiales*

A20 **Electronic and optical properties of hetero-assembled endohedral superatomic clusters**
Takeshi Iwasa[1,2], Atsushi Nakajima[1,2] ; [1] *Nakajima Designer Nanocluster Assembly project*, *JST-ERATO,* [2] *Keio University*

A21 **Electronic structure of rare-earth clusters: from number of 4f-electrons to magnetism**
Lars Peters[1], Saurabh Ghosh[2], Igor di Marco[2], Biplab Sanyal[2], Anna Delin[2], Misha Litcarev[2], Theo Rasing[1], Andrei Kirilyuk[1], Olle Eriksson[2], Mikhail Katsnelson[1] ; [1] *Radboud University Nijmegen,* [2] *Uppsala University*

A22 **Coexistence of Insulating and Metallic States, and other Unusual Electronic and Magnetic Properties of Pure and Doped Zinc Clusters**
Andrés Aguado[1], Andrés Vega[1], Alexandre Lebon[2], Bernd von Issendorff[3] ; [1] *Valladolid University,* [2]*Brest University,* [3] *Universität Freiburg*

A23 **Probing of an Adsorbate-Specific Excited State on an Organic Insulating Surface by Two-Photon Photoemission Spectroscopy**
Masahiro Shibuta[1], Naoyuki Hirata[1,2], Toyoaki Eguchi[1,2], Atsushi Nakajima[1,2] ; [1] *Keio University,* [2] *JST, ERATO, Nakajima Designer Nanocluster Assembly Project*

A24 **Full relativistic calculations of electronic and magnetic properties of small cationic and neutral bismuth clusters**
Josef Anton[1], and Timo Jacob[1], Arne Rosen[2] ; [1] *University of Ulm,* [2]*University of Gothenburg*

A25 **Phase Transition Behavior and Ionic Conductivity of Small Silver Iodide Quantum Dots**
Takayuki Yamamoto[1], Hirokazu Kobayashi[1,2], Yoshiki Kubota[3], Hiroshi Kitagawa[1,2] ; [1] *Kyoto University, CREST, JST,* [3] *Osaka Prefecture University*

A26 **A new structural model for Al_{23}^- magic cluster: A face-sharing bi-icosahedral motif**
Kiichirou Koyasu[1,2], Tatsuya Tsukuda[1,2] ; [1]*The University of Tokyo,* [2] *Kyoto University*

A27 **Non-spherical gold clusters with the lowest-energy intense absorptions: strong correlation between geometric and electronic structures**
Yukatsu Shichibu[1,2], Mingzhe Zhang[2], Katsuaki Konishi[1,2] ; [1] *Hokkaido University,* [2] *Hokkaido University*

A28 **Density functional theory study on hydrogen absorption properties of nano-sized transition metal clusters (1): difference between Pd/Pt bulk and their clusters**
Aya Matsuda, Hirotoshi Mori ; *Ochanomizu University*

A29 **Density functional theory study on hydrogen absorption properties of nano-sized transition metal clusters (2): dependency on composition and internal structures**
Kasumi Miyazaki, Aya Matsuda, Hirotoshi Mori ; *Ochanomizu University*

A30 **Electronic shell closure of Al_{13} by electron donation from PVP**
Tomomi Watanabe[1,2], Kiichirou Koyasu[1,2], Tatsuya Tsukuda[1,2] ; [1] *The University of Tokyo,* [2] *Kyoto University*

A31 **Precise Separation of Metal Clusters Protected by Two-Types of Thiolate Ligands**
Yoshiki Niihori, Miku Matsuzaki, Chihiro Uchida, Yuichi Negishi ; *Tokyo University of Science*

A32 **Ultrafast photoelectron spectroscopy of metal clusters supported on MgO and Si substrates**
Florian Knall[1], Mihai E. Vaida[1], Thorsten M. Bernhardt[1], Hisato Yasumatsu[2], Nobuyuki Fukui[3] ; [1] *University of Ulm,* [2] *Toyota Technological Institute;*
[3] *East Tokyo Laboratory, Genesis Research Institute, Inc.*

A33 **Graphene-supported metal clusters: Well-defined nanostructures for the investigation of photo-induced processes**
Kira Jochmann, Thorsten M. Bernhardt ; *University of Ulm*

A34 **Properties of designed small gallium-nitride clusters**
Tibor Höltzl ; *Furukawa Electric Institute of Technology*

A35 Stabilization of Magic-Numbered $Au_{25}(SR)_{18}$ Cluster
Wataru Kurashige[1], Masaki Yamaguchi[1], Katsuyuki Nobusada[2], Yuichi Negishi[1] ; [1] *Tokyo University of Science,* [2] *Institute for Molecular Science*

A36 Theoretical Study on the Ln Dependence of $Ln(COT)_2$ Photoelectron Spectra
Erika Nakajo, Tomohide Masuda, Satoshi Yabushita ; *Keio University*

A37 Functionalized Gold Nanoclusters as Site-Specific Labels for Imaging of Enteroviruses
Kirsi Salorinne[1], Varpu Marjomäki[2], Tanja Lahtinen[1], Mari Martikainen[2], Jaakko Koivisto[1], Sami Malola[3], Mika Pettersson[1], Hannu Häkkinen[1,3] ; [1] *University of Jyväskylä,* [2] *University of Jyväskylä,* [3] *University of Jyväskylä*

A38 Metal nanoparticle modified electrochemical electrodes for nonenzyme hydrogen peroxide sensing
Jue Wang, Xuejiao Chen, Kaiming Liao, Guanghou Wang, Min Han ; *Nanjing University*

A39 Gold Nanorod Assisted Laser Desorption/Ionization of Oligopeptides
Masanori Fujii[1], Naotoshi Nakashima[1,2,3],Yasuro Niidome[1,2,4] ; [1] *Kyushu University,* [2] *Kyushu University,* [3] *CREST,* [4] *Kagoshima University (Present Affiliation)*

A40 Spontaneous Formation of Gold Glyconanoparticles by Direct Reaction of ω-Glycosilated Alkylsulfanylanilines and $HAuCl_4$
Ryuich Takegawa, Satoaki Onitsuka, Toshiyuki Hamada, Jun-ich Kurawaki, Hiroaki Okamura ; *Kagoshima University*

A41 Nanopore devices for rapid structural analysis of Nanomaterials
Sou Ryuzaki[1], Masateru Taniguchi[2], Koichi Okamoto[1], Kaoru Tamada[1] ; [1] *Kyushu University,* [2] *Osaka University*

A42 Silver acetylide nano helical structure induced by impurities
Shota Ito, Yoshikiyo Hatakeyama, Ken Judai ; *Nihon University*

A43 Rapid cooling of isolated small carbon cluster anions
Takeshi Furukawa[1], Naoko Kono[1], Gen Ito[1], Jun Matsumoto[1], Hajime Tanuma[1], Toshiyuki Azuma[2], Klavs Hansen[3], Haruo Shiromaru[2] ; [1] *Tokyo Metropolitan University,* [2] *Atomic, Molecular and Optical Physics Laboratory, RIKEN,* [3] *University of Gothenburg*

A44 Radiative cooling of laser-heated niobium clusters
Klavs Hansen[1], Yejun Li[2], Vladimir Kaydashev[2], Ewald Janssens[2] ; [1] *University of Gothenburg,* [2] *KU Leuven*

A45 Adsorbing carbon dioxide on fullerenes at 0.37K under the influence of charge: a mass spectrometric and molecular dynamics/DFT study
Stefan Ralser[1], Johannes Postler[1], Alexander Kaiser[1], M. Probst[1], S. Denifl[1], Diethard K. Böhme[2], Paul Scheier[1] ; [1] *Universität Innsbruck,* [2] *York University*

A46 Entropy-driven isomer switching in $Fe^+(H_2O)_n$ probed with IR spectroscopy and free-energy calculations
Kazuhiko Ohashi[1], Jun Sasaki[1], Gun Yamamoto[1], Ken Judai[2], Nobuyuki Nishi[2], Hiroshi Sekiya[1] ; [1] *Kyushu University,* [2] *Institute for Molecular Science*

A47 **Syntheses of Au@PdAg and Au@PdAg@Ag core–shell Nnanorods through distortion induced alloying between Pd shells and Ag atoms over Au nanorods**
Masaharu Tsuji , Koichi Takemura, Chihiro Shiraishi, Keiko Uto, Atsuhiko Yajima[3], Masashi Hattori, Takeshi Daio ; *Kyushu University*

A48 **Ligand-protected gold clusters with novel interfacial structures**
Prasenjit Maity[1], Jun-ichi Nishigaki[1], Tatsuya Tsukuda[1,2] ; [1] *The University of Tokyo,* [2] *Kyoto University*

A49 **Isolation and properties of chiral $Pd_2Au_{36}(SR)_{24}$ cluster**
Noelia Barrabés[1], Bei Zhang[1], Houhua Li[2], Kaziz Sameh[3], Dawid Wodka[1], Clément Mazet[2], Jordi Llorca[4], Thomas Bürgi[1] ; [1] *University of Geneva,* [2] *University of Geneva,* [3] *Superior National School of engineers of Tunis,* [4] *Technical University of Catalonia*

A50 **Alternate shell structure in Fe-Co nanoparticles**
Bheema Lingam Chittari[1], Vijay Kumar[1,2] ; [1]*Dr. Vijay Kumar Foundation(VKF),* [2]*Shiv Nadar University*

A51 **Bond Length Analysis of Au Nanoparticles Synthesized in Ionic Liquids**
Yoshikiyo Hatakeyama[1], Kiyotaka Asakura[2], Ken Judai[1], Keiko Nishikawa[3] ; [1] *Nihon University,* [2] *Hokkaido University,* [3] *Chiba University*

A52 **withdraw**

A53 **Generation of a liquid droplet in a vacuum**
Kota Ando, Masashi Arakawa, Akira Terasaki ; *Kyushu University*

A54 **Vibrational properties of metal nanoparticles: From structural dependence to intrinsic damping**
Huziel E. Sauceda[1], Israel Acuña-Galván[2,3], Ignacio L. Garzón[1] ; [1] *Universidad Nacional Autónoma de México,* [2] *Centro Universitario UAEM Zumpango,* [3] *UAEH, Hidalgo*

A55 **An incorporation of the concept of a bifurcation pathway to global reaction route mapping analyses: An application to Au_5 cluster**
Tetsuya Taketsugu[1,2], Yu Harabuchi[1], Yuriko Ono[1], Satoshi Maeda[1,2] ; [1] *Hokkaido University,* [2] *Kyoto University*

A56 **Stability and morphology of platinum cluster supported on silicon substrate in heating cycles**
Nobuyuki Fukui[1], Hisato Yasumatsu[2] ; [1] *East Tokyo Laboratory, Genesis Research Institute, Inc.,* [2] *Cluster Research Laboratory, Toyota Technological Institute*

A57 **Synthesis of a novel [core+*exo*]-type heptanuclear gold cluster**
Mingzhe Zhang, Yukatsu Shichibu, Katsuaki Konishi ; Hokkaido University

A58 **Exploration on Magic Binary Nanoclusters Consisting of Silicon-Transition Metal Atoms by Reaction with Molecular Oxygen**
Yoshito Sugawara[1], Tomomi Nagase[1], Hironori Tsunoyama[1,2], Atsushi Nakajima[1,2] ; [1] *Keio University,* [2] *Nakajima Designer Nanocluster Assembly Project, JST-ERATO*

A59 **Preparation and redispersible solidification of monodisperse CdSe nanoparticles capped with cysteine in water**
Yasuto Noda, Isao Sawakami, Takuya Kurihara, K. Takegoshi ; *Kyoto University*

A60 Low temperature XAFS study of thiolate-protected Au clusters

Seiji Yamazoe[1,2], Shinjiro Takano[1], Wataru Kurashige[3], Yuichi Negishi[3], Tatsuya Tsukuda[1,2] ; [1] *The University of Tokyo,* [2] *Kyoto University,* [3] *Tokyo University of Science*

A61 Ionic cluster formation using an ion drift-tube with selected-ion injection - Measurement of thermodynamic quantities for H_3O^+ Hydrate

Yoichi Nakai[1], Hiroshi Hidaka[2], Naoki Watanabe[2], Takao M. Kojima[3] ; [1] *RIKEN Nishina Center for Accelerator-Based Science,* [2] *Hokkaido University,* [3] *Atomic Physics Laboratory*, *RIKEN*

A62 Nanoparticle formation by interaction between laser ablated plume and shock waves

Eri Ueno[1], Naoaki Fukuda[2], Hiroshi Fukuoka[3], Minoru Yaga[4], Ikurou Umezu[5], Min Han[6], Toshio Takiya[1] ; [1] *Hitachi Zosen Corporation,* [2] *Kyoto University,* [3] *Nara National College of Technology,* [4] *University of the Ryukyus,* [5] *Konan University,* [6] *Nanjing University*

A63 Structures of small silicon-doped gold cluster cations

Jun Miyawaki, Ko-ichi Sugawara ; *AIST*

A64 Location of dopant M (M = Pd, Ag, Cu) within $Au_{25-x}M_x(SR)_{18}$ studied by XAFS

Seiji Yamazoe[1,2], Wataru Kurashige[3], Katsuyuki Nobusada[2,4], Yuichi Negishi[3] , Tatsuya Tsukuda[1,2] ; [1] *The University of Tokyo,* [2] *Kyoto University,* [3] *Tokyo University of Science,* [4] *Institute for Molecular Science*

A65 Space-Focusing of Spatially Spread Ions in Time-of-Flight Mass Spectrometer

Shun Sarugaku, Ryohei Murakami, Masashi Arakawa, Akira Terasaki ; *Kyushu University*

A66 Understanding and designing nanoalloys for clean energy applications by first principles calculations

Daojian Cheng ; *Beijing University of Chemical Technology*

A67 Conformations of Biomolecular Ions Probed by Proton Transfer Reactions at Various Temperature

Shinji Nonose, Minami Kawashima, Hideo Isono ; *Yokohama City University*

A68 Reactions of Copper Cluster Oxide Anions with Nitric Oxide: Enhancement of Adsorption by Partial Oxidation

Shinichi Hirabayashi[1], Masahiko Ichihashi[2] ; [1] *East Tokyo Laboratory, Genesis Research Institute, Inc.,* [2] *Toyota Technological Institute*

A69 Vibrational Spectroscopy of Aluminum Oxide Cluster Anions: Structure and Reactivity

Xiaowei Song[1,2], Matias R. Fagiani[1,2], Florian A. Bischoff[3], Wieland Schöllkopf[1], Sandy Gewinner[1], Joachim Sauer[3], Knut R. Asmis[1,2] ; [1] *Fritz-Haber-Institut der Max-Planck-Gesellschaft,* [2] *Universität Leipzig,* [3] *Humboldt-Universität Berlin*

A70 Homogeneous deposition of size-selected clusters using Lissajous scanning method

Atsushi Beniya[1], Noritake Isomura[1], Hirohito Hirata[2], Yoshihide Watanabe[1] ; [1] *Toyota Central R&D Labs., Inc.,* [2] *Toyota Motor Corporation*

A71 **Time-of-flight mass spectrometry for reaction product detection in heterogeneous catalysis**
A. Winbauer, M. Tschurl, J. Kiermaier, U. Boesl, U. Heiz ; *Technische Universität München*

A72 **H and O adsorption on $Fe_{13}Pt_{42}$ core-shell nanoparticle**
Bheema Lingam Chittari[1], Vijay Kumar[1,2] ; [1]*Dr. Vijay Kumar Foundation(VKF),* [2]*Shiv Nadar University*

A73 **$Au_{38}(SR)_{24}$ cluster for oxidation catalysis**
Bei Zhang[1], Houhua Li[2], Miguel A.G. Hevia[3], Kaziz Sameh[4], Dawid Wodka[1], Clements Mazet[2], Thomas Bürgi[1], Noelia Barrabés[1] ; [1] *University of Geneva,* [2] *University of Geneva,* [3] *ICIQ,* [4] *Superior National School of Engineers of Tunis*

A74 **A new scalable Matrix Assembly Cluster Source (MACS) operating in reflection mode.**
William D Terry, Feng Yin, Jian Liu, Lu Cao, Richard E Palmer ; *University of Birmingham*

A75 **Theoretical study of the dehydrogenation of isopropanol on Ni_{13} cluster supported on Θ-Al_2O_3(010) surface**
Andrey Lyalin[1], Tetsuya Taketsugu[1,2] ; [1] *Kyoto University,* [2] *Hokkaido University*

A76 **Chemical Reactivity of Rhodium and Copper-doped Rhodium Neutral Clusters**
Masato Takenouchi, Ken Miyajima, Fumitaka Mafuné ; *The University of Tokyo*

A77 **Reduction of N_2 on Pd surfaces at low temperatures**
Junichi Murakami[1], Masayuki Futamata[1], Yukimichi Nakao[2], Shin Horiuchi[2], Kyoko Bando[2], Umpei Nagashima[2], Kazuki Yoshimura[2] ; [1]*Saitama University,* [2]*AIST,*

A78 **Automated prediction of pathways for single bond activations on small gold clusters: A case study of H_2 dissociation on neutral and charged Au_n^m (n = 1-12, m = 0, ±1)**
Min Gao[1], Andrey Lyalin[2], Satoshi Maeda[1,2], Tetsuya Taketsugu[1,2] ; [1] *Hokkaido University,* [2] *Kyoto University*

A79 **Preparation and catalytic application of supported silver clusters**
Masaru Urushizaki[1], Shinjiro Takano[1], Seiji Yamazoe[1,2], Kiichirou Koyasu[1,2], Tatsuya Tsukuda[1,2] ; [1] *The University of Tokyo,* [2] *Kyoto University*

A80 **A Highly Practical and Reusable Zinc Catalyst for Transesterification**
Daiki Nakatake, Yuki Yokote, Ryo Yazaki, Takashi Ohshima ; *Kyushu University*

A81 **Thermal stability and reactivity of manganese oxide clusters**
Kohei Koyama, Ken Miyajima, Fumitaka Mafuné ; *The University of Tokyo*

A82 **Studies on chemical reactions of transition metal clusters with oxygen by using FT-ICR mass spectrometer**
Yuta Tobari[1], Kazuki Ogasawara[2], Yoshinori Sato[2], Makoto Saito[2] , Shohei Chiashi[2], Shigeo Maruyama[2] , Toshiki Sugai[1] ; [1] *Toho University,* [2] *The University of Tokyo*

A83 **First-principle study of small nickel cluster structure and hydrogen dissociation on nickel dimer**
Pham Thi Nu, Ohno Kaoru : *Yokohama National University*

A84 **Clusters on La-Ni Mixed Oxides and its Catalytic Performance for Isomerization of Allylic Alcohols to Saturated Aldehydes**
Tamao Ishida[1,4], Jun Aimoto[1], Akiyuki Hamasaki[1], Hironori Ohashi[1], Tetsuo Honma[2], Takushi Yokoyama[1], Kohei Sakata[3], Mitsutaka Okumura[3], Makoto Tokunaga,[1] ; [1] *Kyushu University,* [2] *JASRI/SPring-8,* [3] *Osaka University,* [4] *Tokyo Metropolitan University*

A85 **withdraw**

A86 **Release of Oxygen from Copper Oxide Cluster Ions by Heat**
Ken Miyajima, Keisuke Morita, Fumitaka Mafuné ; *The University of Tokyo*

A87 **Regenerative synthesis of copper nanoparticles on TiO_2 nanoparticles by photoreduction**
Naoki Nishida, Takuya Aoki, Hideki Tanaka ; *Chuo University*

A88 **Stoichiometry of cationic and anionic vanadium oxide clusters analyzed by ion mobility-mass spectrometry**
Jenna W.J. Wu, Ryoichi Moriyama, Hiroshi Tahara, Keijiro Ohshimo, Fuminori Misaizu ; *Tohoku University*

First-Principles Study of Excited State Evolution in a Protected Gold Complex

Olga Lopez-Acevedo,[1] Ari Ojanperä,[1] and Martti Puska[1]

[1] *COMP Centre of Excellence, Department of Applied Physics, Aalto University, P.O. Box 11100, 00076 Aalto, Finland*

We have studied the photoexcitation dynamics of the protected gold complex Au2(SCH3)(PH3)2+1 [1]. In our calculations, we used a combination of the Delta Self-Consistent-Field method, Ehrenfest dynamics, and the time-dependent density functional theory. Our simulations provide insight into two types of mechanisms that can be tuned to enhance the photoluminescence of protected clusters in solution. Using Bader charge analysis we found that a charge transfer process between ligands appears upon excitation and that a charge transfer from the core toward the ligands takes place during the first tens of femtoseconds of the nonadibatic evolution. A later, hundreds of femtoseconds long reverse charge transfer process results in an asymmetric distribution of charge between the metal atoms. The charge redistribution and the oscillator strength of the excited-to-ground-state stimulated transition are coupled in both mechanisms. These results will help the understanding of emission properties of larger and more complex protected clusters.

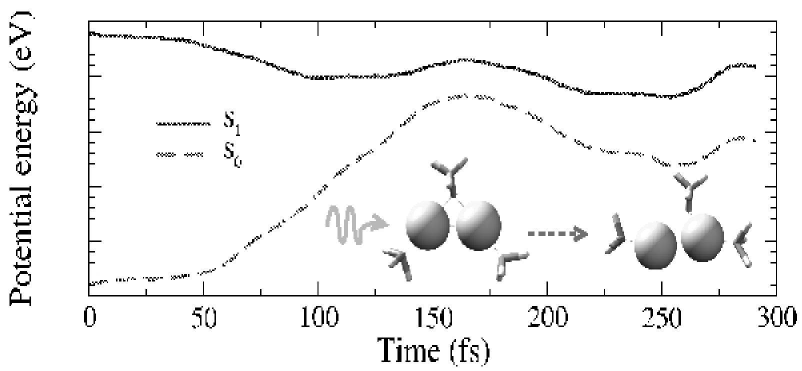

Reference

[1] A. Ojanperä, M. Puska and O. Lopez-Acevedo, J. Phys. Chem. C 117 (2013) page. 11837

Optical properties and structures of isolated gold-silver nanoalloys from molecular beam photodissociation spectroscopy

A. Shayeghi,[1] D. A. Götz,[1] R. L. Johnston,[2] and R. Schäfer[1]

[1] *Eduard-Zintl-Institut für Anorganische und Physikalische Chemie, Technische Universität Darmstadt, Alarich-Weiss-Str. 8, 64287 Darmstadt, Germany*
[2] *School of Chemistry, University of Birmingham, Edgbaston, Birmingham B15 2TT, United Kingdom*

Gold-silver nanoalloys have attracted much attention in the past, especially due to their very interesting optical properties [1]. Here, we present experimental and theoretical studies of optical absorption spectra of $Ag_NAu_M^+$ ($3 \leq N+M \leq 5$) clusters in the photon energy range $\hbar\omega = 1.9 - 4.4$ eV for the first time. The clusters are produced by pulsed laser vaporization and detected using time-of-flight mass spectrometry. The optical response is probed by photodissociation using a tunable ns-laser pulse from an optical parametric oscillator. Absorption spectra are recorded by monitoring the ion signal depletion upon photon absorption, providing a lower limit to absolute photodissociation cross sections. The spectra are compared to optical response calculations in the framework of long-range corrected time-dependent density functional theory, which has been shown to perform well for gold-silver tetramer clusters (N+M = 4) in previous studies [2, 3].
The cluster geometries used in excited state calculations are obtained by an extensive potential energy surface search employing the Birmingham Cluster Genetic Algorithm coupled with density functional theory [4, 5]. We also intend to perform geometry optimizations and subsequent excited state calculations based on coupled cluster theory. These combined theoretical and experimental studies pave the way for a deeper understanding of the gold-silver nanoalloy clusters electronic structure.

Reference(s)

[1] R. Ferrando, J. Jellinek, and R. L. Johnston, Chem. Rev. 108 (2008) 845.
[2] A. Shayeghi, R. L. Johnston, and R. Schäfer, Phys. Chem. Chem. Phys. 15 (2013) 19715.
[3] A. Shayeghi, C. J. Heard, R. L. Johnston, and R. Schäfer, J. Chem. Phys. 140 (2014) 054312.
[4] S. Heiles, A. J. Logsdail, R. Schäfer, and R. L. Johnston, Nanoscale 4 (2012) 1109.
[5] R. L. Johnston, Dalton Transactions, (2003) 4193.

Fluorescent oxidized Si nanoclusters and reversible interactions with solvent

Hanieh Yazdanfar,[1] Mike J. McNally,[1] Gediminas Galinis,[1] Mark Watkins,[1] and Klaus von Haeften[1]

[1] *Department of Physics and Astronomy, University of Leicester, UK*

Fluorescent silicon nanoclusters have been produced by a novel method developed in our group. The process involves the co-deposition of the silicon particles and a liquid jet. A sample of several millilitres, containing clusters 1nm in size, is produced in only few minutes [1, 2]. Aging experiment proves that these fluorescent particles have not agglomerated and remained stable in the solution after several years. Their fluorescence intensity has not changed in 3 years. X-ray photo emission spectroscopy and attenuated total reflection was used to analyse the chemical composition of the materials. The results revealed that all the silicon was oxidized. Hence, the infrared absorption bands were attributed to SiOH, SiH, and SiO_x compounds.

Samples can be produced in different solvents such as water, ethanol, and isopropanol. The wavelength of fluorescence bands depends on the dipole moments of the solvents, the larger the dipole moments, the more the shift to longer wavelengths. Distillation experiments show that the position of fluorescent peaks of the nanoclusters not only depends on chemical reactions between silicon particles and the liquid jet during growth, but also on the solvents that nanoclusters have been kept in. This is inferred from measurements performed after the sample completely dried out and dissolved in another solvent. The sequence was repeated several times using water and ethanol as solvents. Figure 1 shows spectra after four reversible distillation cycles. The results show that the peak position shifts with change of the solvent due to differences in the dipole moments. Lifetime Measurements show that the dipole moment of solvents also influences the life time of nanoclusters as the decay time is observed to vary from 3.7 to 5.6 ns.

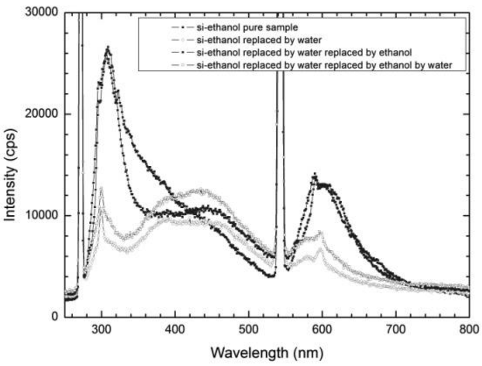

Figure 1. Fluorescence spectra of silicon nano clusters in ethanol and water. The solid symbols show fluorescence spectra for silicon clusters in ethanol, with the peak position at 320 nm. As the sample dried and dissolved into the water, the peak position shifted to 440 nm as is seen in the empty symbols.

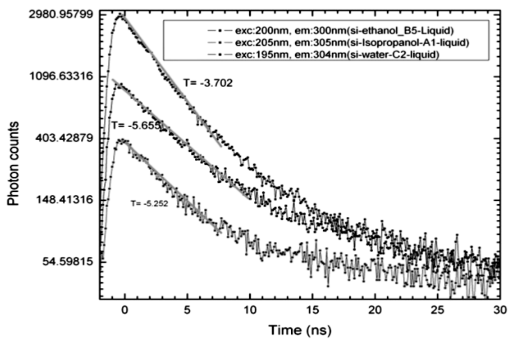

Figure2. Lifetime of silicon nanoparticles in water (top), ethanol (middle), and isopropanol (bottom).

References

[1] G. Torricelli, A. Akraiam, and K. von Haeften, Nanotechnology **22**, 315711 (2011).

[2] G. Galinis, H. Yazdanfar, M. Bayliss, M. Watkins, and K. von Haeften, J. Nanopart. Res. **14**, 1019 (2012).

Single-shot imaging of giant Xe clusters with X-ray free-electron laser

T. Nishiyama[1], C. Bostedt[2], K. R. Ferguson[2], C. Hutchison[1], K. Nagaya[1,3], H. Fukuzawa[3,4], K. Motomura[4], S. Wada[3,5], T. Sakai[1], K. Matsuami[1], T. Tachibana[4], Y. Ito[4], W. Q. Xu[4], S. Mondal[4], T. Umemoto[5], C. Nicolas[6], C. Miron[6], T. Kameshima[7], Y. Joti[7], K. Tono[7], T. Hatsui[3], M. Yabashi[3], K. Ueda[3,4], and M. Yao[1]

[1] *Department of Physics, Kyoto University, Kyoto, Japan*

[2] *SLAC National Accelerator Laboratory, United States of America*

[3] *RIKEN SPring-8 Center, Hyogo, Japan*

[4] *Institute of Multidisciplinary Research for Advanced Materials, Tohoku University, Sendai, Japan*

[5] *Department of Physical Science, Hiroshima University, Hiroshima, Japan*

[6] *Synchrotron SOLEIL, L'Orme des Merisiers, Saint-Aubin, Cedex, France*

[7] *Japan Synchrotron Radiation Research Institute (JASRI), Hyogo, Japan*

X-ray free-electron laser (X-FEL) delivers spatially coherent and extremely intense x-ray pulses, which enables us to study three-dimensional structural analysis of nanoscale single particles. In particular, combination of x-ray scattering and other techniques such as ion time-of-flight (TOF) spectroscopy is expected to provide information on physical properties in connection with structure. This method is especially useful for clusters, whose formation through aggregation can produce many structural isomers.

We report here the results of the small-angle x-ray scattering of sub-micron xenon (Xe) clusters. The experiment was carried out at the experimental hutch 3 of the beamline 3 of SACLA. The power density of X-FEL was around 10^{17} W/cm^2. The wavelength was 2.2 Å (5.5 keV) and the pulse width was 10 femtoseconds.

We observed a clear diffraction image from a single sub-micron Xe cluster even with a single X-FEL pulse. We also obtained fluorescence photons and ion TOF spectra from ionized clusters, and they had strong correlation with the diffraction images.

This study was supported by the X-ray Free Electron Laser Utilization Research Project and the X-ray Free Electron Laser Priority Strategy Program of the MEXT, by JSPS, by the Proposal Program of SACLA Experimental Instruments of RIKEN, and by the IMRAM project.

Ultrafast dynamics in single clusters captured with time-resolved x-ray imaging

D. Rupp,[1] M. Adolph,[1] L. Flückiger,[1] T, Gorkhover,[1,2] M. Krikunova,[1] J.-P. Müller,[1] M. Müller,[1] M. Sauppe,[1] D. Wolter,[1] S. Schorb,[1,2] S. Düsterer,[4] R. Treusch,[4] C. Bostedt,[2,3] and T. Möller[1]

[1] *IOAP, Technische Universität Berlin, Germany*
[2] *LCLS at SLAC National Accelerator Laboratory, Menlo Park, USA*
[3] *PULSE Institute, Stanford University and SLAC, Menlo Park, USA*
[4] *FLASH at DESY, Hamburg, Germany*

Extremely bright and ultrashort x-ray pulses from free-electron lasers have initiated new fields of research. One of the pioneering projects is capturing *molecular movies*, i.e. imaging of single molecules and ultrafast molecular processes with atomic resolution in time and space. The most challenging task is to record a scattering image from a single molecule or cluster before electronic changes and ionic motion within the molecule blur the scattering pattern. In order to approach this goal, we strive towards a profound understanding of ultrafast radiation damage.

Atomic clusters have been successfully used as ideal model systems to study laser-matter interaction. We have recently developed single cluster imaging and simultaneous ion spectroscopy as a novel method delivering unprecedented insight into the FEL-induced ionization and plasma dynamics [1, 2]. Knowing the size of the cluster and the FEL exposure power density from the scattering patterns allows for experiments with extremely well defined initial conditions.

In recent experiments at the FLASH-FEL single large xenon clusters were irradiated by intense soft x-ray pulses. The scattering images of the single clusters revealed the built-up of an inhomogeneous, shell structured, highly charged nanoplasma. The ion spectra of the same, size selected clusters indicate that after the interaction with the pulse, the outermost shells of the cluster blast off while the most part of the dense cluster plasma – though transiently highly charged – recombines to neutral atoms. In time-resolved experiments using an infrared pump-pulse, we could even capture unprecedented speckle-type patterns nanoseconds after photon exposure which we interpret as the signature of a neutral, slowly expanding gas ball.

In order to create an actual movie from non-reproducible, grown particles such as clusters, the initial structure has to be known. Therefore as a next step a novel setup, the “X-ray Movie Camera”, with a multilayer-based split-and-delay unit for x-ray double-pulses up to 500 ps delay is under construction. Using a novel detector design we will be able to capture two spatially separated images, one from the initial particle and one from the same cluster at a later stage of the photo-induced transformation.

[1] C. Bostedt *et al.* PRL **108**, 093401 (2012)
[2] T. Gorkhover *et al.* PRL **108**, 245005 (2012)

Momentum mapping of fragment ions generated upon Coulomb explosions of dichloroethylene isomers in intense laser fields

Yoriko Wada,[1] Hiroshi Akagi,[2] Ryuji Itakura,[2] Tomonari Wakabayashi,[1] and Takayuki Kumada[2]

[1] *Department of Chemistry, Kindai University, Higashi-Osaka, Japan*
[2] *Kansai Photon Science Institute, Japan Atomic Energy Agency, Kizugawa, Kyoto, Japan*

Coulomb explosions are common features observed in the experiments of photon-molecule interactions using femtosecond laser pulses of high peak intensity. Extensive research activities are found in literatures, concerning the understanding of fundamental processes of multi-photon absorption, ionization forming multiply charged ions, and fragmentation followed by Coulomb explosions. Despite the knowledge having been accumulated so far, it is rare to find an extension of the Coulomb explosion process to analytical purposes in the molecular structure research. We present our recent studies on the momentum mapping of fragment ions generated upon Coulomb explosions of three isomers of dichroloethylene to discuss distinguishability of these isomers using the mapping of kinetic characters of fragment ions in a momentum space.

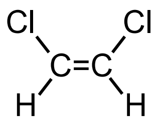
Z-1,2-dichroloethylene

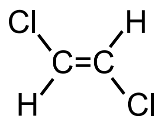
E-1,2-dichroloethylene

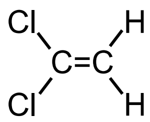
1,1-dichroloethylene

The three isomers, especially *E*-1,2-dichroloethylene, exhibited clearly different patterns in the correlation mapping of directions for the leaving cationic fragments, as already reported in the literature [1]. Moreover, we analyzed the velocity as well as the direction for the fragment ion in a momentum space to find that the momentum-mapping pattern is strongly influenced by the difference in the intensity of laser fields. This is an indication for the next step for an application of the Coulomb explosion to the molecular structure research for some molecular complexes [2-4].

References

[1] T. Yatsuhashi, N. Nakashima, and J. Azuma, J. Phys. Chem. A 117 (2013) 1393.
[2] Y. Wada, T. Wakabayashi, and T. Kato, J. Phys. Chem. B 115 (2011) 8439.
[3] Y. Wada, Y. Morisawa, and T. Wakabayashi, Chem. Phys. Lett. 541 (2012) 54.
[4] Y. Wada, K. Koma, Y. Ohnishi, Y. Sasaki, and T. Wakabayashi, Eur. Phys. J. D 66 (2012) 322.

Vibrational Spectroscopy of Monolayer Protected Gold Clusters: A Close Look at the Au-S Interface

Birte Varnholt,[1] Patric Oulevey,[1] Igor Dolamic,[1] and Thomas Bürgi[1]

[1] *Department of Physical Chemistry, University of Geneva, Geneva, Switzerland*

The nature of the thiolate - gold interface on flat surfaces as well as on nanoparticles is intensively studied recently, mainly triggered by recent structure determination of some thiolate-protected gold clusters, which challenges the standard model developed some time ago for self-assembled monolayers of thiols on gold.[1] Vibrational spectroscopy is one way to discriminate bond strengths and geometry sensitively. The low-wavenumber region, which contains the Au-S and Au-S-C vibrations, can be investigated with far-infrared and Raman spectroscopy. With these means we studied thiolate-protected gold clusters with surface structures known to be composed of monomeric (S-Au-S) and dimeric (S-Au-S-Au-S) binding units.[2,3]

DFT calculations on the well-known $Au_{38}L_{24}$ cluster allow discriminating the spectral contributions of such units. The assignment can be transferred to clusters with different surface composition. A systematic shift of the Au-S-C bending allows estimating the number of monomeric and dimeric units.

Recently, a number of thiolate-protected gold clusters were reported that do not obey the electronic shell closing magic numbers. It is assumed that the ligand structure plays a decisive role for the formation of stable clusters. We will elucidate the spectra of a series of $Au_{25}L_{18}$ clusters with varying aliphatic chain lengths and a number of sterically demanding ligands to obtain insight into ligand-gold and ligand-ligand interactions on the clusters.

The metal-sulfur vibrations are furthermore sensitive to the metal type and therefore allow to shed light on the position of the different metals of bimetallic alloy clusters. The catalytic activity of the latter depends on the availability of the active metal to the substrate (core vs. staples) and vibrational spectroscopy is therefore a valuable tool for their characterization.

References

[1] H. Häkkinen, Nat. Chem. 4 (2012) 443-455

[2] I. Dolamic, B. Varnholt, T. Bürgi, Phys. Chem. Chem. Phys. 15 (2013) 19561-19565

[3] B. Varnholt, P. Oulevey, S. Luber, C. Kumara, A. Dass, T. Bürgi J. Phys. Chem. C 118 (2014) 9604-9611

Vibrational spectroscopy of Au-nanocluster single crystals

Jaakko Koivisto,[1] Kirsi Salorinne,[1] Satu Mustalahti,[1] Tanja Lahtinen,[1]
Sami Malola,[2] Hannu Häkkinen,[1,2] and Mika Pettersson.[1]

[1]Department of Chemistry and [2]Department of Physics, University of Jyväskylä, FI-40014, Jyväskylä, Finland.

We have measured the IR-spectra of $[Au_{25}(PET)_{18}]^{-, 0, +}$ and $Au_{144}(PET)_{60}$ -nanoclusters (PET = phenylethylthiolate, SC_2H_4Ph) in single crystals and solvated in deuterated DCM. In solvated clusters the ligand vibrations are very weakly perturbed by the attachment to the gold cluster, but in the crystals the vibrations are significantly broadened and the peak-shape changes from Lorentzian to Gaussian, indicating inhomogeneous broadening mechanism. For $Au_{25}(PET)_{18}$ crystals structural characteristics found in the X-ray crystal structure, such as the trans/gauche -isometry, is observed in the aliphatic C-H-stretching region, while in the $Au_{144}(PET)_{60}$ crystals these peaks are quite featureless. For the negatively charged $[Au_{25}(PET)_{18}]^-$ -clusters the alkane-chains of the TOA^+ (tetraoctylammonium) -counter-cation show significant disorder in the crystal, which is also observed clearly in the IR-spectrum as strong broadening of the TOA^+ aliphatic C-H -stretching (2800-3000 cm^{-1}) and CH_2-bending (1450 cm^{-1}) modes. Similar broadening seen in the IR-spectrum of crystalline $Au_{144}(PET)_{60}$ indicates that the ligands are found in numerous different conformations in the crystal. The observed disorder of the ligand-layer in the $Au_{144}(PET)_{60}$-crystals indicates that while the cluster cores form a periodic structure in the crystals, the ligand layer between the cores does not. This may explain the difficulties in obtaining single crystal X-ray -structure of the $Au_{144}(PET)_{60}$-cluster. The overtone and combination vibration intensities compared to fundamentals are dramatically increased in the crystals, indicating substantial coupling of the vibrational modes. The intensities of the overtone bands are stronger in Au_{25}-crystals than in Au_{144}, indicating that the effect is caused by the crystal packing rather than the electronic, e.g. surface enhanced IR-absorption, properties of the Au-core.

[1] Koivisto; Salorinne; Mustalahti; Lahtinen; Malola; Häkkinen; Pettersson, *J.Phys.Chem.Lett.*, 2014, 5, p. 387-392.
[2] Zhu; Aikens; Hollander; Schatz; Jin, *J.Am.Chem.Soc.*, 2008, 130, p. 5883-5885.
[3] Heaven; Dass; White; Holt; Murray, *J.Am.Chem.Soc.*, 2008, 130, p. 3754-3755.

Two-color IR-UV spectroscopy of Nb_nC_m clusters

Valeriy Chernyy,[1] Joost Bakker,[2] and Andrei Kirilyuk[1]

[1] *Radboud University Nijmegen, IMM, 6525 AJ Nijmegen, The Netherlands*
[2] *Radboud University Nijmegen, FELIX facility, 6525 ED Nijmegen, The Netherlands*

Infra-red (IR) vibration spectroscopy is a powerful and reliable method for probing vibrational modes, that provide a fingerprint of the cluster geometry [1]. There are several approaches to the measurements of the vibrational spectra, such as IR Resonance Enhanced Multiphoton Ionisation (IR-REMPI) [2], IR Multi Photon Dissociation Spectroscopy [3], or two-color IR-UV ionization spectroscopy [4]. The last technique is interesting not only because of universality, but also as a method with an extra degree of freedom for the electronic states. Here we use IR-UV ionization spectroscopy to study the excitation of vibrational modes and the resulting effect on the ionization process in gas-phase Nb_nC_m clusters. The advantage of this system is that IR-REMPI was shown to work on some of the vibrational lines [5], which provides an excellent starting point.
The experimental approach we used is the following: a cluster is excited by an infrared light pulse (pump), produced by the Free Electron Laser for Infrared eXperiments (FELIX), transferring the cluster from the ground to a vibrationally excited state. After that the excited system can be ionised with the UV pulse with the photon energy that is not sufficient for a single-photon ionisation of the non-excited cluster. In order to record vibrational spectra the experiments were done with fixed UV wavelength as a function of the IR frequency. The ionization efficiency for the two-color IR+UV process was normalized to the efficiency of the UV only process on a shot-to-shot basis.
The observed response types can be divided into three groups: (i) there is a high signal from direct IR-REMPI mechanism, but no increase observed with the additional UV radiation, probably because of the extremely high efficiency of IR-REMPI in these clusters; (ii) the clusters also demonstrate some features on IR-REMPI type of spectra, but these features become stronger and better defined in IR-UV experiment; (iii) the most interesting is where there is no signal from IR-REMPI but there are features in IR-UV type of spectra. The difference indicates the effective temperature of the clusters. A complete set of vibrational spectra is thus obtained for Nb_nC_m clusters; the identification of the geometric conformations with the help of DFT is in progress.

Reference(s)
[1] C. Ratsch et al., J. Chem. Phys. 122, **124302** (2005).
[2] G. von Helden et al., Phys. Rev. Lett. 79, **5234** (1997).
[3] W.J.C. Menezes and M.B. Knickelbein, J. Chem. Phys. 98, **1856** (1993).
[4] A. Fielicke et al., J. Chem. Phys. 131, **171105** (2012).
[5] D. van Heijnsbergen et al., Phys. Rev. Let. 89**, 013401 (**2002**).**

Comparative study of ultrafast relaxation dynamics of $Au_{144}(C_2H_4Ph)_{60}$ and $Au_{102}(pMBA)_{44}$ nanoclusters by using mid-IR transient absorption spectroscopy

Satu Mustalahti[1], Pasi Myllyperkiö[1], Tanja Lahtinen[1], Sami Malola[2], Kirsi Salorinne[1], Jaakko Koivisto[1], Hannu Häkkinen[1,2] and Mika Pettersson[1]

[1] *Department of Chemistry, Nanoscience Center, P.O. Box 35, FI-40014 University of Jyväskylä, Finland*

[2] *Department of Physics, Nanoscience Center, P.O. Box 35, FI-40014 University of Jyväskylä, Finland*

Ultrafast electronic relaxation and vibrational cooling dynamics of $Au_{144}(C_2H_4Ph)_{60}$ and $Au_{102}(p\mathrm{MBA})_{44}$ (*p*MBA = *para*-mercaptobenzoic acid) nanoclusters were studied by using femtosecond transient mid-IR spectroscopy. In this study visible or NIR pump pulses were used to electronically excite the sample and a mid-IR pulse was used to probe the system dynamics by monitoring transient absorption of vibrational modes of the ligands. Solutions of highly monodisperse samples were used for both clusters.

For $Au_{144}(C_2H_4Ph)_{60}$ visible pump pulse prepares an electronic state localized in the gold core. The subsequent electronic relaxation via electron-phonon coupling was found to occur with time constant of 1.5 ps followed by vibrational relaxation and heat dissipation into the solvent with 29 ps time constant. The excitation energy dependence of electronic relaxation time constant, which is typical for metallic clusters, was also observed for Au_{144} species thus conforming previous results [1]. For $Au_{102}(p\mathrm{MBA})_{44}$ cluster a drastically different type of relaxation dynamics similar to that of molecular systems is observed. Also formation of a long lived excited species (> 1 ns lifetime) is observed, which indicates the existence of several pathways for electronic relaxation in Au_{102} species.

The obtained results establish an important correlation between exact cluster composition, and energy relaxation and dissipation dynamics for studied systems. The results also clearly indicate that molecular to metallic behavior transition occurs somewhere between these two cluster sizes as has previously been suggested by studies of the onset for electronic absorbance for $Au_{102}(p\mathrm{MBA})_{44}$ and $Au_{144}(C_2H_4Ph)_{60}$ [2, 3].

References

[1] C. Yi, M. A. Tofanelli, C. J. Ackerson, and K. L. Knappenberger, Jr., J. Am. Chem. Soc. 135 (2013) 18222

[2] E. Hulkko, O. Lopez-Acevedo, J. Koivisto, Y. Levi-Kalisman, R. D. Kornberg, M. Pettersson, and H. Häkkinen J. Am. Chem. Soc. 133 (2011) 3752.

[3] J. Koivisto, S. Malola, C. Kumara, A. Dass, H. Häkkinen, and M. Pettersson J. Phys. Rev. Lett. 3 (2012) 3076.

Characterization of counter ions in solutions using thiol molecules adsorbed on silver nanoparticles

Saori Handa, Yingying Yu, Masayuki Futamata

Graduate School of Science and Engineering, Saitama University, Saitama, Japan

To exploit a gap mode plasmon in surface enhanced Raman scattering (SERS) most efficiently, we formed flocculates of Ag nanoparticles (AgNPs)[1,2] using electrostatic interaction between dissociated p-mercaptobenzoic acid (PMBA), protonated p-aminothiophenol (PATP) and their counter ions, as well as van der Waals force between neutral PMBA, PATP and AgNPs. Adsorbed state of PMBA and PATP in addition to trapped counter ions was elucidated using enormous SERS enhancement in a flocculation method. Indeed, we found that AgNPs coated with PATP-SAM feasibly formed flocculates under uncontrolled pH conditions. Because pH in PATP aqueous solutions (10^{-4} M) is close to neutral, ~8.4, larger than pK_a of 6.1 for the ammonium group ($-NH_3^+$) in PATP, neutral species containing $-NH_2$ are predominant. Accordingly, van der Waals attractive potential much larger than thermal energy between AgNPs adsorbed by neutral PATP-SAM film works for flocculation. In contrast, AgNPs coated with PATP-SAM were isolated at pH=3-4, much lower than pK_a for $-NH_3^+$ in PATP, owing to electrostatic repulsion between AgNPs with protonated amino groups. This was supported by flocculation of AgNPs after the addition of Na_2SO_4 (5 mM) or $HClO_4$ (5 mM), whereas isolated AgNPs were sustained at slightly higher pH with restricted ionic strength such as pH=4-5 in ~10^{-4} M $HClO_4$ solutions. These distinct features depending on ionic strength are explained by DLVO theory for colloidal particles. In contrast, flocculates of AgNP-PATP$^+$…X^{n-}…$^+$PTAP-AgNP (here X^{n-} =SO_4^{2-} or ClO_4^-) provided pronounced SERS spectra of trapped anions such as symmetric stretching mode $\nu_{1S}(SO_4^{2-})$ peak at 975 cm^{-1} and $\nu_{1S}(ClO_4^-)$ peak at 931 cm^{-1} at pH<3 with sufficiently high ionic strength, in addition to those from PATP at 1594, 1490, 1180, 1075, 801, 630, and 389 cm^{-1}. Thus, target anions in solution were successfully trapped and characterized using electrostatic interaction with ammonium cations of PATP-SAM on AgNPs. SERS spectra observed for protonated PATP$^+$ are essentially the same as observed for PATP in literature[3,4]. Electrostatic interaction between PATP$^+$ ($-NH_3^+$) and SO_4^{2-} and ClO_4^- ions was also supported by Raman spectral changes for protonated and neutral PATP molecules. Interestingly, SERS spectrum of neutral PATP observed in flocculates of AgNPs is different from that in literature[3,4], which consists of Raman bands observed here in acidic conditions at 1597, 1490, 1174, 1074, 972, 802, 628, and 390 cm^{-1} attributed to PATP$^+$ ($-NH_3^+$), and those of so-called 'dimer bands' at 1420, 1378 and 1139 cm^{-1} in neutral pH. These SERS spectra in literature are observed for PATP molecule on Ag or Au nanostructures adsorbed from ethanol solutions[3,4]. Our SERS spectra from neutral PATP, adsorbed in acidic conditions followed by the addition of NaOH solution to be pH~8, did not change with duration of laser irradiation at >10μW/μm^2, indicating photochemical dimerization of PATP was suppressed. Probably, this is benefited by immediate flocculation of AgNPs with neutral PATP, of which re-orientation is restricted to cause photochemical reactions at a nanogap. Also huge SERS enhancement (G) of 10^9-10^{10} observed at a nanogap in flocculates of AgNPs assures negligible contribution from plausible dimers at marginal sites, outside the nanogap, with G$\leq 10^4$ on AgNPs, where PATP-SAM may cause photochemical reactions with PATP molecules in solutions. Experimental results using PMBA-SAM films on AgNPs will also be presented at the conference.

References: [1] M. Futamata et al., *J. Phys. Chem. C* **114**, 7502, 2010. [2] Y. Yu et al., *Chem. Phys. Lett.* **560**, 49, 2013. [3] Y. Huang et al., *J. Am. Chem. Soc.* **132**, 9244, 2010. [4] X. Tian et al., *RSC Adv.* **2**, 8289, 2012.

Highly-sensitive gap mode Raman spectroscopy on various substrates

Maho Ishikura, Hiroki Suzuki, Masayuki Futamata*

Graduate School of Science and Engineering, Saitama University, Saitama, Japan

To elucidate extremely small amount of adsorbates, a gap mode in surface enhanced Raman scattering (SERS)[1-3] was applied to various substrates including metals and dielectric materials. We obtained sufficiently large 10^6-10^7 enhancement factor for Raman scattering signals from thiophenol (TP) adsorbed on various substrates such as Au, Pb, Sn, V, Cu, Ni, Zn, Al, Pt, stainless steel, and even on Si by immobilization of gold nanoparticles (AuNPs with a radius of ~15 nm). Furthermore, we found that these enhancement factors are not affected by optical properties of substrates but inherently determined by dielectric properties and sizes of AuNPs. Finite difference time domain (FDTD) calculations anticipate enormous enhancement in electric field at a nanogap between metal nanoparticles and metal substrates at appropriate excitation wavelengths. Indeed, 10^8-10^{10} of Raman enhancement is experimentally obtained for various thiol monolayers on silver substrates after the immobilization of silver nanoparticles (AgNPs)[4,5]. Here, AuNPs were utilized to investigate more details on a gap mode Raman spectroscopy to establish this as an analytical tool. FDTD calculations yielded that: (1) the resonance wavelength for a gap mode is primarily determined by AuNP, i.e. its optical constants and size, which is ~560 nm for a spherical AuNP with a radius (r_{AuNP}) of 15 nm on various metal substrates used here. (2) Not only metal substrates but also dielectrics with large optical constants (ε_{sub}) compared to that of surrounding media (ε_{med}), such as Si with an optical constants larger than 10 (ε_{sub}) at 632 nm in air (ε_{med}=1), provides pronounced enhancement (10^6-10^7) in SERS. This prediction is simply explained by the following equation: $\boldsymbol{p_{sub}}' = \boldsymbol{p} \times (\varepsilon_{sub} - \varepsilon_{med}) / (\varepsilon_{sub} + \varepsilon_{med})$, where mirror image dipole in substrate ($\boldsymbol{p_{sub}}'$) is induced by an electrical dipole in AuNP ($\boldsymbol{p}$). (3) Larger AuNP provides larger enhancement in electric field at a nanogap, for instance enhancement in the electric field from 5.6×10^3 (at r_{AuNP}=15 nm) to 4×10^4 - 9×10^4 (at r_{AuNP}=50 nm) on various metal substrates, yielding 10^9-10^{10} of SERS enhancement. Larger AuNP broadens the width of resonance wavelength, for instance from 80 nm (r_{AuNP}=15 nm) to 190 nm (r_{AuNP}=50 nm), due to increased contribution of multipoles. This observation facilitates wider application of a gap mode in SERS, in which various laser wavelengths are available. Next, we experimentally investigated a gap mode between AuNPs and various substrates, such as Au, Pb, Sn, V, Cu, Ni, Zn, Al, Pt, stainless steel, and Si (ε>10) and BK-7 (ε~2.1) cover slip, to ensure anticipated enhancement in SERS. We found that: (1) immobilization of AuNPs (r_{AuNP}=15 nm) provided pronounced enhancement factors of 10^6-10^7 for TP at a nanogap. (2) Even silicon wafer substrates provided enhancement of ~10^6 in SERS by the immobilization of AuNPs. (3) Larger enhancement in Raman scattering signal was confirmed for larger AuNPs, for instance larger enhancement by a factor of ~10 was observed for Zn and Si substrates for AuNPs with a radius (r) of 50 nm compared to that with r=15 nm. Detailed analysis on the size effect using much larger AuNPs will also be presented. Thus, we confirmed that a gap mode is relevant not only for various metals with large damping, but also for dielectric materials with large optical constants, and larger enhancement factor for larger AuNPs. These observations probably facilitate wider application of highly-sensitive gap mode Raman spectroscopy.

References: [1] P. K. Aravind et al., Surf. Sci. **124**, 506, 1984. [2] K. Ikeda et al., J. Phys. Chem. **116**, 20806, 2012. [3] K. Kim et al., J. Phys. Chem. C **115**, 21047, 2012. [4] H. Suzuki et al., Vibrational Spectrosc. **72**, 105, 2014. [5] H. Chiba et al., Vibrational Spectrosc. **73**, 19, 2014.

In-situ produced BiO_x nanoparticles: Studied in a beam and as deposited by photoelectron spectroscopy

Mikko-Heikki Mikkelä,[1] Maxim Tchaplyguine,[1] Chaofan Zhang[2], Tomas Andersson[2], Erik Mårsell[3] and Olle Björneholm[2]

[1] *MAX IV Laboratory, Lund University, Lund, Sweden*
[2] *Department of Physics and Astronomy, Uppsala University, Uppsala, Sweden*
[3] *Department of Physics, Lund University, Lund, Sweden*

Study of bismuth oxide (BiO_x) nanoparticles has attracted interest due to their relevance for catalytic and medical applications [1,2]. In the present work we have investigated BiO_x nanoparticles in a particle beam – unsupported – and as deposited on Si(111) substrate, using X-ray photoelectron spectroscopy (XPS). The experiments were carried out in MAX IV laboratory, Sweden, at the soft X-ray beamline I411 (hv = 40 – 1500 eV). Studied nanoparticles were formed using reactive sputtering based gas-aggregation source [3] and XPS investigation of unsupported particles in a beam and deposition was carried out in-situ in the same experimental chamber and thus effects of deposition and changes in the properties of unsupported nanoparticles could be investigated.

XPS results suggest that depending on the settings of the reactive sputtering, metallic Bi, combined Bi-BiO_x or pure BiO_x nanoparticles are produced and that relative Bi-BiO_x ratio remains somewhat unchanged upon the deposition. In the previous studies of PbO_x nanoparticles using the same experimental setup [4], a heterogeneous oxide-core and metallic-shell structure was suggested and similar dual component composition is also expected for Bi-BiO_x particles of this work. XPS of deposited particles has been also used to investigate how the oxidation state of the deposited particles might change relative to the unsupported species. In addition to XPS we have also utilized scanning electron microscopy (SEM) to investigate the nanostructures formed by the deposited particles and to obtain information about the particle size.

Reference(s)

[1] L. Zhang, W. Wang, J. Yang, Z. Chen, W. Zhang, L. Zhou, S. Liu, Appl. Catal. A 308 (2006) 105.
[2] K. Bogusz, M. Tehei, C. Stewart, M. McDonald, D. Cardillo, M. Lerch, S. Corde, A. Rosenfeld, H.K. Liua, and K. Konstantinov, RSC Adv. 4 (2014) 24412.
[3] M. Tchaplyguine, S. Peredkov, H. Svensson, J. Schulz, G. Öhrwall, M. Lundwall, T. Rander, A. Lindblad, H. Bergersen, S. Svensson, M. Gisselbrecht, S. Sorensen, L. Gridneva, N. Mårtensson, and O. Björneholm, Rev. Sci. Instrum 77 (2006) 033106.
[4] C. Zhang, T. Andersson, S. Svensson, O. Björneholm, and M. Tchaplyguine, Phys. Rev. B 87 (2013) 035402.

Photofragment-ion imaging from mass-selected cluster ions using a linear-type tandem reflectron

Kenichi Okutsu, Kenichiro Yamazaki, Keijiro Ohshimo, and Fuminori Misaizu

Department of Chemistry, Graduate School of Science, Tohoku University, 6-3 Aoba, Aramaki, Aoba-ku, Sendai 980-8578, Japan

We have been studying photodissociation dynamics of mass-selected cluster ions by using a reflectron time-of-flight mass spectrometer combined with an ion-imaging detector. In the present study, we have developed an apparatus of a linear-type tandem reflectron, in place of an angular-type reflectron which was used in our previous study [1]. Using this apparatus we are ultimately aiming to obtain highly-resolved photofragment-ion images which satisfy velocity map imaging conditions. After construction of the apparatus, the performance has been checked by the ultraviolet photodissociation experiment of an Mg^+-Ar complex ion.

Fig. 1 shows a schematic diagram of the apparatus. Magnesium-argon binary cluster ions including Mg^+-Ar were produced by laser vaporization, and they were mass-selected by the time-of-flight mass spectrometer. The Mg^+-Ar ion was then reflected with the "1st reflectron". Because no pulsed voltage was applied on the "2nd reflectron" at this moment, the ions pass through these electrodes without changing their velocities. After the first reflection, the ions were irradiated with linearly polarized dissociation laser (fourth harmonic of a Nd:YAG laser, 266 nm) at the middle of the two reflectrons. Photofragment Mg^+ ions were then reflected with the 2nd reflectron, and detected as ion images by micro channel plate with phosphor screen. Finally the optical image signals were accumulated using a CCD camera.

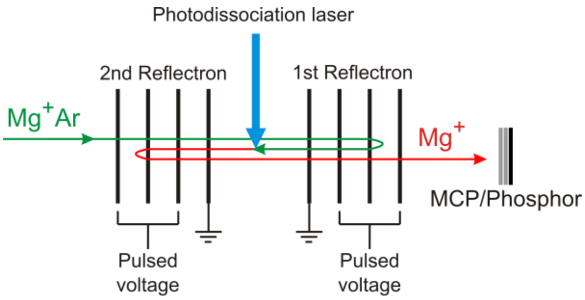

Fig. 1 Schematic diagram of the apparatus

Electronic transition applied in this experiment has a localized nature of $3p_z \leftarrow 3s$ excitation on Mg^+, and thus the transition dipole moment is parallel to the Mg-Ar bond axis [2]. The Mg^+ fragment image was observed as shown in Fig. 2, by changing the polarization direction of the dissociation laser (***E***) with respect to the ion beam direction (***Z***). The split ion image of Mg^+ parallel to ***E*** was observed at ***E***⊥***Z*** condition, as expected.

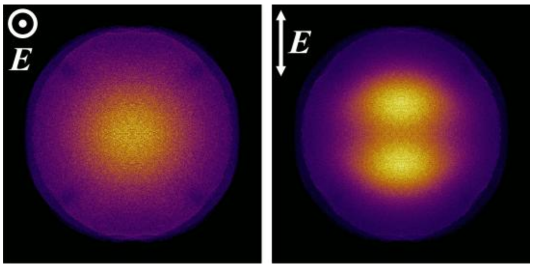

Fig. 2 Observed images of fragment ion Mg^+ for ***E*** // ***Z*** (left), ***E***⊥***Z*** (right)

References

[1] H. Hoshino, Y.Yamakita, Y.Suzuki, M.Saito, K.Koyasu, and F. Misaizu, 16th ISSPIC, B25 (2012).

[2] J. S. Pilgrim, C. S. Yeh, K. R. Berry, and M. A. Duncan, J. Chem. Phys. 100 (1994) 7945.

Time Resolved Study of EUV-FEL Triggered Nano-Plasma of Rare-Gas Clusters

K. Nagaya[1,2], T. Sakai[1], T. Nishiyama[1], K. Matsunami[1], S. Yase[1], M. Yao[1], H. Fukuzawa[2,3], K. Motomura[3], T. Tachibana[3], S. Mondal[3], K. Ueda[2,3], S. Wada[2,4], H. Hayashita[4], N. Saito[2,5], T. Togashi[2,6], M. Nagasono[2], M. Yabashi[2]

[1] Department of Physics, Kyoto University, Kyoto 606-8502, Japan
[2] RIKEN SPring-8 Center, Kouto 1-1-1, Sayo, Hyogo 679-5148, Japan
[3] Institute of Multidisciplinary Research for Advanced Materials, Tohoku University, Sendai 980-8577, Japan
[4] Department of Physical Science, Hiroshima University, Higashi-Hiroshima 739-8256, Japan
[5] National Metrology Institute of Japan, AIST, Tsukuba 305-8568, Japan
[6] Japan Synchrotron Radiation Research Institute, Hyogo 679-5198, Japan

The free electron laser (FEL) light sources based on self-amplified spontaneous-emission (SASE) are opening new research fields of the interaction of matters with intense laser pulses in the short wavelength region. Pioneering works for rare-gas clusters [1-3] revealed the importance of nano-plasma formation for the FEL-matter interaction process. Here we discuss nano-plasma dynamics using pump-probe scheme, which was proposed by the molecular dynamics simulations study for small rare-gas clusters [4]. We carried out EUV-FEL pump – near infra-red (NIR) laser probe experiments at the SPring-8 compact SASE source (SCSS) test facility [5].

We have carried out time-of-flight (TOF) measurements of fragment ions from xenon clusters (N~5,000) and neon clusters (N~5,000) as a function of delay time (Δt) between the EUV-FEL pulse (λ =51nm for xenon clusters and 61nm for neon clusters) and the NIR laser pulse (λ =800nm). We confirmed the emission of energetic highly charged xenon ions up to around Xe^{15+} for xenon clusters from the analysis of TOF spectra, suggesting the enhanced heating of nano-plasma due to surface plasma resonance. The signature of surface plasma resonance gives an evidence for the nano-plasma formation from rare-gas clusters by intense EUV-FEL irradiation. We found similar enhancement of highly charged ions for neon cluster, though the delay time dependence is different between xenon cluster and neon cluster, suggesting the difference of the nature of nano-plasma produced by EUV-FEL irradiation.

We are grateful to SCSS Test Accelerator Operation Group at RIKEN for continuous support in the course of the studies. This study was supported by the X-ray Free Electron Laser Utilization Research Project and the X-ray Free Electron Laser Priority Strategy Program of Ministry of Education, Culture, Sports, Science, and Technology of Japan (MEXT), by Grants-in-Aid (No. 23241033 and No. 23600006) from the Japan Society for the Promotion of Science (JSPS).

Reference(s)

[1] C. Bostedt et al., New J. Phys. 12 (2010) 083004.
[2] B. Ziaja, H.Wabnitz, F.Wang, and E.Weckert, T. Moeller, Phys.Rev. Lett. 102, 205002 (2009).
[3] M. Arbeiter and Th. Fennel, Phys. Rev. A 82, 013201 (2010).
[4] C. Siedschlag and J. M. Lost, Phys. Rev. A 71, 031401(R) (2005).
[5] H. Shintake et al., Nature Photon. 2, 555 (2008).

X-ray absorption spectroscopy of size-selected cerium oxide clusters

Tetsuichiro Hayakawa,[1] Masashi Arakawa,[2] Shun Sarugaku,[2] Kota Ando,[2] Kenichiro Tobita,[2] Tomonori Ito,[2] Kazuhiro Egashira,[1] and Akira Terasaki[2,3]

[1] *East Tokyo Laboratory, Genesis Research Institute, Inc., Chiba, Japan*
[2] *Department of Chemistry, Kyushu University, Fukuoka, Japan*
[3] *Cluster Research Laboratory, Toyota Technological Institute, Chiba, Japan*

Bulk ceria (Ce_mO_n) exhibits oxygen storage/release behavior and is applied to catalysts or catalyst supports. It is known that the charge state of Ce atoms and the oxygen storage behavior of ceria are closely related to each other. We are investigating cerium oxide clusters as model systems of active sites of ceria catalysts by using X-ray absorption spectroscopy (XAS). XAS is a powerful tool to investigate electronic (and geometric) properties of multi-element systems because of its element specificity. In this study, local charge states of Ce and O atoms in size-selected free cerium oxide clusters are probed via spectral shifts in X-ray absorption.

Cerium oxide cluster ions are produced by a magnetron sputtering cluster ion source, transported by ion-guides and ion-deflectors, size-selected by a quadrupole mass filter, and admitted into a linear quadrupole RF ion-trap. The linear ion trap accumulates size-selected cluster ions, which are otherwise extremely dilute. The ions thus stored are irradiated with a soft X-ray beam from a synchrotron (BL-7A in Photon Factory, KEK, Japan), and are fragmented upon X-ray absorption. An X-ray absorption spectrum is measured through the fragment-ion yield as a function of the photon energy.

X-ray absorption of small cerium oxide clusters ($Ce_mO_n^+$; m=2, 3) was measured in the energy range of Ce M-edge (ca. 880 eV) and O K-edge (ca. 530 eV). CeO^+, Ce^+ and Ce^{2+} were produced as dominant fragment ions, while background ion signal was negligibly weak. X-ray absorption spectra in Ce M-edge region consisted of two prominent peaks corresponding to Ce M_5- and M_4-“white lines”. The Ce M-edge spectra of $Ce_2O_3^+$ and $Ce_2O_5^+$ show higher peak energies and smaller M_5/M_4 intensity ratio for $Ce_2O_5^+$ than for $Ce_2O_3^+$. These features indicate that Ce atoms in $Ce_2O_5^+$ are more positively charged than in $Ce_2O_3^+$, which is consistent with the higher oxygen content in the former. Systematic blue-shifts in the spectra were clearly observed also for $Ce_3O_n^+$ with increase in n. In the presentation, charge states of Ce and O atoms will be discussed in the context of geometric structures of the clusters.

Photodepletion spectroscopy of silver cluster cations in a temperature-controlled ion trap

Tomonori Ito, Kenichiro Tobita, Masashi Arakawa, and Akira Terasaki

Department of Chemistry, Kyushu University, Fukuoka, Japan

Optical properties of metal vary dramatically with its size, e.g. metal nanoparticles exhibit broad spectra caused by collective excitation of electrons, whereas atoms show spectral lines resulting from transitions between atomic orbitals. Metal clusters provide an opportunity to investigate emergence of a collective behavior of electrons in the intermediate size range. Electronic structures should be reflected in a spectral profile of absorption, which depends on the cluster size and temperature. In this work, we report photodissociation action spectra of silver cluster cations with a focus on size and temperature dependence for a systematic study of electronic transitions in metal clusters.

Silver cluster cations, Ag_n^+ (n = 8–14), were produced with a magnetron sputtering ion source and mass-selected by a quadrupole mass filter. They were stored in a linear radio-frequency ion trap and irradiated with an UV laser tunable between 285 and 335 nm. Dissociation yields were evaluated as decrease in the parent ions by laser irradiation, i.e., the "photodepletion" method was employed.

Figure 1 shows photodissociation action spectra of Ag_9^+ measured at 300 and at ~110 K. The spectrum at 300 K shows four broad peaks with full widths at half maximum (FWHM) of about ~0.1 eV. When the ion trap and the buffer gas were cooled down to ~110 K, the peaks became narrower and some of them were blue-shifted. The observed spectral profiles show that the optical absorption originates not from collective electronic excitation but rather from single-electron transitions between molecular orbitals, as evaluated by widths and integrated intensities of absorption. The spectral sharpening at a lower temperature is attributable to lowering the vibrational quantum number in the initial ground electronic state, which reduces hot-band contributions. Temperature-dependent spectra with similar integrated absorption intensities were observed as well for Ag_n^+ (n = 8–14). These results imply that molecular nature of electronic structures is retained at least up to n = 14.

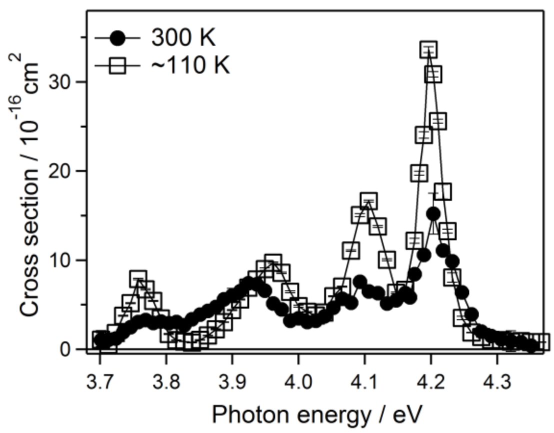

Figure 1. Photodepletion spectra of Ag_9^+ measured at room temperature (closed circles) and ~110 K (open squares).

Geometry, Electronic, and Magnetic properties as well as selective O_2 and CO adsorption on Au_nRh_m clusters

Marcela .R. Beltrán[1], Fernando. Buendía[1]

[1]*Universidad Nacional Autónoma de México, Instituto de Investigaciones en Materiales, Apdo. Postal 70-360, C.P. 04510, Del. Coyoacán, México D.F. México*

The chemical reactivity of gas-phase transition metal clusters toward various molecules has been the subject of numerous investigations, motivated by the intrinsic interest in clusters as novel nanoscale catalysts, as well as by the lessons that may be learnt from such studies pertaining to catalysis by supported metal clusters and the adsorption and reactivity mechanisms of extended metal surfaces. Recently there has been a growing interest in the chemical properties of gold nano clusters and their potential use as nanocatalysts. In early experiments a definite pattern of oxygen adsorption to negatively charged small gold clusters has been detected, where only anionic clusters with an even number of atoms (odd number of valence electrons) showed significant O2 uptake[1], whereas odd-numbered clusters either did not exhibit any propensity for reaction with oxygen[1] or showed very weak reactivity. Also gold cluster anions that show a propensity for oxygen adsorption can also coadsorb carbon monoxide, thus suggesting them as possible model catalysts for the CO oxidation reaction[2,3]. Base on those studies A systematic study of the stability of gold rhodium clusters, their electronic and magnetic properties as well as their behavior under oxygen rich and CO rich simulated atmospheres is presented. This study has been done using density functional theory calculations. Their Infra red spectra, their binding energies, as well as their vertical and adiabatic detachment energies are presented and discussed. On the other hand their dissociation energies for different evaporation channels have also been calculated. The influence of adsorbant atom(s) on the surface structure and the stability of the clusters is also discussed.

References

[1] Bokwon Yoon, Hannu Hakkinen, and Uzi Landman, J. Phys. Chem. A, 4066, 107 2003

[2] Ajay M. Joshi, W. Nicholas Delgas and Kendall T. Thomson, J. Phys. Chem. B. 23373, 110, 2006

[3] Mitsutaka Okumura, Yasutaka Kitagawa, Masatake Haruta, Kizashi Yamaguchi, Applied Catalisis A: General, 37, 291, 2005

AB INITIO STUDY OF CATIONIC, ANIONIC AND NEUTRAL Au_nRh_m CLUSTERS

Fernando Buendía[1] and Marcela R. Beltrán[1]

[1]*Universidad Nacional Autónoma de México, Instituto de Investigaciones en Materiales, C.P. 04510, México D.F. México*

The determination of the geometric structure of transition metal clusters is a vital step towards understanding cluster properties. Therefore any effort in this direction is essential for the future possible applications and to the development of new technologies. Bimetallic clusters have drawn considerable attention in recent years due to its capacity to enhance their electronic and catalytic properties. In particular, transition metal doped gold clusters have been extensively investigated both, experimentally as well as theoretically [1,2]. These systems are interesting as doping with transition metal atoms strongly changes the properties of the host cluster. The geometric structures, relative stabilities, magnetic moments, and vibrational spectra of small cationic, anionic and neutral Au_nRh_m clusters have been systematically studied through density functional theory (DFT) [3]. Our results show that the transition metal doping of gold clusters play a special roll in their stabilities and their chemical activity.

References

[1] W. Bouwen, F. Vanhoutte, F. Despa, S. Bouckaert, S. Neukermans, L. T. Kauhn, H. Weidele, P. Lievens, R. E. Silverans, Chem. Phys. Lett. 314, 227 (1999)

[2] M. Heinebrodt, N. Mailinowski, F. Tast, W. Branz, I. M. L. Billas, T. P. Martin, J. Chem. Phys. 110, 9915 (1999)

[3] R. Ahlrichs; M. Bär; M. Häser; H. Horn; C. Kölmel, Chem. Phys. Lett.162, 165 (1989)

Electronic and optical properties of hetero-assembled endohedral superatomic clusters

Takeshi Iwasa[1,2] and Atsushi Nakajima[1,2]

[1] *Nakajima Designer Nanocluster Assembly project*, *JST-ERATO, Japan*
[2] *Department of Chemistry, Keio University, Yokohama, Japan*

Multielement gas-phase clusters including endohedrally doped silicon or aluminum magic clusters show intriguing physicochemical properties such as electronic, magnetic, and optical properties. Since these properties are dependent on the cluster size and compositions, the use of designer endohedral clusters as potential building blocks for novel optoelectronic devices is attractive challenging issue. For example, endohedral silicon and aluminum clusters such as $Si_{16}M$ (M=Sc, Ti, V) and $Al_{12}X$ (X=B, Si, P) are known to possess highly symmetric structures and atom-like electronic shells. When M=Ti and X=Si, these clusters show the closed electronic shell, like noble gas atoms. Replacements of the endohedral atoms to those in the neighboring groups such as Sc or V for $Si_{16}Ti$ and B or P for $Al_{12}Si$ give hole or electron, respectively, in the electronic shell, invoking the *p*- or *n*-type semiconductor.

We have previously demonstrated that the $Si_{16}M$ clusters are possible building blocks to fabricate cluster-based *p-n* or *p-i-n* junctions through the density functional theory study on the hetero-assembly of $Si_{16}M$ clusters [1]. In the present study, the electronic and optical properties of hetero-assembly of $Al_{12}X$ are studied and the results are compared to those of $Si_{16}M$. Furthermore, the electronic structures are analyzed by projecting the Kohn-Sham orbitals of the monomer units into the spherical harmonics to classify them from a superatom perspective [2].

The HOMOs and LUMOs of a hetero-assembly of $Al_{12}B$-$Al_{12}P$ dimer are fairly localized to $Al_{12}B$ and $Al_{12}P$ units, respectively, and can be labeled as FG and DG hybridized states. The hetero-dimer has substantial charge carriers, which are estimated as the difference in electron counts from the closed-shell $Al_{12}Si$, with slight charge depletion in contrast to the case of $Si_{16}M$. The charge depletion occurs due to the electron delocalization, because the frontier orbitals of $Al_{12}X$ consist mainly of surface Al atoms, whereas the frontier orbitals of $Si_{16}M$ localize to endohedral M atoms. Analyses on the UV-Vis spectrum of the hetero-dimer, simulated by time-dependent DFT calculations, show that the charge-transfer excited states would occur from $Al_{12}B$ to $Al_{12}P$ in energy range up to 4 eV. These results suggest the potential applications of these clusters to fabricate *p-n* junction for photovoltaic cells. When one or two $Al_{12}Si$, which can correspond to an insulating semiconductor, is inserted between the hetero dimer, it is found to enhance the dipole moment of the hetero-assembled clusters.

References

[1] T. Iwasa and A. Nakajima, J. Phys. Chem. C **116** (2012) 14071-14077.
[2] T. Iwasa and A. Nakajima, J. Phys. Chem. C **117** (2013) 21551-21557.

Electronic structure of rare-earth clusters: from number of 4f-electrons to magnetism

Lars Peters[1], Saurabh Ghosh[2], Igor di Marco[2], Biplab Sanyal[2], Anna Delin[2], Misha Litcarev[2], Theo Rasing[1], Andrei Kirilyuk[1], Olle Eriksson[2], and Mikhail Katsnelson[1]

[1] *Radboud University Nijmegen, Institute for Molecules and Materials, Nijmegen, The Netherlands*
[2] *Department of Physics and Astronomy, Uppsala University, Uppsala, Sweden*

The majority of rare-earth atoms (with the exception of La, Ce, Gd and Lu) are divalent, while most of the rare-earth bulk systems (except α-phase Ce, Eu and Yb) are trivalent [1]. In other words, an atom is described by the $4f^{n+1}6s^2$ configuration and the bulk by the $4f^n[spd]^3$ one. Thus, by going from the atomic limit to the bulk limit one 4f-electron is transferred to the [spd]-band. What happens in the regime between these two limits, the cluster regime, is completely unknown. Will the cluster be divalent, trivalent or perhaps mixed-valent? The resulting electronic structure plays a major role in the resulting cluster properties, such as magnetism, polarizability or conductivity.
We address this fundamental question by using density functional theory (DFT) calculations. This DFT in its conventional form (LDA or GGA) is derived in the limit of a (nearly) uniform electron gas and is therefore only suitable for weakly correlated delocalized electron systems. However, we are dealing with the opposite case, that of strongly correlated localized electron systems. Therefore, DFT is used to describe the delocalized [spd]-electrons in the cluster only and for the 4f-electrons a special approach is used. This approach is known as the Born-Haber cycle [2] and allows us to accurately examine the required energy differences between a divalent, trivalent and mixed-valent cluster. This is done by first evaluating the energy differences in DFT between $4f^n[spd]^3$, $4f^{n+1}[spd]^2$ and $4f^{n+x}[spd]^{3-x}$ configurations in which intra and inter 4f-couplings are completely excluded. Second, this exclusion is corrected for by using experimental data on the isolated rare-earth atom, which is justified since the 4f-shell in the atom, cluster or bulk is essentially the same.
As a result we derive that for example all Tb clusters are pure trivalent, while Sm and Tm clusters show an abrupt change from pure divalent to pure trivalent at respectively a size of 8 and 6. In contrast to expectations, no mixed-valence state was observed in the transition region.
With the electronic structure established we may proceed to understand the magnetic interactions and resulting configuration of the rare-earth clusters. For example for Sm it follows directly from Hund's rules that a divalent cluster is non-magnetic (J=0), while a trivalent cluster is magnetic (J=2.5). In other words, the magnetism should only appear in clusters of 8 atoms and larger. Also we show for Tb-clusters that the exchange coupling can be understood in terms of a competition between double-exchange and super-exchange.

[1] Jensen, J. and Mackintosh, A.R. *Rare Earth Magnetism* (Clarendon Press, Oxford, 1991)
[2] Delin, A., Fast, L., Johansson, B., Wills, J. M. and Eriksson, O. Method for calculating valence stability in lanthanide systems. *Phys. Rev. Lett.* **79**, 4637-4640 (1997)

Coexistence of Insulating and Metallic States, and other Unusual Electronic and Magnetic Properties of Pure and Doped Zinc Clusters

Andrés Aguado,[1] Andrés Vega,[1] Alexandre Lebon,[2] and Bernd von Issendorff[3]

[1] *Department of Theoretical, Atomic and Optical Physics, Valladolid University, Spain*
[2] *Laboratoire de Magnétisme de Bretagne, Brest University, France*
[3] *Physikalisches Institut, Universität Freiburg, Germany*

How many of the several attributes of the bulk metallic state persist in a nanoparticle containing a finite number of atoms of a metallic element? Do all those attributes emerge suddenly at a well defined cluster size or do they rather evolve at different rates and in a broad size range? In this poster, we address these fundamental questions through a conjoint experimental/theoretical investigation of zinc clusters with up to 73 atoms. We show that the evolution of metallic properties with size is not monotonous and rather displays reentrant insulating behavior at several sizes following an electronic shell closing. Additionally, we report the observation of novel coexistence phenomena involving different electronic phases: for some sizes, metallic and insulating electronic states coexist within a single, Janus-like, nanoparticle; for the rest of sizes, we report the coexistence of two weakly interacting metallic phases with different dimensionalities, localized respectively at the shell and the core of the nanoparticle. This is due to an anomalously long core-shell separation, which equips the shell and coreregions with largely independent structural, vibrational and thermal properties, only weakly correlated to each other.

In a second part of the poster, we demonstrate that the cluster Zn_{17} doped with an endohedral Cr impurity can be qualified as a magnetic superalkali cluster. We explain the origin of its high stability, its low vertical ionization potential and its high total spin magnetic moment which amounts to $6\mu_B$, exactly the value of the isolated Cr atom. With the aim of exploring the possibility of designing a bistable magnetic nanoparticle, with a corresponding inter-unit exchange coupling, we also consider the assembling of two such units through different contact regions and in different magnetic configurations. Furthermore, we analyze up to which extent is the Zn shell able to preserve the electronic properties of the embedded Cr atom, both against coalescence of the two superatoms forming the magnetically bistable nanoparticle, and upon the adsorption of an O_2 molecule or even under an over-saturated oxygen atmosphere. Our results are discussed not only emphasizing the fundamental physical and chemical aspects, but also with an eye on the new prospects that those $Cr@Zn_{17}$ magnetic superalkali clusters (and others of similar kind) may open in spintronics-, molecular electronics- or biomedical-applications.

Probing of an Adsorbate-Specific Excited State on an Organic Insulating Surface by Two-Photon Photoemission Spectroscopy

Masahiro Shibuta,[1] Naoyuki Hirata,[1,2] Toyoaki Eguchi,[1,2] and Atsushi Nakajima[1,2]

[1] *Department of Chemistry, Faculty of Science and Technology, Keio University, Japan*
[2] *JST, ERATO, Nakajima Designer Nanocluster Assembly Project, Japan*

Controlled assembly of functionalized nanoclusters or molecules is one of the promising candidates to create novel nanomaterials. Although electrically conductive material, metals and semiconductors, are often used as substrates, physical properties of adsorbed nanoclusters or molecules are largely disturbed due to the strong interaction between adsorbates and substrates. In this study, photo-excited electronic states of a ferrocene (Fc) molecule adsorbed on decanethiolate self-assembled monolayer (SAM) formed on Au(111) substrate, which is known to be chemically inert and electrically insulating [1], have been investigated by using two-photon photoemission spectroscopy (2PPE). We have found that, on the SAM surface, Fc interacts with the substrate very weakly and newly forms the excited states specific to isolated molecules adsorbed on an insulating substrate [2].

A top of Figure 1 shows photon energy dependence of 2PPE spectra for 0.3 monolayer (ML) of Fc on SAM plotted against an intermediate energy relative to Fermi level (E_F). By Fc adsorption, a peak labeled A* appeared at E_F + 2.6 eV. The intensity of A* was enhanced at the photon energy of 4.5 – 4.6 eV, indicating that electrons in A* are resonantly excited from Fc-derived the highest occupied molecular orbital (HOMO) located at E_F – 1.9 eV. The polarization dependence of 2PPE spectra (Fig. 1 bottom) indicates that the electrons in A* are bound perpendicular to the surface because it is only probed by *p*-polarized photon. It has been reported that, for a free Fc molecule in gas phase, the first molecular Rydberg state is formed at 5.1 eV above HOMO, which is about 0.5 eV higher than resonance photon energy of A* (4.5 – 4.6 eV). From these experimental findings, it has been concluded that the A* is an excited state bound not only to the excited hole formed at the adsorbed Fc but also to the positive image charge induced in the substrate. The A* is therefore specific to the isolated adsorbate on electrically insulating substrate. Such an adsorbate-specific excited state, which is not formed in a free molecule, will be responsible for unique properties characteristic of adsorbates on the surface.

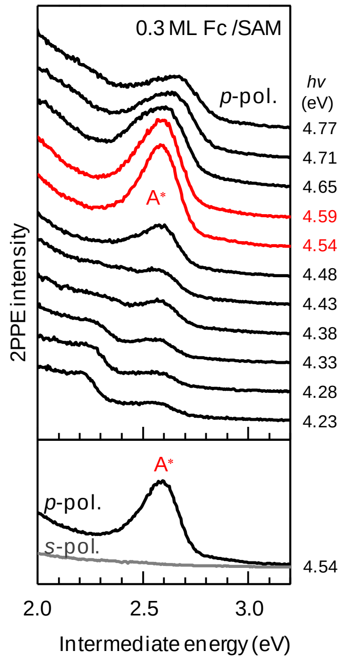

Figure 1. Photon energy (hv) and polarization dependent 2PPE spectra of 0.3 ML Fc on SAM.

Reference
[1] M. Shibuta, N. Hirata, R. Matsui, T. Eguchi, A. Nakajima, J. Phys. Chem. Lett. 3 (2012) 981.
[2] M. Shibuta, N. Hirata, T. Eguchi, A. Nakajima, J. Am. Chem. Soc. 136 (2014) 1825.

Full relativistic calculations of electronic and magnetic properties of small cationic and neutral bismuth clusters

Josef Anton[1], and Timo Jacob[1], and Arne Rosen[2]

[1]*Department of Electrochemistry, University of Ulm, Ulm, Germany*
[2]*Department of Physics, University of Gothenburg,Gothenburg, Sweden*

Group-V elements show huge variability in their electrical, mechanical, and thermal properties – ranging from gaseous nitrogen to solid and brittle bismuth. Within the group-V elements, bismuth is the only metal while arsenic and antimony are classed as semi-metals [1]. Under ambient conditions the most stable crystalline form of both bismuth and its lighter group V congeners is a rhombohedral layered structure (α-As, α-Sb, α-Bi) with each atom surrounded by three nearest neighbors within the layer and three atoms at a larger distance in the adjacent layers. In α-Bi, these intra- and inter-layer distances differ by only 15% approaching the simple cubic structure with a coordination number of six. Furthermore, unlike P_4 (white phosphorous) and As_4 (yellow arsenic) a solid Bi_4 form is unknown [1].
Relativistic effects such as the stabilization of the $np_{1/2}$-orbital, destabilization of the $np_{3/2}$-orbital and spin-orbit coupling lead to a drastic changes in electronic and magnetic properties of a single atom from Phosphor to Element 115 in group V [2]. For instance, in lighter elements of this group, P, As, and Sb, their outermost p-levels are splitted by less than 0.6 eV and the p-electrons are coupled according to the well-known LS-coupling scheme while in the heavy Element 115 the Spin-Orbit (SO) splitting of the outermost p-levels is about 4.7 eV and the p-electrons are coupled according to the jj-coupling scheme. Relativistic effects in Bi-atom where the fine splitting of the p-levels is about 1.8 eV are very pronounced and lead to a break down the LS-coupling scheme but they are still not strong enough to couple the p-electrons according to jj-coupling scheme. These differences in the electronic structures of the atoms in the group V cause also the differences in the properties of their molecules and atomic clusters [2]. Thus, a proper theoretical description of electronic and magnetic properties of e.g. Bi-clusters requires a self-consistent treatment of all relativistic effects in the clusters.
In this contribution we will present our full relativistic 4-componet calculations on electronic and magnetic properties of small cationic and neutral Bi-clusters which were performed with our full relativistic DFT-code [3]. We also will compare our results with the recently published experimental results [4].

References

[1] N. N. Greenwood and A. Earnshaw, *Chemistry of the Elements*, 2nd Ed., Elsevier, 1997
[2] V. Pershina, A. Borschevsky, J. Anton, and T. Jacob, J. Chem. Phys. **132**, 194314 (2010).
[3] J. Anton, B. Fricke, E. Engel, *Phys. Rev. A*, **69**, 012505 (2004).
[4] R. Kelting *et al.,* J. Chem. Phys. **136**, 154309 (2012).

Phase Transition Behavior and Ionic Conductivity of Small Silver Iodide Quantum Dots

Takayuki Yamamoto,[1] Hirokazu Kobayashi,[1,2] Yoshiki Kubota,[3] and Hiroshi Kitagawa[1,2]

[1] *Division of Chemistry, Graduate School of Science, Kyoto University, Kyoto, Japan*
[2] *Core Research for Evolutional Science and Technology (CREST), Japan Science and Technology Agency (JST), Tokyo, Japan*
[3] *Department of Physical Science, Graduate School of Science, Osaka Prefecture University, Osaka, Japan*

Much effort has been made to realize all-solid-state batteries. Silver iodide has been extensively studied as one of the candidates for ionic conductors in solid electrolytes because the high-temperature α-phase shows superionic conductivity due to a sublattice melting of silver ions. Below 147 °C, bulk silver iodide undergoes a structural phase transition from the α-phase into the poorly-conducting β/γ-phase, thereby limiting its application. On the other hand, nanoparticles show different phase behavior from bulk due to nano-size effect. Recently, we discovered that the α-phase survives at lower temperature with decreasing particle size [1]. For 10 nm silver iodide nanoparticles, the α- to β/γ-phase transition temperature was 40 °C. In this work, we have synthesized small silver iodide quantum dots and investigated their phase transition behavior and ionic conductivity.

The silver iodide quantum dots were synthesized by a liquid phase method. Silver nitrate and sodium iodide, and poly[N-vinyl-2-pyrrolidone] were used as the precursors and the protective agent, respectively. The transmission electron microscopy (TEM) image showed that obtained quantum dots were monodispersed and the mean diameter was estimated to be 3.0 ± 0.7 nm (Figure inset). The powder X-ray diffraction (PXRD) pattern suggested the formation of silver iodide quantum dots (Figure). From differential scanning calorimetry, it was found that the synthesized quantum dots have no phase transition of silver iodide up to 250 °C. The ionic conductivity was investigated by impedance analysis.

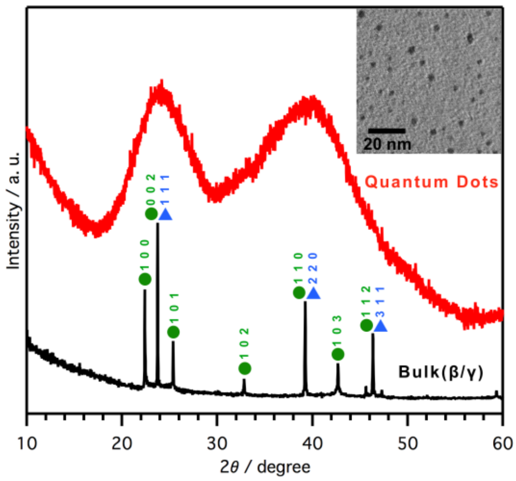

Figure. PXRD patterns of bulk silver iodide and quantum dots (inset: TEM image of silver iodide quantum dots)[2]

Reference(s)

[1] R. Makiura, T. Yonemura, T. Yamada, M. Yamauchi, R. Ikeda, H. Kitagawa, K. Kato, and M. Takata, Nat. Mater. 8 (2009) 476.

[2] T. Yamamoto, H. Kobayashi, and H. Kitagawa, Chem. Lett. Published online: DOI: 10.1246/cl.140409.

A new structural model for Al_{23}^{-} magic cluster: A face-sharing bi-icosahedral motif

Kiichirou Koyasu[1,2] and Tatsuya Tsukuda[1,2]

[1] *Department of Chemistry, School of Science, The University of Tokyo, Tokyo, Japan*
[2] *Elements Strategy Initiative for Catalysts and Batteries, Kyoto University, Kyoto, Japan*

Metal clusters of Na, Al, and Au have been viewed as "superatoms" which accommodate valence electrons in their discrete superatomic orbitals. High stability of magic clusters has been explained by the closure of the electronic shells when the total number of valence electrons are 8, 18, 20, 34, 40,.... For example, magic clusters Al_{13}^{-} and Al_{23}^{-} observed in the gas phase have been viewed as superatoms in which 40 and 70 valence electrons are accommodated within icosahedral and fcc-based cores (structure **1** in Fig. 1a), respectively [1]. In contrast, Au superatoms have been synthesized by protection with ligands, such as thiolates (SR) and phosphines. The icosahedral Au_{13}^{5+} superatomic core with 8 electrons is formed in $Au_{25}SR_{18}^{-}$ [2,3]. In addition, three types of quasi-molecules made of two Au_{13} superatoms, Au_{23}^{9+}, Au_{25}^{11+}, Au_{25}^{9+} with bi-icosahedral (bi-Ih) motifs have been reported so far [4].
Motivated by the successful synthesis of bi-Ih Au clusters, we investigated the possibility that Al_{23}^{-} takes a face-sharing bi-Ih structure by DFT calculations (B3LYP/6-311++G**). We found that isomer **2** (Fig. 1b) with a bi-Ih motif is a local minimum structure, although it is less stable than isomer **1** (Fig. 1a) by 0.97 eV. The vertical detachment energies, VDEs, of isomers **1** and **2** were calculated to be 3.16 and 3.17 eV, respectively (Fig. 1). These VDE values are close to that determined by photoelectron spectroscopy (3.57 eV) [5]. On the basis of these results, we propose a face-sharing bi-ih motif as a possible structure of the magic cluster, Al_{23}^{-}. In order to gain an insight into the bonding scheme between two Al_{13} superatoms, we compared the shapes of molecular orbitals of Al_{13}^{-} and Al_{23}^{-}. It is concluded that constructive overlap of 1F and 2P superatomic orbitals of deformed Al_{13} (D_{3d}) units is responsible for the bonding of two Al_{13} superatoms in Al_{23}^{-}.

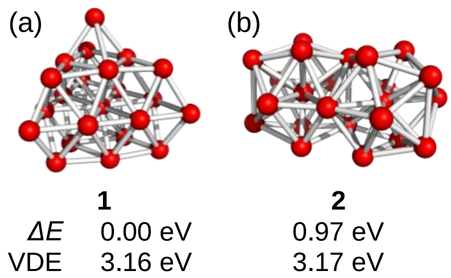

Fig. 1 Optimized structures, relative stability (*ΔE*), and VDE for Al_{23}^{-}.

References

[1] A. Aguado and J. M. López, J. Chem. Phys. 130 (2009) 064704.
[2] M. W. Heaven et al., J. Am. Chem. Soc. 130 (2008) 3754.
[3] Z. Manzhou et al., J. Am. Chem. Soc. 130 (2008) 5883.
[4] J. Nishigaki, K. Koyasu, and T. Tsukuda, Chem. Rec. in press, DOI: 10.1002/tcr.201402011.
[5] J. Akola et al., Phys. Rev. B 62 (2000) 13216.

Non-spherical gold clusters with the lowest-energy intense absorptions: strong correlation between geometric and electronic structures

Yukatsu Shichibu,[1,2] Mingzhe Zhang,[2] and Katsuaki Konishi[1,2]

[1] *Faculty of Environmental Earth Science, Hokkaido University, Sapporo, Japan*
[2] *Graduate School of Environmental Science, Hokkaido University, Sapporo, Japan*

Subnanometer-sized gold clusters with gold atoms of ~10 have attracted considerable attention because they are expected to show unique size- and/or structure-dependent physicochemical properties.[1] While conventional monophosphine-ligated gold clusters favored spherical geometries and typically took on brownish colors,[2] we found that a series of non-spherical Au_n clusters (n = 6, 7, 8, 11) belonging to "[core+*exo*] motif" exhibit unusual absorption properties during the systematic study on diphosphine-ligated gold clusters.[3-6]

Fig.1 top shows geometric structures of [core+*exo*]-type $[Au_6(dppp)_4]^{2+}$ (**1**), $[Au_7(dppp)_4]^{3+}$ (**2**), $[Au_8(dppp)_4Cl_2]^{2+}$ (**3**) and $[Au_{11}(dppe)_6]^{3+}$ (**4**) from single-crystal X-ray diffraction analyses (dppp = $Ph_2P(CH_2)_3PPh_2$, dppe = $Ph_2P(CH_2)_2PPh_2$). Interestingly, the Au_6 structure of **1** can be interpreted as an elemental unit of **2 - 4** and the other Au_n (n = 7, 8, 11) structures are described as growth or fusion of the Au_6. Moreover, each of their absorption spectra exhibited the lowest-energy intense band in visible region (Fig.1 bottom). These isolated bands have never been seen in the spectra of monophosphine-ligated gold clusters and were all assigned to simple HOMO-LUMO intraband (6sp → 6sp) transitions from density functional theory (DFT) calculation. So the attachment of only one Au atom to a polyhedral core could develop such an unusual absorption. The strong correlation between the shapes and electronic structures of the clusters is discussed from an electron system (4e) and the jellium model.

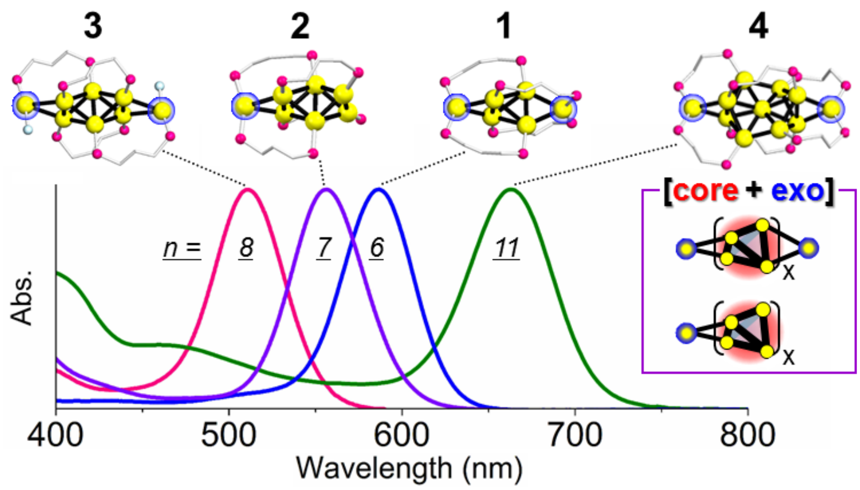

Figure 1. Skeletal structures and absorption spectra of Au_n clusters (n = 6, 7, 8, 11; **1** - **4**). Inset shows [core+*exo*] motif, in which one or two *exo* Au atoms are attached to centered polyhedral Au cores.

References

[1] T. Tsukuda, *Bull. Chem. Soc. Jpn.* 85 (2012) 151. [2] K. P. Hall, D. M. P. Mingos, *Prog. Inorg. Chem.* 32 (1984) 237. [3] Y. Shichibu *et al.*, *to be submitted*. [4] Y. Shichibu, K. Konishi, *Inorg. Chem.* 52 (2013) 6570. [5] Y. Shichibu, Y. Kamei, K. Konishi, *Chem. Commun.* 48 (2012) 7559. [6] Y. Kamei, Y. Shichibu, K. Konishi, *Angew. Chem. Int. Ed.* 50 (2011) 7442.

Density functional theory study on hydrogen absorption properties of nano-sized transition metal clusters (1): difference between Pd/Pt bulk and their clusters

Aya Matsuda and Hirotoshi Mori

Department of Chemistry and Biochemistry, Ochanomizu University, Japan

[Introduction] Hydrogen storage is essential to utilize hydrogen energy in a practical manner. Various kinds of hydrogen absorbing materials have been proposed. One of the best-known hydrogen storage materials is bulk palladium (Pd). As the hydrogen absorption of bulk Pd start from H-adsorption on its surface, it has been expected that the hydrogen absorbing ability can be improved by nanoparticulation. However, Yamauchi *et al*. experimentally showed that the simple expectation is not correct, *i.e.* nano-sized Pd has lower hydrogen absorbing ability [1]. They also found that platinum (Pt), which belongs to same group 10, does not shown any hydrogen absorption in a bulk form and manifests hydrogen absorbing ability by nanoparticulation. However, the origin of the differences of hydrogen absorption ability among these inorganic metal systems has not been understood. The object in this study is to explain the differences of the hydrogen absorption properties from a theoretical point of view.

[Methods] A set of DFT calculations at the RI-PBE/def-SV(P) level of theory was performed to investigate electronic structures of Pd_{55}, Pt_{55}, bulk Pd, and bulk Pt. First, geometries of the inorganic metal clusters were optimized with cubooctahedral (O_h) symmetry, which was observed in X-ray diffraction experiments [1,2]. As the crystal structure of bulk Pd and Pt have been reported, we used the experimental parameters for electronic band structure calculation of the bulks. Then, using cubic grid points with an interval of 0.25 Å, interaction energies between an H atom and Pd_{55}, Pt_{55}, bulk Pd and bulk Pt were evaluated.

[Results] The most stable hydrogen diffusion path predicted for Pd_{55} is shown in Fig. 1. Similar path was also obtained for Pt_{55}. Our calculations show that the hydrogen in Pd_{55} is the more stable than that in Pt_{55}. The results well correspond to experimental observation by Yamauchi *et al*. The most stable hydrogen absorption site is octahedral (O_h) site, of which H absorption energies for Pd_{55} and Pt_{55} in O_h site are -0.54 eV and -0.18 eV, respectively. To discuss the difference of interaction energy between absorbed H atom and M_{55} (M=Pd, Pt), we decompose the interaction energy by their physicochemical origins; electrostatic, repulsive, polarizable and dispersion interaction. The difference of repulsive interaction energy between Pd and Pt system is the largest (2.03 eV), which makes the difference of stability. It was clarified that the instability of H atom in Pt_{55} is due to relativistic expansion of electronic distribution (Fig. 2). In the poster session, difference between cluster and bulk will be discussed in detail.

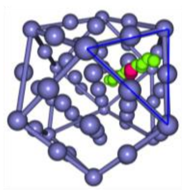

Fig. 1 The most stable H diffusion path in Pd_{55}

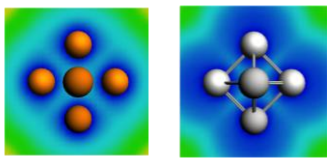

Fig. 2 The electron diffusion of Pd_6 (left) and Pt_6 (right)

[References] [1] M. Yamauchi *et al.*, *J. Phys. Chem. C,* **112**, 3294 (2008) [2] M. Yamauchi *et al.*, *Synth. Met.*, **135,** 757, (2003)

Density functional theory study on hydrogen absorption properties of nano-sized transition metal clusters (2): dependency on composition and internal structures

Kasumi Miyazaki, Aya Matsuda and Hirotoshi Mori

Department of Chemistry and Biochemistry, Ochanomizu University, Japan

[Introduction] Hydrogen storage is essential to utilize hydrogen energy in a practical manner. Promising materials for hydrogen storage are nano-sized transition metal clusters. It was reported by Yamauchi *et al*. that nano-sized mixed transition metal (alloy) clusters show different hydrogen absorbing properties from pure transition metal clusters. They also found that the hydrogen absorbing ability can be tuned by composition and internal structures of the mixed metals, e.g. Pd/Pt alloy cluster of which composition of Pt is ca. 10% shows better hydrogen absorption ability (0.40 H/M) [1] than pure Pd cluster (0.30 H/M) [2]. Although these experimental observations anticipate the finding of novel materials for hydrogen storage, the mechanism for the tuning for hydrogen absorbing properties has not been well understood. Using density functional theory calculations, recently, we studied the mechanism from a molecular level point of view. In this presentation, we will discuss relationships among chemical composition, internal structure, electronic structure, and hydrogen storage property of nano-sized mixed transition metal clusters.

[Methods] A set of DFT calculations at the RI-PBE/def-SV(P) level of theory was performed to investigate electronic structures of Pd/Pt mixed clusters (Pd_{55}, $Pd_{50}Pt_5$, $Pd_{42}Pt_{13}$, $Pd_{28}Pt_{27}$, and Pt_{55}). First, geometries of the clusters were optimized. For the mixed metal clusters, core-shell type and solid-solution type structures were take into account. Interactions between an H and the Pd/Pt mixed clusters were evaluated.

[Results] A set of H-absorption interaction potential energy curves along normal directions to (111) surface of Pd_{55}, Pt_{55}, and core-shell type $Pd_{42}Pt_{13}$ are shown in Fig. 1. Our calculation showed that all the clusters shown in this figure can absorb an H atom inside, as observed experimentally. Since the potential minima for Pt_{55} is much shallower than the others (and the position of energy minima is just below the surface), it well explain the fact that Pt nano particle can absorb H atoms, but the amount of them is small (0.15 M/H). It was also well explained that the core-shell type $Pd_{42}Pt_{13}$ has similar H absorption property to the Pd_{55}. Kobayashi *et al*. reported that adsorbed H atoms distribute on the interface between Pt core and Pd shell [3]. Our calculation reproduced their observation. In the poster session, dependency on alloy composition will be discussed. The case of solid solution type cluster will be also discussed.

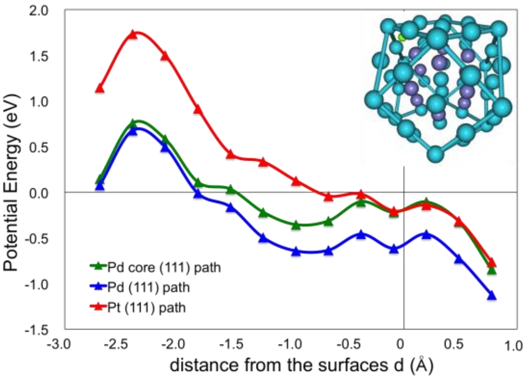

Fig. 1 H-absorption potential energy curves for Pd_{55}, Pt_{55}, and core-shell type $Pd_{13}Pt_{42}$ shown in r.h.s.

[References] [1] H. Kobayashi *et al.*, J. Am. Chem. Soc., **132**, 5576 (2010) [2] M. Yamauchi *et al.*, *J. Phys. Chem. C,* **112**, 3294 (2008) [3] H. Kobayashi *et al.*, J. Am. Chem. Soc., **130**, 1818 (2010)

Electronic shell closure of Al_{13} by electron donation from PVP

Tomomi Watanabe,[1,2] Kiichirou Koyasu,[1,2] and Tatsuya Tsukuda[1,2]

[1] *Department of Chemistry, The University of Tokyo, Tokyo, Japan*
[2] *Elements Strategy Initiative for Catalysts and Batteries, Kyoto University, Kyoto, Japan*

Ligands play an important role in stabilizing metal clusters by steric protection and regulating the number of the electrons for the closure of electronic shells in the clusters [1]. For example, the number of valence electrons in the Au_{13} clusters protected by electron-withdrawing ligands such as thiolates and halides is adjusted to be 8. In contrast, we can expect that Al_{13} clusters having 39 electrons can be electronically stabilized by donating one electron from the protecting ligands. Polyvinylpyrrolidone (PVP) is a candidate for an electron donating stabilizer as demonstrated experimentally [2] and theoretically [3] for stabilization of Au clusters. In this study, we computationally investigated the stabilization of Al_{13} by electron donation from PVP.

N–Ethyl–2–pyrrolidone (EP) was used as model of PVP. Geometrical structures of $Al_{13}(EP)_n$ (n = 0–4) were optimized by DFT at the level of B3LYP/6-31G(d) using Gaussian 09 package. Global and local minima structures were confirmed by vibrational analysis. The binding energy of the EP ligand (*BE*) and increment of the Mulliken charge on the Al_{13} core (ΔQ) were estimated.

The optimized structures of $Al_{13}(EP)_1$ are shown in Table 1. In isomer **1**, EP is bounded to Al_{13} through the carbonyl oxygen with a binding energy of 1.11 eV, whereas EP is weakly bound to Al_{13} in isomer **2**. The electronic charge of Al_{13} core is increased by –0.36e in isomer **1**, indicating that EP can act as electron donating ligand to Al_{13}. The second and third EP ligands also stabilized Al_{13} by electron donation through carbonyl O atom. The ΔQ value of $Al_{13}(EP)_3$ was almost –1e. This indicates that the electronic shell of Al_{13} is closed by electron donation from three EP ligands.

Table 1. The optimized structure, *BE* and ΔQ of $Al_{13}(EP)_1$.

	Isomer 1	**Isomer 2**
Optimized structure	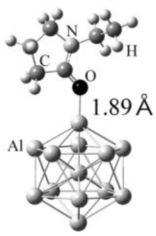	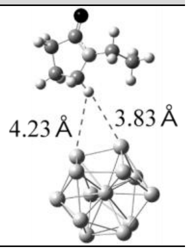
BE (eV)	1.11	0.01
ΔQ	–0.36	–0.02

References

[1] M. Walter et al., Proc. Natl. Acad. Sci. U.S.A. 105 (2008) 9157.
[2] H. Tsunoyama et al., J. Am. Chem. Soc. 131 (2009) 7086.
[3] M. Okumura et al., Chem. Phys. Lett. 459 (2008) 133.

Precise Separation of Metal Clusters Protected by Two-Types of Thiolate Ligands

Yoshiki Niihori[1], Miku Matsuzaki[1], Chihiro Uchida[1], and Yuichi Negishi[1]

[1] *Department of Applied Chemistry, Tokyo University of Science, Tokyo, Japan*

[Introduction] Thiolate-protected gold clusters have attracted a great deal of attention as new functionalized nano-materials. It will be able to change their chemical/physical properties by changing the surrounding ligands. However, in many cases, the synthesis of cluster with multiple types of thiolate ligands results in a distribution of composition of the cluster-surface. To control the function of the cluster by changing the composition of cluster-surface, precise separation technique is required. Herein we report precise separation of metal clusters protected by two-types of ligands by use of high-performance liquid chromatography (HPLC).

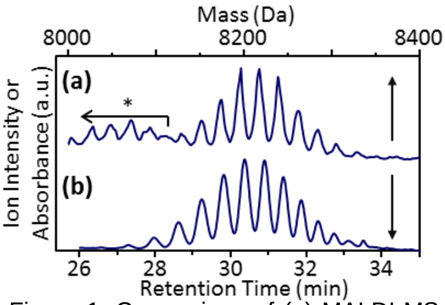

Figure 1. Comparison of (a) MALDI-MS and (b) linear-gradient chromatogram of as-prepared cluster..

[Experiment] $Au_{24}Pd$ clusters protected by two-types of thiolate ligands are synthesized by using ligand exchange reaction with $Au_{24}Pd(SR_1)_{18}$ and incoming thiol (R_2SH) in solution system. As-prepared $Au_{24}Pd(SR_1)_{18-n}(SR_2)_n$ (n = 0-18) clusters were separated by using HPLC with reverse phase column. To achieve precise separation, we applied following two-types of gradient programs. 1) Linear-gradient program; the mobile phase was substituted from methanol to THF linearly. 2) Step-gradient program; the mobile phase was substituted from methanol to methanol/THF mixture intermittingly. In the chromatogram, each fraction were corrected and characterized with MALDI-Mass spectrometry.

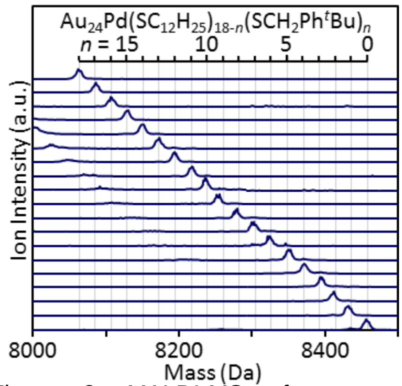

Figure 2. MALDI-MS of separated clusters.

[Result and Discussion] Figure 1 indicates the comparison of MALDI-MS and linear-gradient chromatogram of as-prepared $Au_{24}Pd(SC_{12}H_{25})_{18-n}$-$(SCH_2Ph^tBu)_n$ cluster. In MALDI-MS, each peak were assigned to $PdAu_{24}(SC_{12}H_{25})_{18-n}(SCH_2Ph^tBu)_n$ with different n. Figure 2 presents MALDI-MS of each corrected fractions.

We found that all the clusters with individual combination of two-types of ligands were separated precisely.[1] Same experiment has been done by changing the combination of two-types of thiolate/setenolate ligands and metal cores (Au_{25}, Au_{38}). We found that our method has general versatility for separation of various metal clusters with two-types of ligands. Figure 3 indicates step-gradient chromatogram of $Au_{24}Pd(SC_2H_4Ph)_{18-n}(SC_{12}H_{25})_n$ cluster. Several fine peaks were observed in Figure 3(a) and multiple sub-peaks in one peak were observed. We attributed these sub-peaks to coordination isomers. We found that when a step-gradient used, it could be possible to separate clusters with higher resolution.[2]

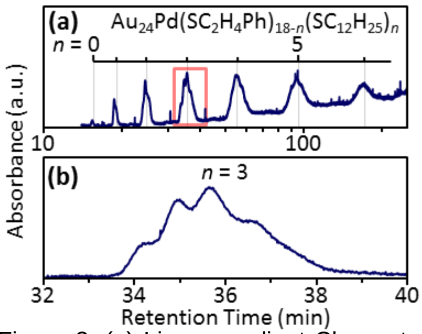

Figure 3. (a) Linear-gradient Chromato-gram and (b) expanded chromatogram of squared area in (a).

[1] Y. Niihori, M. Matsuzaki, T. Pradeep, Y.Negishi, *J. Am. Chem. Soc.*, 135, (2013) 4946-4949.
[2] Y. Niihori, M. Matsuzaki, C. Uchida, Y. Negishi, *Nanoscale*, in Press, (2014).

Ultrafast photoelectron spectroscopy of metal clusters supported on MgO and Si substrates

Florian Knall,[1] Mihai E. Vaida,[1] Thorsten M. Bernhardt,[1]
Hisato Yasumatsu,[2] and Nobuyuki Fukui[3]

[1] *Institute of Surface Chemistry and Catalysis, University of Ulm, Ulm, Germany*
[2] *Cluster Research Laboratory, Toyota Technological Institute;*
In [3] East Tokyo Laboratory, Genesis Research Institute, Inc., Chiba, Japan

The dynamics of photoexcited electrons of metal clusters supported on ultrathin oxide films[1,2] and on Si(111) substrates[3] are discussed on the basis of time-resolved two photon photoemission spectra measured at different wavelengths by means of a time-of-flight energy analyzer in combination with a femtosecond laser. One- and two photon processes for the photo-emission have been observed.

References

[1] M.E. Vaida, T. Gleitsmann, R. Tchitnga, T.M. Bernhardt, J. Phys. Chem. C 113 (2009) 10264.
[2] M.E. Vaida, T. Gleitsmann, R. Tchitnga, T.M. Bernhardt, Phys. Status Solidi B 247 (2010) 1139.
[3] H. Yasumatsu, T. Hayakawa, T. Kondow, Chem. Phys. Lett. 487 (2010) 279.

* This research was supported by JSPS Invitation Fellowship Program, Summer Program and Postdoctoral Fellowship, and the Special Cluster Research Project of Genesis Research Institute, Inc.

Graphene-supported metal clusters: Well-defined nanostructures for the investigation of photo-induced processes

Kira Jochmann,[1] Thorsten M. Bernhardt[1]

[1] *University of Ulm, Institute of Surface Chemistry and Catalysis, 89069 Ulm, Germany*

During the last decade considerable attention was drawn to the growth of graphene on metal single crystal surfaces, where it provides an ideal template for the ordered growth of regular metal cluster arrays. Building on various investigations about the detailed growth of these cluster super-lattices, we make use of the possibility to easily grow nanostructures with equally spaced and mono-disperse clusters for fundamental research in laser selective photochemistry.

Our new experimental setup enables time-resolved measurements due to a femtosecond laser system on the one hand and surface analysis via scanning tunnelling microscopy on the other hand. In first light interaction measurements time-resolved two-photon photoemission spectroscopy (2PPES) was applied to gain an insight into the unoccupied electronic structure of the Ir(111)/graphene/Ir cluster system at different graphene and cluster coverages. In subsequent experiments the combination of femtosecond laser pump-probe mass spectrometry with resonance enhanced multi-photon ionization and STM will be employed to reveal photo-dissociation dynamics of our probe molecule methyl bromide with spatio-temporal resolution.

Properties of designed small gallium-nitride clusters

Tibor Höltzl[1]

[1] *Furukawa Electric Institute of Technology, Budapest, Hungary*

Geometry and electronic structure of small gallium-nitride clusters was investigated using quantum chemical methods. Most of the nano-scale studies focus on the difference between the macroscopic and the nano-scale materials. In contrast, our work emphasizes the flexibility of the nano-design which aims to construct structures with desired properties. Our goal was to construct gallium-nitride clusters with similar geometric structure to the bulk material.

We have found that simple design principles (which are adapted based on the publications of sphalerite indium-phosphide) can be successfully used to design various cluster sizes with the desired properties. The underlying method is simple: the coverage of the surface of the cluster is the most important factor which determines the electronic and the geometric structure. The cluster has to be covered such that every atom in it must participate in four chemical bonds from which one and only one is dative, while the remaining ones are covalent.

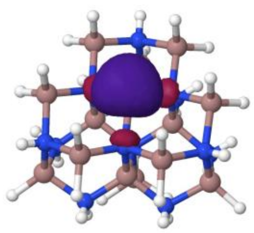

ters was supported by our computation of the cluster with different coverages.

hods can be used to study various physical and . Geometrical structure of even a small cluster is estingly, the specific heat per GaN units of very

Jmol

Also, the surface modification of the gallium nitride clusters opens the way toward small clusters with the desired properties. Clusters with several different coverages and reaction sites were constructed and investigated. The chemical behavior of these reaction sites is highly different. On one site this shows that the surface modification of these type of clusters can be applied to obtain a desired chemical behavior, which would be useful e.g. in catalyst design. On the other hand, it also emphasizes the importance of the role of the chemical bonding around the gallium reaction site, also in a larger system. This could also influence the surface growth of the bulk.

Stabilization of Magic-Numbered $Au_{25}(SR)_{18}$ Cluster

Wataru Kurashige,[1] Masaki Yamaguchi,[1] Katsuyuki Nobusada,[2] and Yuichi Negishi[1]

[1] *Department of Applied Chemistry, Tokyo University of Science, Tokyo, Japan*
[2] *Department of Theoretical and Computational Molecular Science, Institute for Molecular Science, Okazaki, Japan*

1. Introduction

Small gold clusters protected by ligands are of interest in both fundamental and applied research because they exhibit size specific optical and physical properties. Of such clusters, thiolate-protected gold clusters (Au:SR), especially $Au_{25}(SR)_{18}$ has been the most extensively studied. Recently, we have attempted to synthesized more stable clusters than $Au_{25}(SR)_{18}$ (Fig. 1). In consequence, we succeeded in synthesizing a thiolate-protected $Au_{24}Pd(SR)_{18}$ cluster, which is a mono-Pd-doped cluster of $Au_{25}(SR)_{18}$ and a selenolate-protected $Au_{25}(SeR)_{18}$. We compared their stability with those of $Au_{25}(SR)_{18}$. The results indicated that Pd doping and selenolate protection increase a stability of the cluster against the degradation in solution.

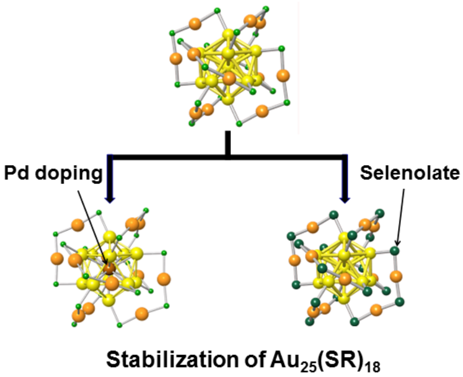

Fig. 1. Our object

2. Experiment

Thiolate-protected $PdAu_{24}(SR)_{18}$ (**1**) was isolateted by Brust method and reverse phase HPLC and Selenolate-protected $Au_{25}(SeR)_{18}$ (**2**) was isolated by that and solvent extraction. These isolated compounds were characterized by UV-vis spectrum, ESI, MALDI, LDI mass spectrum, TGA, TEM image, X-ray diffractogram and X-ray photoelectron spectra. And we investigated these stability in solution by pursuing time dependence of UV-vis spectrum.

3. Results and discussion

Only one peak was observed in the MALDI mass spectrum of **1**, assigned to $Au_{24}Pd(SR)_{18}$ [1]. On the other hand, only one peak was observed in the ESI mass spectrum of **2**, assigned to $Au_{25}(SeR)_{18}$ [2]. These results indicate that these clusters were isolated in high purity using our methods. Regarding stability in solution between $Au_{25}(SR)_{18}$ and $Au_{24}Pd(SR)_{18}$, the relative ion intensity of $Au_{25}(SR)_{18}$ decreases over time, and after 30 days the mass spectrum exhibits only the peak attributed to $Au_{24}Pd(SR)_{18}$. And we also did similar experiment between $Au_{25}(SR)_{18}$ and $Au_{25}(SeR)_{18}$. The absorption spectrum of $Au_{25}(SR)_{18}$ changed gradually over time, whereas that of $Au_{25}(SeR)_{18}$ exhibited only a slight change, even after two days. These results indicate that $Au_{24}Pd(SR)_{18}$ and $Au_{25}(SeR)_{18}$ are more stable than $Au_{25}(SR)_{18}$ in solution[3], [4].

Reference(s)

[1] Y. Negishi, W. Kurahige, Y. Niihori, T. Iwasa and K. Nobusada, Phys. Chem. Chem. Phys., 12 (2010) 6219.
[2] Y. Negishi, W. Kurahige and U. Kamimura, Langmuir (Letter), 27 (2011) 12289.
[3] W. Kurahige, M. Yamaguchi, K. Nobusada and Y. Negishi, J. Phys. Chem. Lett., 3 (2012) 2649.
[4] Y. Negishi, W. Kurahige, Y. Niihori and K. Nobusada, Phys. Chem. Chem. Phys. (Perspective), 15 (2013) 18736.

Theoretical Study on the Ln Dependence of $Ln(COT)_2^-$ Photoelectron Spectra

Erika Nakajo, Tomohide Masuda, and Satoshi Yabushita

Department of Chemistry, Keio University, Yokohama, Japan

Lanthanide (Ln) complexes are attractive for their novel properties originating from the core-like open-shell 4f orbitals. The sandwich cluster $Ln(COT)_2^-$, consisting of Ln metal and 1,3,5,7-cyclooctatetraene (COT) ligands with the D_{8h} symmetry is an important synthetic unit towards the multiply-layered structures which have a great potential as magnetic and optical nanowires. We have theoretically analyzed the electronic structure of a series of $Ln(COT)_2^-$ and the corresponding neutral complexes, to simulate the recently reported anion photoelectron spectra[1]. Fig. 1 shows the orbital interaction scheme of $Gd(COT)_2^-$. The valence MOs with the energy order $e_{1g} < e_{1u} < e_{2g} < e_{2u}$ consist mainly of the COT π orbitals (L_π and L_δ). Compared to the COT orbitals, the large energy gap between e_{2u} and e_{2g}, and the level inversion of e_{1g} and e_{1u} on sandwiching are both simply attributed to the symmetrically allowed mixings with the Ln 5d and 5p orbitals. However, to explain the Ln dependence of these MO energies (Fig.2), several complicated factors should be considered: (1) the shortening of the Ln-COT distance resulting from lanthanide contraction, (2) the very strong intramolecular electrostatic interaction in the ionic bonding system[2], and (3) the covalent orbital interaction. Interestingly, even with the shortening of the Ln-COT distance, the metal-ligand orbital overlaps remain constant or even decrease due to the simultaneous contraction of the Ln atomic orbitals. Although the Ln 4f orbitals have little contribution to the metal-ligand covalency, they are known to contribute to the stabilization of neutral $Ln(COT)_2$ through a specific metal-ligand interaction[3]. Because of the non-negligible magnitude of the orbital overlap (from 0.05 in Ce to 0.02 in Yb), configuration interaction involving $4f\delta(e_{2u})$ and the ligand $L_\delta(e_{2u})$ occurs in a spin-dependent manner. For middle-range Ln, this interaction was indeed observed as the splitting of the X peak in the anion PE spectra that correspond to the photodetachment from the HOMO (e_{2u}) [1]. The Ln dependence of this interaction is explained with a simple model relevant to the 4f configuration, with taking into account the energy difference and the overlap between $4f\delta(e_{2u})$ and the ligand $L_\delta(e_{2u})$. The experimentally observed X peak splittings thus have been proved as an interesting example that shows the remarkable interaction between the Ln 4f and the ligand electrons.

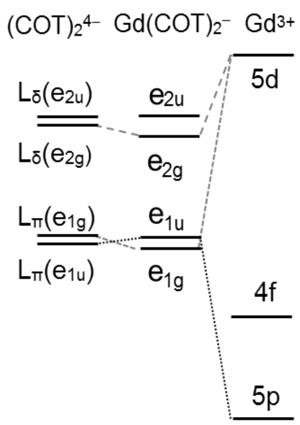

Fig.1: Qualitative orbital interaction scheme of $Gd(COT)_2^-$

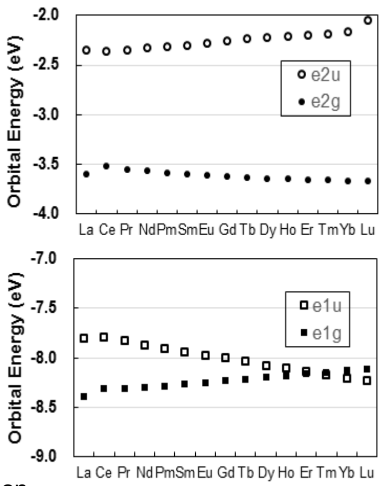

Fig.2: Valence orbital energies

[1] N. Hosoyal, K. Yada, T. Masuda, E. Nakajo, S. Yabushita, and A. Nakajima, J. Phys. Chem. A 118 (2014) 3051.
[2] R. Takegami, N. Hosoya, J. Suzumura, A. Nakajima, and S. Yabushita, J. Phys. Chem. A 109 (2005) 2476.
[3] W. Liu, M. Dolg, and P. Fulde, Inorg. Chem. 37 (1998) 1067.

Functionalized Gold Nanoclusters as Site-Specific Labels for Imaging of Enteroviruses

Kirsi Salorinne,[1] Varpu Marjomäki,[2] Tanja Lahtinen,[1] Mari Martikainen,[2] Jaakko Koivisto,[1] Sami Malola,[3] Mika Pettersson,[1] and Hannu Häkkinen[1,3]

[1] *Department of Chemistry, Nanoscience Centre, University of Jyväskylä, Finland*
[2] *Department of Biology and Environmental Sciences, Nanoscience Centre, University of Jyväskylä, Finland*
[3] *Department of Physics, Nanoscience Centre, University of Jyväskylä, Finland*

Monolayer protected gold nanoclusters of a few nanometers in size have proven to be promising site-specific labels for various biomolecules due to their unique properties that come from the small size and molecule-like characteristics that can be studied e.g. by transmission electron microscopy (TEM).[1-4] In addition, by properly designing the protecting monolayer to include specific linker molecules to allow site-specific conjugation to biomolecules, this technique enables the investigation of different mechanisms or pathways of complex biomolecules, or tracking of the biomolecule-gold cluster conjugates inside cells using the appropriate imaging technique. Here we describe a recent success in labeling of enteroviruses for TEM studies by maleimide-functionalized $Au_{102}(pMBA)_{44}$ clusters (pMBA = para-mercaptobenzoic acid).[5]

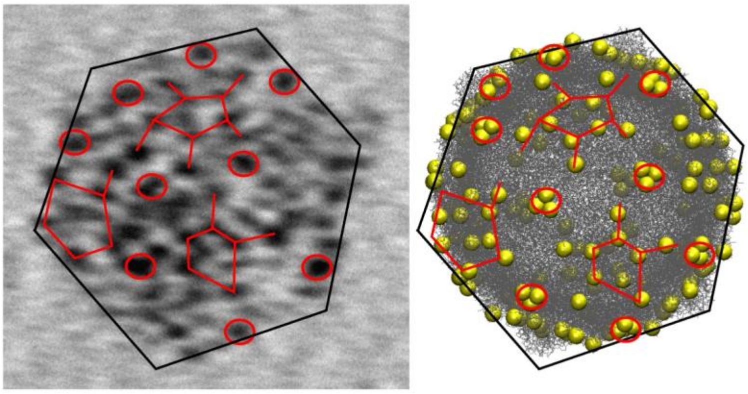

Reference(s)
[1] C. J. Ackerson, R. D. Powell and J. H. Hainfeld, Method Enzymol. 481 (2010) 195.
[2] C. J. Lin, C. Lee, J. Hsieh, H. Wang, J. K. Li, J. Shen, W. Chan, H. Yeh and W. H. Chang, J. Med. Biol. Eng. 29 (2009) 276.
[3] T. Tsukuda, Bull. Chem. Soc. Jpn. 85 (2012) 151.
[4] H. Qiang, M. Zhu, Z. Wu and R. Jin, Acc. Chem. Res. 45 (2012) 1470.
[5] V. Marjomäki, T. Lahtinen, M. Martikainen, J. Koivisto, S. Malola, K. Salorinne, M. Pettersson and H. Häkkinen, Pros. Natl. Acad. Sci. 111 (2014) 1277.

Metal nanoparticle modified electrochemical electrodes for nonenzyme hydrogen peroxide sensing

Jue Wang[1], Xuejiao Chen[1], Kaiming Liao[1], Guanghou Wang[2] and Min Han[1]

[1]*National Laboratory of Solid State Microstructures and Department of Materials Science and Engineering, Nanjing University, Nanjing 210093,China*
[2]*National Laboratory of Solid State Microstructures and Department of Physics, Nanjing University, Nanjing 210093, China*

Rapid, accurate, stable, sensitive and low cost detection of H_2O_2 is very important in various fields including clinical diagnostics, environmental analysis and food industry [1–3]. Dense metal (palladium, silver) nanoparticle arrays coating on glass carbon electrodes (GCEs) with good dispersity were fabricated by using gas phase cluster beam deposition. The nanoparticle modified electrodes show enhanced electrocatalytic activity toward the reduction of H_2O_2 with a very low overpotential [4]. With an optimized nanoparticle coverage, a high selective nonenzyme sensing platform for stable detection of H_2O_2 with a low detection limit (1×10^{-7} M), high sensitivity ($5.65\times10^{-1}AM^{-1}CM^{-2}$) as well as a wide linear range from 1.0×10^{-6} to 6.0×10^{-3}M was realized. The electrodes also show a very quick response to the concentration change of H_2O_2, with a current rise time of less than 1 s, which is faster than all the silver or palladium based electrodes.

References
[1] S.A. Kumar, S.F. Wang and Y.T. Chang, Thin Solid Films 518 (2010) 5832–5838.
[2] G.H. Zhang, N.B. Yang, Y.L. Ni, J. Shen, W.B. Zhao and X.H. Huang, Sensors and Actuators B: Chemical 158 (2011) 130–137.
[3] M. Delvaux, A. Walcarius and S. Demoustier-Champagne, Analytica Chimica Acta 525 (2004) 221–230.
[4] K.M. Liao, P. Mao, Y.H. Li, Y.L. Nan, F.Q. Song, G.H. Wang and M. Han, Sensors and Actuators B: Chemical 181 (2011) 125–129.

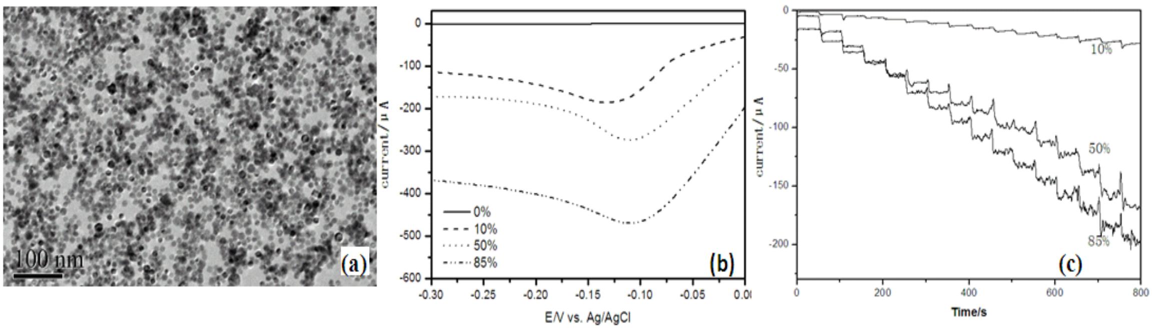

Fig.1. (a) TEM image of the Pd clusters deposited on amorphous carbon film surface. (b) The linear sweep stripping voltammetry (LSSV) measurements of the Pd NPs/GCE with different nanoparticle coverage in 0.01M H_2O_2 (0.05M PBS, pH=7.4) at the scan rates of 0.05V/s. (c) The amperometric responses of the Pd NPs/GCE with different nanoparticle coverage deposition times upon successive addition of H_2O_2 into gently stirred 0.05 M PBS (pH 7.4) at −0.11V.

Gold Nanorod Assisted Laser Desorption/Ionization of Oligopeptides

Masanori Fujii,[1] Naotoshi Nakashima,[1,,2,3] and Yasuro Niidome[1,2,4]

[1] *Department of Applied Chemistry, Kyushu University, Fukuoka, Japan*
[2] *I2CNER WPI, Kyushu University, Fukuoka, Japan*
[3] *CREST, Tokyo, Japan*
[4] *Kagoshima University, Kagoshima, Japan (Present Affiliation)*

In Surface Assisted Laser Desorption/Ionization Time-of-Flight Mass Spectrometry (SALDI-MS), nanostructured surfaces absorb photons and assist in desorption and ionization of sample molecules. We have been reported highly efficient SALDI processes using gold nanorods on an ITO plate previously[1,2]. Here, we controlled the aggregation of gold nanorods, and evaluated their SALDI efficiencies.

Gold nanorods with aspect ratios of about 5 (51 ± 7 nm and 9.7 ± 1.1 nm in longitudinal and transverse directions, respectively) were coated with poly(sodium styrenesulfonate) (PSS) and deposited on an ITO plate. ITO plates were repeatedly immersed in a PSS-nanorod solution to control the degree of aggregation of the gold nanorods. The nanorod-ITO plates were used for SALDI-MS measurements to detect an oligopeptide (angiotensin I) cast on the plates. A MALDI-MS machine (Autoflex III, Bruker Daltonics) was used for the mass spectrometry.

Fig. 1 shows the S/Ns of the mass signals plotted against the full width at half maximum (FWHM) of longitudinal SP bands for gold nanorods on the ITO plates. For the plates showing 250-350 nm SP bandwidths, the SALDI efficiencies depended on which spots were chosen for the mass spectrometry to be performed at. Intense signals were randomly obtained, which strongly suggested that there were a few extraordinary spots that showed highly efficient SALDI processes.

In the case of plates that the FWHM values were 250-350, SEM observation indicated that small aggregates, consisting of a few nanorods, formed on the plates. Image analysis of the SEM images showed that the efficient SALDI processes originated from small aggregates consisting of 3 to 8 nanorods. Isolated gold nanorods and large aggregates of nanorods did not show efficient SALDI processes. The longitudinal SP bands of the gold nanorods could be used as an indicator to obtain the size-controlled nanorod-aggregates. This approach should be advantageous for the preparation of highly sensitive and reproducible SALDI plates.

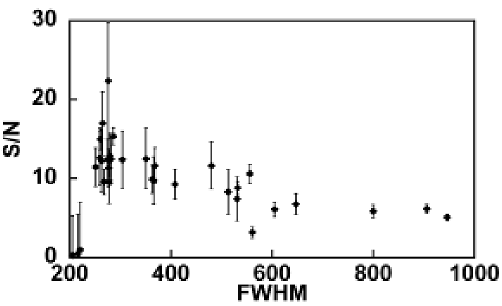

Fig. 1 S/Ns for the mass signals of angiotensin I plotted against the FWHM of longitudinal SP bands for gold nanorods on the ITO plates.

Reference

[1] Y. Nakamura, Y. Tsuru, M. Fujii, Y. Taga, A. Kiya, N. Nakashima and Y. Niidome, *Nanoscale* 3(2011)3793.

[2] M. Fujii, N. Nakashima, T. Niidome, and Y. Niidome, *Chem. Lett.*, 43(2014) 131.

Spontaneous Formation of Gold Glyconanoparticles by Direct Reaction of ω-Glycosilated Alkylsulfanylanilines and $HAuCl_4$

Ryuich Takegawa, Satoaki Onitsuka, Toshiyuki Hamada, Jun-ich Kurawaki, and Hiroaki Okamura

Department of Chemistry and Bioscience, Graduate School of Science and Engineering, Kagoshima University, Kagoshima, Japan

Gold glyconanoparticles were easily prepared by simply mixing $HAuCl_4$ and ω-glycosilated alkylsulfanylanilines in methanol. The ^{1}H NMR and absorption spectra and TEM images of the resulting nanoparticles indicated the formation of aggregated nanoparticles that were covered with sugar molecules. The specific and reversible interaction of the glyconanoparticles and lectin protein (concanavalin A, Con A) was also confirmed.

We have earlier reported a new method to prepare stable gold nanoparticles covered with a single organic species using $HAuCl_4$ and *N*-acylbenzenethiol, where benzenethiol acts as a "reductive stabilizer" that reduces the Au^{3+} ion and stabilizes the resulting gold nanoparticles by coordinating to their surfaces [1].

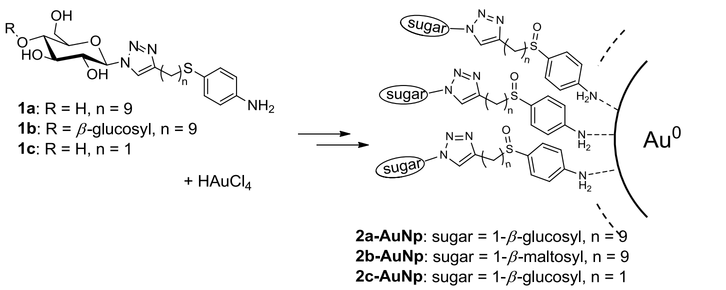

Scheme 1 Plausible structure of gold glyconanoparticle

Using this result, we developed new reductive stabilizers, ω-glycosilated alkylsulfanylaniline **1a**-**c**, which spontaneously afforded gold glyconanoparticles when mixed with $HAuCl_4$ in methanol. The expected pathway to form the gold glyconanoparticle and its plausible structure are shown in Scheme 1. The absorption spectrum and TEM image of the resulting deep-blue solution clearly indicated the formation of aggregated nanoparticles, which may be constructed by interparticle hydrogen bonding of the surface sugar moiety (Fig. 1).

The specific and reversible interaction of the glyconanoparticle **2c-AuNp** and Con A was confirmed by the formation of an orange precipitate of the **2c-AuNp**-Con A aggregate, which was dissolved by the subsequent addition of mannose.

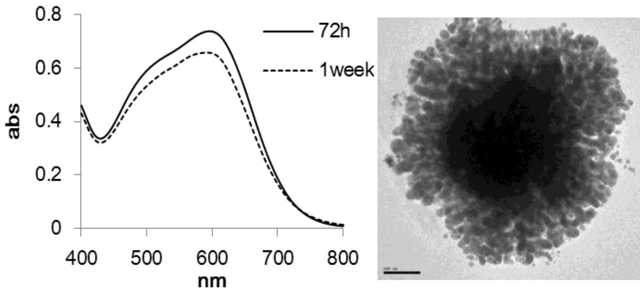

Fig. 1 Absorption of spectra (left) and TEM image (right, scale bar 100 nm) of **2a**-**AuNp**

Reference

[1] H. Okamura, J. Kurawaki, T. Iwagawa, T. Hamada, M. Kawashima, Chem. Lett. 39 (2010) 1258-1260.

Nanopore devices for rapid structural analysis of Nanomaterials

Sou Ryuzaki,[1] Masateru Taniguchi,[2] Koichi Okamoto,[1] and Kaoru Tamada[1]

[1] *Institute for Materials Chemistry and Engineering, Kyushu University, Fukuoka, Japan*
[2] *The Institute of Scientific and Industrial Research, Osaka University, Osaka, Japan*

Rapid structural analysis methods for biomolecules consisting of single or several molecules in solution represent innovative technologies to reveal their functions because the functions strongly depend on their own structures. However, there presently exist no rapid structural analysis methods for single nanomaterials in solutions. Nanopore technologies have the capacity to investigate the volume and shape of single nanomaterials in solutions owing to changes in ionic currents passing through the nanopores. Nanopores must have high spatial and time resolutions to determine the structures of single nanomaterials.

Here we report the development of low-aspect-ratio nanopores with a spatial resolution of 35.5 nm and a fast current amplifier, resulting in realization of ultrafast time resolutions of 1.0 μs. Combining state-of-the-art technologies with multiphysics simulation methods to translate ionic current data into structures of nanomaterials passing through a nanopore, we have achieved rapid structural analysis of single gold nanorods, single polystyrene (Pst) beads, and single dumbbell-like Pst beads in aqueous solutions. The present nanopore devices will be innovative technologies for the fields of nanobiodevices and structural biology.

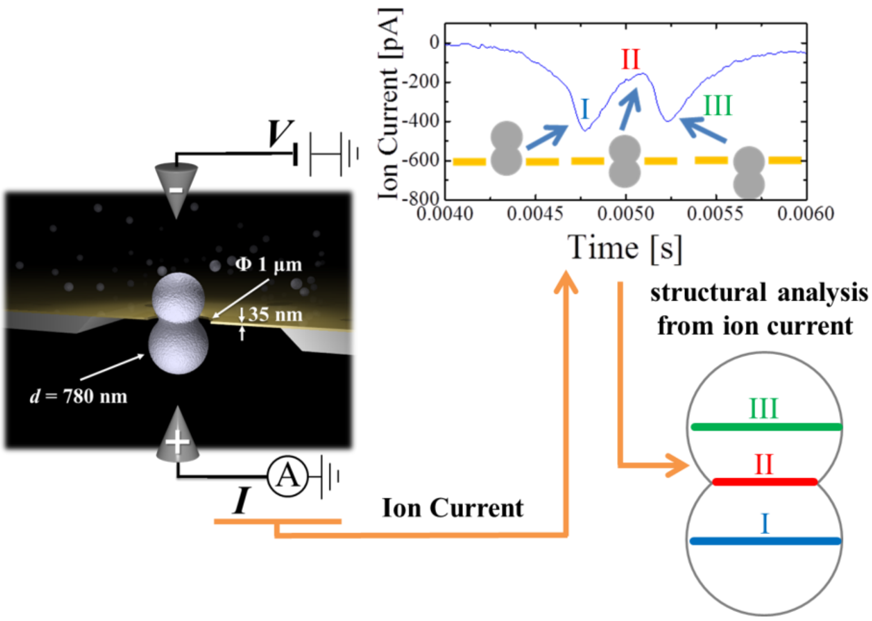

Figure 1. Schematic illustration of the present structural analysis method using a nanopore. A low aspect ratio nanopore is capable of structural analysis like a 3D scanner because the shape of ion current blockade due to a material translocation in a nanopore reflects the tomograms of the material passing through the nanopore.

Silver acetylide nano helical structure induced by impurities

Shota Ito,[1] Yoshikiyo Hatakeyama,[1] and Ken Judai[1]

[1] *Department of Physics, College of Humanities and Sciences, Nihon University, Tokyo, Japan*

Silver tolylacetylide does not have chiral center carbon, and is an achiral molecule. However, it turned out that twisted nano ribbon structures, chiral helices, were generated by recrystallization in solution phase. We have investigated for the chiral origin how the achiral molecules aggregate to the chiral nano helical structure. The solvent for recrystallization was changed between methanol, ethanol, 1-propanol, and 1-butanol systematically. Fast recrystallization solvent such as methanol was observed as twisted nanoribbon structures, and the other side, slower solvent such as 1-butanol was as straight non-twisted nanoribbon structures. Helical and non-helical structures can be controlled by recrystallization solvent. Crystallization speed, in other words, quality of crystal by crystallization kinetics is important for twisted nanoribbon structure [1].

An additional experiment showed that light irradiation made solution color changing to red and enhancement of twisting nanoribbon structures. The light irradiation produced decomposition of silver acetylide and dimerization reaction. The dimerization of acetylide indicated red color, and displacement of crystal by the decomposed compounds enhanced crystal tension and twisting.

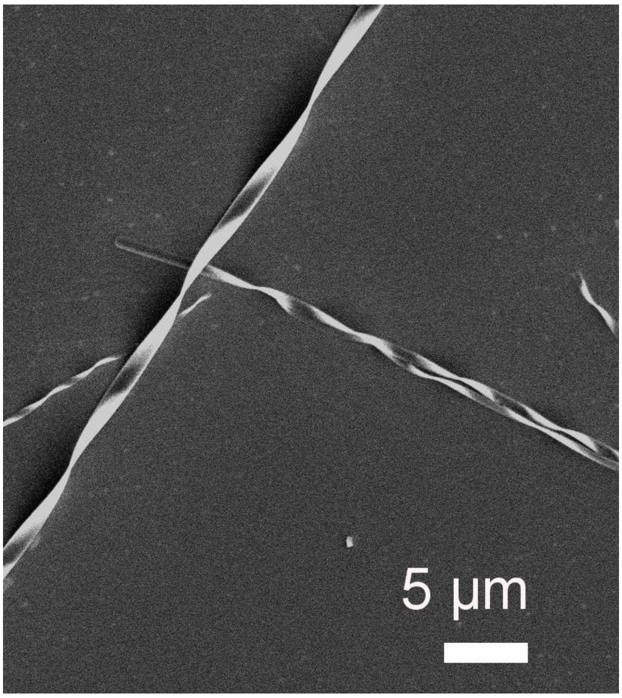

Figure: Scanning Electron Microscopy (SEM) image of twisted silver tolylacetylide.

Reference

[1] K. Judai, Y. Hatakeyama, and J. Nishijo, *J. Nanosci.* (2013) 545430.

Rapid cooling of isolated small carbon cluster anions

Takeshi Furukawa,[1] Naoko Kono,[1] Gen Ito,[1] Jun Matsumoto,[2] Hajime Tanuma,[1] Toshiyuki Azuma,[3] Klavs Hansen,[4] and Haruo Shiromaru[2]

[1] *Department of Physics, Tokyo Metropolitan University, Tokyo, Japan*
[2] *Department of Chemistry, Tokyo Metropolitan University, Tokyo, Japan*
[3] *Atomic, Molecular and Optical Physics Laboratory, RIKEN, Saitama, Japan*
[4] *Department of Physics, University of Gothenburg, Gothenburg, Sweden*

For vibrationally excited molecules, radiative cooling is usually a rather inefficient cooling pathway. We have found that even-numbered carbon cluster anions radiate significantly faster than odd-numbered ones, and much faster than by infrared (IR) radiation. Chain-form neutral carbon clusters have filled or half-filled degenerate highest π orbitals depending on the parity. This is the origin of the even/odd alternation in the electron affinities. It will also be reflected in the excitation spectra of the anions, and in the even/odd alternation in the radiative cooling of small carbon cluster anions.

The experiments were performed using the electrostatic ion storage ring at TMU, where we observed time-resolved electron emission from $C_{4\text{-}7}^-$ anions on the timescale of a hundred microsecond and longer after laser excitation [1]. The decays were observed to be thermal. For C_5^- and C_7^-, the time profile of the emission rate in the delayed reaction shows that the anions were cooled slowly by IR radiations (timescale: tens of millisecond). On the other hand, the electron emission rate of C_4^- and C_6^- after laser excitation decreased anomalously fast, on less than a few tens of microseconds. By comparing the calculated emission rates, we concluded that this process was due to the electronic transitions *via* low-lying electronic excited states after the inverse internal conversion (IIC) process, i.e., the conversion of energy from vibrationally excited states to electronically excited states. Although this IIC process is usually suppressed due to the small statistical weight of the excited state, it may dominate the cooling dynamics for isolated molecules. It should be noted that IIC-accelerated cooling of trapped ions has so far been found only for large molecular ions (e.g. anthracene cation [2]) and the fast cooling of $C_{4,6}^-$ shows that the mechanism is present also for very small ions. For the evolution of interstellar molecules, where two-body collisions produce highly excited products and radiative cooling determines whether they survive intact, the IIC process will be more important for smaller molecules.

References

[1] M. Goto et al., J. Chem. Phys. 139 (2013) 054306; K. Najafian, et al., J. Chem. Phys. 140 (2014) 104311; G. Ito et al., Phys. Rev. Lett. 112 (2014) 183001.
[2] S. Martin et al., Phys. Rev. Lett. 110 (2013) 163003.

Radiative cooling of laser-heated niobium clusters

Klavs Hansen,[1] Yejun Li,[2] Vladimir Kaydashev,[2] and Ewald Janssens[2]

[1] *Department of Physics, University of Gothenburg, 41296 Gothenburg, Sweden*
[2] *Laboratory of Solid State Physics and Magnetism, KU Leuven, 3001 Leuven, Belgium*

Thermal radiation and thermionic emission have been established as important decay channels of highly excited clusters that are made of refractory materials [1,2]. In most materials, the activation energy for evaporation of a massive fragment (atom or molecule) is lower than the ionization energy, which strongly favors loss of atoms in unimolecular reactions. For refractory materials, the high binding energy makes the thermionic emission channel competitive and also radiative cooling, i.e., thermal emission of photons, appears on the timescale (about 100 μs) defined by molecular beam devices [3]. Thermal photon emission is not an activated process and is only suppressed relative to atomic evaporation due to the large frequency factor of the latter. This is different at low energy where a crossover from atomic evaporation or thermionic emission to radiative cooling occurs.

Clusters of niobium are known to emit atoms, electrons, and photons in thermal processes on the nano- and microsecond timescales [4]. Only a few experimental studies tried to quantify the radiation emitted by recording the black-body radiation spectra of laser-heated clusters and of clusters heated by oxidation [5].

In the present work, we study for the first time the competition between atomic evaporation and thermionic emission as decay channels of excited size-selected refractory metal clusters. The radiative cooling of small laser-heated Nb_n^+ ($8 \leq n \leq 22$) clusters has been measured. The emitted power was determined by the quenching effect on the metastable decay, employing two different experimental protocols. The radiative power decreases slightly with cluster size and shows no strong size-to-size variations. The magnitude is 40-50 keV/s at the timescale of several microseconds, which is the measured crossover time from evaporative to radiative cooling.

Reference(s)

[1] G. Ganteför et al., Phys. Rev. Lett. 77 (1996) 4524.
[2] Y. Toker et al., Phys. Rev. A 76 (2007) 053201.
[3] K. Hansen and E.E.B. Campbell, J. Chem. Phys. 104 (1996) 5012.
[4] V.J.F. Lapoutre et al., J. Chem. Phys. 139 (2013) 121101.
[5] U. Frenzel et al., Z. Phys. D 40 (1997) 108.

Adsorbing carbon dioxide on fullerenes at 0.37K under the influence of charge: a mass spectrometric and molecular dynamics/DFT study

Stefan Ralser[1], Johannes Postler[1], Alexander Kaiser[1], M. Probst[1], S. Denifl[1], Diethard K. Böhme[2], and Paul Scheier[1]

[1] *Institut für Ionenphysik und Angewandte Physik, Universität Innsbruck, Austria*
[2] *Department of Chemistry,York University, Toronto, ON, Canada M3J 1P3*

In the current era of climate change, it is essential to know and to understand the basic properties of constituents involved in this phenomenon. Especially the binding of greenhouse gases to suitable materials is of particular interest to find efficient sinks that will reduce the amount of such substances in the atmosphere [1]. In the present study, we focus on the greenhouse gas carbon dioxide and its adsorption properties on carbonaceous materials. In this context, various materials including graphites, graphenes and nanotubes have been explored [2, 3, 4]. Here we report the adsorption of CO_2 on neutral and charged buckminster fullerenes (C_{60}).

C_{60}, together with CO_2 is embedded in superfluid helium nanodroplets at 0.37K via a pickup process. Electron collisions with the doped He nanodroplets results in charged complexes of the form $C_{60}(CO_2)_n$ that are analyzed utilizing mass spectrometry.

For cationic clusters significantly more CO_2 molecules can be accommodated in the first shell around the C_{60} fullerene. According to molecular dynamic simulations and DFT calculations, this gain results from a reorientation of the CO_2 axis with respect to the center of the positively charged C_{60}. Mass spectrometrically determined shell closures are 35 and 48 for the anions and cations, respectively which agrees very well with the calculated shell closures. The first shell of CO_2 around a neutral C_{60} contains 44 molecules according to our simulations.

This work was supported by the FWF, Wien (P23657, I978 and P26635)

References

[1] D.M. D'Alessandro, B. Smit and J.R. Long, Angew. Chem. Int. Ed.49 (2010) 6058-6082
[2] E.J. Bottani, V. Bakaev and W. Steele, Chem. Eng. Sci. 49 (1994) 2931-2939
[3] A. Kumar M.S. Ramaprabhu, AIP Advances 1 (2011) 032152
[4] M. Cinke et. al., Chem. Phys. Lett. 376 (2003) 761-766

Entropy-driven isomer switching in $Fe^+(H_2O)_n$ probed with IR spectroscopy and free-energy calculations

Kazuhiko Ohashi,[1] Jun Sasaki,[1] Gun Yamamoto,[1]
Ken Judai,[2] Nobuyuki Nishi,[2] and Hiroshi Sekiya[1]

[1] *Department of Chemistry, Kyushu University, Fukuoka, Japan*
[2] *Institute for Molecular Science, Okazaki, Japan*

We have investigated coordination and solvation structures of metal ions through gas-phase spectroscopy. For $Fe^+(H_2O)_n$ (n = 3–8), we already reported IR photodissociation spectra in the OH stretch region [1]. The spectral features were consistent with isomers with 2-fold linear coordination, but they were not lowest in energy from DFT calculations. We aim at resolving the discrepancy by considering temperature (entropy) effects on isomer distributions of $Fe^+(H_2O)_n$.

Geometries of $Fe^+(H_2O)_n$ were optimized and harmonic vibrational frequencies were computed at the B3LYP/6-311+G(2df) level by using GAUSSIAN 09 package. Partition functions and then free energies of low-lying isomers were evaluated under rigid-rotor/harmonic-oscillator approximation.

Here we focus on $Fe^+(H_2O)_8$; figure displays the optimized geometries and free energies of three isomers of $Fe^+(H_2O)_8$ with a coordination number of 2, 3, and 4. (4+4) is lowest in free energy at T = 0–75 K. The ordering of (4+4) and (2+4+2) inverts at 75 K and that of (4+4) and (3+5) at 200 K. (2+4+2) becomes increasingly stable with increasing temperature. At 250–300 K, (4+4) and (3+5) are higher in free energy than (2+4+2) by 24–31 and 19–21 kJ mol^{-1}, respectively.

At lowest T, (4+4) should be dominant, because it is favorable in enthalpy. Meanwhile, (2+4+2) has a larger number of lower-frequency vibrations than (4+4), because outer-shell waters are bound less rigidly; their contribution to entropy is rather large. Owing to the entropy effect, (2+4+2) becomes abundant at higher T. We conclude that IR observation of 2-coordinated isomers is reasonable, because T = 250–300 K is estimated for $Fe^+(H_2O)_{5\text{–}8}$ under investigation.

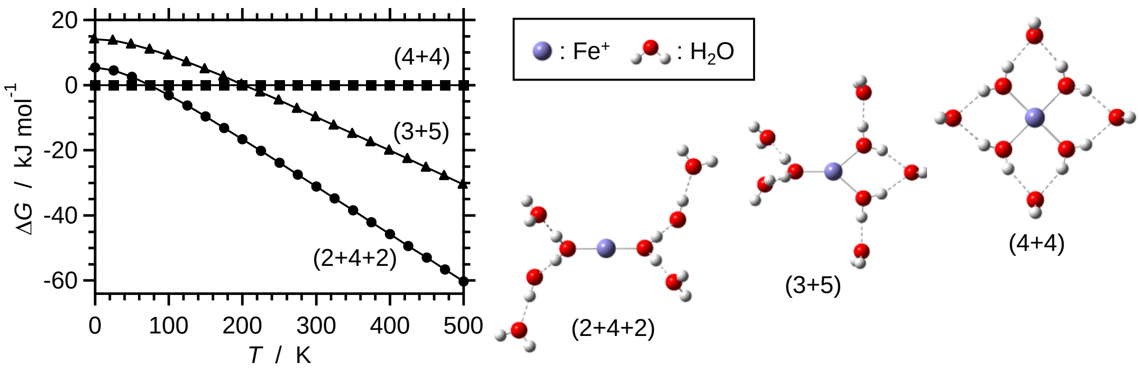

Fig. Optimized geometries for three isomers of $Fe^+(H_2O)_8$ and free energy of (2+4+2) and (3+5) relative to (4+4) as a function of temperature in the 0–500 K range.

[1] K. Ohashi et al., ISSPIC XVI (2012) A30.

Syntheses of Au@PdAg and Au@PdAg@Ag core–shell Nnanorods through distortion induced alloying between Pd shells and Ag atoms over Au nanorods

Masaharu Tsuji,[1,2,3] Koichi Takemura,[2] Chihiro Shiraishi,[2] Keiko Uto,[1] Atsuhiko Yajima,[3] Masashi Hattori,[1] and Takeshi Daio[4]

[1] *Institute for Materials Chemistry and Engineering, Kyushu University, Kasuga, Japan*
[2] *Department of Applied Science for Electronics and Materials, Kyushu University, Kasuga, Japan*
[3] *Department of Automotive Science, Kyushu University, Kasuga, Japan*
[4] *International Research Center for Hydrogen Energy, Kyushu University, Fukuoka, Japan*

Nobel Au@PdAg and Au@PdAg@Ag core–shell nanorods (NRs) having PdAg alloy shells were synthesized using Au@Pd NRs as seeds. Their crystal structures and growth mechanisms were examined using transmission electron microscopic (TEM), TEM–energy dispersed X-ray spectroscopic (EDS), XRD, ultraviolet (UV)–visible (Vis)–near infrared (NIR) extinction spectroscopic data. In the first step, rectangular or dumbbell-type Au@Pd seeds were prepared by reducing H_2PdCl_4 with ascorbic acid in an aqueous solution in the presence of Au NRs as seeds and cetyl trimethyl ammonium bromide (CTAB).[1] In the second step, when Ag^+ ions were reduced with ascorbic acid and CTAB in the presence of rectangular or dumbbell-type Au@Pd NRs as seeds and CTAB, Au core PdAg alloy shells were formed with maximum Ag contents of about 16 or 24%, respectively, after 10 min heating at 60 °C. The driving force of alloying between Pd shells and Ag atoms is distortion of Pd layers over Au NRs on the basis of peak shifts and broadening of XRD data. At longer reaction times over 10 min, the content of Ag exceeds its maximum solubility in Pd shells, and then the second Ag shells were epitaxially grown over Au@PdAg NRs via a single island-growth mechanism. In this mechanism, crystal growth of Ag shells over Au@Pd-Ag cores starts from the formation of single nuclei on a wide side PdAg alloy facet followed by growth to one rectangular rod shell and further growth of neighboring rectangular rod shells having {100} facets, as shown in Fig. 1.

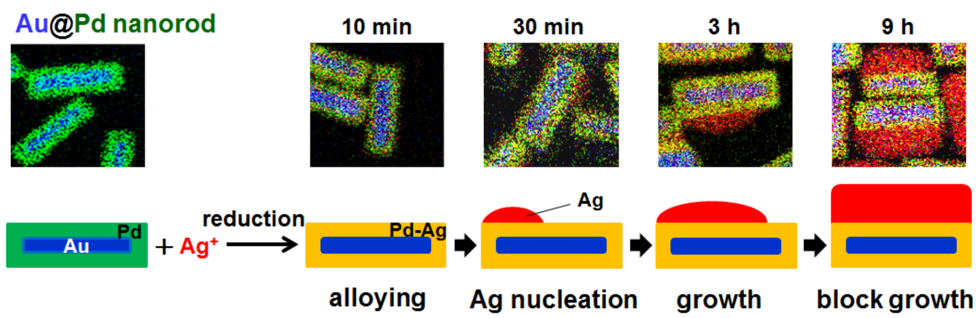

Fig. 1. TEM-EDS images and growth mechanism of rectangular Au@PdAg@Ag nanorod.

Reference
[1] M. Tsuji, K. Ikedo, K. Uto, M. Matsunaga, Y. Yoshida, et al., CrystEngComm, 15 (2013) 6553.

Ligand-protected gold clusters with novel interfacial structures

Prasenjit Maity,[1] Jun-ichi Nishigaki,[1] Tatsuya Tsukuda[1,2]

[1] *Department of Chemistry, School of Science, The University of Tokyo, Tokyo, Japan*
[2] *Elements Strategy Initiative for Catalysts and Batteries, Kyoto University, Kyoto, Japan*

We present two topics on development of new ligand-protected Au clusters by controlling the interfacial structures.

1. Protection of Gold Clusters by Bulky Thiolates [1, 2]

Bulky arenethiols, EindSH (Eind = 1,1,3,3,5,5,7,7-octaethyl-*s*-hydrindacen-4-yl) and DppSH (Dpp = 2,6-diphenylphenyl), were used as protecting ligands with an aim to suppress the formation of –SR–[Au(I)–SR–]$_n$ oligomers on the Au core. $Au_{41}(SEind)_{12}$ and $Au_{25}(SDpp)_{11}$ were obtained by mixing of the hydrosol of small (diameter<2 nm) PVP-stabilized Au clusters and the toluene solution of the corresponding thiol and subsequent etching process. As expected, the ligand-to-Au ratios of $Au_{41}(SEind)_{12}$ and $Au_{25}(SDpp)_{11}$ are significantly smaller than those of Au:SR reported so far. Structural characterization of these isolated clusters suggests that the bulky thiolates are bonded directly to the surface of Au_{41} with twisted pyramidal motif and Au_{25} with vertex-shared bi-icosahedral motif.

2. Protection of Gold Clusters by Terminal Alkynes [3–5]

Gold clusters protected by terminal alkynes, 1-octyne (OC-H), phenyl acetylene (PA-H) and 9-ethynyl-phenanthrene (EPT-H), were prepared by the ligand exchange of the small (diameter<2 nm) Au:PVP clusters. Vibrational spectroscopy revealed that the terminal hydrogen is lost during the ligand exchange. A series of precisely-defined gold clusters, $Au_{34}(PA)_{16}$, $Au_{54}(PA)_{26}$, $Au_{30}(EPT)_{13}$, $Au_{35}(EPT)_{18}$, and $Au_{41\text{-}43}(EPT)_{21\text{-}23}$, were synthesized and characterized in detail to obtain further insight into the interfacial structures. An upright configuration of the alkynes on Au clusters was suggested from the Au to alkyne ratios and photoluminescence from the excimer of the EPT ligands. EXAFS analysis implied that alkynyl carbon is bound to bridged or hollow sites on the Au cluster surface.

Reference(s)

[1] J. Nishigaki, R. Tsunoyama, H. Tsunoyama, N. Ichikuni, S. Yamazoe, Y. Negishi, M. Itoh, T. Matsuo, K. Tamao, and T. Tsukuda, *J. Am. Chem. Soc.* 134 (2012) 14295.
[2] J. Nishigaki, S. Yamazoe, S. Kohara, A. Fujiwara, W. Kurashige, Y. Negishi, and T. Tsukuda, *Chem. Commun.* 50 (2014) 839.
[3] P. Maity, H. Tsunoyama, M. Yamauchi, S. Xie, and T. Tsukuda, *J. Am. Chem. Soc.* 133 (2011) 20123.
[4] P. Maity, T. Wakabayashi, N. Ichikuni, H. Tsunoyama, S. Xie, M. Yamauchi, and T. Tsukuda, *Chem. Commun.* 48 (2012) 6085.
[5] P. Maity, S. Takano, S. Yamazoe, T. Wakabayashi, and T. Tsukuda, *J. Am. Chem. Soc.* 135 (2013) 9450.

Isolation and properties of chiral $Pd_2Au_{36}(SR)_{24}$ cluster

Noelia Barrabés,[1] Bei Zhang,[1] Houhua Li,[2] Kaziz Sameh,[3] Dawid Wodka,[1] Clément Mazet,[2] Jordi Llorca[4] and Thomas Bürgi[1]

[1] *Depart. of Physical Chemistry*, *University of Geneva, Geneva, Switzerland*

[2] *Depart. of Organic Chemistry*, *University of Geneva, Geneva, Switzerland*

[3] *Depart. of Industrial Engineering, Superior National School of engineers of Tunis, Tunis, Tunisia*

[4] *Institute of Energy Technologies and Centre for Research in Nano Engineering, Technical University of Catalonia, Barcelona, Spain*

Doping of thiolated gold nanoclusters ($Au_n(SR)_m$) with metals such as Pd or Pt leads to the stability and properties enhancement of $Au_n(SR)_m$ clusters [1]. One of the most promising property of some of $Au_x(SR)_n$ clusters is their intrinsic chirality even though the stabilizing ligand is achiral. However, up to now not much attention has been paid to the chirality of doped thiolate-protected gold nanoclusters. Following a reported synthesis protocol [2], $Pd_xAu_{n-x}(SR)_{24}$ nanoclusters have been synthesized and separated by chiral HPLC chromatography leading to the isolation of the two enantiomeric forms of $Pd_2Au_{36}(SR)_{24}$, which show chiroptical signal by circular dichroism (CD) spectroscopy.

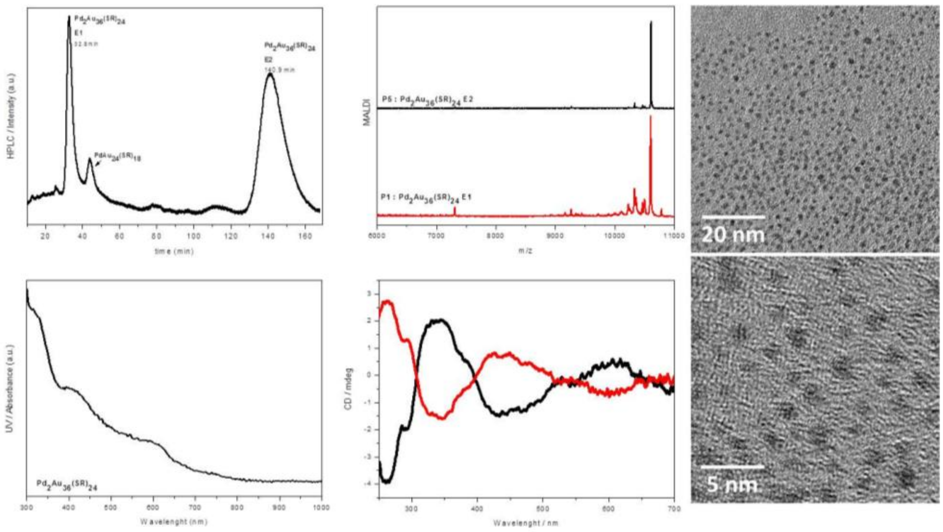

Figure 1. Isolation and characterization of enantiopure $Pd_2Au_{36}(SR)_{24}$

The ability to separate and store enantiomers of Pd doped clusters at room temperature enables us to study their racemization by CD and their structure by XAFS, XPS and HRTEM. It revealed the possibility of Pd doping at the surface of the thiolated gold cluster. Furthermore, Pd doping substantially affects the flexibility of the Au(Pd) – S interface.

References

[1] R.Jin and K.Nobusada, *Nano Research.* 7 (2014) 285

[2] Y.Negishi,K.Igarashi, K.Munakata, W.Ohgake and K.Nobusada,*Chem.Commun.*48(2012) 660

Alternate shell structure in Fe-Co nanoparticles

Bheema Lingam Chittari[1] and Vijay Kumar,[1,2]

[1]*Dr. Vijay Kumar Foundation(VKF), 1969 Sector 4, Gurgaon 122001, Haryana, India*
[2]*Center for Informatics, School of Natural Sciences, Shiv Nadar University, Chithera, Gautam Budh Nagar - 203207, U.P., India*

FeCo alloys have received much attention because of their high permeability and saturation magnetization in magnetic applications. Nanoalloys of Fe-Co are of interest as the magnetic moments in nanoparticles are generally enhanced as it is the case for pure Fe clusters and assemblies of such nanoparticles are attractive for developing improved magnets. It is important to understand the atomic distributions in such nanoparticles as the magnetic behavior could be sensitive to the distribution of atoms. We have explored from *ab initio* calculations the atomic structure and alloying behavior in small nanoparticles of Fe-Co alloys by considering 55-atom Mackay icosahedron of Fe-Co in which a 13-atom icosahedron is covered by 42 atoms. This has 20 triangular faces, 12 vertices and 30 atoms on the edges. We optimized different distributions of Fe and Co atoms and find that the optimized structures remain icosahedral and are ferromagnetic. Among all the distributions we studied, the one with alternate shells of Co-Fe_{12}-Co_{42} has the lowest energy with 4.5 eV/atom binding energy and 107 μ_B magnetic moments. In the case when Fe atoms form the complete core (Fe_{13}) and Co atoms form a complete shell i.e $Fe_{13}Co_{42}$ core-shell structure, we find that the energy is 0.43 eV higher and the magnetic moments increase to 108 μ_B. Our results suggest that Fe atoms are preferred in the core and Co on the surface and this is in agreement with the notion that the element with lower surface energy tend be on the surface. In the lowest energy alternate shell structure the magnetic moment on each Fe atom is 2.4 μ_B, the central Co atom has 0.9 μ_B whereas each of 30 edge Co atoms has 1.7 μ_B and the 12 vertex atoms have 1.9 μ_B magnetic moments. We shall further discus the charge transfer and electronic structure in these nanoalloys.

This work has been supported by the Asian Office of Aerospace Research and Development (AOARD)

[1] B.L. Chittari and V. Kumar, to be published.

Bond Length Analysis of Au Nanoparticles Synthesized in Ionic Liquids

Yoshikiyo Hatakeyama,[1] Kiyotaka Asakura,[2] Ken Judai,[1] and Keiko Nishikawa[3]

[1] *College of Humanities and Sciences, Nihon University, Tokyo, Japan*
[2] *Catalysis Research Center, Hokkaido University, Hokkaido, Japan*
[3] *Graduate School of Advanced Integration Science, Chiba University, Chiba, Japan*

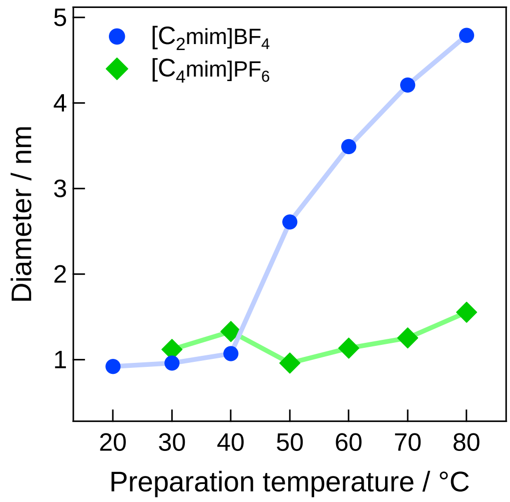

Figure 1. The size of maximum abundance in AuNPs in two ionic liquids.

Au nanoparticles (AuNPs) of varied sizes were synthesized in ionic liquids using sputter deposition technique. As these AuNPs are dispersed freely in each ionic liquid without any stabilizing agents, they are occasionally called naked-AuNPs. To characterize the structure of AuNPs, the values of peak positions were extracted as the size of maximum abundance in AuNPs in each ionic liquid from size distribution curve obtained by small-angle X-ray scattering (SAXS). Figure 1 shows the size of maximum abundance in AuNPs synthesized in 1-ethyl-3-methyl imidazolium tetrafluoroborate ([C_2mim]BF_4) and 1-butyl-3-methyl imidazolium hexafluorophosphate ([C_4mim]PF_6). Their sizes were controlled by the types of ionic liquid[1] and the temperatures[2] during sputter deposition. To elucidate the Au-Au bond length of AuNPs in relation to the particle size, X-ray absorption fine structures (XAFS) at Au L_3-edge were measured. From the analyses of XAFS, it was revealed that the bond lengths of Au-Au for AuNPs with the size of about 1nm are 2.76–2.81 Å in contrast to 2.88 Å for bulk Au. Comparing our present results by SAXS and XAFS with previously-reported theoretical studies, we come to the conclusion that the surfaced Au atoms of the naked-AuNPs in ionic liquids have shorter bond length compared to inner atoms.

Acknowledgement

XAFS experiments were performed under the approval of the Photon Factory Program Advisory Committee (Proposal No. 2007G518 and 2009G090). The present study was supported by a Grand-in-Aid for Scientific Research (No. 17073002 for K. N.) on Priority Area "Science on Ionic Liquids" from the Ministry of Education, Culture, Sports, Science and Technology of Japan.

References

[1] Y. Hatakeyama, M. Okamoto, T. Torimoto, S. Kuwabata, and K. Nishikawa, J. Phys. Chem. C 113 (2009) 3917.
[2] Y. Hatakeyama, S. Takahashi, and K. Nishikawa, J. Phys. Chem. C 114 (2010) 11098.

withdraw

Generation of a liquid droplet in a vacuum

Kota Ando, Masashi Arakawa, and Akira Terasaki

Department of Chemistry, Kyushu University, Fukuoka, Japan

Liquids in a vacuum provide opportunities to apply gas-phase experimental techniques such as mass spectrometry to chemical species in condensed phases. For example, biological molecules are to be introduced in a manner closer to a native environment, i.e., in an aqueous solution, which can be analyzed by mass spectrometry to extract structural information about solvation. In turn, materials produced in the gas phase, such as metal clusters, are to be injected in a liquid for performing wet chemistry. These ideas motivate us to develop a method to generate a liquid droplet in a vacuum.

A schematic of the experimental apparatus is shown in Figure 1. A droplet with a diameter of 50−100 μm was generated on demand by a piezo-driven droplet nozzle, which was inserted into a vacuum chamber. The droplet was illuminated by a pulsed strobe LED and was monitored by using a camera for characterization. The liquid-sample reservoir was evacuated simultaneously with the chamber to avoid a spontaneous flow of the sample liquid into the chamber through the nozzle. The pressure inside the chamber was reduced down to 17 Pa using a rotary pump with 1.6 Ls^{-1} pumping speed.

In the present experiment, pure water and ethylene glycol were examined. The sample liquids were deaerated in advance to avoid release of solute gases in a vacuum. In the case of pure water, the droplet generation was possible down to the 17 Pa. However, when the vacuum was below the vapor pressure of water (2.3 kPa at 293 K), the droplet generation was not persistent due to occasional boiling in the nozzle. In this respect, ethylene glycol was easier to handle, enabling droplet formation regularly at 17 Pa, because its vapor pressure is much lower.

Liquid-to-solid phase transition in a vacuum was examined by illuminating the droplet with linearly polarized light; scattered light should be depolarized, when a droplet is frozen. However, it was found that a pure water droplet is not frozen even at 8.2 ms after generation at 21 Pa. The survival of the liquid phase was further supported by thermodynamic simulation of droplet temperature as a function of time. Figure 2 shows a cooling rate calculated for a water droplet with 74-μm in diameter at 0 Pa. The temperature was predicted to be 240 K at 8.2 ms after generation. This result implies that evaporative cooling down to 240 K is too fast for the water droplet to be frozen. This is consistent with a previous report on homogeneous nucleation rates in a nitrogen atmosphere showing a time constant of more than tens of second at 240 K [1].

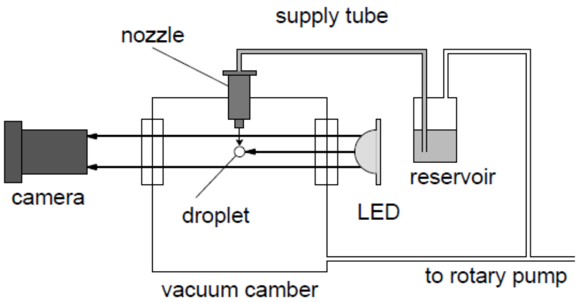

Figure 1. Experimental apparatus

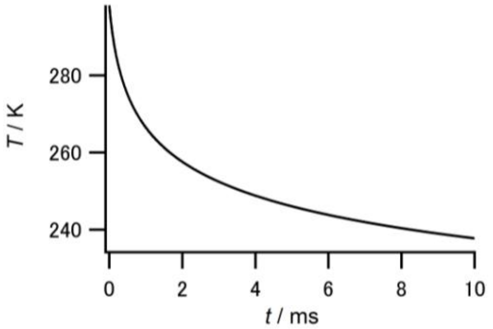

Figure 2. A cooling rate calculated for a water droplet with 74-μm in diameter at 0 Pa

[1] P Stöckel, I. M. Weidinger, H. Baumgärtel, and T. Leisner, J. Phys. Chem. A 109 (2005) 2540

Vibrational properties of metal nanoparticles: From structural dependence to intrinsic damping

Huziel E. Sauceda,[1] Israel Acuña-Galván,[2,3] and Ignacio L. Garzón[1]

[1] *Instituto de Física, Universidad Nacional Autónoma de México, Apartado Postal 20-364, 01000 México, D.F., Mexico*
[2] *Centro Universitario UAEM Zumpango, Estado de México, C.P. 55600, Mexico*
[3] *Escuela Superior de Tizayuca, UAEH, Hidalgo, C.P. 43800, Mexico*

The experimental and theoretical study of vibrations of metal nanoparticles has become a fruitful research field because of the lack of answers to fundamental questions as well as the potential applications in Nanotechnology. Here, we report a detailed analysis on the morphological dependence of the vibrational density of states (VDOS) for crystalline (FCC) as well as icosahedral and decahedral silver and gold nanoparticles (NP). Gold nanorods (GNR) of similar size are also studied. On the other hand, a careful study of the intrinsic damping of the launched breathing mode (BM) on a gold NP is presented. The interactions between metal atoms were modeled by the n-body Gupta potential. Using the well-known fact that the VDOS strongly depends on the morphology of the NP[1,2] and recent experimental measurements of the VDOS for Ag and Au NP[3,4], we have deduced the crystalline structure of the NP from the experiment by a direct comparison of the VDOS (see Figure). In the study of the launched BM, we obtain a simple linear dependence of the damping time with temperature, t_D=-aT+b, and consequently, the quality factor also depends in the same way. For applications of metal NP as a nanoresonators, this is a very important result because it describes the behavior of the system's quality factor under changes of temperature.

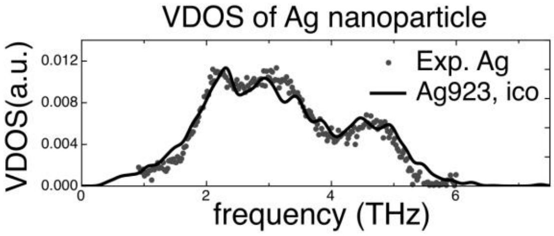

References

[1] H.E. Sauceda, D. Mongin, P. Maioli, A. Crut, M. Pellarin, N. Del Fatti, F. Vallée and I.L. Garzón, J. Phys. Chem. C 116 (2012) 25147.

[2] H.E. Sauceda, F. Salazar, L.A. Pérez and I.L. Garzón, J. Phys. Chem. C 117 (2013) 25160.

[3] M. Bayle, P. Benzo, N. Combe, C. Gatel, C. Bonafos, G. Benassayag, R. Carles, Phys. Rev. B 89 (2014) 195402.

[4] M. Bayle, N. Combe, N. Sangeetha, G. Viau, R. Carles, Nanoscale (2014), accepted.

An incorporation of the concept of a bifurcation pathway to global reaction route mapping analyses: An application to Au_5 cluster

Tetsuya Taketsugu,[1,2] Yu Harabuchi,[1] Yuriko Ono,[1] and Satoshi Maeda[1,2]

[1] *Department of Chemistry, Faculty of Science, Hokkaido University, Sapporo, Japan*
[2] *Elements Strategy Initiative for Catalysts and Batteries, Kyoto University, Kyoto, Japan*

For a given polyatomic system, the global reaction route mapping (GRRM) analyses can give a global map of reaction pathways which connect all possible minima *via* the corresponding transition states (TSs) through the respective intrinsic reaction coordinates (IRCs) on the potential energy surface (PES) [1]. The IRC is determined definitely as a steepest descent pathway in mass-weighted coordinates, starting from TS to reactant and product minima, for each elementary reaction. Sometimes the IRC accompanies a valley-ridge inflection (VRI) point, which causes a bifurcation of the valley paths. Fig. 1 illustrates two different cases of VRI occurrences: (a) non-totally symmetric VRI and (b) totally symmetric VRI. As shown in Fig. 1, the IRC itself cannot bifurcate at VRI points because a direction of the IRC is defined mathematically as the negative energy gradient. Therefore, in a global map of reaction pathways obtained by GRRM analyses, the bifurcation of reaction pathways are not taken into account.

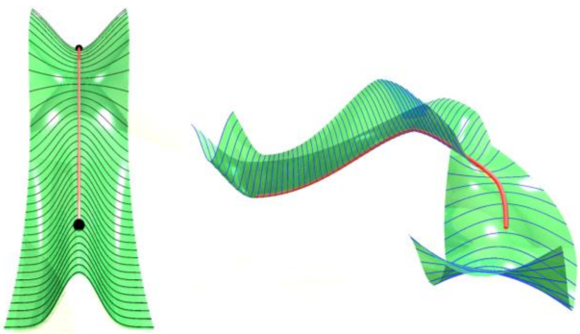

(a) non-totally symmetric (b) totally symmetric

Fig. 1. Schematic illustrations of VRI occurrences

The bifurcation of reaction pathways has been studied in many aspects [2-6], but all previous studies focused on the specific reaction pathway of the specific reaction. In the present study, we first applied the GRRM analyses to Au_5 cluster, as an example, by DFT(PBEPBE)/lanL2DZ calculations. It is shown that Au_5 cluster has five minima and 14 transition states, which are connected via IRCs. Then, we carried out normal mode analyses at chosen points along the respective IRCs, and calculated vibrational frequencies of all transverse modes from the projected Hessians. As the results, the VRI points are found along four different IRCs. These VRI points are successfully related to one of product minima which are not directly connected by the IRC. The detailed discussions will be give in the presentation.

References

[1] S. Maeda, K. Ohno, and K. Morokuma, Phys. Chem. Chem. Phys., **15** (2013) 3683.
[2] T. Taketsugu and T. Hirano, J. Chem. Phys., **99** (1993) 9806.
[3] T. Taketsugu, N. Tajima, and K. Hirao, J. Chem. Phys., **105** (1996) 1933.
[4] T. Yanai, T. Taketsugu, and K. Hirao, J. Chem. Phys., **107** (1997) 1137.
[5] Y. Harabuchi and T. Taketsugu, Theo. Chem. Acc., **130** (2011) 305.
[6] Y. Harabuchi, A. Nakayama, and T. Taketsugu, Comp. Theo. Chem., **1000** (2012) 70.

Stability and morphology of platinum cluster supported on silicon substrate in heating cycles

Nobuyuki Fukui,[1] and Hisato Yasumatsu,[2]

[1] *East Tokyo Laboratory, Genesis Research Institute, Inc., Ichikawa, Japan*
[2] *Cluster Research Laboratory, Toyota Technological Institute, Ichikawa, Japan*

Size selected clusters supported on a substrate are model systems appropriate for studying functional subnano-materials due to the advantage to design the surface structure precisely as well as their behaviors far different from the corresponding bulk and even nano-particles.

We have succeeded to construct monatomic –layered uni-size Pt cluster disks on a Si(111)- 7x7 surface stably at 300 K, which induce two-dimensional charge polarization[1,2]. Considering importance for their advanced application to catalysis, we investigated the stability and morphology of the cluster disks in heating cycles under a UHV condition by means of scanning tunneling microscopy (STM) [3].

It was found by statistical analysis of the STM images that the diameter and height of the cluster disk remain unchanged after heating at 673 K (see Figure1). Therefore, it is reasonable that the cluster disk is stable in heating at 673 K. Considering the diffusion of Si atoms in Pt/Si binary systems below 600K, the higher thermal stability of the Pt cluster disk on the Si(111)-7x7 surface is likely due to strong Pt-Pt interaction in the disk, which prevents the diffusion of the Si and Pt atoms into the Pt cluster disks and the silicon substrate, respectively.

However, the height of the cluster disk tends to increase with the heating temperature above 673 K. It is also reasonable that Si atoms of the substrate diffuse into the cluster disk.

When the samples are heated at 900 K, the number density of the cluster disk containing Si atoms is increased dramatically. It seems that the one or few Pt atoms in the cluster disk also start to diffuse on the substrate surface in addition to diffusion of Si atoms into the cluster disk.

After heating at 1000 K, bigger island appear on a single-crystal Si surface as a result of the diffusion of the Pt atoms into bulk.

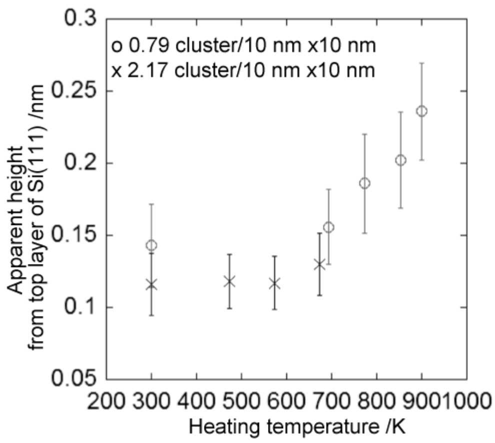

Figure 1: Temperature dependence of Apparent height of Pt_{30} disk at two cluster density

Reference(s)

[1] H.Yasumatsu et.al, J. Chem. Phys.,123(2005) 12470

[2] H.Yasumatsu et.al, Chem. Phys. Lett.,487(2010) 279

[3] N Fukui and H. Yasumatsu, Eur.Phys.J.D. 67 (2013)81/1-4

Synthesis of a novel [core+*exo*]-type heptanuclear gold cluster

Mingzhe Zhang,[1] Yukatsu Shichibu,[1,2] and Katsuaki Konishi[1,2]

[1] *Graduate School of Environmental Science, Hokkaido University, Sapporo, 060-0810, Japan*
[2] *Faculty of Environmental Earth Science, Hokkaido University, Sapporo, 060-0810, Japan*

Subnanometer-sized clusters with nuclearity of around 10 have recently attracted much interest, not only due to the fundamental aspects of their unique nuclearity- and structure-dependent optical and electronic properties but also to their potential in the development of novel nanomaterials and catalysts. Previously we have shown that $[Au_6(dppp)_4]^{2+}$ (**1**), $[Au_8(dppp)_4Cl_2]^{2+}$ and $[Au_{11}(dppe)_6]^{3+}$ (dppp = $Ph_2P(CH_2)_3PPh_2$, dppe = $Ph_2P(CH_2)_2PPh_2$) adopt unusual [core+*two*] geometries having two *exo* gold atoms attached to the polyhedral cores, and demonstrated their geometry-dependent optical properties and electronic structures [1-3]. Herein, we report the first example of trivalent heptanuclear gold cluster $[Au_7(dppp)_4]^{3+}$ (**2**) with a [core+*one*] structure. **2** synthesized by the growth reaction of **1** in the presence of silver ion (Fig.1). Single-crystal X-ray structural analysis of **2** revealed that it had an edge-sharing bi-tetrahedral core with one edge-bridging gold atom at one side of the *exo* positions. This structure can be viewed as a derivative of the precursor **1**, in which one of the *exo* gold atoms of **1** accommodate an extra Au(I). But interestingly, the growth reaction of **1** to form **2** didn't proceed by using gold ion. Like other [core+*exo*] type gold clusters, UV-vis absorption spectrum of **2** showed an isolated absorption band, which was assigned to HOMO-LUMO electronic transition. So these [core+*exo*] clusters can be considered to show common absorption properties. In addition, **2** also showed an evident photoluminescence band at 642 nm (Fig.2).

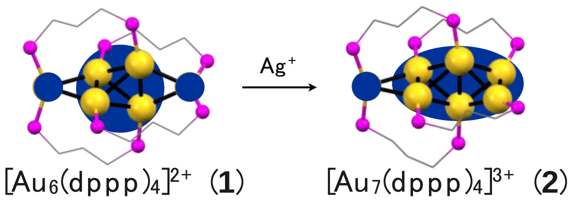

Fig.1 Skeletal structures of cluster **1** and **2**.

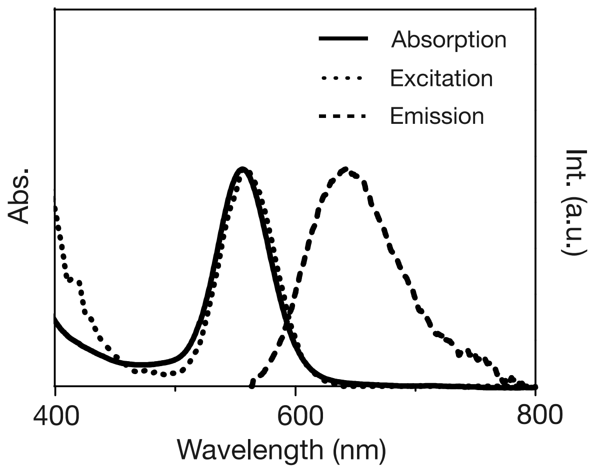

Fig.2 Absorption, emission (λ_{ex} = 555 nm) and excitation (λ_{em} = 642 nm) spectra of **2**.

References
[1] Y. Kamei, Y. Shichibu, and K. Konishi, *Angew. Chem. Int. Ed*. *50* (2011) 7442.
[2] Y. Shichibu, Y. Kamei, and K. Konishi, *Chem. Commun*. *48* (2012) 7559.
[3] Y. Shichibu, and K. Konishi, *Inorg. Chem*. *52* (2013) 6570.

Exploration on Magic Binary Nanoclusters Consisting of Silicon-Transition Metal Atoms by Reaction with Molecular Oxygen

Yoshito Sugawara,[1] Tomomi Nagase,[1] Hironori Tsunoyama,[1,2] and Atsushi Nakajima[1,2]

[1] *Department of Chemistry, Keio University, Japan*
[2] *Nakajima Designer Nanocluster Assembly Project, JST-ERATO, Japan*

Nanoclusters (NCs) with early transition metal (M=Groups 3–5 elements) encapsulated in a Si_{16} cage have been received intensive research interest[1-3] because of their size-specific stability originating from concerted electronic and geometric shell closing. Replacement of interior metal atom with other elements is one of the potential method to open up wide functionality of metal-silicon binary NCs. In this study, we investigated magic numbers in binary NCs consisting of silicon (Si) and late transition metal (M=Pd, Ni, and Rh) by utilizing a magnetron type NC ion source combined with reaction with molecular oxygen (O_2). Since the O_2 exposure causes etching reactions of NC ions, the reaction enhances the relative population of magic NC ions with metal encapsulation, such as $M@Si_{16}^{+/-}$, in M-Si binary NCs. Magic numbers in the M-Si NCs (M=Pd, Ni, and Rh) were investigated by the etching reaction and their origin was discussed based on the metal-element dependence.

Positive and negative ions of binary NCs were generated by a magnetron type NC source[4] and size distributions were monitored by a quadrupole mass spectrometer. Magic number behaviors were investigated by the comparison of mass spectra with or without the reaction with O_2; the pristine NCs were reacted with O_2 at the downstream of the NC source, which was introduced as effusive beam perpendicular to the NC beam.

Figure 1 shows representative mass spectra of Pd-Si binary NC cations with or without reaction of O_2. Without reaction of O_2, a series of Si_n^+, $PdSi_n^+$, and $Pd_2Si_n^+$ cations were observed (Fig. 1 top). After the reaction (Fig. 1 bottom), the intensities of $PdSi_{10}^+$ and $PdSi_{13}^+$ become relatively prominent as compared with the other $PdSi_n^+$ ions. The similar magic number behavior was also observed in Ni-Si binary NC cations, where both Ni and Pd belong to group 10 in the periodic table. However, the magic number behavior was not observed apparently at the same sizes in Rh (group 9)-Si binary cations after reacting with O_2, although the intensity of $RhSi_5^+$ was relatively strong. Therefore, the common magic numbers of MSi_{10}^+ and MSi_{13}^+ observed for M=Pd and Ni were attributable to isoelectronic characteristics of the binary NCs, because the atomic radii of Ni and Pd are different, while those of Rh and Pd are almost similar.

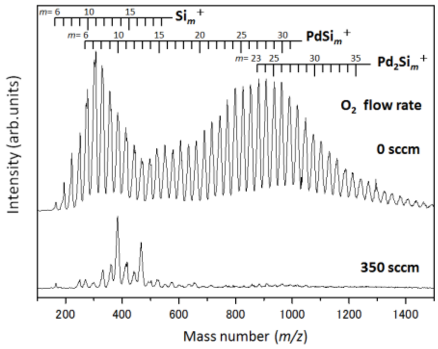

Figure 1. Mass spectra of Pd-Si NC cations.
(source conditions; Ar 122 sccm, He 200 sccm, Power 50 W)

References
[1] K. Koyasu *et al*., J. Am. Chem. Soc. 127 (2005) 4998. [2] J. T. Lau *et al*., J. Chem. Phys. 134 (2011) 041102. [3] P. Claes *et al*., Phys. Rev. Lett. 107 (2011) 173401. [4] H. Tsunoyama *et al*., Chem. Lett. 42 (2013) 857.

Preparation and redispersible solidification of monodisperse CdSe nanoparticles capped with cysteine in water

Yasuto Noda, Isao Sawakami, Takuya Kurihara, and K. Takegoshi

Division of Chemistry, Graduate School of Science, Kyoto University, Kyoto, Japan

In this presentation we report on the preparation of monodisperse CdSe nanoparticles (NPs) capped with cysteine in water and the redispersible solidification without destruction. Using solid-state NMR, we studied the details of the interaction providing the reversibility between the capping cysteine and the CdSe NPs.

The synthetic procedure of CdSe NPs is as follows: Se and Cd precursor solutions were prepared with dissolving elemental Se in Na_2SO_3 aq. and $Cd(OH)_2$ in cysteine aq. with the cysteine/Cd ratio of 4, respectively. Then the solutions were mixed in room temperature so as to be the Cd/Se ratio of 2 under pH of ca. 13 adjusted with NaOH aq. As shown Fig. 1(a), the solution showed the sharp absorption peak with the FWHM of 13 nm, which indicates monodisperse CdSe NPs were grown.

The CdSe NPs powder was obtained by adding acetone as an antisolvent to the solution after pH adjustment of 11 followed by drying with a vacuum pump after centrifugation. The absorption spectrum after redispersion of the obtained powder into water resembled one before the solidification closely as shown Fig. 1(b). Moreover, the powder XRD pattern showed any clear peaks indicating coalescence of CdSe NPs. Thus the CdSe NPs could be solidified without destruction.

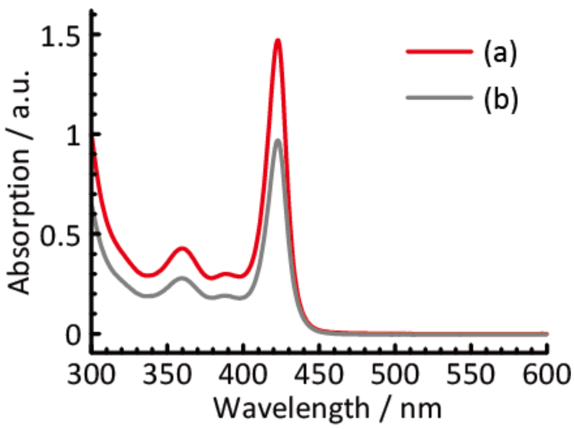

Figure 1 Absorption spectra of CdSe NPs aq. (a) just after preparation and (b) redispersed after solidification.

In order to investigate the stability of CdSe NPs, solid-state ^{13}C NMR was performed. The $\{^1H\}$-^{13}C cross-polarization magic-angle spinning NMR spectrum showed the thiol and amino groups bound to CdSe NPs, while the carbonyl group did not. Moreover, any free cysteines were observed. Thus, the CdSe NPs should be covered with cysteine monolayers.

This work is supported by JSPS KAKENHI Grant Number 25888009.

Low temperature XAFS study of thiolate-protected Au clusters

Seiji Yamazoe,[1,2] Shinjiro Takano,[1] Wataru Kurashige,[3] Yuichi Negishi,[3] and Tatsuya Tsukuda[1,2]

[1] *Department of Chemistry, School of Science, The University of Tokyo, Tokyo, Japan*
[2] *ESICB, Kyoto University, Kyoto, Japan*
[3] *Department of Applied Chemistry, Faculty of Science, Tokyo University of Science, Tokyo, Japan*

X-ray absorption spectroscopy (XAFS) is a powerful tool to probe the local structure of a specific element. Recently, we determined by Pd K-edge EXAFS that a Pd dopant atom in $Au_{24}Pd_1(SC_{12}H_{25})_{18}$ is located at the center of icosahedral Au core [1]. However, EXAFS data of thiolate-protected Au clusters measured at RT underestimate the coordination numbers (CNs) of Au-Au bonds determined by the single crystal XRD, which is probably due to thermal fluctuation of Au atoms in the small clusters. We report herein that detailed structure information can be obtained from EXAFS data recorded in wide *k* region at <10 K. We also demonstrate the softening of the Au-Au bond by the analysis of the temperature dependence.

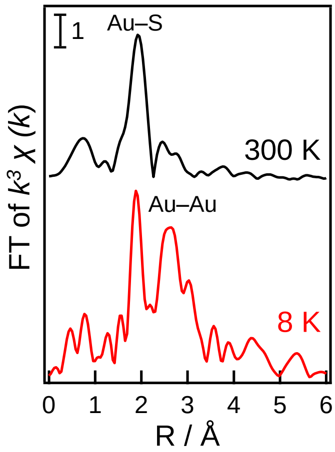

Fig. 1 Au L_3-edge FT-EXAFS spectra of $Au_{25}(SC_2H_5Ph)_{18}$ at 300 K and 8 K

The XAFS spectra of $Au_{25}(SC_2H_5Ph)_{18}$, $Au_{38}(SC_2H_5Ph)_{24}$, and $Au_{144}(SC_2H_5Ph)_{60}$ at Au L_3-edge were recorded at BL01B1 beam line in SPring-8. Fig. 1 shows the Au L_3-edge Fourier transformed (FT) EXAFS spectra of $Au_{25}(SC_{12}H_{25})_{18}$ measured at 300 and 8 K. The peaks assigned to the Au–Au bonds are clearly discernible at 8 K. This is due to the suppression of thermal fluctuation of Au atoms. Curve fitting analysis for Au_{25} cluster was performed assuming one Au–S bond and two types of Au–Au bonds (Table 1). The bond lengths and CNs of the Au–S and Au–Au bonds obtained from the curve fitting analysis agreed well with those determined from the single crystal X-ray analysis [2]. Similar results were obtained for $Au_{38}(SC_2H_4Ph)_{18}$ and $Au_{144}(SC_2H_4Ph)_{60}$. Finally, the Einstein temperature (θ_E), which is related to the bond stiffness, of each bond was estimated from the temperature-dependent Debye-Waller factors.

Table 1 Result of curve fitting analysis and structural parameters obtained from X-ray single crystal analysis of $Au_{25}(SC_2H_5Ph)_{18}$

Sample	Atom	CN[a]	*r* (Å)[b]	DW[c]	*R* (%)[d]
$Au_{25}(SC_2H_4Ph)_{18}$ at 8 K	S	1.6(2)	2.321(4)	0.0049(12)	12.0
	Au1	1.4(8)	2.759(17)	0.0034(33)	
	Au2	1.9(1.1)	2.906(29)	0.0072(118)	
$Au_{25}(SC_2H_4Ph)_{18}$ Single crystal [2]	S	1.4	2.33		
	Au1	1.4	2.784		
	Au2	1.9	2.948		

[a]CN: coordination number, [b]*r*: bond length, [c]DW: Debye-Waller factor, [d]*R*: R factor

References

[1] Y. Negishi et al., J. Phys. Chem. Lett. 4 (2013) 3579.
[2] M. A. MacDonald et al., J. Phys. Chem. C 115 (2011) 15282.

Ionic cluster formation using an ion drift-tube with selected-ion injection - Measurement of thermodynamic quantities for H_3O^+ Hydrate

Yoichi Nakai[1], Hiroshi Hidaka[2], Naoki Watanabe[2] and Takao M. Kojima[3]

[1] *RIKEN Nishina Center for Accelerator-Based Science, Wako, Saitama 351-1098, Japan*
[2] *Institute of Low Temperature Science, Hokkaido University, Sapporo 060-0819, Japan*
[3] *Atomic Physics Laboratory*, *RIKEN, Wako, Saitama 351-0198, Japan*

For the decades, ion-induced nucleation has attracted attentions as one of important processes for gas-phase nucleation because a free-energy barrier for growth of particles decreases by electrostatic attractive forces originating from polarization of atoms/molecules, e.g., as shown for the classical liquid drop model. In particular, ionic cluster formation, an early stage of the ion-induced nucleation, is a significant research subject since it governs the subsequent stages.

Thus far, the ionic cluster formation has been widely investigated from various research points of view. In many of experimental studies, however, the formation processes were triggered in a reactant gas including parent molecules of core ions by discharge, a pulsed electron beam, radiation sources, and so on. In such a situation, various ionic species can be produced together with desired ionic core ions. Thus, initial ionic reactions were not well defined, generally. In order to eliminate reactions by undesired ions, we developed an experimental apparatus, an ion drift-tube with selected-ion injection [1-3], where only specific parent ions are injected to a reaction cell.

We measured H_3O^+ hydrate, i.e., $H_3O^+(H_2O)_n$ cluster ions, produced in a mixed gas of helium and water in the temperature range from 224 to 403K and estimated the Gibbs free-energy changes for the stepwise association of a water molecule, $H_3O^+(H_2O)_{n-1} + H_2O \rightarrow H_3O^+(H_2O)_n$. The thermodynamic quantities, the enthalpy changes and the entropy changes, were also estimated. The obtained values are reasonably consistent with those of the preceding investigations [4,5]. In addition, we also show the experimental results of $NO^+(H2O)_n$ formation briefly, which we recently measured [6].

Reference(s)
[1] H. Böhringer and F. Arnold, Int. J. Mass Spectrom. and Ion Phys. 49 (1983) 61.
[2] T. M. Kojima et al., Z. Phys. D: At., Mol. Clusters 22 (1962) 645.
[3] H. Tanuma et al., Rev. Sci. Instrum. 71 (2000) 2019.
[4] NIST Chemistry WebBook, http://webbook.nist.gov/chemistry/.
[5] K. D. Froyd and E. R. Lovejoy, J. Phys. Chem. A 107 (2003) 9800.
[6] H. Hidaka et al., poster presentation in this symposium.

Nanoparticle formation by interaction between laser ablated plume and shock waves

Eri Ueno[1], Naoaki Fukuda[2], Hiroshi Fukuoka[3], Minoru Yaga[4], Ikurou Umezu[5]
Min Han[6] and Toshio Takiya[1]

[1] *Hitachi Zosen Corporation, Osaka, Japan*
[2] *Office of Society-Academia Collaboration for Innovation, Kyoto University, Kyoto, Japan*
[3] *Department of Mechanical Engineering, Nara National College of Technology, Nara, Japan*
[4] *Department of Mechanical Systems Engineering, University of the Ryukyus, Okinawa, Japan*
[5] *Department of Physics, Konan University, Kobe, Japan*
[6] *Department of Materials Science and Engineering, Nanjing University, Nanjing, China*

Pulsed laser ablation in background gas is one of techniques to produce nanoparticles with a precisely specified size. Production of nanoparticles with the desired size is possible because the conditions for evaporated mass and ambient gas pressure can be independently controlled [1]. Although observation of the laser ablation processes by spectroscopic methods gives an information on the plume expansion dynamics, effect of shock wave is not clear [2]. Shock waves generated in the early stage of the laser ablation process reflect and diffract at the substrate. These make the clarification of the nanoparticle formation process difficult. Hitherto, little papers have discussed effect of these shock waves on the plume dynamics and nanoparticle formation processes[3][4]. We investigated the interaction between laser ablated plumes and shock waves using one- and/or two-dimensional Eulerian fluid dynamics equations combined with a classical nucleation model in supersaturated vapors. We found that the rate of nanoparticle formation becomes higher when a plume locates between the target and substrate and reflected shock wave passes through the plume. In that case, a sudden change in temperature could be generated near the interference between the shock wave and the plume, followed by the formation of nanoparticles in the narrow region.

References

[1] N. G. Semaltianos, Crit. Rev. Solid State Mater. Sci., 35-2, (2010) 105. (Journals)
[2] G.W.Yang, Prog. Mat. Sci., 52, (2007) 662-664. (Journals)
[3] M.Han et al., Phys. Lett., A302, (2002)182. (Journals)
[4] M. Yaga, T. Takiya and Y. Iwata: Shock waves, 14-5/6, (2005) 403. (Journals)

Structures of small silicon-doped gold cluster cations

Jun Miyawaki and Ko-ichi Sugawara

National Institute of Advanced Industrial Science and Technology (AIST), Tsukuba, Japan

Gold nano-clusters have been attracting much attention because of their catalytic properties and their size-dependency of geometries and reactivity has been investigated experimentally and theoretically. Doping effect of foreign atom(s) on the structures and reactivity of gold clusters is also interesting subject. Since photoelectron spectra of the silicon-doped gold cluster anions were observed by Wang and co-workers [1], a number of theoretical works have been reported in this decade on the structures of silicon-doped gold clusters, but they are mostly limited to the neutral and anionic species. In the present study, structural evolutions of the silicon-doped gold cluster cations, $Au_nSi_m^+$, have been investigated for n=1-6 and m=1,2 using density functional theory calculations.

Shorter bond length and larger dissociation energy of $AuSi^+$ compared with Au_2^+ and Si_2^+ suggest that Au-Si bond is stronger than Au-Au bond and Si-Si bond in their diatomic cations. Doping of silicon atom(s) in the pure gold cluster cations causes significant change on their structures. Most of the structures of the lowest energy $Au_nSi_m^+$ (n=1-6,m=1,2) isomers correspond to those of the counterpart $Si_mH_n^+$, i.e., Au/H analogy found for the neutrals and anions by Wang's group [1,2] holds for the cations as well. For n=1-4, the structures of Au_nSi^+ are the same as the corresponding SiH_n^+ cations. However, Au_5Si^+ has the penta-coordinated capped square prism structure which is different from the experimentally observed SiH_3^+-H_2 structure of SiH_5^+. Au_6Si^+ is built based on Au_5Si^+ motif, which may be taken as beginning of the Au_n-Si-Au structure reported for the larger clusters. For $Au_nSi_2^+$, the most stable isomers have the same structures as $Si_2H_n^+$ in n=2, 3, and 5. In case of n=4, second stable isomer has the same structure as Au_4Si_2 concluded from PES experiment [2] although the most stable isomer has the different structure. $Au_6Si_2^+$ has the different structure from the experimentally confirmed D_{3d} H_3Si-SiH_3^+ structure.

References

[1] B. Kiran, X. Li, H.-J. Zhai, L.-F. Cui, L.-S. Wang, Angew. Chem. Int. Ed. 43 (2004) 2125.
[2] X. Li, B. Kiran, L.-S. Wang, J. Phys. Chem. A 109 (2005) 4366.

Location of dopant M (M = Pd, Ag, Cu) within $Au_{25-x}M_x(SR)_{18}$ studied by XAFS

Seiji Yamazoe,[1,2] Wataru Kurashige,[3] Katsuyuki Nobusada,[2,4] Yuichi Negishi,[3] and Tatsuya Tsukuda[1,2]

[1] *Department of Chemistry, School of Science, The University of Tokyo, Tokyo, Japan*
[2] *ESICB, Kyoto University, Kyoto, Japan*
[3] *Department of Applied Chemistry, Faculty of Science, Tokyo University of Science, Tokyo, Japan*
[4] *Department of Theoretical and Computational Molecular Science, Institute for Molecular Science, Okazaki, Japan*

One of the ubiquitous thiolate-protected Au clusters, $Au_{25}(SR)_{18}$, has an icosahedral Au_{13} core surrounded by six $-SR-(Au-SR)_2$-oligomers (Fig. 1)[1]. Recently, bimetallic clusters $Au_{25-x}M_x(SR)_{18}$ (M = Pd[2], Ag[3], Cu[4]) have been successfully synthesized. However, it has not yet been revealed which site is the dopant M occupies among three sites; core-center (Au_C), core-surface (Au_S), or oligomer (Au_O). In this work, the location of M within $Au_{25-x}M_x(SR)_{18}$ was studied by X-ray absorption spectroscopy (XAFS).

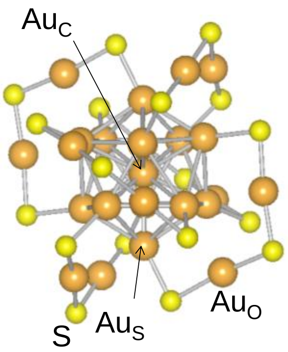

Fig. 1 Structure of $Au_{25}(SR)_{18}$.[1] The R groups are omitted for simplicity.

Bimetallic clusters $Au_{24}Pd_1(SC_{12}H_{25})_{18}$, $Au_{25-x}Ag_x(SC_2H_4Ph)_{18}$ (x=1–4), and $Au_{25-x}Cu_x(SC_2H_4Ph)_{18}$ (n=1–3) were synthesized according to the previously reported methods[2-4]. The XAFS spectra at Pd K-, Ag K-, Cu K-, and Au L_3-edges were recorded at BL01B1 beam line in SPring-8. Structures of bimetallic cluster models, M_P, obtained by replacing Au_P with M were optimized by density functional theory (DFT) using PBE0 functional. Then, EXAFS oscillations of the optimized models were simulated by FEFF8[5]. Fig. 2 shows the Pd K-edge EXAFS spectrum of $Au_{24}Pd_1(SC_{12}H_{25})_{18}$ and the simulated EXAFS spectra of the Pd_C, Pd_S, and Pd_O. The EXAFS oscillation pattern experimentally obtained agrees well with that of Pd_C, which is the most stable structure[6]. Similar analysis revealed that Ag dopants occupy core-surface sites in $Au_{25-x}Ag_x(SC_2H_4Ph)_{18}$ whereas Cu dopants are located at the oligomer sites in $Au_{25-x}Cu_x(SC_2H_4Ph)_{18}$.

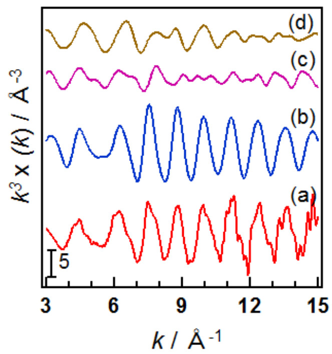

Fig. 2 Pd-K edge EXAFS spectra of $Au_{24}Pd_1(SC_{12}H_{25})_{18}$ obtained by (a) experiment, (b) Pd_C, (c) Pd_S, and (d) Pd_O models.

References:

[1] M.W. Heaven et al., J. Am. Chem. Soc., 130 (2008) 3754.
[2] Y. Negishi et al., Phys. Chem. Chem. Phys. 12 (2010) 6219.
[3] Y. Negishi et al., Chem. Commun. 46 (2010) 4713.
[4] Y. Negishi et al., J. Phys. Chem. Lett. 2 (2012) 2209.
[5] A. L. Ankudinov et al., Phys. Rev. B., 58 (1998) 7565.
[6] Y. Negishi et al., J. Phys. Chem. Lett., 4 (2013) 3579.

Space-Focusing of Spatially Spread Ions in Time-of-Flight Mass Spectrometer

Shun Sarugaku, Ryohei Murakami, Masashi Arakawa, and Akira Terasaki

Department of Chemistry, Kyushu University, Fukuoka, Japan

A time-of-flight mass spectrometer (TOF-MS) is a powerful tool for rapid analysis over a wide range of masses within tens of micro seconds. Focusing of ions is crucial in TOF-MS to achieve high resolution. The standard technique is the Wiley-McLaren type, where spatial distribution of ions is compensated for by a double electric-field configuration, so-called space-focusing. However, space-focusing does not work well when the spatial spread of ions is too large. Here we demonstrate that the mass resolution is improved even for ions spread over the entire accelerator region of TOF-MS by applying a non-linear electric potential to the accelerator.

We constructed TOF-MS illustrated in Fig.1. An ion beam was introduced coaxially to the flight path. The ions were extracted toward an ion detector by applying pulsed voltages to electrodes EL1 and EL2. All the electrodes had a 20-mm diameter ion-inlet aperture. The aperture of EL2 was with a metal mesh for an ordinary linear electric potential in the accelerator, whereas the mesh was removed when applying a non-linear potential.

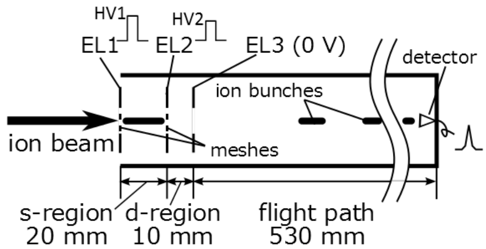

Fig. 1. A schematic view of the present time-of-flight mass spectrometer.

Figure 2(a) shows a TOF mass spectrum of an ion beam of Ag_7^+ from a continuous cluster-ion source, which filled the entire s-region of the TOF accelerator. The mass resolution was very low with meshes on all the electrodes. It was found by ion-trajectory simulation that ions near the exit of the s-region at t = 0 μs have TOF shorter than the rest of the ions. The resolution was improved by applying a non-linear potential so that these ions are accelerated by less voltages and thus have longer TOF. Figure 2(b) shows a TOF mass spectrum improved by this method.

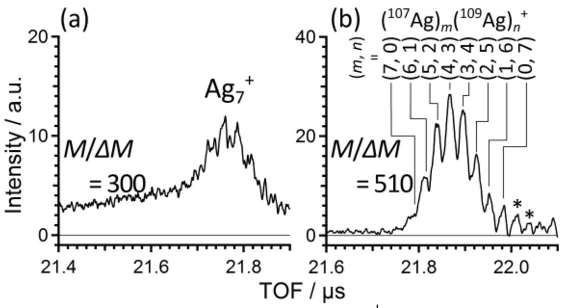

Fig. 2. TOF mass spectra of Ag_7^+ measured with meshes on all the electrodes (a), and on EL1 only (b). The peaks marked with asterisks are ringing noise.

The TOF-MS was further combined with a linear ion trap. Ions were trapped for 50 ms, extracted from the trap, and introduced coaxially to the flight path, which produced a quasi- continuous ion beam. We were able to separate isotopomers of Ag_3^+ clearly as shown in Fig. 3.

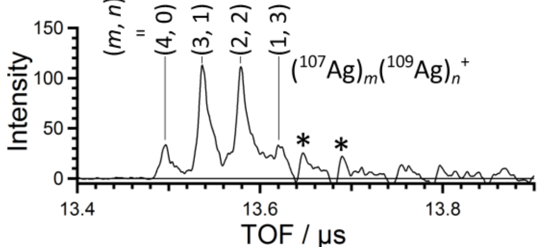

Fig. 3. A TOF mass spectrum of Ag_3^+ extracted from a linear ion trap.

Understanding and designing nanoalloys for clean energy applications by first principles calculations

Daojian Cheng*

State Key Laboratory of Organic-Inorganic Composites, Beijing University of Chemical Technology, Beijing 100029, P.R. China

**E-mail: chengdj@mail.buct.edu.cn*

With respect to the catalysts, alloy surfaces and nanoalloys have been employed to improve the catalytic activity of oxygen reduction reaction (ORR), CO oxidation, and CO_2 conversion. Here, first principles density functional theory (DFT) calculations have been used to study the oxygen reduction reaction (ORR) activity of Pt-based alloy surfaces and nanoalloys,[1,2] CO oxidation activity of Au-Pd nanoalloys,[3,4] and CO_2 conversion activity of Cu-Ni nanoalloys.[5,6] In addition, new TiO_2-based photocatalysts have been developed by DFT calculations.[7-11]

References:

1) Wenjie Xu, **Daojian Cheng*,** Mang Niu, Xiaohong Shao*, and Wenchuan Wang, Modification of the adsorption properties of O and OH on Pt–Ni bimetallic surfaces by subsurface alloying **Electrochimica Acta** 76, 440-445(2012)
2) **Daojian Cheng*,** Wenchuan Wang, Tailoring of Pd–Pt bimetallic clusters with high stability for oxygen reduction reaction **Nanoscale** 4, 2408-2415 (2012)
3) Mingjiang Li and **Daojian Cheng*, J. Phys. Chem. C** 2013, 117, 18746−18751
4) **Daojian Cheng***, Haoxiang Xu, Alessandro Fortunelli*, **Journal of Catalysis** 2014, 314, 47–55
5) Yang Yang and **Daojian Cheng***, Role of Composition and Geometric Relaxation in CO2 Binding to Cu-Ni Bimetallic Clusters **J. Phys. Chem. C** 2014, 118, 250-258
6) **Daojian Cheng*,** Fabio R. Negreiros, Edoardo Aprà and Alessandro Fortunelli*, Computational approaches to the chemical conversion of carbon dioxide **ChemSusChem,** 2013, 6, 944 – 965
7) M. Niu, W. Xu, X. Shao*, **Daojian Cheng***, Enhanced photoelectrochemical performance of rutile TiO(2) by Sb-N donor-acceptor coincorporation from first principles calculations, ***Applied Physics Letters*** **99** (2011).
8) M. Niu, **Daojian Cheng***, D. Cao*, Enhanced photoelectrochemical performance of anatase TiO2 by metal-assisted S-O coupling for water splitting, ***International Journal of Hydrogen Energy*** **38**, 1251 (2013).
9) M. Niu, **Daojian Cheng***, D. Cao*, Understanding Photoelectrochennical Properties of B-N Codoped Anatase TiO2 for Solar Energy Conversion, ***Journal of Physical Chemistry C*** **117**, 15911 (2013).
10) M. Niu, **Daojian Cheng***, D. Cao*, Understanding the Mechanism of Photocatalysis Enhancements in the Graphene-like Semiconductor Sheet/TiO2 Composites, ***Journal of Physical Chemistry C*** **118**, 5954 (2014).
11) M. Niu, **Daojian Cheng***, D. Cao*, SiH/TiO2 and GeH/TiO2 Heterojunctions: Promising TiO2-based Photocatalysts under Visible Light, ***Scientific reports*** **4**, 4810 (2014).

Conformations of Biomolecular Ions Probed by Proton Transfer Reactions at Various Temperature

Shinji Nonose, Minami Kawashima, and Hideo Isono

Graduate School of Nanobioscience, Yokohama City University, Japan

Investigations of gas-phase protonated biomolecules are motivated by the growing prevalence of electrospray ionization (ESI) mass spectrometry, which produce gas-phase biomolecular ions. Access to biomolecules in the gas phase provides the opportunity to study them in isolated states. The advantage of gas-phase studies is that ideas can be tested as finite molecular systems. In the preset study, proton transfer from multiply-protonated protein and peptide ions to gaseous molecules was studied in the gas phase. Absolute reaction rate constants for proton transfer were determined from intensities of parent and product ions in the mass spectra. Temperature dependence of reaction rate constants and branching fractions for proton transfer was measured. An issue that is attracting considerable attention is vacuo conformations might resemble structural evolution that originates in temperature change in the gas phase.

A home-made tandem mass spectrometer with ESI was used for measurements. Multiply-charged protein and peptide ions were produced by ESI of a dilute solution in methanol-water mixture including acetic acid. The charge-selected protein and peptide ions emerging from a quadrupole mass spectrometer (QMASS) were admitted into a collision cell with octapole ion trap. The collision cell was filled with He including gaseous molecules. Primary, secondary, and aromatic amines were chosen as target molecules. Temperature dependence of reaction rate constants and branching fractions for proton transfer from multiply-charged protein and peptide ions to the target molecules was measured, by changing temperature of the collision cell. The parent and product ions were mass-analyzed by a time-of-flight mass spectrometer equipped with reflectron.

Proton transfer from the protein and peptide ions to the target molecules was occurred by collisions in the cell. Absolute reaction rate constants for proton transfer were estimated with intensity of ions in the mass spectra. In any protein and peptide ions, the reaction rate increased rapidly with increase of charge states. By changing temperature of the collision cell in region from 280 to 470 K, temperature dependence of reaction rate constants and branching fractions for proton transfer was measured. Dramatic change was observed for distribution of product ions and reaction rate constants. These results would correlate to conformation change of protein and peptide ions with change of temperature, which originates in self-solvation to protons by hydrophilic residues in polypeptide chains, delocalization of charges with self-solvation, and Coulomb repulsion between charges.

References

[1] S. Nonose, T. Okamura, K. Yamashita, A. Sudo, Chemical Physics, **419** (2013) 237–245.
[2] S. Nonose, K. Yamashita, A. Sudo, M. Kawashima, Chemical Physics, **423** (2013) 182–191.

Reactions of Copper Cluster Oxide Anions with Nitric Oxide: Enhancement of Adsorption by Partial Oxidation

Shinichi Hirabayashi,[1] and Masahiko Ichihashi[2]

[1] *East Tokyo Laboratory, Genesis Research Institute, Inc., Ichikawa, Japan*
[2] *Cluster Research Laboratory, Toyota Technological Institute, Ichikawa, Japan*

Recently we have found that a carbon monoxide molecule is oxidized by copper oxide cluster anions, and in this reaction the deformation of the clusters and the resulting change of their electronic structures facilitate the progress of the reaction [1]. Here, we show that a nitrogen monoxide, NO, molecule can adsorb onto the copper oxide anions efficiently [2], and this adsorption leads to the reduction of NO.

Reactivity measurements were performed by use of a tandem-type mass spectrometer. Copper cluster ions were produced by the ion-sputtering of copper targets, and oxidized by oxygen molecules. Then bare or oxidized copper cluster ions were mass-selected by a quadrupole mass filter (QMF), and allowed to pass through a reaction cell filled with NO gas. Product ions and unreacted parent cluster ions were mass-analyzed by the second QMF.

In the reactions of $Cu_nO_2^-$ with NO at the collision energy of 0.2 eV, the following products were observed,

$$Cu_nO_2^- + NO \rightarrow Cu_nO_2(NO)^-, \quad (1)$$

$$Cu_nO_2^- + NO \rightarrow Cu_{n-1}O_2(NO)^- + Cu. \quad (2)$$

The total reaction cross sections are shown in Fig. 1, and even-sized clusters have relatively large cross sections in $n \geq 8$. NO adsorption is often accompanied by the release of a Cu atom from $Cu_8O_2^-$, $Cu_{10}O_2^-$ and $Cu_{12}O_2^-$ as indicated in reaction (2). On the other hand, Cu_n^- have significantly small cross sections in comparison with $Cu_nO_2^-$. Further, we measured the reaction cross sections of $Cu_8O_4^-$ and $Cu_8O_6^-$ for comparison, and found that only $Cu_8O_2^-$ has a large reaction cross section (see Fig. 2). In order to elucidate this specific reactivity, we calculated the reaction diagram of $Cu_nO_m^-$ + NO by using DFT, and this suggests that the energy of the transition state between the molecular and the dissociative adsorption of NO reduces remarkably by the partial oxidation of the copper cluster anions.

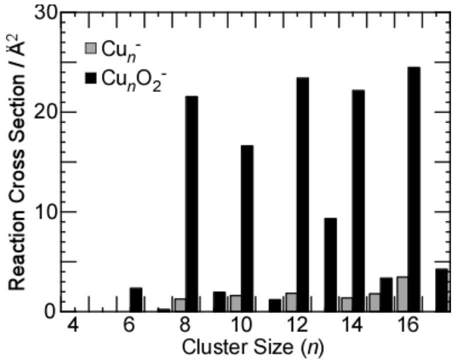

Fig.1: Reaction cross sections of Cu_n^- and $Cu_nO_2^-$.

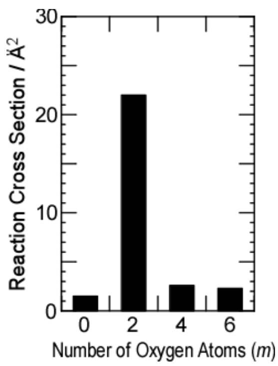

Fig.2: Reaction cross sections of $Cu_8O_m^-$.

References
[1] S. Hirabayashi, Y. Kawazoe, and M. Ichihashi, Eur. Phys. J. D 67 (2013) 35.
[2] S. Hirabayashi, and M. Ichihashi, J. Phys. Chem. A 118 (2014) 1761.

Vibrational Spectroscopy of Aluminum Oxide Cluster Anions: Structure and Reactivity

Xiaowei Song,[1,2] Matias R. Fagiani,[1,2] Florian A. Bischoff,[3] Wieland Schöllkopf,[1] Sandy Gewinner,[1] Joachim Sauer[3] and Knut R. Asmis[1,2]

[1] *Fritz-Haber-Institut der Max-Planck-Gesellschaft, Faradayweg 4-6, 14195 Berlin, Germany.*

[2] *Wilhelm-Ostwald-Institut, Universität Leipzig, Linnéstr. 2, 04103 Leipzig, Germany*

[3] *Institut für Chemie, Humboldt-Universität Berlin, Brook-Taylor-Str. 2, 12489 Berlin, Germany*

Aluminum oxides serve as highly efficient heterogeneous catalysts and catalyst supports. In particular, they are used for methane activation and promote various H/D exchange processes.[1] However, a molecular level understanding of the elementary reaction mechanisms and the nature of the involved active sites remains limited. Spectroscopic studies on size-selected gas phase clusters [2,3] can aid in gaining insight into the concepts governing these processes. Here, we use infrared photodissociation in combination with the intense and widely-tunable radiation from the IR free electron laser FHI-FEL [4] to study the structure and reactivity of aluminum oxide cluster anions in the gas phase. The nominally electronic closed shell clusters $(AlO_2)(Al_2O_3)^-_{x=0-3}$ as well as the open shell clusters $AlO_{x=1-4}$ and $Al_2O_{x=3-6}$ are probed. Structures are assigned based on a comparison of the IRPD spectra of the H_2-tagged cluster anions to simulated IR spectra from electronic structure calculations. The terminal Al-O stretching modes involving singly-coordinated oxygen atoms are found in-between 950 and 1200 cm^{-1}. Al-O stretching modes involving doublyand triply-coordinated O-atoms lie lower in energy (600-950 cm^{-1}) and O-Al-O bending modes are found below 600 cm^{-1}. For some of the open-shell cluster anions reactions with the H_2-messenger molecules are observed. The underlying reaction mechanism is studied in more detail in our ion trap setup, i.e., rate constants are determined from concentration profiles measured as a function of the reaction time and the ion trap temperature. Preliminary results from the reactivity studies of the clusters anions with water are also shown.

References

[1] Wang Z., Wu X., Zhao Y., Ma J., Ding X., He S.,Chem. Eur. J. 17, 3449-3457 (2011).

[2] G. Santambrogio, E. Janssens, S. Li, T. Siebert, G. Meijer, K.R. Asmis, Jens Döbler, M. Sierka, J. Sauer, J. Am. Chem. Soc. 130, 15143-15149 (2008).

[3] Sierka, J. Döbler, J. Sauer, G. Santambrogio, M. Brümmer, L. Wöste, E. Jannsens, G. Meijer, K.R. Asmis, Angew. Chem. Int. Ed. 46, 3372-5 (2007).

[4] Schöllkopf, W., Gewinner, S., Erlebach, W., Heyne, G., Junkes, H., Liedke, A., et al. (2013). In Proceedings of FEL 2013, New York, NY, USA (pp. 657-660).

Homogeneous deposition of size-selected clusters using Lissajous scanning method

Atsushi Beniya[1], Noritake Isomura[1], Hirohito Hirata[2] and Yoshihide Watanabe[1]

[1] *Toyota Central R&D Labs., Inc., 41-1 Yokomichi, Nagakute, Aichi 480-1192, Japan* ,
[2] *Toyota Motor Corporation, 1200 Mishuku, Susono, Shizuoka 410-1193, Japan*

Size-selected atomic clusters on surfaces are a subject of considerable interest because of their distinctive size-dependent catalytic properties. Conventionally, the cluster deposited surfaces were prepared by irradiating the sample surface to cluster ion beam. In order to investigate deposited isolated clusters, it is crucial to define the cluster coverage. However, due to intensity distribution of the ion beam, deposition with homogeneous coverage is difficult. In this work, homogeneous deposition of size-selected Pt clusters could be performed using Lissajous scanning method.

In this experimental setup, figure 1, ion beam was focused by einzel lenses, and then deflected to orthogonal X and Y directions. Ion beam scanning was performed by applying triangle wave to X and Y electrodes with an irrational frequency ratio f_X/f_Y, and consequently the ion trajectory fills a sample surface [1]. Cluster distribution on surfaces was analyzed using scanning x-ray photoelectron spectroscopy (analysis area < 0.05 mm^2). Figure 2 shows the Pt 4f intensity distribution of $Pt_n/TiO_2(110)$. Without deflector, figure 2(a) and 2(c), Pt clusters were deposited with a FWHM of 4 mm. Using the ion scanning, figure 2(b) and 2(d), homogeneous distribution could be achieved. Cluster distribution was also analyzed using scanning tunneling microscopy (STM), and summarized in Table 1. Density of deposited clusters was independent of position. Thus, homogeneous cluster deposition could be performed using the Lissajous scanning method.

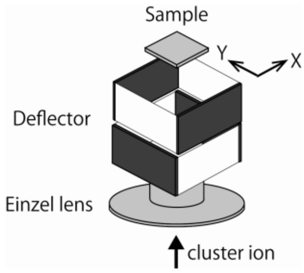

Fig. 1. Experimental set up of ion optics with deflector.

[1] A. Bazaei, Y. K. Yong, and S. O. R. Moheimani, Rev. Sci. Instrum. 83 (2012) 063701.

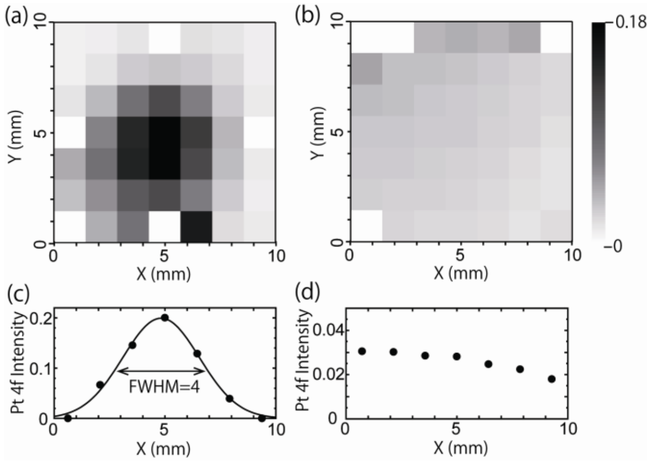

Fig. 2. Pt 4f intensity of (a) $Pt_4/TiO_2(110)$ prepared without deflector, and (b) $Pt_{15}/TiO_2(110)$ prepared with deflector. (c) Line profile at Y=5 mm of fig. 2(a), and (d) that of fig. 2(b).

Table. 1. Pt atomic density of $Pt_{15}/Al_2O_3/NiAl(110)$ estimated using STM.

X (mm)	Pt density ($\times 10^{13}$ atoms/cm^2)
2.5	1.72
5.0	1.77
7.5	1.78

Time-of-flight mass spectrometry for reaction product detection in heterogeneous catalysis

A. Winbauer[1], M. Tschurl[1], J. Kiermaier[1], U. Boesl[1], U. Heiz[1]

[1] *Chemistry Department, Technische Universität München, Germany*

Mass spectrometry is a very powerful analytical tool for the study of heterogeneous catalysis. It is often used to study reaction processes by analyzing the reaction products, both in a qualitative and in a quantitative way.

Typically, mass spectrometers work by using electron impact ionization, where discrimination between isomers is difficult to achieve. Fragmentation patterns of the isomers must differ to a large extent to be distinguishable.

A powerful and soft method for selective ionization is REMPI (Resonant Enhanced Multiphoton Ionization). In this technique a laser of specific wavelength is employed to ionize a single isomer through resonant intermediate states. Other isomers are not ionized as they are non resonant at the energy used [1].

A new experimental setup was built for the study of catalytic reactions on metal clusters supported on single crystal surfaces under UHV conditions. Custom ion optics were designed to incorporate the crystal support and enable future desorption-ionization studies and enantioselective laser mass spectrometry.

In this work we present our experimental setup, in which we combine time of flight mass spectrometry and resonance enhanced multiphoton ionization for investigation of products formed via surface reactions. It will thus be possible to examine the selectivity of catalytic reactions on size selected clusters. Furthermore, we will show first experimental results, for example wavelength scans and sensitivity tests and first TPD measurements on Pd (643) and Pt (111).

Reference

[1] U. Boesl, R. Weinkauf, C. Weickhardt, E. W. Schlag, *International Journal of Mass Spectrometry and Ion Processes* **131** (1994) 87-124.

H and O adsorption on $Fe_{13}Pt_{42}$ core-shell nanoparticle

Bheema Lingam Chittari[1] and Vijay Kumar,[1,2]

[1]*Dr. Vijay Kumar Foundation(VKF), 1969 Sector 4, Gurgaon 122001, Haryana, India*
[2]*Center for Informatics, School of Natural Sciences, Shiv Nadar University, Chithera, Gautam Budh Nagar - 203207, U.P., India*

Nanoalloys of Pt have been shown to exhibit significant improvements in their catalytic properties compared with pure Pt clusters [1-2]. We have carried out *ab initio* calculations on $Fe_{13}Pt_{42}$ nanoparticles having 55 atoms. It has been found that for this size Mackay icosahedral structure has the lowest energy with the Fe atoms forming an icosahedral core and Pt atoms forming the shell. Note that Fe_{13} free cluster also tend to have an icosahedral structure while for Pt clusters triangular faces are preferred [3] and in this nanoparticle structure both these aspects are satisfied. This core-shell nanoparticle has 48 μ_B magnetic moments with ferromagnetic coupling. The magnetic moments on Fe atoms are close to the value in free Fe clusters which is about 3.0 μ_B per atom while the magnetic moments on Pt atoms have the value of about 0.21 μ_B. The Bader charge analysis shows charge transfer from Fe core to Pt atoms. The charge transfer is more significant to Pt atoms on the edges. Further calculations have been performed to understand the variation in H and O adsorption on pure Pt_{42} nanoparticle and Pt_{42} surface in the core-shell $Fe_{13}Pt_{42}$ nanoparticle. We considered H and O atoms on vertex, face, bridge, and edge sites and found that the H adsorption on the bridge site shows higher binding energy where it interacts with two Pt atoms and *reduces* the magnetic moment significantly to 41 μ_B. The H adsorption energy on $Fe_{13}Pt_{42}$ is 2.39 eV. On the other hand oxygen adsorption is favored on a face site where it interacts with three Pt atoms and there is an *increase* in the magnetic moment to 50 μ_B from the value for the free $Fe_{13}Pt_{42}$ nanoparticle. The O adsorption energy on $Fe_{13}Pt_{42}$ is 5.81 eV. Similar calculations of H and O on pure Pt_{42} nanoparticle show higher binding energies of 2.96 eV and 6.40 eV for H and O, respectively. The H and O atoms adsorb, respectively, on an edge and face site of pure Pt_{42} similar to the case of $Fe_{13}Pt_{42}$. These results suggest significant reduction in the biding energy on Pt when there is Fe core and that the Pt_{42} in a core shell nanoparticle structure behaves entirely different from its pure Pt_{42} structure.

References

[1] J. Jang, E. Lee, J. Park, G. Kim, S. Hong and Y. Kown, Sci. Rep. 3 (2013) 2872.
[2] S. Guo, S. Zhang and S. Sun, Angew. Chem. Int. Ed., 52 (2013) 8526.
[3] V. Kumar and Y. Kawazoe, Phys. Rev. B 77, (2008) 205418.

This work has been supported by Asian Office of Aerospace Research and Development.

$Au_{38}(SR)_{24}$ cluster for oxidation catalysis

Bei Zhang,[1] Houhua Li,[2] Miguel A.G. Hevia, [3] Kaziz Sameh,[4] Dawid Wodka,[1] Clements Mazet,[2] Thomas Bürgi[1] and Noelia Barrabés[1]

[1] *Department of Physical Chemistry*, *University of Geneva, Geneva, Switzerland*
[2] *Department of Organic Chemistry, University of Geneva, Geneva, Switzerland*
[3] *Institute of Chemical Research of Catalonia (ICIQ), Tarragona, Spain*
[4] *Depart. of Industrial Engineering, Superior National School of Engineers of Tunis, Tunis, Tunisia*

Thiolate protected gold nanoclusters ($Au_n(SR)_m$) have been shown catalytically active and selective in several hydrogenation and oxidation reactions[1]. Among them, $Au_{38}(SR)_{24}$ nanocluster bears intrinsically chiral features due to the arrangement of the protecting ligands on the surface of the cluster, which makes it promising in enantioselective catalysis. As a preliminary test, the stability of $Au_{38}(SR)_{24}$ nanocluster in the oxidation of sulfide is investigated by in -situ UV-vis measurements and MALDI. A relation between the catalytic activity and the decomposition of the Au_{38} cluster was observed. Previous experience evidences enhancement of catalytic activity of $Au_n(SR)_m$ clusters through the removal of thiol ligands by thermal treatments [2]. In order to correlate the thermal treatment effect on the ligands and metal cluster stability, PM-IRRAS, TG, TPD/R/O coupled with mass spectrometer, XANESS and TEM studies have been performed. The influence of the nature of the support material has been evaluated by supporting $Au_{38}(SR)_{24}$ nanocluster on inert oxide as Al_2O_3 and reducible oxide as CeO_2.

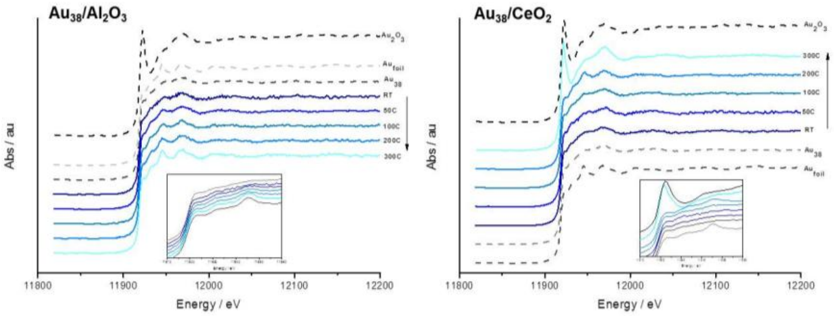

Figure 1. XANESS of insitu thermal treatment of supported $Au_{38}(SR)_{24}$ cluster

Different interaction, stability and reactivity are observed to depend on the kind of support employed under thermal treatments. TPD/R/O connected with mass spectrometer studies showed decomposition of the ligands starting at low temperatures (around 80°C) with two main fragmentation steps, which may be related with the different staple configurations. XANESS studies show the formation of cationic Au in the case of using reducible oxide as CeO_2.

Reference(s)

[1] S. Yamazoe, K Koyasu, and T. Tsukuda, Accounts of Chemical Research, 2014, 47, 816
[2] X. Nie, C. Zeng, X. Ma, H. Qian, Q. Ge, H. Xua and R. Jin, Nanoscale, 2013, 5, 5912

A new scalable Matrix Assembly Cluster Source (MACS) operating in reflection mode.

William D Terry, Feng Yin, Jian Liu, Lu Cao, Richard E Palmer.

Nanoscale Physics Research Laboratory, School of physics and Astronomy, University of Birmingham, Birmingham, B15 2TT, UK

Both fundamental issues [1] and applications [2] are driving the increasing interest in size-selected clusters. However one of the constraints on the field is the limited flux of size-selected clusters generally available (for an exception see ref [3]). We have demonstrated the Matrix Assembly Cluster Source, which employs the ion sputtering of co-condensed cluster atoms and rare gas atoms (e.g. Ar^+ and Ar/Ag respectively) operating in transmission mode. Here we demonstrate cluster samples characterized by HAADF (High Angle Annular Dark Field) STEM (Scanning Transmission Electron Microscopy) imaging [4], generated by MACS in reflection mode. We achieve a 1% conversion factor from incident ion beam to cluster beam (~3μA to 30nA). Investigation of the incident ion beam and cluster collection angles shows the maximum cluster yield is found when the sum of the two is 110° (i.e. sum of incident and reflection angles). The average size of clusters produced (100-600 atoms) is dependent on the concentration of cluster material in the rare gas matrix. This type of cluster source appears to be scalable and a scale up of cluster production by six or more orders of magnitude to lighter industrial applications seems feasible ultimately. This maybe achieved using commercially available 100mA sources which would produce ~1mA at current conversion factors.

References

[1] Walt A. de Heer, Rev Mod Phys, 65, 3 (1993) 611-676.
[2] Matake Haruta, Catalysis today, 36, 1, (1997) 153-166.
[3] K Wegner, S Vinati, P Piseri, A Antonini, A Zelioli, E Barborini, C Ducati and P Milani, Nanotechnology 23 (2012) 185603.
[4] Z. W. Wang, R. E. Palmer, Phys Rev Lett 108 (2012) 245502.

Theoretical study of the dehydrogenation of isopropanol on Ni_{13} cluster supported on Θ-Al_2O_3(010) surface

Andrey Lyalin,[1] and Tetsuya Taketsugu[1,2]

[1] *Elements Strategy Initiative for Catalysts and Batteries (ESICB), Kyoto University, Kyoto, Japan*
[2] *Department of Chemistry, Faculty of Science, Hokkaido University, Sapporo, Japan*

Hydrogenation and dehydrogenation reactions are major contributors to many industrial chemical processes. Many of such processes require using expensive precious metal catalysts. Therefore, extensive efforts are underway to develop efficient alternatives to traditional catalytic processes [2]. Recently, it has been demonstrated that nickel nanoparticles supported on Θ- and γ-forms of Al_2O_3 can serve as effective catalysts for dehydrogenation of secondary alcohols [1]. In spite of the great potential of nickel nanoparticles as catalysts for dehydrogenation reactions the mechanisms of such processes are largely not understood.

In the present work we report the results of theoretical investigation of the catalytic activity of Ni_{13} cluster supported on Θ-Al_2O_3(010) surface for the dehydrogenation of isopropanol (C_3H_8O). The calculations are carried out using methods of density functional theory (DFT) with the use of PBE functional and projector augmented wave (PAW) technique as implemented in PWSCF code. It is demonstrated that dehydrogenation of C_3H_8O on the free Ni_{13} cluster is a two-step process with the first H transfer from the alcohol hydroxyl group followed by C-H bond cleavage. Our calculations show, that H transfer from OH group of C_3H_8O to Ni_{13} is the reaction limiting step with the barrier of 0.95 eV, while the C-H bond cleavage requires the barrier of 0.41 eV. In the case of Ni_{13} clusters supported on Θ-Al_2O_3(010) the isopropanol molecule adsorbs on top of the surface Al atom in the close vicinity of the nickel cluster, which results in decrease of the H transfer barrier up to 0.1 eV due to formation of complementary adsorption sites at metal/support interface.

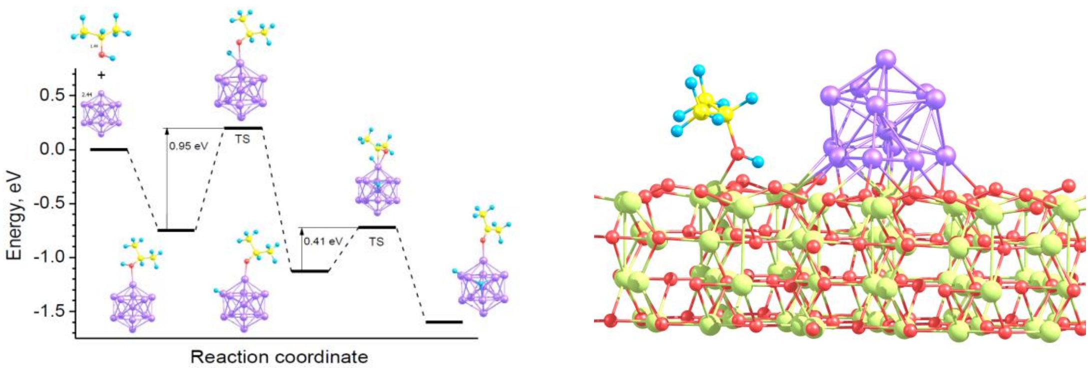

Figure 1. Energy diagram for dehydrogenation of C_3H_8O on the free Ni_{13} (left) and adsorption of isopropanol in the vicinity of Ni_{13} cluster supported on Θ-Al_2O_3(010) surface (right).

References

[1] S. E. Davis. M. S. Ide, R. J. Davis, Green Chem. 15 (2013) 17.
[2] K. Shimizu, K. Kon, K. Shimura, S.S.M.A. Hakim, J. Catal. 300 (2013) 242.

Chemical Reactivity of Rhodium and Copper-doped Rhodium Neutral Clusters

Masato Takenouchi, Ken Miyajima, and Fumitaka Mafuné

School of Arts and Sciences, The University of Tokyo, Japan

Catalyst containing rhodium has been extensively studied because of its high reactivity to convert NO_x to N_2 and CO to CO_2. In our group, Yamada et al. has reported that Rh oxide neutral clusters have more efficient reactivity with N_2O than Rh neutral clusters [1]. In this study, we generated copper-doped rhodium neutral clusters and investigated the reactivity with N_2O.

Rh_nCu_m (n = 7-14, m = 0, 1) clusters were generated by the laser ablation of Rh and Cu rods in a helium carrier gas. The clusters are photoionized by a F_2 excimer laser (λ =157 nm) and mass analyzed. $Rh_nCu_mO_p$ (p = 1-4) were produced by the reaction with N_2O. When the concentration of N_2O is sufficiently high, oxygen transfer reactions occur in a following sequence:

$$Rh_nCu_m + N_2O \rightarrow Rh_nCu_mO + N_2 \qquad (1)$$

$$Rh_nCu_mO + N_2O \rightarrow Rh_nCu_mO_2 + N_2 \qquad (2)$$

Rate constants k_1 and k_2 were defined for above reactions. Fig.1 shows the rate constants (k_1 and k_2) of neutral Rh_n and Rh_nCu clusters. It was found that the size-dependence of rate constants shows the similar trends between $Rh_{n-1}Cu$ and Rh_n clusters. The enhancement of second oxidation step (k_2>k_1) was found for pure and doped rhodium clusters. From this result, we can conclude that metal atom substitution of a Rh atom by a Cu atom gives no significant change on the reactivity of $Rh_{n-1}Cu$ and Rh_n clusters.

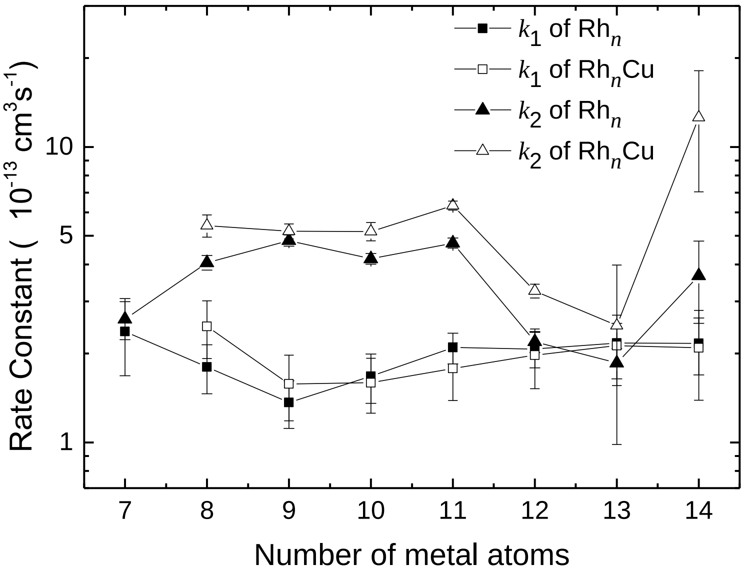

Fig.1 Rate constants k_1, k_2 of the reactions of neutral Rh_n and $Rh_{n-1}Cu$ clusters with N_2O

Reference

[1] A. Yamada, K. Miyajima, F. Mafuné *Phys. Chem. Chem. Phys.,* **2012**, *14*, 4188-4195

Reduction of N_2 on Pd surfaces at low temperatures

Junichi Murakami[1], Masayuki Futamata[1], Yukimichi Nakao[2], Shin Horiuchi[2], Kyoko Bando[2], Umpei Nagashima[2] and Kazuki Yoshimura[3]

[1]*Graduate School of Science and Engineering, Saitama University, Saitama, Japan*

[2]*Nanosystem Research Institute, National Institute of Advanced Industrial Science and Technology (AIST), Tsukuba, Japan*

[3]*Materials Research Institute for Sustainable Development, AIST, Nagoya, Japan*

In nature N_2 is reduced to NH_3 on the FeMo cluster located at the reaction center of the nitrogenase enzyme. On the cluster, N_2 is activated in molecular form at room temperature (RT). This is in marked contrast to the Haber-Bosh process for industrial NH_3 production in which the process begins with cleaving the strong triple bond of N_2 at a very high temperature like 500 °C.
A possibility of directly reducing a N_2 molecule to NH_3 on a metal surface at low temperatures (LT), in a manner similar to that of nitrogenase, was discussed by Nϕrskov's group [1]. However, such a process has not been experimentally verified. In the symposium we present data showing the low-temperature reduction of N_2 to NH_3 takes place on Pd surfaces. Palladium is known to dissociate H_2 below RT. For N_2 adsorption, on the other hand, clean Pd surfaces are known not to adsorb N_2. However, it has been reported that once a Pd surface is contaminated with nitrogen, it easily adsorbs N_2 in molecular form at and above RT [2]. Although the nature of the adsorbed N_2 has not been elucidated, if N_2 molecules adsorbed on Pd surfaces are activated, exposure of the Pd surfaces to N_2 and H_2 may result in reduction of N_2, leading to the formation of NH_3 at LT.
We used X-ray photoelectron spectroscopy for various Pd samples such as thin Pd films, Pd plates and Pd fine particles to study interactions of the surfaces with N_2 and H_2. We found (1) H_2 dissociates on the oxidized Pd surfaces at and above RT (as have been reported), (2) N_2 is adsorbed by the Pd surfaces probably in molecular form, (3) nitrogen species on Pd surfaces react with H from H_2 and are reduced to NH_3 and (4) the resultant NH_3 desorbs from the surface at least above 70 °C. Thus elementary steps needed to catalytically convert N_2 to NH_3 with H_2 proceed on Pd surfaces at the low temperatures.
It has been reported that N_2 is adsorbed by small Pd clusters [3]. A theoretical calculation for N_2 adsorption on a Pd cluster (Pd_8) shows N_2 is adsorbed with a side-on geometry and activated, which is similar to N_2 adsorption on small tungsten clusters [4]. Thus we believe cluster-like structures on the Pd surfaces are responsible for the N_2 adsorption and activation.

References

[1] T. H. Rod, A. Logadottir and J. K. Nϕrskov, J. Chem. Phys. **112** (2000) 5343.

[2] E. Miyazaki, I. Kojima and S. Kojima, Langmuir **1** (1985) 264.

[3] P. Fayet, A. Kaldor and D. M. Cox, J. Chem. Phys. **92** (1990) 254.

[4] J. Murakami and W. Yamaguchi, Sci. Rep. **2**, article number 407 (2012).

Automated prediction of pathways for single bond activations on small gold clusters: A case study of H_2 dissociation on neutral and charged Au_n^m (n = 1-12, m = 0, ±1)

Min Gao,[1] Andrey Lyalin,[2] Satoshi Maeda[1,2] and Tetsuya Taketsugu[1,2]

[1] *Department of Chemistry, Faculty of Science, Hokkaido University, Sapporo, Japan*
[2] *Elements Strategy Initiative for Catalysts and Batteries, Kyoto University, Kyoto, Japan*

We report the results of a systematic theoretical investigation of single-bond activation pathways for hydrogen molecule catalyzed by small metal clusters. As it is known, the number of isomers and adsorption sites on cluster surface increases drastically with the growth in cluster size. Therefore, a systematic search for the optimal pathways of chemical reactions on metal cluster surfaces becomes an extremely complicated task and requires urgent development of novel automated computational methods.

In the present study, a new theoretical approach to find metal-cluster-catalyzed single bond activation pathways is introduced [1]. The proposed approach combines two automated reaction path search techniques: the anharmonic downward distortion following (ADDF) and the artificial force induced reaction (AFIR) methods, developed in our previous works [2]. A simple model reaction of the H−H bond activation catalyzed by Au_n^m (n = 1–12, m = 0, ±1) clusters is considered as an example. Systematic analysis of the structure-dependent reactivity of small gold clusters is performed. It is demonstrated that the most stable structures of the gold clusters are not always highly reactive as shown in Fig.1. Therefore, several isomeric structures must be taken into account for adequate description of the reaction rates at finite temperatures. The influence of the charge state of gold clusters on H_2 dissociation is also investigated. It is shown that excess of a positive charge on gold cluster can promote the adsorption and dissociation of H_2 molecule. The proposed approach can serve as a promising tool for investigation of the chemical reactions catalyzed by small metal clusters. More details will be shown in poster presentation.

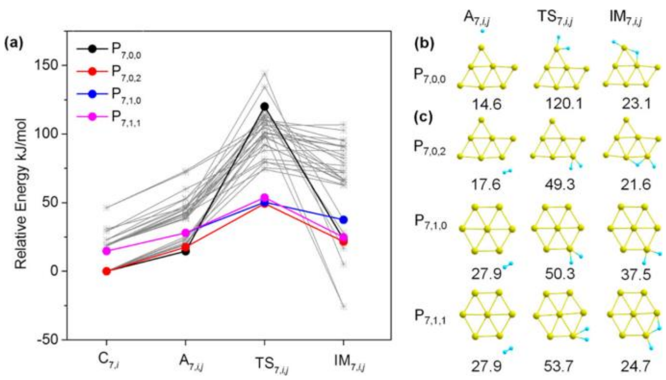

Fig.1 (a) Potential energy profiles for H_2 dissociation on isomers of Au_7. (b) Structures along the pathway starting from the most favorable adsorption geometry. (c) Structures along the three lowest pathways [1].

References
[1] M. Gao, A. Lyalin, S. Maeda, and T. Taketsugu, J. Chem. Theo. Comput. 10 (2014) 1623.
[2] S. Maeda, K. Ohno, and K. Morokuma, Phys. Chem. Chem. Phys.15 (2013) 3683.

Preparation and catalytic application of supported silver clusters

Masaru Urushizaki,[1] Shinjiro Takano,[1] Seiji Yamazoe,[1,2] Kiichirou Koyasu,[1,2] and Tatsuya Tsukuda[1,2]

[1] *Department of Chemistry, School of Science, The University of Tokyo, Tokyo, Japan*
[2] *ESICB, Kyoto University, Kyoto, Japan*

Silver clusters smaller than 1 nm show size-specific catalysis for hydrogenation of nitroaromatics [1]. In order to understand the origin of size-specific catalysis and to optimize the catalytic performance of Ag clusters, it is required to synthesize Ag clusters with atomically-precise size. This work is aimed to synthesize size-controlled Ag clusters on metal oxides by applying the method we developed for the synthesis of supported Au clusters using thiolate-protected Au clusters [2]. In this work, we used atomically-precise Ag clusters protected by 4-melcaptobenzoicacid (MBA), $Ag_{44}(MBA)_{30}^{4-}$ [3].

The silver clusters, $M_4Ag_{44}(MBA)_{30}$ (M = Cs and Na), were synthesized by the method reported in ref [4]. UV-vis spectrum of the products (Fig. 1a) shows that the $Ag_{44}(MBA)_{30}^{4-}$ clusters were successfully synthesized. Then, $Ag_{44}(MBA)_{30}$ clusters were adsorbed on metal oxides (Al_2O_3 or TiO_2) by mixing them in DMF. Reflectance spectrum of $Ag_{44}(MBA)_{30}/Al_2O_3$ (Fig. 1b) showed similar features observed in the absorption spectrum of $Ag_{44}(MBA)_{30}$ (Fig. 1a). This indicates that $Ag_{44}(MBA)_{30}$ clusters are adsorbed on alumina in the intact form. Finally, the $Ag_{44}(MBA)_{30}/Al_2O_3$ composite was calcined in vacuo at 450 ^{o}C to remove the thiolates for catalytic application. Reflectance spectrum after the calcination (Fig.1c) showed no surface plasmon resonance peak at ~400 nm which is characteristic for Ag nanoparticles. This observation implies that the aggregation of silver clusters is negligible during the calcination conditions we employed. This calcined clusters catalyzed reduction of 4-nitrophenol to 4-aminophenol.

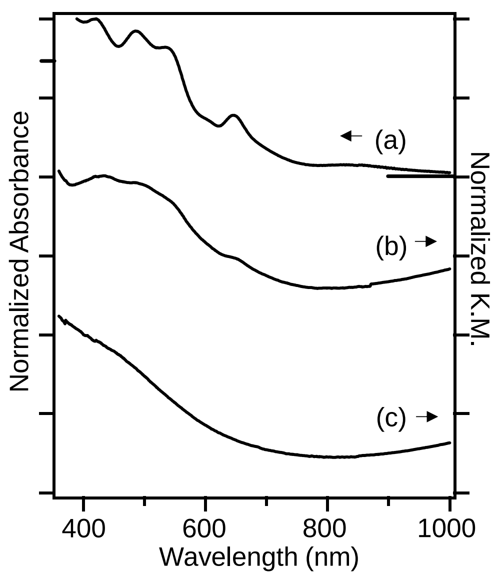

Figure.1 (a) UV-vis absorption spectrum of $Ag_{44}(MBA)_{30}$, and diffuse reflectance spectra of $Ag_{44}(MBA)_{30}/Al_2O_3$ (b) before and (c) after calcination.

References
[1] K.-I. Shimizu et al., J. Catal. 270 (2010) 86.
[2] S. Yamazoe et al., Acc. Chem. Res. 47 (2014) 816.
[3] K. M. Harkness et al., Nanoscale 4 (2012) 4269.
[4] A. Desireddy et al., Nature 501 (2013) 399.

A Highly Practical and Reusable Zinc Catalyst for Transesterification

Daiki Nakatake,[1] Yuki Yokote,[1] Ryo Yazaki[1] and Takashi Ohshima[1]

[1] *Graduate School of Pharmaceutical Sciences, Kyushu University, Fukuoka, Japan*

~Introduction~

Ester compounds are ubiquitous in various biologically active natural products and drugs. General methods for ester synthesis rely on condensation reagent or reactive acylating reagent, resulting in the generation of stoichiometric amounts of unwanted waste. Catalytic transesterification, which generates only lower alcohols as co-products, is more desirable in terms of atom-economy. We recently reported tetranuclear zinc cluster [$Zn_4(OCOCF_3)_6O$] (Figure 1.), which catalyzed transesterification under almost neutral conditions with wide functional group tolerance (Scheme 1.) [1]. This zinc catalyst, however, has still much room for improvement, because handling under an inert gas atmosphere was necessary due to its hygroscopic nature, and the reactions of sterically hindered 2° and 3° alcohols were quite slow.

Figure 1.

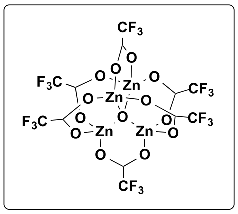

$Zn_4(OCOCF_3)_6O$

Scheme 1.

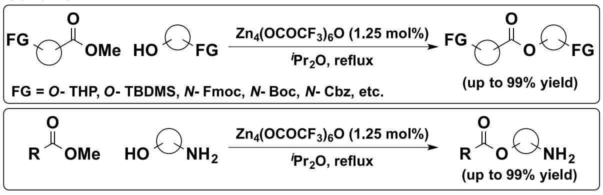

~This Work~

We developed a new highly stable zinc/bis-imidazole ligand complex (Scheme 2.). This zinc complex catalyzed transesterification reaction without special care regarding air and moisture with expanded substrate scope [2]. The complex showed higher catalytic activity than the zinc cluster catalyst itself. In addition, the complex also catalyzed carbonate formation and oxazoline formation under the optimized conditions. This stable nature of the complex made it possible to recover and reuse the catalyst at least five times without significant loss of activity.

Scheme 2.

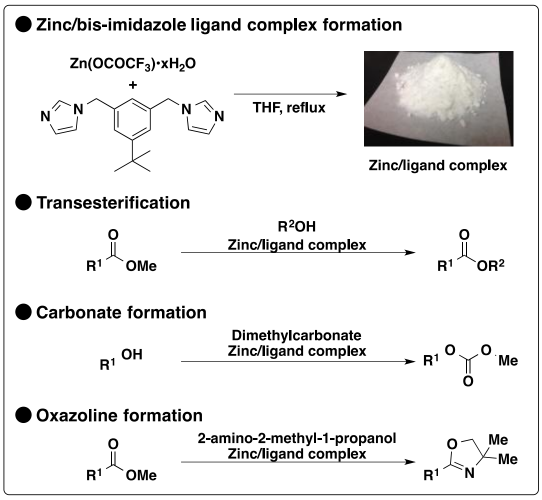

References

[1a] Iwasaki, T.; Maegawa, Y.; Hayashi, Y.; Ohshima, T.; Mashima, K. *J. Org. Chem.* **2008,** *73,* 5147. [1b] Ohshima, T.; Iwasaki, T.; Maegawa, Y.; Yoshiyama, A.; Mashima, K. *J. Am. Chem. Soc.* **2008,** *130,* 2944. [1c] Maegawa, Y.; Ohshima, T.; Hayashi, Y.; Agura, K.; Iwasaki, T.; Mashima, K. *ACS Catal.* **2011,** *1,* 1178. [2] PCT/JP2014/58876.

Thermal stability and reactivity of manganese oxide clusters

Kohei Koyama, Ken Miyajima, and Fumitaka Mafuné

School of Arts and Sciences, The University of Tokyo, Tokyo, Japan

Manganese oxide is known to react with CO and NO in the states of bulk and nanoparticle [1, 2]. In this study, we examined thermal stability and reactivity with CO of cationic manganese oxide clusters with and without heating process of clusters.

$Mn_nO_m^+$ clusters were generated by the laser ablation of a Mn metal target in 0.1% oxygen seeded helium carrier gas. Clusters passed through a reaction gas cell and an extension tube heated with a resistive heater before expansion into a vacuum. Fig. 1 shows abundance distribution of $Mn_nO_m^+$ clusters ($4 \leq n \leq 9$), indicating $Mn_nO_m^+$ clusters ratio with $n : m = 2 : 3$ were abundantly formed at room temperature. As temperature increased to 425 °C, oxygen rich clusters and $Mn_nO_m^+$ clusters having the composition of $n : m = 2 : 3$ decreased and instead, oxygen deficient clusters increased.

Fig. 2 shows abundance ratios of $Mn_nO_m^+$ clusters ($n = 8$) as a function of temperature. $Mn_8O_{11}^+$, $Mn_8O_{12}^+$ and $Mn_8O_{14}^+$ were generated at room temperature. As temperature increased, oxygen rich clusters decreased and oxygen poor clusters increased. For example, $Mn_8O_{12}^+$ decreased while $Mn_8O_{10}^+$ increased between 100 °C to 200 °C. It is considered that the oxygen molecule was desorbed by heating. $Mn_nO_m^+ \rightarrow Mn_nO_{m-2}^+ + O_2$

Knowing thermal stabilities of $Mn_nO_m^+$ clusters, we examined reactivity with CO. $Mn_nO_m^+$ clusters forms CO attached products by the reaction with a CO gas at room temperature. As desorption of CO was observed by heating up to 100 °C, the bonding between CO and cluster is suggested to be very weak.

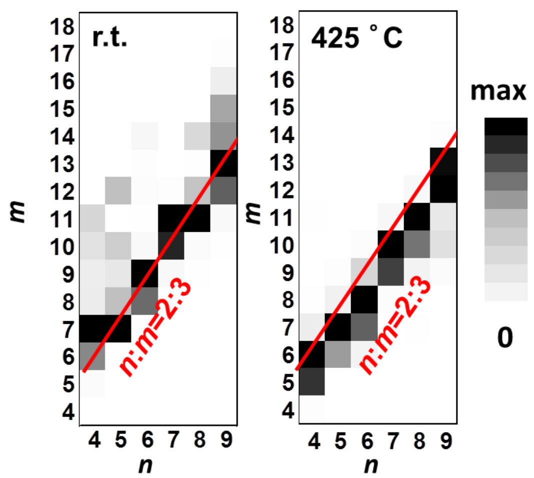

Fig. 1 Map of abundance distribution of $Mn_nO_m^+$ clusters at r.t. and 425 °C.

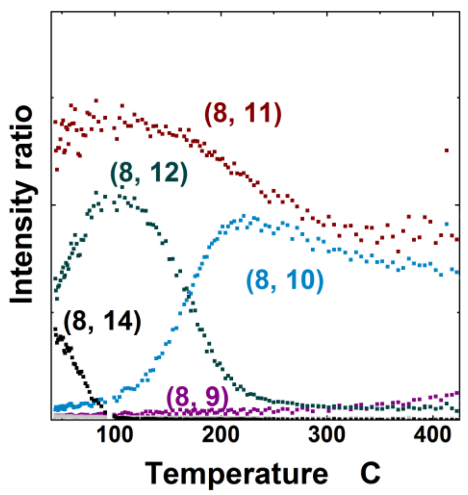

Fig. 2 Abundance ratio of $Mn_nO_m^+$ clusters ($n = 8$) increasing temperature .

Reference(s)

[1] S. Royer, D. Duprez, Chem. Cat. Chem. 2011, 3, 24.
[2] J. Shan, et al, J. Phys. Chem. C 2013, 117, 8329.

Studies on chemical reactions of transition metal clusters with oxygen by using FT-ICR mass spectrometer

Yuta Tobari,[1] Kazuki Ogasawara,[2] Yoshinori Sato,[2] Makoto Saito,[2] Shohei Chiashi,[2] Shigeo Maruyama,[2] and Toshiki Sugai[1]

[1] *Department of Chemistry, Toho University, Funabashi, Japan*
[2] *Department of Mechanical Engineering, The University of Tokyo, Tokyo, Japan*

Transition metal oxide clusters have been used as industrial catalysts with their unique size effects. However, their size dependence and oxidation reactivity are not well known. Here we present studies on reactions of transition metal clusters with O_2 by using FT-ICR.

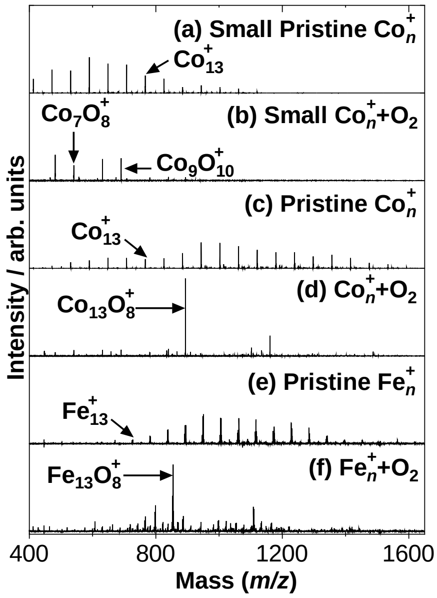

Fig. 1 Mass spectra of metal and metal oxide clusters.

Details of experimental apparatus and techniques have been described elsewhere [1]. Metal clusters were produced by a laser vaporization cluster source and were injected and trapped in a cell under a magnetic field of 6 T. The trapped clusters were thermalized in several seconds and were then exposed to oxygen for 100-1000 ms. The pressure of O_2 of the cell were approximately 5×10^{-7} Torr. Figure 1 shows mass spectra of pristine metal (M_n^+: M = Co or Fe) clusters and product metal oxide clusters ($M_nO_{2m}^+$) with/without O_2, respectively. When the pristine cluster (Co_n^+) size distribution was smaller (n = 6-18) in Fig. 1a, the products were $Co_nO_{2m}^+$ (n = 5-11, $2m$ = 6-12) without any magic numbers (Fig. 1b). The ratios of $2m/n$ were 1.1-1.3. When the cluster size was larger (n = 8-28) as shown in Fig. 1c, we can observe a salient magic number of $Co_{13}O_8^+$ [2] with the much lower ratio of $2m/n$ = 0.6. The production condition of $Co_{13}O_8^+$ clarifies that it is derived from larger parent pristine clusters (Co_n: n >13) through dissociative oxidation processes [3]. The intensity analyses also support the production processes with the fact that $Co_{13}O_8^+$ is much more abundant than the pristine Co_{13}^+. Figures of 1e and 1f show almost identical cluster distributions of Fe_n and Fe_nO_{2m} to those of Co_n and Co_nO_{2m} in Figs. 1c and 1d. The results together with their intensity analyses reveal universal dissociative oxidation processes of transition metal clusters.
Our preliminary reaction rate analyses reveal that the obtained rate constants of Co_n and Fe_n (n = 7-26) are similar to the Langevin ion-molecule collision rate constant ($k_L \sim 5.3 \times 10^{-10}$ cm^3 s^{-1}), which is consistent to the studies on $Ni_n + O_2$ (n = 2-15) reported by Sugawara and Koga [4].

References

[1] S. Inoue and S. Maruyama, Jpn. J. Appl. Phys. 47 (2008) 1931.
[2] Q. Sun, et al., Phys. Rev. B 62 (2000) 8500.
[3] F. Liu, F. X. Li, and P. B. Armentrout, J. Chem. Phys. 123 (2005) 064304.
[4] K. Sugawara and K. Koga, Chem. Phys. Lett. 409 (2005) 197.

First-principle study of small nickel cluster structure and hydrogen dissociation on nickel dimer

Pham Thi Nu and Ohno Kaoru

Department of Physics, Graduate School of Engineering, Yokohama National University, Yokohama 240-8501, Japan

With the aim of improving the active surface to total metal volume ratio, nanoparticles have been used for years in the field of catalysis. It has been reported that in compared with traditional supported Ni catalysts, Ni nanocluster catalysts have a potential of having high activity and selectivity particularly in hydrocarbon hydrogenation reactions [1]. Theoretical calculation plays an important role in predicting the properties of a small cluster.

Recently it has been reported that the hydrogen capacity of hydrogen storage materials such as graphites and metal hydrides is enhanced by adding a small amount of metal nanoparticles such as platinum and nickel [2,3]. The phenomenon is described as “hydrogen spillover” process, in which the H atoms are created on a metal surface and migrate to the surface of the support.

Using the all-electron mixed basis approach program [4,5], which was developed in our group, Sahara et al.[6] have performed TDDFT simulations of a simple system composed of nickel dimer and hydrogen molecule. We are studying the stable structure of small nickel clusters. The results are compared with other theoretical and experimental data in terms of geometric structure and spin multiplicity. After finding the stable structure of nickel dimer, we perform the molecular dynamics (MD) simulation of hydrogen dissociation on nikel dimer. Our MD simulation result shows a possibility that hydrogen molecule is dissociated into two hydrogen atoms (see Fig.1).

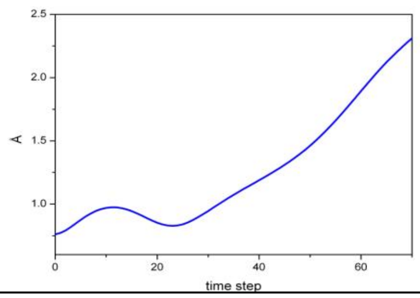

Fig1. The distance of two hydrogen atoms in MD simulation

References

[1] G.Schmid, V.Maihack, F.Lantermann, and S.Peschel, J. Chem.Soc. Dalton Trans. 589 (1996).

[2] Y. W. Li and R. T. Yang, J. Phys. Chem. C 111, 11086 (2007).

[3] M. A. Miller, C. -Y. Wang, G. N. Merrill, J. Phys. Chem. C 113, 3222 (2009).

[4] T. Ohtsuki, K. Ohno, K. Shiga, Y. Kawazoe, Y. Maruyama, and K. Masumoto, Phys. Rev. Lett. 81, 967 (1998); Phys. Rev. B 60, 1531 (1999).

[5] Y. Noguchi, O.Sugino, M. Nagaoka, S.Ishii, and K.Ohno, J. Chem. Phys. 137, 024306 (2012)

[6] R. Sahara, H. Mizuseki, M. H. F. Sluiter, K. Ohno, and Y. Kawazoe, RSC Advances 3, 12307-12312 (2013)

Clusters on La-Ni Mixed Oxides and its Catalytic Performance for Isomerization of Allylic Alcohols to Saturated Aldehydes

Tamao Ishida,[1,5] Jun Aimoto,[1] Akiyuki Hamasaki,[1] Hironori Ohashi,[2] Tetsuo Honma,[3] Takushi Yokoyama,[1] Kohei Sakata,[4] Mitsutaka Okumura,[4] Makoto Tokunaga,[1]

[1] *Department of Chemistry, Kyushu University, Fukuoka, Japan*
[2] *Faculty of Arts and Science, Kyushu University, Fukuoka, Japan*
[3] *Japan Synchrotron Radiation Research Institute (JASRI/SPring-8), Hyogo, Japan*
[4] *Department of Chemistry, Osaka University, Osaka, Japan*
[5] *Research Center for Gold Chemistry, Tokyo Metropolitan University, Tokyo, Japan*

Isomerization of allylic alcohols into aldehydes is one of the important processes for chemical industries. Supported gold nanoparticles have been used for oxidative amination of alcohols (N-alkylation and N-alkylidenation of amines with alcohols), in which hydrogen-borrowing mechanisms are working.

In this work,[1] we have attempted this strategy for the Au-catalyzed isomerization of 2-propen-1-ol and *trans*-2-octen-1-ol. Among the Au catalysts with simple oxide supports, Au/NiO exhibited the highest catalytic activity with excellent selectivity. In addition, a mixed metal oxide support consisting of Ni and La considerably improved the results. The catalysts were characterized by X-ray absorption fine structure (XAFS) measurements, which revealed Au in Au/La-Ni-O-H_2 exist as small clusters (coordination number of Au–Au bond is 6.8). We also carried out DFT calculation using a Au_6 cluster for the catalyst model.

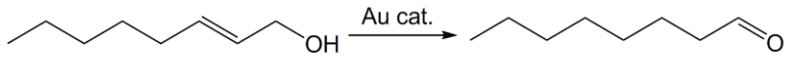

Table 1. Isomerization of *trans*-2-octen-1-ol.[a]

Entry	Catalyst	Solvent	Conv. (%)[b]	Yield (%)[b]
1	Au/NiO	dioxane	61	51
2	Au/La_2O_3	dioxane	8	3
3	Au/La-Ni-O (1/1)	dioxane	98	83
4	Au/La-Ni-O-H_2 (1/1)	dioxane	87	87

[a] Au 1 mol%, N_2 (0.1 MPa), 100 ºC, 24 h.

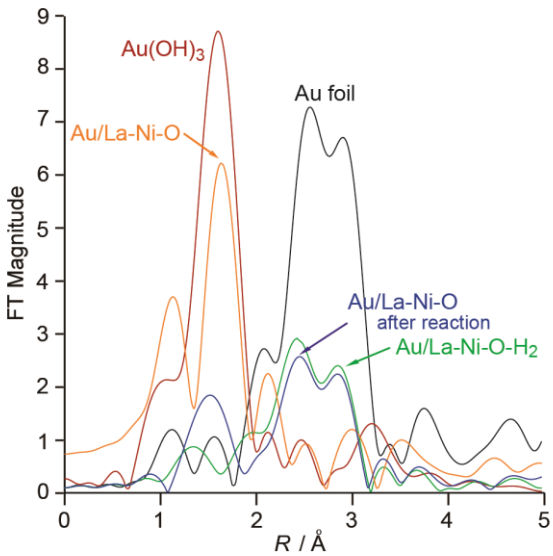

Figure 1. Au L_3-edge radial structure functions of Au/NiO and Au/La-Ni-O.

Reference

[1] T. Ishida, J. Aimoto, A. Hamasaki, H. Ohashi, T. Honma, T. Yokoyama K. Sakata, M. Okumura, and M, Tokunaga, Chem. Lett. In press (doi:10.1246/cl.140369).

withdraw

Release of Oxygen from Copper Oxide Cluster Ions by Heat

Ken Miyajima, Keisuke Morita, and Fumitaka Mafuné

School of Arts and Sciences, The University of Tokyo, Tokyo, Japan

Copper oxide clusters, $Cu_nO_m^+$, were prepared in the gas phase by laser ablation of a copper rod in the presence of 0.5% oxygen in a He carrier gas. The cluster ions were heated up to 1000 K at downstream of the cluster source (post-heating), and the stoichiometry of $Cu_nO_m^+$ (n = 4−19) was examined using mass spectrometry [1].

As shown in Figures 1a, and b, temperature programmed desorption experiments revealed that an oxygen molecule is released from oxygen-rich $Cu_nO_m^+$ (m/n > 2/3), forming $Cu_nO_m^+$ (n:m ~ 3:2). Oxygen molecules are further released from cluster ions to form $Cu_nO_m^+$ (n:m ~ 2:1) at the higher temperatures, suggesting that a Cu atom tends to take +1 charge state at high temperatures (Fig. 1c).

Figure 2 shows that oxygen-rich $Cu_{14}O_{10}^+$ and $Cu_{14}O_{12}^+$ release an oxygen molecule during the heating in the range of 298–550 K and 350–700 K, respectively. Water adducts which are produced by the impurities in the vacuum chamber are also observed in the temperature of < 600 K. Other $Cu_nO_m^+$ clusters also show the similar profiles. It was found that copper oxide clusters having $Cu_nO_m^+$ (n:m ~ 3:2) withstand a high temperature of 500 K.

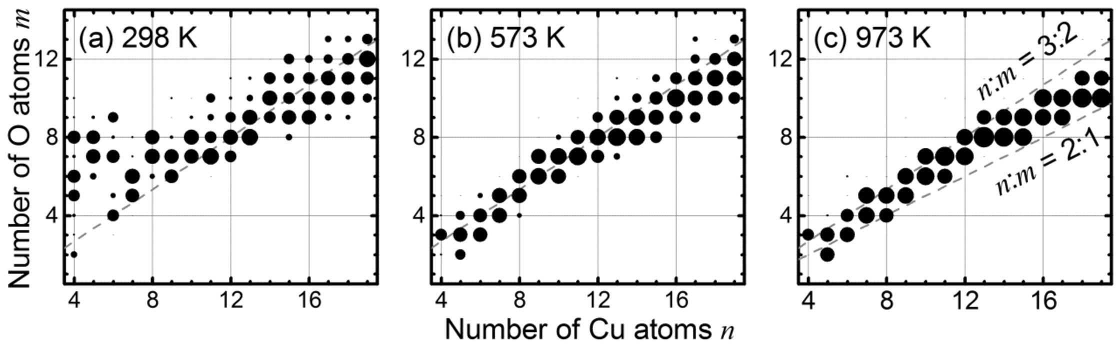

Figure 1 Mass abundance of $Cu_nO_m^+$ clusters: (a) without heating treatment, (b and c) after heating treatment. Area of each bubble is proportional to the normalized intensity ($Cu_nO_m^+/\sum_m Cu_nO_m^+$).

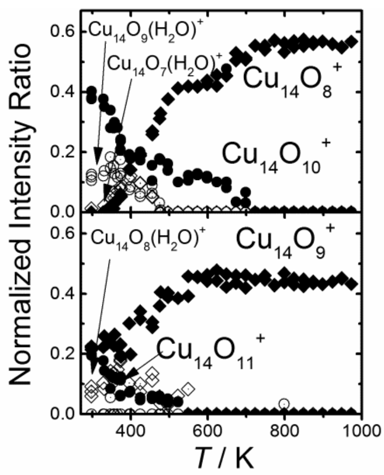

Figure 2 Temperature programmed desorption spectra of $Cu_{14}O_m^+$ clusters. Open symbols correspond to the water adducts.

Reference

[1] K. Morita, K. Sakuma, K. Miyajima, F. Mafuné, J. Phys. Chem. A 117 (2013) 10145-10150.

Regenerative synthesis of copper nanoparticles on TiO_2 nanoparticles by photoreduction

Naoki Nishida, Takuya Aoki, and Hideki Tanaka

Department of Applied Chemistry, Chuo University, Tokyo, Japan

Copper nanoparticle has attracted interest due to their potential contribution to a wide variety of areas, including optical and electronic applications. Meanwhile, regenerative property of synthesis process of nanoparticles is an important subject in science and technology because of deeply understanding of growth and decomposition mechanism of nanoparticles besides sustainability of metal resources. In this study, we investigated the regenerative synthesis of copper nanoparticle on titanium oxide through the photoreduction of copper acetate.

The synthesis of copper nanoparticles by photoreduction was carried out using a similar method reported previously [1,2]. Copper acetate powder and titanium oxide nanoparticles dispersion were dissolved in ethanol. The mixed solution was photoirradiated using a high-pressure Hg lamp for 24 h at room temperature.

Figure 1 shows extinction spectra with photoirradiation at 24 h. A peak of surface plasmon band for copper nanoparticles is observed at ~580 nm. When the copper nanoparticles solution was exposed to fresh air, the signal of surface plasmon band was decreaced. Additionally, surface plasmon peaks were red shift with exposure time. These coincidences imply that the copper nanoparticles were etched by exposure to fresh air. Furthermore, when the decomposed solution was re-photoirradiated, surface plasmon band for copper nanoparticles were observed again. It was proved that the formation and decomposition of copper nanoparticles could be alternately repeated by using the present method. These results have inspired us to develop applications for novel catalysts recycled by photoirradiation and optical devices that can be switched by photoirradiation and air exposure.

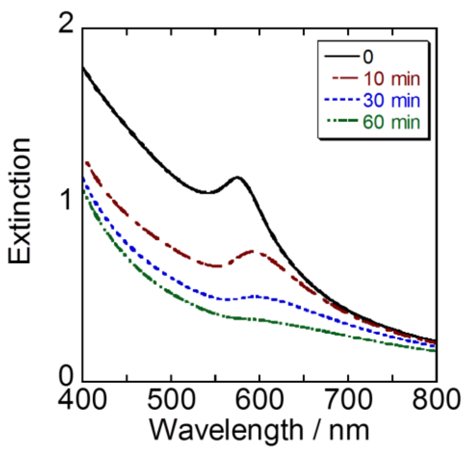

Figure 1. Extinction spectra of copper nanoparticles for air-exposure time.

References

[1] N. Nishida, A. Miyashita, N. Hashimoto, H. Murayama and H. Tanaka, Eur. Phys. J. D 63 (2011) 307.

[2] N. Nishida, A. Miyashita, T. Tsukuda and H. Tanaka, Chem. Lett. 42 (2013) 168.

Stoichiometry of cationic and anionic vanadium oxide clusters analyzed by ion mobility-mass spectrometry

Jenna W.J. Wu, Ryoichi Moriyama, Hiroshi Tahara, Keijiro Ohshimo, and Fuminori Misaizu

Department of Chemistry, Graduate School of Science, Tohoku University, 6-3 Aoba, Aramaki, Aoba-ku, Sendai 980-8578, Japan

Bulk vanadium oxides are widely studied due to their various usages in industry as oxidization catalyst. Structures and reactions of small vanadium oxide clusters, $V_mO_n^{+/-}$, are also being studied intensively. In this study, stable compositions of anionic and cationic vanadium oxide clusters up to m = 60 are identified and discussed.

Vanadium oxide cluster ions generated by laser vaporization were injected into a drift cell with an energy of 250 eV by a pulsed electric field. Collision-induced dissociations occur at the entrance of the cell, then the product ions pass through the cell by applied electrostatic field. The ions were detected in the later TOF mass-analysis process.

The stoichiometry components have a dependency on parity of the vanadium atom numbers, which is caused by the open and closed shell effect in the formation of clusters [1]. Odd numbered $V_mO_n^{+/-}$ clusters are closed-shell species with fully oxidized vanadium atoms; on the contrary even numbered $V_mO_n^{+/-}$ clusters are open-shell species containing uneven number of electrons.

In cationic odd numbered vanadium oxide clusters, $(VO_2)(V_2O_5)_x^+$ and $(VO)(V_2O_5)_x^+$ are mainly observed (listed according to the level of intensity); also, $(V_2O_4)(V_2O_5)_x^+$ and $(V_2O_5)_x^+$ are observed for even numbered clusters as shown in Figure 1. Similar to the cations, the anions also have several stable species corresponding to the number of vanadium atoms, yet, they exhibit in one-oxygen rich stoichiometry. For the odd numbered vanadium oxides $(VO_3)(V_2O_5)_x^-$ and $(VO_2)(V_2O_5)_x^-$ are observed; the even numbered are $(V_2O_5)_x^-$ and $(V_2O_4)(V_2O_5)_x^-$.

The above ions are in good agreement with photodissociation products for the small vanadium oxide clusters where m < 10 [2]. Additionally, the relatively stable species observed are due to terminal oxygen dissociation in the cluster formation and interaction processes. These characteristics are applicable to sizes up to m = 60.

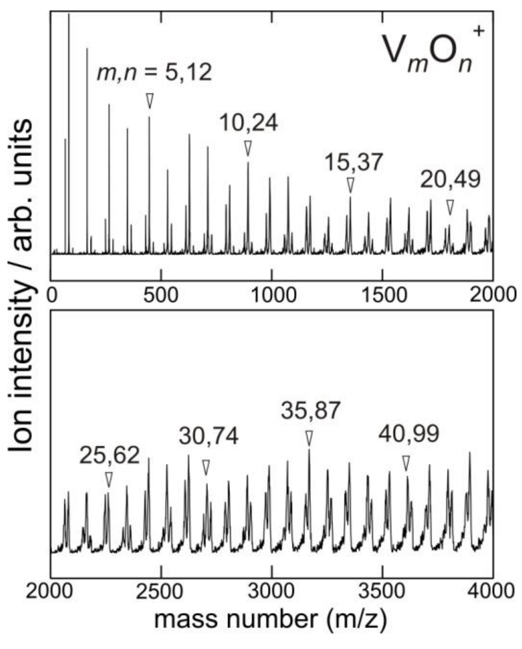

Figure 1. Cationic vanadium oxide clusters with even and odd numbered stoichiometry.

References
[1] G. Santambrogio, M. Brummer, and K. R. Asmis, Phys. Chem. Chem. Phys. 10 (2008) 3992.
[2] K. S. Molek, T. D. Jaeger, and M. A. Duncan, J. Chem. Phys. 123 (2005) 144313.

ISSPIC XVII
Fukuoka, 2014

POSTER SESSION B

September 11th, Thursday
16:30 - 18:30

Electron correlation: magnetism and superconductivity	B1-B11
Energy-related topics & Environmental studies	B12-B15
Optical properties and plasmonics	B16-B26
Carbon-based nanomaterials	B27-B35
Device-oriented topic	B36-B40
Structure and thermodynamics	B41-B63
Reactivity and catalysis	B64-B89

B1 **Anomalous Hall Effect in Uniform Fe nanocluster-Assembled Films**
Junbao Wang[1], Wenbo Mi[2], Laisen Wang[1], Qinfu Zhang[1], Dongliang Peng[1] ; [1] *Xiamen University,* [2] *Tianjin University*

B2 **Magnetism and exchange interaction in small Terbium clusters**
Andrei Kirilyuk[1], Saurabh Ghosh[2,3], Biplab Sanyal[3], Lars Peters[1], Chris van Dijk[1], John Bowlan[4], Anna Delin[3], Igor Di Marco[3], Walt de Heer[4], Mikhail I. Katsnelson[1], Olle Eriksson[3] ; [1] *Radboud University Nijmegen, IMM,* [2] *Cornell University,* [3] *Uppsala University,* [4] *Georgia Institute of Technology*

B3 **Relation between valence of iron ions in maghemite nanoparticles and their saturation magnetization**
Keita Kobayashi, Kazunari Nojiri, Tomoyuki Terai, Tomoyuki Kakeshita , Hidehiro Yasuda ; *Osaka University*

B4 **Magnetization and Mössbauer Study of Partially Oxidized Iron cluster Films Deposited on HOPG**
Nils Tarras-Wahlberg[1], Saeed Kamali[2], Mats Andersson[1,3], Christer Johansson[4], Arne Rosen[1,5] ; [1] *Gothenburg University and Chalmers University of Technology,* [2] *University of California, Davis,* [3] *Chalmers University of Technology,* [4] *Acreo Swedich ICT AB,* [5] *Gothenburg University*

B5 **Term rules for small aluminum clusters**
Daisuke Yoshida, Hannes Raebiger ; *Yokohama National University*

B6 **Self-doping of ultrathin insulating films by transition metal atoms**
Z. Li[1], H.-Y. T. Chen[2], K. Schouteden[1], L. Giordano[2], M. I. Trioni[3], E. Janssens[1], V. Iancu[1], C. Van Haesendonck[1], P. Lievens[1], G. Pacchioni[2] ; [1]*KU Leuven,* [2]*Università di Milano-Bicocca,* [3]*CNR - National Research Council of Italy, ISTM*

B7 **withdraw**

B8 **Probing the phonon density of states and its effect on superconductivity in Sn nanoparticles, nano-islands, and cluster-assembled films**
K. Houben[1], S. Couet[1], J. Jochum[1], D. Pérez[1], M. Bisht[1], M.Trekels[1], T. Picot[1], R. Rüffer[2], M.Y. Hu[3], S.A. Brown[4], F.M. Peeters[5], P. Lievens[1], A. Vantomme[1], K. Temst[1], M.J. Van Bael[1] ; [1] *KU Leuven* [2] *European Synchrotron Radiation Facility (ESRF),* [3] *Argonne National Laboratory,* [4] *University of Canterbury,* [5] *Universiteit Antwerpen*

B9 **X-ray absorption spectroscopy of free, size selected, singly metal doped silicon clusters**
Vicente Zamudio-Bayer[1,2], Linn Leppert[3], Konstantin Hirsch[2,4], Arkadiusz Ławicki[2], Andreas Langenberg[2,4], Jochen Rittmann[2,4], Martin Kossick[2,4], Marlene Vogel[2,4], Robert Richter[2,4], Thomas Möller[4], Akira Terasaki[5,6], Stephan Kümmel[3], Bernd von Issendorff[1], Julian Tobias Lau[2] ; [1]*Universität Freiburg,* [2] *Helmholtz-Zentrum Berlin für Materialien und Energie GmbH,* [3] *Universität Bayreuth,* [4] *Technische Universität Berlin,* [5] *Toyota Technological Institute,* [6] *Kyushu University*

B10 **Magnetic moments of chromium-doped gold clusters: The Anderson impurity model in finite systems**
K. Hirsch[1, 2], V. Zamudio-Bayer[5], A. Langenberg[1, 2], M. Niemeyer[1, 2], B. Langbehn[1, 2], T. Möller[2], A. Terasaki[3, 4], B. v. Issendorff[5], J. T. Lau[1] ; [1]*IHelmholtz-Zentrum Berlin für Materialien und Energie GmbH,* [2]*Technische Universität Berlin,* [3]*Toyota Technological Institute,* [4]*Kyushu University,* [5]*Universität Freiburg*

B11 **Superconducting properties of nanoparticles and small clusters**
T. Picot[1], H. Wang[1], K. Houben[1], A. Hillion[1], S. Bals[2], S.A. Brown[3], E. Janssens[1], P. Lievens[1], A. Vantomme[2], K. Temst[1], M.J. Van Bael[1] ; [1] *KU Leuven,* [2] *Universiteit Antwerpen,* [3] *University of Canterbury*

B12 **Formic Acid Oxidation Catalytic Properties of Pd Nanoparticles Prepared by Physical Vapor Deposition**
L.S. Wang, M. Lei, J.B. Wang, C.Y. Zou, D.L. Peng ; *Xiamen University*

B13 **Fabrication of Si nanoparticles from Si swarf and the application to hydrogen generation source**
Taketoshi Matsumoto[1], Katsuya Kimura[1], Kentaro Imamura[1], Masao Takahashi[1], Yayoi Kanatani[2], Tohru Higo[2], Hikaru Kobayashi[2] ; [1] *Osaka University, CREST-JST,* [2] *Nisshin Kasei Co., Ltd., CREST-JST*

B14 **Structural and optical properties of "Cauliflower" silicon nanoparticles**
Wingjohn Tang[1], Joren Eilers[1], Marijn van Huis[1], Da Wang[1], Ruud Schropp[2], Andries Meijerink[1], Alfons van Blaaderen[1], Marcel Di Vece[1] ; [1]*Utrecht University,* [2] *ECN, TU/e*

B15 **Sulfuric acid clusters in atmospheric particle formation: insights from computational approaches**
Henning Henschel, Oona Kupiainen-Määttä, Theo Kurtén, Ville Loukonen, Tinja Olenius, Hanna Vehkamäki ; *University of Helsinki*

B16 **Photoluminescence properties of Si nanoparticles fabricated from Si swarf: fluorescence enhancement by organic molecules**
Masanori Maeda, Taketoshi Matsumoto, Hikaru Kobayashi ; *Osaka University, CREST, Japan Science and Technology Agency*

B17 **$Ag_{44}SR_{30}$: What comes after the structure is solved?**
Lars Gell, Hannu Häkkinen ; *University of Jyväskylä*

B18 **Information on Quantum States Pervades the Absorption Spectra of the $Au_{144}(SR)_{60}$ Nanocluster**
H.-Ch. Weissker[1,2], V.D. Thanthirige[4], K. Kwak[5], D. Lee[5], G. Ramakrishna[4], R.L. Whetten[3], X. López-Lozano[3] ; [1] *Aix-Marseille Univ., CNRS,* [2] *European Theoretical Spectroscopy Facility,* [3] *The University of Texas at San Antonio,* [4] *Western Michigan University,* [5] *Yonsei University*

B19 **Preparation of non-toxic gold submicron-sized particles using laser-induced melting in liquids**
Takeshi Tsuji[1], Yuuma Higashi[2], Masaharu Tsuji[2], Yoshie Ishikawa[3], Naoto Koshizaki[3] ; [1] *Shimane University,* [2] *Kyushu University,* [3]*AIST,* [4]*Hokkaido University*

B20 **Polymer-protected fluorescent platinum nanoclusters and their application**
Xin Huang, Hidekazu Ishitobi, Yasushi Inouye ; *Osaka University,*

B21 **Electrochemical Reactions and Spectral Changes of Gold-Silver Core-shell Nanorods on ITO Plates**
Yuki Hamsaki[1], Naotoshi Nakashima[1,2,3], Yasuro Niidome[1,2,4] ; [1] *Kyushu University,* [2] *I2CNER WPI, Kyushu University,* [3] *CREST,* [4] *Kagoshima University (Present Affilication)*

B22 **Novel thiolate-protected gold clusters with sub-2 nm sized and fcc cores: synthesis and optical property**
Shinjiro Takano[1], Seiji Yamazoe[1,2], Kiichirou Koyasu[1,2], Tatsuya Tsukuda[1,2] ; [1] *The University of Tokyo,* [2] *Kyoto University*

B23 **Gold ultrathin nanowires and nanorods: First observation of surface plasmon resonance**
Ryo Takahata[1], Seiji Yamazoe[1,2], Kiichirou Koyasu[1,2], Tatsuya Tsukuda[1,2] ; [1] *The University of Tokyo,* [2] *Kyoto University*

B24 **Controlled formation of highly luminescent silver clusters in zeolite matrices via high-brilliance soft X-ray irradiation**
Didier Grandjean[1], Eduardo Coutino-Gonzalez[1], Maarten Roeffaers[1], Kristina Kvashnina[2], Eduard Fron[1], Bert Sels[1], Johan Hofkens[1], Peter Lievens[1] ; [1] *KU Leuven,* [2] *ESRF*

B25 **One-step Synthesis and Characterization of Benzenthiol Derivative-protected Gold Clusters**
Takuya Ishida[1], Yukina Takahashi[1], Hiroaki Okamura[2], Junichi Kurawaki[2], Sunao Yamada[1] ; [1] *Kyushu University,* [2] *Kagoshima University*

B26 **Ultrafast Strong Field Ionization of Small Metal Clusters**
Dennis Dieleman, Valeriy Chernyy, Theo Rasing, Andrei Kirilyuk ; *Radboud University*

B27 **Monocarbon cationic cluster synthesis from methane-nitrogen mixtures embedded in He nanodroplets and their calculated binding energies**
Iogann Tolbatov, Sylwia Ptasinska, Daniel M. Chipman ; *University of Notre Dame*

B28 **Genuinely amorphous carbon produced from explosive nano acetylide**
Ken Judai, Naoyuki Iguchi, Yoshikiyo Hatakeyama ; *Nihon University,*

B29 **Evaluation of the ratio of metal/semiconductive single-wall carbon nanotubes separated in two immiscible aqueous solution phases by utilizing Raman spectroscopy**
Shinzo Suzuki[1], Naoki Kanazawa[1], Akira Ono[2], Yohji Achiba[3] ; [1] *Kyoto Sangyo University,* [2] *Kanagawa University,* [3] *Tokyo Metropolitan University*

B30 **Growth of single-wall carbon nanotubes on the porous glass (PG) sheet by using ACCVD technique**
Shinzo Suzuki[1], Kyohei Nagao[1], Yosuke Ito[1], Nobuaki Ito[2], Hiroshi Nagasawa[3], Yohji Achiba[4] ; [1] *Kyoto Sangyo University,* [2] *JAIST,* [3] *Nano-support Co. Ltd.,* [4] *Tokyo Metropolitan University*

B31 **Analysis of the products of single-walled carbon nanotube growth with the aid of density functional theory calculations**
Arne Rosén[1], Yunguo Li[2], J. Andreas Larsson[4], Hamid Reza Barzebar[3], Thomas Wågberg[3] ; [1]*University of Gothenburg,* [2]*Royal Institute of Technology,* [3]*Umeå University,* [4]*Luleå University of Technology*

B32 **Bonding and Spin-polarized Transport of Co Atomic Chain on Graphene with Topological Line Defects**
Cheng-huan Jiang[1, 2], Gui-xian Ge[1], Jian-guo Wan[1], Guang-hou Wang[1] ; [1] *Nanjing University,* [2] *Communication University*

B33 **Metallic sp^2 carbon nanomaterials with octagons showing high density of states at the Fermi level: A first principles study**
Yusuke Noda, Shota Ono, Kaoru Ohno ; *Yokohama National University*

B34 **Simultaneous formation of fullerenes and polyynes by laser ablation in the gas phase at room temperature**
Hitomi Endo[1], Yuki Taguchi[1], Yurika Abe[1],Tomonari Wakabayashi[2], Takeshi Kodama[1], Yohji Achiba[1], Haruo Shiromaru[1] ; [1] *Tokyo Metropolitan University,* [2] *Kinki University*

B35 **Pressure dependence of production of carbon nanotubes by High-temperature Pulsed-arc Discharge**
Hayato Kikuchi, Atsushi Shimaya, Hiroki Koizumi, Ryota Jinnouchi, Katsuhide Terada, Toshiki Sugai ; *Toho University*

B36 **Ligand exchange reactions on transition metal oxo clusters and applications in materials chemistry**
Johannes Kreutzer, Ulrich Schubert ; *Vienna University of Technology*

B37 **Extending the Sizes and Charge States of Polyanionic Metal Clusters**
Steffi Bandelow[1], Franklin Martinez[1,2], Gerrit Marx[1], Lutz Schweikhard[1], Albert Vass[1] ; [1] *Ernst-Moritz-Arndt University Greifswald,* [2] *present address: University of Rostock*

B38 **Surface immobilization of gas-phase-synthesized nanoclusters toward construction of nanoelectronics**
Masato Nakaya[1,2], Takeshi Iwasa[1,2], Hironori Tsunoyama[1,2], Toyoaki Eguchi[1,2], Atsushi Nakajima[1,2] ; [1]*Nakajima Designer Nanocluster Assembly Project, JST,* [2] *Keio University,*

B39 **Generation of small and stable Si nanoparticles using a liquid jet co-deposition method**
Gediminas Galinis, Oliver Youle, Hanieh Yazdanfar, Mike J. McNally, Mumin M. Koç, Gauthier Torricelli, Mark Watkins, Klaus von Haeften ; *University of Leicester*

B40 **Enhanced quantum coherence in graphene by Pd cluster deposition and its zero-temperature saturation**
Fengqi Song, Junhao Han, Yuyuan Qin, Guanghou Wang ; *Nanjing University*

B41 **The hydrogen Bonded Networks in Hydrated Halogen Anions**
Chiaki Ishibashi[1], Suehiro Iwata[2], Kaoru Onoe[1], Hidenori Matsuzawa[1] ; [1] *Chiba Institute of Technology,* [2]*Keio University*

B42 **Formation of regular polyicosahedral structure during growth of large Lennard-Jones clusters from their global minimum**
Wieslaw Polak ; *Lublin University of Technology*

B43 **Structures and dielectric properties of neutral lead clusters**
D.A. Götz[1], A. Shayeghi[1], R.L. Johnston[2], P. Schwerdtfeger[3], R. Schäfer[1] ; [1] *Technische Universität Darmstadt,* [2] *University of Birmingham,* [3] Massey University

B44 **Fabrication of Ag cluster by a novel laser ablation of nanocolloid target**
Teppei Nishi, Yusuke Akimoto, Shuji Kajiya, Kosuke Kitazumi, Naoko Takahashi, Yoshihide Watanabe ; *Toyota Central R&D Labs., Inc.*

B45 **Solvation Chemistry of Water-Soluble Thiol-Protected Gold Nanocluster Au_{102} from DOSY NMR Spectroscopy and DFT Calculations**
Tanja Lahtinen, Kirsi Salorinne, Sami Malola, Jaakko Koivisto, Hannu Häkkinen ; *University of Jyväskylä*

B46 **Size-dependent structures of iron oxide cluster ions studied by ion mobility mass spectrometry**
Tatsuya Komukai, Ryoichi Moriyama, Keijiro Ohshimo, uminori Misaizu ; *Tohoku University*

B47 **Fabrication of Rh nanoframes through dissolution of Au cores of Au@Rh core-shell nanorods by the addition of HCl**
Yukinori Nakashima, Masashi Hattori, Masaharu Tsuji ; *Kyushu University*

B48 **Effect of Core Size on Au-Pt Core-Shell Nanoparticles for Oxygen Reduction Reaction**
Saki Hirose[1], Yoshikiyo Hatakeyama[2], Ken Judai[2], Takeshi Morita[1], Keiko Nishikawa[1] ; [1]*Chiba University,* [2]*Nihon University*

B49 **Melting of Weakly-Bound Systems by Monte Carlo Simulations – Applications to Mercury and Argon under High Pressure**
Elke Pahl[1], Jonas Wiebke[1], Peter Schwerdtfeger[1], Florent Calvo[2] ; [1] *Massey University Auckland,* [2] *ILM*

B50 **Design of Three-shell Icosahedral Matryoshka Clusters $A@B_{12}@A_{20}$ (A = Sn, Pb; B = Mg, Zn, Cd, Mn) Including a New Type of Magnetic Superatoms**
Xiaoming Huang [1], Jijun Zhao [*1,2], Yan Su [1], Zhongfang Chen [3], R. Bruce King [*4] ; [1] *Dalian University of Technology,* [2] *Beijing Computational Science Research Center,* [3] *University of Puerto Rico,* [4] *University of Georgia*

B51 **Structures, electronic and magnetic properties of $Fe_2Ge_n^-$ and $Cr_2Ge_n^-$ (n=3-12) clusters from DFT calculations and photoelectron spectra**
Xiaoqing Liang[1], Xiaoming Huang[1], Jijun Zhao[1*], Hongguang Xu[2], Weijun Zheng[2] ; [1]*Dalian University of Technology,* [2] *Chinese Academy of Sciences*

B52 **Geometric, electronic, and magnetic structure of Fe_xO_y clusters**
Remko Logemann, Gilles de Wijs, Mikhail Katsnelson, Andrei Kirilyuk ; *Radboud University Nijmegen*

B53 **Redispersibility of Solid State Cysteine-Capped CdSe Nanoparticles Depending on pH Values of These Aqueous Solution**
Takuya Kurihara, Yasuto Noda, K. Takegoshi ; *Kyoto University*

B54 **Structural Stability in icosahedral Ni-Zr-Nb ternary clusters**
Nobuhisa Fujima[1], Toshiharu Hoshino[1], Mikio Fukuhara [2] ; [1] *Shizuoka University,* [2] *Tohoku University*

B55 **Synthesis of Porphyrin-face Coordinated Au Clusters and Their Interfacial Interaction**
Masanori Sakamoto[1,2], Daichi Eguchi[1], Toshiharu Teranishi[1] ; [1] *Kyoto University,* [2] *PRESTO-JST*

B56 **Origin of Magic Stability for Aluminum-Boron Binary Nanoclusters**
Tomomi Nagase [1], Shoichiro Suga[1], Hironori Tsunoyama[1,2], Atsushi Nakajima[1,2] **;** [1]*Keio University,* [2]*Nakajima Designer Nanocluster Assembly Project, JST-ERATO*

B57 **Geometrical structures of vanadium oxide cluster ions studied by ion mobility mass spectrometry**
Ryoichi Moriyama, Jenna W. J. Wu, Hiroshi Tahara, Keijiro Ohshimo, Fuminori Misaizu ; *Tohoku University*

B58 **Synthesis of stable gold clusters face-coordinated by porphyrin derivatives containing disulfide groups**
Daichi Eguchi[1], Masanori Sakamoto[1,2], Toshiharu Teranishi[1] ; [1] *Kyoto University,* [2] *JST-PRESTO*

B59 **Observation of halogen adsorbates on magic numbered gold clusters stabilized by polyvinylpyrrolidone**
Setsuka Arii[1], Satoru Muramatsu[1], Seiji Yamazoe[1, 2],Kiichirou Koyasu[1, 2], Tatsuya Tsukuda[1, 2] ; [1] *The University of Tokyo,* [2] *Kyoto University*

B60 **Secondary ion emission from micro droplets induced by fast ion impacts**
Takuya Majima[1], Tatsuya Nishio[2], Kensei Kitajima[2], Yoshiki Oonishi [2], Hiroki Ueda[2], Hidetsugu Tsuchida[1], Akio Itoh[1,2] ; [1] *Kyoto University,* [2] *Kyoto University*

B61 **Drift time measurements of H_3O^+ hydrate formed by NO^+ injection into drift tube filled with H_2O/buffer gas at low temperatures**
Hiroshi Hidaka[1], Yoichi Nakai[2], Takao M. Kojima[3], Naoki Watanabe[1] ; [1] *Hokkaido University,* [2] *RIKEN Nishina Center for Accelerator-Based Science,* [3] *Atomic Physics Laboratory*, *RIKEN*

B62 **Solid-state absorption properties and crystal structures of di-alkynylated octanuclear gold clusters**
Mizuho Sugiuchi, Naoki Kobayashi, Yukatsu Shichibu, Katsuaki Konishi ; *Hokkaido University*

B63 **Helium droplets doped with sulfur and C_{60}**
Martina Harnisch[1], Nikolaus Weinberger[1], Stephan Denifl[1], Paul Scheier[1], Olof Echt[1,2] ; [1] *University of Innsbruck,* [2] *University of New Hampshire*

B64 **Size- and Isomer-Dependent Reactivity of Nickel Oxide Cluster Ions Studied by Ion Mobility Mass Spectrometry**
Keijiro Ohshimo, Shohei Azuma, Tatsuya Komukai, Ryoichi Moriyama, Fuminori Misaizu ; *Tohoku University*

B65 **Protected but Accessible: Oxygen Activation by Calixarene-stabilized Undecagold Cluster**
Xi Chen, Hannu Häkkinen ; *University of Jyväskylä*

B66 **The origin of the high selectivity and catalytic activity of small ruthenium clusters in the methanation of CO**
Sandra M. Lang[1], Thorsten M. Bernhardt[2], Marjan Krstić[2], Vlasta Bonačić-Koutecký[2,3] ; [1] *University of Ul,* [2] *University of Split*
[3] *Department of Chemistry, Humboldt-University Berlin*

B67 **Low-temperature catalytic activity of CO oxidation driven by strong electronic interaction between Pt-Ag bi-element cluster and Si surface**
Hisato Yasumatsu[1], Nobuyuki Fukui[2] ; [1] *Toyota Technological Institute,* [2] *Genesis Research Institute, Inc.*

B68 **Dynamics of truly monodisperse cluster catalysts under the STM**
Y. Fukamori, F. Knoller, M. König, F. Esch, U. Heiz ; *Technische Universität München*

B69 **Effects of Ir addition on gas-phase and supported Au nanoclusters towards catalytic CO oxidation**
Laura Michelle Jiménez-Díaz, Luis Antonio Pérez ; *Universidad Nacional Autónoma de México*

B70 **Theoretical investigation for isomerizaiton of allyl alcohol over Au cluster**
Mitsutaka Okumura[1,2], Kohei Tada[1], Kohei Sakata[1,] Hiroaki Koga[2] , Takashi Kawakami[1], Shusuke Yamanaka[1] ; [1] *Osaka University,* [2] *Kyoto University*

B71 **Synthesis of Ag@Pd/TiO_2 catalysts in an aqueous solution for the hydrogen generation from decomposition of formic acid at room temperature**
Daisuke Shimamoto, Masashi Hattori, Takeshi Daio , Masaharu Tsuji ; *Kyushu University*

B72 **Reaction of aluminum cluster cations with a mixture of O_2 and H_2O gases: Formation of hydrated-alumina clusters**
Masashi Arakawa, Kei Kohara, Akira Terasaki ; *Kyushu University*

B73 **Adsorption and catalytic activation of the molecular oxygen on the metal supported h-BN**
Andrey Lyalin[1], Akira Nakayama[1,2], Kohei Uosaki[3], Tetsuya Taketsugu[1,2] ; [1] *Kyoto University,* [2] *Hokkaido University,* [3] *GREEN, NIMS*

B74 **Reductive Activation of CO_2 by Cobalt Cluster Anions**
Akimaro Yanagimachi[1], Kiichirou Koyasu[1,2], Tatsuya Tsukuda[1,2] ; [1] *The University of Tokyo,* [2] *Kyoto University*

B75 **Theoretical study on the isomerization of small gold clusters induced by O_2 adsorption**
Min Gao[1], Daisuke Horita[1], Yuriko Ono[1], Andrey Lyalin[2], Satoshi Maeda[1,2], Tetsuya Taketsugu[1,2] ; [1] *Hokkaido University,* [2] *Kyoto University*

B76 **Materials Development for Realization of Carbon-Neutral Energy Cycles**
Miho Yamauchi ; *Kyushu University, JST-CREST*

B77 **Adsorption and decomposition of NO on foreign metal-doped copper cluster cations**
Shinichi Hirabayashi[1], Masahiko Ichihashi[2] ; [1] *Genesis Research Institute, Inc.,* [2] *Toyota Technological Institute*

B78 **withdraw**

B79 **Base catalysis of $[Nb_6O_{19}]^{8-}$ and $[Nb_{10}O_{28}]^{6-}$**
Shun Hayashi[1], Seiji Yamazoe[1,2], Kiichirou Koyasu[1,2], Tatsuya Tsukuda[1,2] ; [1] *The University of Tokyo,* [2] *Kyoto University*

B80 **FT-ICR study of chemical reaction of acetonitrile molecules on cobalt clusters**
Kazuki Ogasawara[1], Yuta Tobari[2], Yoshinori Sato[1], Makoto Saito[1], Shohei Chiashi[1] ,Toshiki Sugai[2], Shigeo Maruyama[1] ; [1] *The University of Tokyo,* [2] *Toho University*

B81 **Gold Nanoparticle-Catalyzed C–H Bond Functionalization for Biaryl Synthesis**
Yoshiyuki Mise[1], Shohei Aikawa[1], Tamao Ishida[1,4], Ryota Akebi[1], Akiyuki Hamasaki[1], Hironori Ohashi[1], Tetsuo Honma[2], Tetsuro Tsuji[3], Yasushi Yamamoto[3], Mitsuru Miyasaka[3], Takushi Yokoyama[1], Makoto Tokunaga[1] ; [1] *Kyushu University,* [2] *JASRI/SPring-8,* [3] *UBE Industries Ltd.,* [4] *Tokyo Metropolitan University*

B82 **Gas Phase Modeling of the Catalytically Active Centers in Iron Sulfur Proteins**
Heiko Heim, Thorsten M. Bernhardt, Sandra M. Lang ; *University of Ulm*

B83 **Thermal stability and reactivity with CO molecules of cerium oxide and gold-appended cerium oxide clusters**
Toshiaki Nagata, Ken Miyajima, Fumitaka Mafuné ; *The University of Tokyo*

B84 **Enhancement of photocatalytic activity of TiO_2 nanoparticles by addition of Ag nanoparticles**
Mari Yonemura, Naoki Nishida, Hideki Tanaka ; *Chuo University*

B85 **Towards the Creation of Functionalized Metal Nanoclusters and Highly Active Photocatalytic Materials Using Thiolate-Protected Magic Gold Clusters**
Yuichi Negishi ; *Tokyo University of Science*

B86 **Formation and structural analysis of composite of Ag nanoplates with TiO_2 nanoparticles**
Hiroki Nanjyo, Ken Iwai, Naoya Kinoshita, Naoki Nishida, Hideki Tanaka ; *Chuo University*

B87 **Instantaneous cooling of metal clusters by collision with rare gas clusters – Incorporation mechanism of a cobalt cluster ion into an argon cluster**
Hideho Odaka[1], Masahiko Ichihashi[2] ; [1] *East Tokyo Laboratory, Genesis Research Institute, Inc.*, [2] *Toyota Technological Institute*

B88 **Surface oxide luminescence of Silicon nanoclusters**
Hanieh Yazdanfar, Gediminas Galinis, Mike J. McNally, Mumin. M. Koç, Oliver Youle, Gauthier Torricelli, Mark Watkins, Klaus von Haeften ; *University of Leicester*

B89 **Autoionization in cluster Coulomb explosion studied by magnetic time-of-flight ion imaging**
C. Schaal, R. Irsig, S. Skruszewicz, J. Tiggesbäumker, K.-H. Meiwes-Broer ; *Universität Rostock*

Anomalous Hall Effect in Uniform Fe nanocluster-Assembled Films

Junbao Wang,[1] Wenbo Mi,[2] Laisen Wang[1] Qinfu Zhang[1] and Dongliang Peng[1]

[1] *Department of Materials Science and Engineering, Xiamen University, Xiamen, China*
[2] *Department of Applied Physics, Tianjin University, Tianjin, China*

Recently, the anomalous Hall effect (AHE) in ferromagnets has gained increasing attentions due to its controversial mechanisms [1,2]. Usually, in some heterogeneous systems the deviations from the scaling law ($\rho_{xy}^{A} \propto \rho_{xx}^{\gamma}$, γ=1, 2) between the saturated AHE resistivity (ρ_{xy}^{A}) and longitudinal resistivity (ρ_{xx}) were observed. However, so far few attempts have been made to study the relation between the different γ and the size distribution of nanoparticles. In this work, the uniform Fe nanocluster-assembled films with different thicknesses (t_a=160-1200 nm) were prepared by plasma-gas-condensation method. By Quantum Design physical property measurement system, we measured the magnetic and electrical transport properties of the samples ranging from 5 to 375 K. As shown in the inset of Fig. 1, ρ_{xy} was calculated from $V_{xy}t_a/I$, where V_{xy} is the transverse voltage, I the applied DC current. It is found that the Fe nanoclusters possess "core-shell" structure. Compared with bulk Fe, four-order (~2.4 $\times10^{-8}$ ΩcmG^{-1}) enhancement of the AHE coefficients was observed for the film with t_a=1200 nm at 300 K. The ρ_{xy}^{A} firstly increases and further decreases with the increasing temperature in the range of 5-375 K. Moreover, ρ_{xy}^{A} decreases with the increase of ρ_{xx} in log-log scales and following a new scaling relation of $\log(\rho_{xy}^{A}/\rho_{xx}) = a_0 + b_0 \log \rho_{xx}$ (Fig. 1).

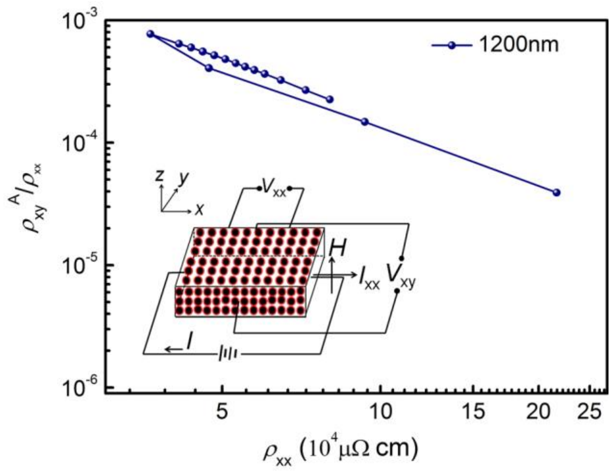

Fig. 1 The plot of $\log(\rho_{xy}^{A}/\rho_{xx}) - \log \rho_{xx}$ for the film with t_a=1200 nm.
In inset shows schematic of contact arrangement and Hall effect measurements.

Reference(s)

[1] P. He, L. Ma, Z. Shi, G. Y. Guo, J. G. Zheng, Y. Xin and S. M. Zhou, Phys. Rev. Lett, 109 (2012) 066402.

[2] Z. B. Guo, W. B. Mi, A. Manchon, J. Q. Li, B Zhang, P. G. Barba and X. X. Zhang, Appl. Phys. Lett, 102 (2013) 062413.

Magnetism and exchange interaction in small Terbium clusters

Andrei Kirilyuk[1], Saurabh Ghosh[2,3], Biplab Sanyal[3], Lars Peters[1], Chris van Dijk[1], John Bowlan[4], Anna Delin[3], Igor Di Marco[3], Walt de Heer[4], Mikhail I. Katsnelson[1], and Olle Eriksson[3]

[1] *Radboud University Nijmegen, IMM, Heyendaalseweg 135, 6525 AJ Nijmegen, The Netherlands*
[2] *School of Applied and Engineering Physics, Cornell University, Ithaca, New York 14853, USA*
[3] *Department of Physics and Astronomy, Uppsala University, Box 516, 751 20 Uppsala, Sweden*
[4] *School of Physics, Georgia Institute of Technology, Atlanta, Georgia 30332, USA*

The rare-earth metals have similar crystal structures, which arise from the relatively unchanged electronic structure of the valence shells as the localised 4f-shell is being filled [1]. In spite of this, their magnetic structures vary significantly [2]. This is directly related to the mechanism of the exchange interaction in these materials where the spin-polarized 4f wavefunctions of each atom do not overlap but are responsible for a large magnetic moment. In contrast, the spd electrons are delocalized and form bands, leading to rather complicated Fermi surfaces. The exchange interaction known as Ruderman-Kittel-Kasuya-Yosida (RKKY) interaction between the localised 4f moments is mediated by these delocalised electrons. It is long-ranged and results in the oscillatory behaviour of the magnetic coupling as a function of the separation between the atoms [3], described by the electron wavevectors at the Fermi surface. In a periodic lattice this causes certain frustrations and results in several magnetic phases, from simple ferromagnetism to antiferromagnetic helical [2,4]. When the system size is reduced, electronic wavefunctions mediating the exchange are constrained by the boundaries. Because of this, surfaces often show magnetic properties drastically different from the bulk [5]. The behavior becomes even more extreme if the size of the whole system is comparable to the length scale of the bulk exchange.
Here we follow, both experimentally and theoretically, the development of magnetism in Tb clusters from the atomic limit and adding one atom at a time. The exchange is, surprisingly, shown to drastically increase compared to that of the bulk, and to oscillate as a function of the interatomic distance. Unlike the bulk, the oscillation is not caused by the RKKY mechanism. Instead, the exchange is shown to be driven by finite size effects, leading to the variations of the exchange between ferromagnetic double-exchange and antiferromagnetic super-exchange mechanisms. As a consequence, the magnetic moment oscillates with cluster size in exact agreement with experimental data. Therefore the finite size effects and quantum confinement are key parameters when designing new rare-earth based magnets.

Reference(s)

[1] A. Delin, L. Fast, B. Johansson, J.M. Wills, O. Eriksson, Phys. Rev. Lett. 79 (1997) 4637
[2] J. Jensen and A.R. Mackintosh, Rare Earth Magnetism (Clarendon Press, Oxford, 1991)
[3] D.A. Goodings, J. Phys. C (Proc. Phys. Soc.), ser. 2, vol. 1 (1968) 125
[4] L. Nordström and A. Mavromaras, Europhys. Lett. 49 (2000) 775
[5] E. Vescovo, C. Carbone, and O. Rader, Phys. Rev. B 48 (1993) 7731.

Relation between valence of iron ions in maghemite nanoparticles and their saturation magnetization

Keita Kobayashi,[1] Kazunari Nojiri,[2] Tomoyuki Terai,[2] Tomoyuki Kakeshita[2] and Hidehiro Yasuda[1,2]

[1] *Research Center for Ultra-High Voltage Electron Microscopy, Osaka University, Ibaraki, Osaka 567-0047, Japan*

[2] *Division of Materials and Manufacturing Science, Graduate School of Engineering, Osaka University, Suita, Osaka 565-0871, Japan*

Since solid state properties of nanomaterials strongly depend on the size, to understand detailed mechanism of size dependence of the properties is important for practical application of novel nanomaterials. Especially, clarification of mechanism of size dependency of magnetic properties has been required because nano magnetic materials have been expected as key materials for development of high density storage media and medical applications.

In this study, to clarify the mechanism of diameter dependence of magnetic properties of magnetic nanomaterials, maghemite (γ-Fe_2O_3) nanoprticles with various diameter distributions were prepared by coprecipitation, and the saturation magnetization and the microscopic structures and electronic states of these nanoparticles were compared by vibrating sample magnetometry, transmission electron microscopy, and electron energy loss spectroscopy.

Although transmission electron diffractometry did not reveal any structural differences between nanoparticles, we found, by electron energy loss spectroscopy, that the valence of iron ion in the nanoparticles tended to change from Fe^{3+} to Fe^{2+} with decreasing the saturation magnetization. These results suggest that the decreasing saturation magnetization is attributed to increase of oxygen deficiency density in the nanoparticles.

This work was supported by KAKENHI (#25790003) from JSPS. The authors thank Mr. M. Fujisaki (Renovation Center of Instruments for Science Education and Technology, Osaka University) for ICP measurements, and Hayashibara Co., Ltd. for providing a portion of reagent used in this study.

Magnetization and Mössbauer Study of Partially Oxidized Iron cluster Films Deposited on HOPG

Nils Tarras-Wahlberg[1], Saeed Kamali[2], Mats Andersson[1,3], Christer Johansson[4], and Arne Rosen[1,5]

[1] *Experimental Physics, Gothenburg University and Chalmers University of Technology, SE-412 96, Göteborg, Sweden*

[2] *Department of Chemistry, University of California, Davis, California 95616, USA*

[3] *Department of Applied Mechanics, Chalmers University of Technology, SE-412 96, Göteborg, Sweden*

[4] *Acreo Swedich ICT AB, Arvid Hedvalls Backe 4, SE-400 14, Göteborg, Sweden*

[5] *Department of Physics, Gothenburg University, SE-412 96 , Göteborg, Sweden*

Iron clusters produced in a laser vaporization source were deposited to form cluster-assembled thin films with different thicknesses on highly oriented pyrolytic graphite substrates. The development of oxidation of the clusters with time, up to three years, was investigated by magnetic measurements using an alternating gradient magnetometer [1]. Furthermore, to receive information about the oxidation states, clusters of ^{57}Fe were studied using Mössbauer spectroscopy. The magnetic analysis shows a time evolution of the saturation magnetization, remanence, and coercivity, determined from the hysteresis curves characteristic of a progressing oxidation. The different thicknesses of the iron cluster films as well as a protective layer of vanadium influence the magnetic properties when the samples are subjected to oxidation with time. While the saturation magnetization and remanence decrease and reach half the initial values for almost all the samples after three years, the coercivity increases for all samples and is more substantial for the thickest sample with a vanadium protective layer. This value is three folded after three years. Furthermore, based on a core-shell model and using the saturation magnetization values we have been able to quantitatively calculate the amount of the increase of Fe-oxide as a function of time. The Mössbauer spectroscopy shows peaks corresponding to iron metal and maghemite.

Reference(s)

[1] N. Tarras-Wahlberg, S. Kamali, M. Andersson, C. Johansson, A. Rosén, Journal of Magnetism and Magnetic Materials **367**, 40 (2014)

Term rules for small aluminum clusters

Daisuke Yoshida, Hannes Raebiger

Department of Physics, Yokohama National University, Yokohama, Japan

The ground states terms of isolated atoms are determined by Hund's rules, which are explained by the lowering of the electronuclear attraction energy [1-3]. For molecules and clusters, such term rules do not exist. We search for such terms rules by first principles calculation of small Al clusters. Bulk Al is paramagnetic, but in low dimensional structures Al atoms may spontaneously align their spins. Al_n clusters with even $n = 2, 4, 6, 8$ have spin-triplet ground states [3-6]. Al_3 on the other hand has spin-doublet (low spin) state and spin-quadruplet (high spin) configurations, but which one of these is the ground state remains unsolved [7-10]. Our present benchmark study confirms that Al dimer has the $^3\mathrm{P}_u$ high spin ground state and unambiguously shows that Al trimer has the $^2A'_1$ low spin ground state. Al dimer is consistent with both Hund's first and second rules, but the ground state term cannot be explained by traditional interpretations [1-4,11-13]. Al trimer violates Hund's rule. Al dimer's high spin term is stabilized by Fermi correlation, whereas Al trimer's low spin is stabilized by Coulomb correlation which overwhelms Fermi correlation. We show that all the molecular terms of dimer and trimer can be described by simple rules pertaining to bonding structures and symmetries. This mechanism is described by our high accuracy variational calculation.

References

[1] J. Katriel and R. Pauncz, Adv. in Quantum Chem. 10, 143 (1977).
[2] R. J. Boyd, Nature 310, 480 (1984).
[3] T. Oyamada, K. Hongo, Y. Kawazoe, and H. Yasuhara, J. Chem. Phys. 133, 164113 (2010).
[4] G. Pacchioni, D. Plavˇsić, and J. Koutecký, Ber. Bunsenges. Phys. Chem. 87, 503 (1983).
[5] L. Pettersson, C. W. Bauschlicher, and T. Halicioglu, J. Chem. Phys. 87, 2205 (1987).
[6] C. W. Bauschlicher, H. Partridge, S. R. Langhoff, P. R. Taylor, and S. P. Walch, J. Chem. Phys. 86, 7007 (1987).
[7] D. M. Cox, D. J. Trevor, R. L. Whetten, E. A. Rohlfing, and A. Kaldor, J. Chem. Phys. 84, 4651 (1986).
[8] J. A. Howard, R. Sutcliffe, J. S. Tse, H. Dahmane, and B. Mile, J. Phys. Chem. 89, 3595 (1985).
[9] J. Tse, J. Chem. Phys. 92, 2488 (1990).
[10] Y. M. Hamrick, R. J. Vanzee, and W. Weltner, J. Chem. Phys. 96, 1767 (1992).
[11] J. C. Slater, Phys. Rev. 34, 1293 (1929).
[12] J. H. Van Vleck, J. Chem. Phys. 3, 807 (1935).
[13] J. P. Colpa and R. E. Brown, J. Chem. Phys. 68, 4248 (1978).

Self-doping of ultrathin insulating films by transition metal atoms

Z. Li,[1,*] H.-Y. T. Chen,[2] K. Schouteden,[1] L. Giordano,[2] M. I. Trioni,[3] E. Janssens,[1] V. Iancu,[1] C. Van Haesendonck,[1] P. Lievens,[1] and G. Pacchioni[2]

[1]*Laboratory of Solid-State Physics and Magnetism, KU Leuven, BE-3001 Leuven, Belgium*
[2]*Dipartimento di Scienza dei Materiali, Università di Milano-Bicocca, I-20125 Milano, Italy*
[3]*CNR - National Research Council of Italy, ISTM, I-20133 Milano, Italy*

Deposition of metal atoms on solid surfaces is usually employed to study nucleation and growth of metal nanoparticles that are relevant for heterogeneous catalysis, sensors, optical and magnetic data storage, etc. Growth of ultrathin films of insulating materials on a metallic substrate prior atom deposition can provide additional control of the coupling of the metal adsorbates with the metallic substrate [1–3]. Soft landing of metal atoms on insulating thin layers is typically noninvasive and results in cluster growth with little or no surface damage.

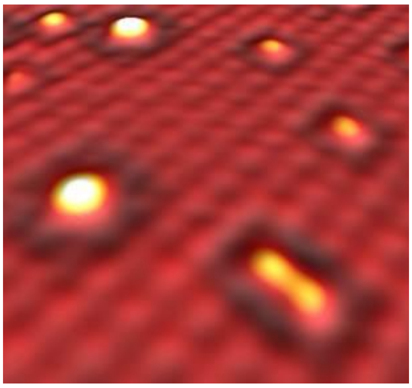

Here, we demonstrate an uncommon case of spontaneous doping by transition metals on ultrathin insulating films. Individual magnetic atoms (Co and Cr) are deposited on atomically thin NaCl films on Au(111). Two different adsorption sites are revealed by high-resolution scanning tunneling microscopy (STM), i.e., at Na and at Cl locations. Using density functional based STM simulations, we show that the magnetic atoms substitute with either a Na or Cl atom of the NaCl surface, resulting in cationic and anionic dopants with a high thermal stability. Moreover, since the dopants bear large localized magnetic moments, the dimers represent an ideal system to study magnetic interactions between diluted magnetic impurities in an insulating matrix. By mapping the local density of states, the dependence of the magnetic coupling between neighboring magnetic atoms on their separation is investigated [4]. The here reported self-doping of an insulating material by magnetic atoms may open a novel route to tune catalytic, optical, magnetic, and transport properties of materials.

Reference(s)
[1] J. Repp, et al., Science 305 (2004) 493.
[2] J. Repp, et al., Phys. Rev. Lett. 95 (2005) 225503.
[3] C. F. Hirjibehedin, et al., Science 317 (2007) 1199.
[4] Z. Li, et al., Phys. Rev. Lett. 112 (2014) 026102.

withdraw

Probing the phonon density of states and its effect on superconductivity in Sn nanoparticles, nano-islands, and cluster-assembled films

K. Houben[1], S. Couet[2], J. Jochum[1], D. Pérez[2], M. Bisht[2], M.Trekels[2], T. Picot[1], R. Rüffer[3], M.Y. Hu[4], S.A. Brown[5], F.M. Peeters[6], P. Lievens[1], A. Vantomme[2], K. Temst[2], M.J. Van Bael[1]

[1] *Laboratory of Solid-State Physics and Magnetism, KU Leuven, Belgium*
[2] *Instituut voor Kern- en Stralingsfysica, KU Leuven, Belgium*
[3] *European Synchrotron Radiation Facility (ESRF), Grenoble, France*
[4] *Advanced Photon Source (APS), Argonne National Laboratory, Illinois USA*
[5] *MacDiarmid Institute for Advanced Materials and Nanotechnology, University of Canterbury, NZ*
[6] *Departement Fysica, Universiteit Antwerpen, Belgium*

Phonons influence many material properties, such as thermal and mechanical behavior. Furthermore, the electron-phonon interaction lies at the basis of Cooper-pair formation and is therefore of crucial importance in conventional phonon-mediated superconductivity. As worked out in the Eliashberg formalism, the phonon density of states (PDOS) directly determines key superconducting parameters such as the electron-phonon coupling strength and the critical temperature T_C. When reducing the system dimensions down to the nanometer scale, phonon confinement effects and the appearance of surface phonon modes result in deviations in the phonon density of states with respect to the corresponding bulk PDOS [1]. Such phonon confinement effects may in turn induce changes of the superconducting properties [2]. While the phonon spectrum of bulk systems is well understood, considerably less is known about the vibrational behavior in nanostructures because of the difficulty of experimentally probing atomic vibrations at this scale.

Tin (Sn) is known as a weak-coupling superconductor with a bulk T_C of 3.72 K. Significant T_C enhancements have been observed in weak-coupling superconducting nanostructures [3], which are (partially) ascribed to confinement effects of the phonon spectrum. In this work, we have experimentally measured the PDOS of embedded Sn nanoparticles in SiO_2, Sn cluster-assembled layers and Sn nano-islands by nuclear inelastic scattering (NIS) of synchrotron radiation which specifically probes the ^{119}Sn isotope [2]. The PDOS of all these nanoscale Sn systems show clear modifications compared to that of a reference bulk Sn sample, such as an energy redistribution of the phonon modes or the appearance of new modes. Moreover, T_C enhancements well above 10% were detected in the superconducting properties and we have disentangled to what extent this is attributable to the observed phonon confinement effects. For the thicker Sn islands, we can conclude that phonon confinement does explain the modified T_C, while for the smaller islands and cluster-assembled Sn films other effects like electron confinement become more important.

Reference(s)

[1] B. Roldan Cuenya et al., Phys. Rev. B 64 (2001) 235321.
[2] S. Couet et al., Phys. Rev. B 88 (2013) 045437.
[3] B. Abeles et al., Phys. Rev. Lett. 17 (1966) 632.

X-ray absorption spectroscopy of free, size selected, singly metal doped silicon clusters

Vicente Zamudio-Bayer[1,2], Linn Leppert[3], Konstantin Hirsch[2,4], Arkadiusz Ławicki[2], Andreas Langenberg[2,4], Jochen Rittmann[2,4], Martin Kossick[2,4], Marlene Vogel[2,4], Robert Richter[2,4], Thomas Möller[4], Akira Terasaki[5,6], Stephan Kümmel[3], Bernd von Issendorff[1] and Julian Tobias Lau[2]

[1]Fakultät für Physik, Universität Freiburg, Stefan-Meier-Straße 21, 79104 Freiburg, Germany
[2]Institut für Methoden und Instrumentierung der Forschung mit Synchrotronstrahlung, Helmholtz-Zentrum Berlin für Materialien und Energie GmbH, Albert-Einstein-Straße 15, 12489 Berlin, Germany
[3]Theoretische Physik IV, Universität Bayreuth, 95440 Bayreuth, Germany
[4]Institut für Optik und Atomare Physik, Technische Universität Berlin, Hardenbergstraße 36, 10623 Berlin, Germany
[5]Cluster Research Laboratory, Toyota Technological Institute, 717-86 Futamata, Ichikawa, Chiba 272-0001, Japan
[6]Department of Chemistry, Kyushu University, 6-10-1 Hakozaki, Higashi-ku, Fukuoka 812-8581, Japan

The size dependent magnetic properties and electronic structure of small, 3d transition metal doped silicon clusters have been studied spectroscopically. The cluster ions were size selected, stored in a liquid Helium cooled ion trap and irradiated with the x-ray beam from an undulator at the BESSY II synchrotron facility. The x-ray absorption and x-ray magnetic circular dichroism (XMCD) at the $L_{2,3}$-edges of the single 3d transition metal impurity were measured in ion yield mode [1]. Special emphasis was placed on the influence that the encapsulation of the single impurity at the exo- to endohedral doping transition has on the magnetic moment. Information on the geometries of the clusters was obtained by combining the experimental results with density functional theory calculations. By applying the XMCD sum rules [2], it was furthermore possible to resolve the spin and orbital contribution to the impurity's magnetic moment as a function of the cluster's chemical composition and geometry. The correlation of magnetic moment with dopant coordination and metal silicon nearest-neighbor distance observed in this model systems can be generalized to bulk dilute magnetic semiconductors.

Reference(s)

[1] V. Zamudio-Bayer, L. Leppert, K. Hirsch, A. Langenberg, J. Rittmann, M. Kossick, M. Vogel, R. Richter, A. Terasaki, T. Möller, B. v. Issendorff, S. Kümmel, and J. T. Lau, Phys. Rev. B, 88, 115425 (2013)

[2] B. T. Thole, P. Carra, F. Sette, and G. van der Laan, Phys. Rev. Lett., 68, 1943 (1992); P. Carra, B. T. Thole, M. Altarelli, and X. Wang, Phys. Rev. Lett., 70, 694 (1993)

Magnetic moments of chromium-doped gold clusters: The Anderson impurity model in finite systems

K. Hirsch[1, 2], V. Zamudio-Bayer[5], A. Langenberg[1, 2], M. Niemeyer[1, 2], B. Langbehn[1, 2], T. Möller[2], A. Terasaki[3, 4], B. v. Issendorff[5] and J. T. Lau[1]

[1]*Institut für Methoden und Instrumentierung der Forschung mit Synchrotronstrahlung, Helmholtz-Zentrum Berlin für Materialien und Energie GmbH, Albert-Einstein-Straße 15, 12489 Berlin, Germany*

[2]*Institut für Optik und Atomare Physik, Technische Universität Berlin, Hardenbergstraße 36, 10623 Berlin, Germany*

[3]*Cluster Research Laboratory, Toyota Technological Institute, 717-86 Futamata, Ichikawa, Chiba 272-0001, Japan*

[4]*Department of Chemistry, Kyushu University, 6-10-1 Hakozaki, Higashi-ku, Fukuoka 812-8581, Japan*

[5]*Fakultät für Physik, Universität Freiburg, Stefan-Meier-Straße 21, 79104 Freiburg, Germany*

A long standing problem in condensed matter physics is the interaction of a single magnetic impurity with a free electron gas resulting in interesting many body phenomena like the Kondo effect. In recent years substantial progress was obtained by pushing the experiments to atomic scales. Here we want to follow this approach and investigate the interaction of a single magnetic impurity with a finite free electron gas. $CrAu_n^+$ clusters serve as a model system [1]: We can show that the size dependence of the local spin magnetic moment of $CrAu_n^+$ clusters can be well described within a modified version of the Anderson impurity model taking into account the highly discretized density of states of the gas phase gold host [2,3]. The interaction of the localized impurity states with the electron bath of the gold matrix is governed by quantum confinement in the host. We show that the size of the impurity spin magnetic moment can be controlled by the size of the energy gap in the host density of states. This introduces the possibility to even restore the spin degree of freedom of the impurity atom although absent in the corresponding bulk material.

Reference(s)

[1] K. Hirsch et al., submitted to Phys. Rev. Lett.
[2] P. W. Anderson, Phys. Rev. **124**, 41 (1961).
[3] K. Hirsch et al., submitted to Phys. Rev. B

Superconducting properties of nanoparticles and small clusters

T. Picot[1], H. Wang[2], K. Houben[1], A. Hillion[1], S. Bals[3], S.A. Brown[4], E. Janssens[1], P. Lievens[1], A. Vantomme[2], K. Temst[2], M.J. Van Bael[1]

[1] *Laboratory of Solid-State Physics and Magnetism, KU Leuven*
[2] *Instituut voor Kern- en Stralingsfysica, KU Leuven*
[3] *Elektronenmicroscopie voor Materiaalonderzoek*, *Universiteit Antwerpen*
[4] *The MacDiarmid Institute for Advanced Materials and Nanotechnology*, *University of Canterbury*

We present two different approaches to study the superconducting properties of small particles with a size ranging from a few nanometers down to the sub-nanometer scale with clusters made of a countable number of atoms. In the first approach, ion implantation has been used to synthesize Pb nanoparticles with a diameter ranging from 8 to 20 nm inside an Al matrix [1]. Detailled structural characterization of the nanocomposite material shows the highly epitaxial relation between the nanoparticles and the crystalline matrix. The Al/Pb nanocomposites display a single superconducting transition temperature increasing linearly with the amount of Pb. Our experimental data can be well described by superconducting proximity effect models for strongly coupled superconductors with a value of the electron-phonon coupling constant for the Pb nanoparticles of $\lambda = 1.2$ slightly lower than in bulk Pb ($\lambda = 1.55$). Our analysis reveals the high quality of the matrix-nanoparticle interface obtained by ion implantation synthesis. In the second approach, nanoparticles and small clusters are produced using a magnetron sputtering cluster source equipped with a high resolution RF quadrupole mass filter and a UHV deposition chamber compatible with in situ STM. We give a general overview of the source and the cluster size distribution in different production regimes. Perspectives are discussed to study the superconducting properties of small size-selected deposited clusters.

Reference(s)

[1] H. Wang et al. Supercond. Sci. Technol. 27 (2014) 015008

Formic Acid Oxidation Catalytic Properties of Pd Nanoparticles Prepared by Physical Vapor Deposition

L.S. Wang [a], M. Lei, J.B. Wang, C.Y. Zou and D.L. Peng [b]

Department of Materials Science and Engineering, College of Materials, Xiamen University, Xiamen 361005, P. R. China

Corresponding authors: [a] wangls@xmu.edu.cn; [b] pengdl@xmu.edu.cn

Pd catalysts in nanoscale showed better catalysis efficiency for formic acid oxidation, and hold a great potential to replace Pt due to its lower cost and more resistance to CO poisoning.[1] However, traditional chemosynthesis has been a long standing challenge in obtaining Pd nanoparticles with ultraclean surface. Fortunately, these problems are expected to be resolved by physical vapor deposition which is different from traditional chemosynthesis. [2]

In this work, Pd nanoparticles were synthesized under the high vacuum and inert gas condition by using the plasma-gas-condensation clusters deposition apparatus (see Fig.1), and softly landed on the glassy carbon plate (GCP) directly. The Pd cluster-assembled films whose packing density was only about 30% for bulk Pd were obtained. The Pd catalysts prepared here have many advantages including ultraclean surface, small size and porous stacks which can achieve more active sites, larger specific surface area and effective contact area in catalytic reaction, therefore, the excellent electrocatalytic activities including a large electrochemical surface area (100.0 $m^2 g^{-1}$), a high current density peak of formic acid oxidation (0.58 mA cm^{-2} and 0.55 mA μg^{-1}Pd) and considerable stability have been obtained. Furthermore, the effects of substrate temperatures on catalytic activity have been studied.

Based on what we have discussed above, we supposed that our recent research would focus wide interests among chemists and material scientists, and desirable to share with other researchers as soon as possible. Further investigation is carrying out in in our laboratory currently.

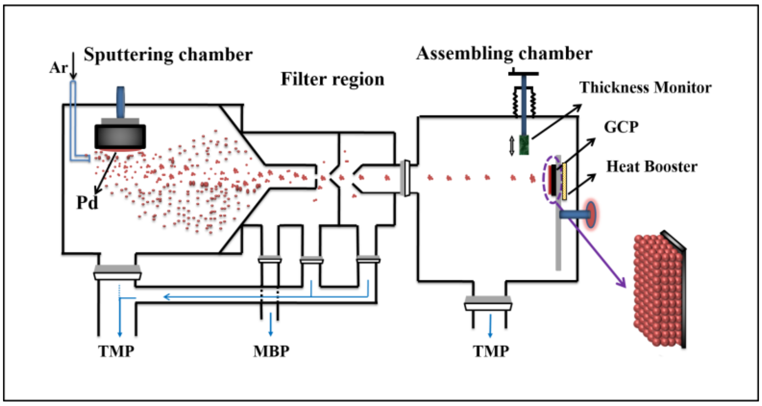

Fig. 1. Schematic diagram of Pd NC deposition process in the nanoparticle composite deposition system.

Reference(s)

[1] V. Mazumder, M. Chi, M. N. Mankin, Y. Liu *et al.*, Nano letters 12 (2012) 1102-1106.

[2] L.S. Wang, R.T Wen, Y. Chen, D.L. Peng, T. Hihara, Appl. Phys. A 103 (2011) 1015-1020.

Fabrication of Si nanoparticles from Si swarf and the application to hydrogen generation source

Taketoshi Matsumoto,[1] Katsuya Kimura,[1] Kentaro Imamura,[1] Masao Takahashi,[1] Yayoi Kanatani[2] Tohru Higo,[2] and Hikaru Kobayashi[2]

[1] *ISIR, Osaka University and CREST-JST, Ibaraki, Japan*
[2] *Nisshin Kasei Co., Ltd. and CREST-JST, Osaka, Japan*

Si nanoparticles have a potential for a hydrogen generation source [1]. We have developed a fabrication method of Si nanoparticles from Si swarf applicable to light emitting materials [2] and solar cells [3]. Si swarf is an industrial waste generated during slicing Si ingots for fabrication of solar cells and LSI, and thus, the production cost for Si nanoparticles can be reduced remarkably by use of Si swarf. In this study, the Si nanoparticles are produced from Si swarf and the reaction mechanism with water to generate hydrogen is investigated.

Si swarf was milled with a beads mill to fabricate Si nanoparticles. X-ray diffraction patterns showed clear peaks assigned to crystalline Si. The volume distribution of Si nanoparticles evaluated using the algorism proposed by Ida et al.[4] showed the maximum distribution diameter of 6.1 nm. An SiO_2 layer on Si nanoparticles was etched in 50wt% HF aqueous solutions, followed by rinse with ultrapure water. Si nanoparticles were immersed in 40wt% HNO_3 to form ultrathin SiO_2 layer to prevent Si nanoparticles from floating on the solutions.

Si nanoparticles were immersed in 100 ml water of pH controlled with KOH. The hydrogen generation rate for the initial 2.5 min reached to ~400 ml/min.g at 50°C and pH of 13, i.e., 1000 ml hydrogen was produced from 1 g Si nanoparticles in 2.5 min. The hydrogen generation stopped when ~1100 ml/g hydrogen was generated due to formation of an SiO_2 layer on the Si nanoparticle surface as indicated by X-ray photoelectron spectra. By removal of the SiO_2 layer with HF solutions, ~500 ml/g hydrogen was generated again to from these Si nanoparticles. The hydrogen generation rate and also the total evolved hydrogen volume decreased by a decrease in pH of the solutions. It is concluded that in the case of high pH, the Si dissolution reaction is predominant while the reaction for SiO_2 formation on Si nanoparticle surface is dominant for low pH.

References

[1] F. Erogbogbo, T. Lin, P.M. Tucciarone, K.M. LaJoie, L. Lai, G.D. Patki, P.N. Prasad, and M.T. Swihart, Nano Lett. 13 (2013) 451.
[2] T. Matsumoto, M. Maeda, J. Furukawa, W.-B. Kim, and H. Kobayashi, J. Nanopart. Res. 16 (2014) 2240.
[3] M. Maeda, K. Imamura, T. Matsumoto, and H. Kobayashi, Appl. Surf. Sci. *in press*.
[4] T. Ida, S. Shimazaki, H. Hibino, H. Toraya, J. Appl. Crystal. 36 (2006) 1107.

Structural and optical properties of "Cauliflower" silicon nanoparticles

Wingjohn Tang[1], Joren Eilers[2], Marijn van Huis[1], Da Wang[1], Ruud Schropp[3], Andries Meijerink[2], Alfons van Blaaderen[1], Marcel Di Vece[1 4]

[1]Soft Condensed Matter, Debye Institute for Nanomaterials Science, Utrecht University, Princetonplein 5, 3584 CC Utrecht, The Netherlands
[2]Condensed Matter and Interfaces, Debye Institute for Nanomaterials Science, Utrecht University, Princetonplein 5, 3584 CC Utrecht, The Netherlands
[3]Energy research Center of the Netherlands (ECN), Solar Energy, High Tech Campus Building 5, 5656 AE Eindhoven; and Eindhoven University of Technology (TU/e), Department of Applied Physics, Plasma & Materials Processing, P.O. Box 513, 5600 MB Eindhoven
[4]Nanophotonics—Physics of Devices, Debye Institute for Nanomaterials Science, Utrecht University, P.O. Box 80000, 3508 TA Utrecht, The Netherlands

The photovoltaics (PV) market is currently dominated by silicon based solar cell technology because of its relative ease of production and its consistence of abundant and non-toxic materials only. Although new concepts and materials are intensively investigated to increase efficiencies even more, silicon remains a very attractive PV material. Combining silicon with one of such new concepts, the quantum dot, may lead to enhanced device performance[1]. The advantage of silicon quantum dots are their tunable band gap, which can be employed in a tandem cell, and the direct optical transition, which increases absorption.
In this work we produced silicon nanoparticles with a gas aggregation cluster source by magnetron sputtering. The silicon particles were deposited on a substrate and investigated with a suit of techniques such as transmission electron microscopy (TEM), Raman spectroscopy and (time resolved) photoluminescence spectroscopy. Various stages of silicon nanoparticle formation were identified, depending on the cluster source operational parameters. 'Cauliflower'-like particles of about 50-100 nm exhibited the most interesting optical features. They are likely formed by aggregation of smaller silicon nanoparticles and are an intermediate state towards large crystalline particles. These 'cauliflower' silicon particles contain pockets of crystalline and amorphous silicon (a-Si). In agreement with the direct bad gap of a-Si, a photoluminescence signal belonging to this state was measured [2]. Although the dimensions of the a-Si pockets are small, no quantum confinement effects could be observed, likely due to the very close proximity of neighbouring particles. In this study we explored the optical and structural properties of 'cauliflower' silicon nanoparticles, which forms a diving board to using cluster source produced silicon particles for PV.

Reference(s)

[1] G. Conibeer, Mat. Today, **10**, 42 (2007)
[2] A. Vivas Hernandez et al. J. of Physics: Conf. Series **61**,1233 (2007)

Sulfuric acid clusters in atmospheric particle formation: insights from computational approaches

Henning Henschel,[1] Oona Kupiainen-Määttä,[1] Theo Kurtén,[2] Ville Loukonen,[1] Tinja Olenius,[1] and Hanna Vehkamäki[1]

[1] *Department of Physics, University of Helsinki, Helsinki, Finland*
[2] *Department of Chemistry, University of Helsinki, Helsinki, Finland*

A significant fraction of atmospheric aerosol particles are formed in the atmosphere from condensable vapors. The phenomenon is often initiated by sulfuric acid, with the most likely other key participants in the lower troposphere being ammonia, amines and other organic compounds. The very first steps of the process involving the formation of stable clusters are among the most challenging to approach, both theoretically and experimentally. Earlier theories based on macroscopic thermodynamics have failed to reproduce experimental particle formation rates; at present, molecular-level computational chemistry and physics are the state-of-the-art tools to study atmospheric clustering processes, and have produced thus far the best agreement with observations.

The palette of computational methods ranges from electronic structure calculations and molecular dynamics simulations to kinetic cluster population models. While static minimum-energy calculations may reveal the general trends in cluster stability, first-principles molecular dynamics simulations describe the atomic-level movement in a complex of molecules and dynamics related to collisions and cluster rearrangement [1]. To study a larger population of clusters interacting with each other, cluster free energies from electronic structure calculations can be converted into evaporation rates and incorporated into kinetic models [2]. This provides a means to assess the formation rate of clusters of a specific size in given conditions, but also a possibility for a direct comparison with experiments through mass spectrometer measurements of cluster distributions. While the description of collision and evaporation processes in this type of simulation is not as rigorous as can be achieved with molecular dynamics, the approach reproduces observed trends [2], and can thus be used to predict the general behavior of a cluster population.

Our recent cluster kinetics simulations for clusters containing sulfuric acid, ammonia and dimethylamine provide information on the relative potential of the different bases to enhance sulfuric acid driven clustering. The effect of water in these systems is current work-in-progress. In addition to cluster formation in the conditions of laboratory or field measurements, simulations can be used to study the effect of measurement methods, such as chemical ionization [3].

References

[1] V. Loukonen et al., Chem. Phys. 428 (2014) 164–174.
[2] J. Almeida et al., Nature 502 (2013) 359–363.
[3] O. Kupiainen-Määttä et al., J. Chem. Phys. A 117 (2013) 14109–14119.

Photoluminescence properties of Si nanoparticles fabricated from Si swarf: fluorescence enhancement by organic molecules

Masanori Maeda, Taketoshi Matsumoto, and Hikaru Kobayashi

The Institute of Scientific and Industrial Research, Osaka University and CREST, Japan Science and Technology Agency, Ibaraki, Japan

Light emitting Si nanoparticles have attracted much interest because of their unique and applicative characteristics (e.g., controllability of emission wavelength, biocompatibility and surface sensitivity) [1]. We have developed a method of fabricating blue light emitting Si nanoparticles from Si swarf, which is a waste generated during slicing Si ingots to produce Si wafers for solar cell use [2]. In this study, we have produced blue and green light luminescent Si nanoparticles by use of a simple method, and observed their fluorescence enhancement effect of adsorbed organic molecules. Si swarf generated by use of the fixed-abrasive method was milled by use of a beads mill. After milling, transmission electron microscope (TEM) and X-ray diffraction (XRD) observation clearly showed the presence of many Si nanoparticles with diameters less than 10 nm. Si nanoparticles etched with HF solutions exhibited green photoluminescence (PL) under UV irradiation. The PL peak clearly showed blue shifts by an increase in the excitation energy. This result indicates that the green PL originates from band-to-band transition of Si nanoparticles with the quantum confinement effect. After filtering and extracting by 9,10-dimethylanthracene (DMA) containing hexane plus water without HF etching, on the other hand, Si nanoparticles showed strong blue PL. The PL spectra of blue PL Si nanoparticles have no dependence on the excitation energy. In addition, the spectral feature is very similar to that of DMA. Therefore, it can be concluded that blue PL arises from DMA molecules adsorbed on Si nanoparticles. The PL intensity is much higher than that of DMA-containing hexane. The increased PL intensity is attributed to enhancement of UV absorption by Si nanoparticles, followed by transfer of electron-hole pairs to DMA and recombination there. From these results, we propose two different methods to control the PL wavelength; 1) control of the size of Si nanoparticles, and 2) control of adsorbed species on Si nanoparticles.

References

[1] Z. Kang, Y. Liu, and S-T. Lee, Nanoscale 3 (2011) 777-791.

[2] T. Matsumoto, M. Maeda, J. Furukawa, W-.B. Kim, and H. Kobayashi, J. Nanopart. Res. 16 (2014) 2240-1-7.

$Ag_{44}SR_{30}$: What comes after the structure is solved?

Lars Gell,[1] Hannu Häkkinen[1,2]

[1] *Department of Chemistry, Nanoscience Center, University of Jyväskylä, Jyväskylä, Finland*
[2] *Department of Physics, Nanoscience Center, University of Jyväskylä, Jyväskylä, Finland*

The crystal structure of $Ag_{44}SR_{30}^{4-}$ has gained considerable attention since its simultaneous publication by Zhen and Bigioni groups. Various modifications like different R groups, replacement of the inner silver core with gold as well as sulfur with selenium have already been discovered. [1,2,3] In this study we will discuss the influence of cluster charge and electron withdrawing ligands on the optical absorption spectra as well as the plasmonic nature of this nanoparticle. We show that the cluster can bind up to four protons reducing its high charge of four minus to zero. Furthermore the possibility of producing magnetic nanoclusters upon doping with manganese will be discussed.

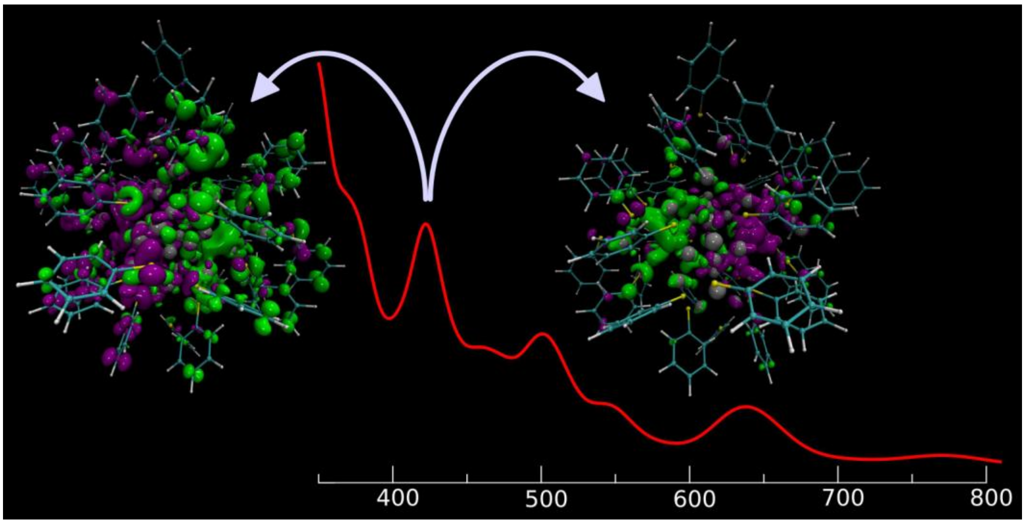

Figure1: The plasmon like nature of $Ag_{44}SR_{30}^{4-}$ upon excitation around 400 nm is shown. The counter interacting field of the silver-d states (right) and ligand+silver-s states (left) can be seen from the induced density as well as the contribution of the phenyl rings to the plasmonic peak.

Reference(s)

[1] H. Yang, Y. Wang, H. Huaqi, L. Gell, L. Lehtovaara, S. Malola, H. Häkkinen and N. Zheng, Nat. Comm. 2013, 4-2422

[2] I. Chakraborty, W. Kurashige, K. Kanehira, L. Gell, H. Häkkinen, Y. Negishi and T. Pradeep. Phys. Chem. Lett. 2013, 4, 3351

[3] A. Desireddy, B.E. Conn, J. Gou, B. Yoon, R. N. Barnett, B. M. Monahan, K. Kirschbaum, W. P. Griffith, R. L. Whetten, U. Landman, T. P. Bigioni, Nature, 2013, 501, 399

Information on Quantum States Pervades the Absorption Spectra of the $Au_{144}(SR)_{60}$ Nanocluster

H.-Ch. Weissker[1,2], V.D. Thanthirige[4], K. Kwak[5], D. Lee[5],
G. Ramakrishna[4], R.L. Whetten[3], X. López-Lozano[3]

[1] *Aix-Marseille Univ., CNRS, CINaM UMR 7325, 13288 Marseille, France.*
[2] *European Theoretical Spectroscopy Facility, France; www.etsf.eu.*
[3] *Department of Physics and Astronomy, The University of Texas at San Antonio. One UTSA Circle, San Antonio, Texas 78249, USA.*
[4] *Department of Chemistry, Western Michigan University, 1903 West Michigan Avenue, 49008-5413 Kalamazoo, Michigan, USA.*
[5] *Department of Chemistry, Yonsei University, Seoul 120-749, Korea.*

The prevalent view in recent decades has been that noble-metal clusters of intermediate size necessarily have smooth optical absorption spectra of low information content in the near-IR, VIS and near-UV regions. At most, one expects a broad, smooth localized surface-plasmon resonance feature. [1,2] In the present study, we demonstrate that, in contradistinction to the commonly held view, the optical absorption of the most widely applied gold cluster, the thiolate-protected $Au_{144}(SR)_{60}$, exhibits a rich spectrum of bands that are individually visible over the entire near-IR, VIS and near-UV regions (1.0–4.0 eV), demonstrating high information content related to the quantum size effects which distinguish the nanoparticles from the bulk materials.[3] The contributions of different parts of the cluster-ligand compound to the spectra are analyzed. The results were obtained owing to low-temperature measurements on ultrahomogeneous samples and realistic quantum-theoretical simulation (~2,500 active electrons) using time-dependent density-functional theory. [4-6]

References

[1] Qian, H., Zhu, Y. & Jin, R., Proc. Natl Acad. Sci. USA 109, 696–700 (2012).
[2] Malola, S., *et al.*, ACS Nano. 7, 10263–10270 (2013).
[3] de Heer, W. A., Rev. Mod. Phys. 65, 611–676 (1993).
[4] López-Lozano, X.; Mottet, C.; Weissker, H.-Ch.; J. Phys. Chem. C, 117, 3062–3068 (2013).
[5] López-Lozano, X.; Barron, H.; Mottet, C.; Weissker, H.-Ch., Phys. Chem. Chem. Phys. 16, 1820–1823 (2014).
[6] Weissker H.-Ch., *et al.*, Nature Communications, 5, 3785, (2014).

Preparation of non-toxic gold submicron-sized particles using laser-induced melting in liquids

Takeshi Tsuji[1], Yuuma Higashi[2], Masaharu Tsuji[2], Yoshie Ishikawa[3], Naoto Koshizaki[3]

[1]*Interdisciplinary Faculty of Science and Engineering, Shimane University, Matuse, Japan*

[2]*Institute of Advanced Materials Chemistry, Kyushu University, Kasuga, Japan*

[3]*National Institute of Advanced Industrial Science and Technology, Tsukuba, Japan*

[4]*Faculty of Engineering, Hokkaido University, Sapporo, Japan*

Recently, laser processes in liquid phase, such as laser ablation in liquids, attract much attention as alternative methods to prepare colloidal materials. A remarkable benefit of laser processes is that the use of undesirable reagents in the synthesis process can be minimized. The laser-induced melting in liquids method, in which colloidal nanoparticles (NPs) are irradiated by non-focused laser beam at moderate fluence, is a novel and conventional technique to prepare spherical submicron-sized particles (SSMPs) with narrow size distribution. In the previous report, we revealed that control of the agglomeration conditions of the source Au NPs is important to obtain Au SSMPs efficiently [1]. Therefore, in the previous study, tri-sodium citrate was used as a stabilizing reagent. In the present work, NaCl, is employed as a stabilizing reagent to prepare "non-toxic" gold SSMPs. Differing from citrate, NaCl is not decomposed and no unnecessary byproduct is formed by laser irradiation.

The source NPs were prepared by using laser ablation of a Au plate immersed in a NaCl aqueous solution. It was confirmed that the stabilization of the source NPs was increased with increasing concentration of NaCl [2]. The non-focused laser beam at 532 nm of a Nd:YAG laser was used to induce melting of the source NPs.

Fig. 1 shows the SSMPs produced from the source NPs in a 0.05 mM NaCl solution. SSMPs was not produced from the source NPs in a 0.1 mM NaCl solution. This result shows that NaCl can be used to control the agglomeration conditions of the source NPs. On the other hand, it has been revealed that the difference in the protective effect for the source gold NPs between NaCl and citrate significantly influences on the formation process of SSMPs.

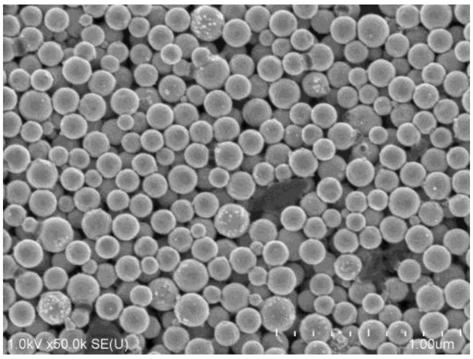

Fig. 1 Au SSMPs produced by the laser-induced melting of the source Au NPs stabilized by 0.05 mM NaCl.

References

[1] T. Tsuji, T. Yahata, M. Yasutomo, K. Igawa, M. Tsuji, Y. Ishikawa, N. Koshizaki, PCCP, 15 (2013) 3099.

[2] J.P. Sylvestre, S. Poulin, A.V. Kabashin, E. Sacher, M. Meunier, J.H.T. Luong, J. Phys. Chem. B, 108 (2004) 16864.

Polymer-protected fluorescent platinum nanoclusters and their application

Xin Huang,[1] Hidekazu Ishitobi,[1, 2] and Yasushi Inouye[1, 2, 3]

[1] Graduate School of Frontier Biosciences, Osaka University, 1-3 Yamada-oka, Suita, Osaka 565-0871, Japan

[2] Department of Applied Physics, Osaka University, 2-1 Yamada-oka, Suita, Osaka 565-0871, Japan

[3] Photonics Advanced Research Center, Osaka University, 2-1 Yamada-oka, Suita, Osaka 565-0871, Japan

Noble metal nanoclusters (M NCs) consisting of a few to several tens of atoms exhibit molecule-like behaviors such as size-dependent fluorescence of which the emission wavelengths can be adjusted by controlling the number of atoms in M NCs. Compared to common fluorophores, M NCs have plenty of merits, such as water solubility, ultra-small size, and easy surface modification. Recently, fluorescent gold and silver nanoclusters (Au NCs and Ag NCs) have been already prepared and used for labeling the living cells as probes, while the fluorescent properties of the platinum nanoclusters (Pt NCs) are rarely discussed. In this presentation, we demonstrate three kinds of different-colored (blue, green, and yellow-emitting) fluorescent Pt NCs. For blue and green-emitting Pt NCs, four-generation poly(amidoamine) dendrimers (PAMAM(G4-OH)) were employed as a template.[1-2] Then we removed PAMAM dentrimers from the synthesized Pt NCs via ligand exchange with thiol mercaptoacetic acid (MAA) after reduction. Since these Pt NCs have the high quantum yield and considerably low cytotoxicity, they were successfully applied for bio-mark of chemokine receptors in the living HeLa cells by binding to an antibody through a conjugated protein. On the other hand, the yellow-emitting fluorescent Pt NCs with excellent photo-stability against both of pH and most metal ions were prepared by a facile method using hyperbranched polyethyleneimine (PEI) as a stabilizing agent.[3] These fluorescent Pt NCs were applied to the sensitive and quantitative detection for Co^{2+} ions and the limit of detection was 500 nM. In future, fluorescent Pt NCs with longer-wavelength are expected to be produced by precise control of the size.

References

[1] S.-I. Tanaka, J. Miyazaki, D. K. Tiwari, T. Jin, and Y. Inouye, Angew. Chem. Int. Ed., 50, (2011) 431-435.

[2] S.-I. Tanaka, K. Aoki, A. Muratsugu, H. Ishitobi, T. Jin, and Y. Inouye, Opt. Mater. Express, 3, (2013) 157-165.

[3] X. Huang, K. Aoki, H. Ishitobi, and Y. Inouye, ChemPhysChem, 15, (2014) 642-646.

Electrochemical Reactions and Spectral Changes of Gold-Silver Core-shell Nanorods on ITO Plates

Yuki Hamsaki,[1] Naotoshi Nakashima,[1,,2,3] and Yasuro Niidome[1,2,4]

[1] *Department of Applied Chemistry, Kyushu University, Fukuoka, Japan*
[2] *I2CNER WPI, Kyushu University, Fukuoka, Japan*
[3] *CREST, Tokyo, Japan*
[4] *Kagoshima University, Kagoshima, Japan (Present Affilication)*

Au-Ag core-shell nanorods, of which spectroscopic properties corresponded to those of anisotropic silver nanoparticles, are chemically unstable in the absence of reducing agent. Oxidation of the silver shells gradually proceeded in an aqueous solution and accompanied by changes in their shapes. In order to allow quantitative evaluation of the shape changes, a constant potential electrolysis, to oxidize the silver shells, coupled with high resolution SEM analysis is herein performed. Oxidation processes of the silver shells in a KCl solution are discussed. Well-controlled oxidation of silver shells is a potential way to give a new class of anisotropic core-shell nanoparticles.

During electrolysis, the peak corresponding to the longitudinal SP band shifted to the shorter wavelength region (Figure 1A). This shift indicated a decrease in the aspect ratios of the core–shell nanorods. In a SEM image, oval nanoparticles and thin gold nanorods were observed. The silver shells form water-soluble dichloride complexes ($AgCl_2^-$) that diffuse in the bulk solution, leaving core gold nanorods behind.

Figure 1B shows size distribution of the core-shell nanorods at 10 s after electrolysis in the KCl solution. The smaller portion of the bimodal size distribution is associated with the gold nanorods, while the larger group corresponds to the core–shell nanorods. The distribution indicates that the core–shell nanorods remain anisotropic shapes even after the 10 s electrolysis. It should be noted that there are a few spherical particles that are plotted on the line indicating the aspect ratio is one. This indicated that oxidation of silver shells occurred at the corners of the silver shells.

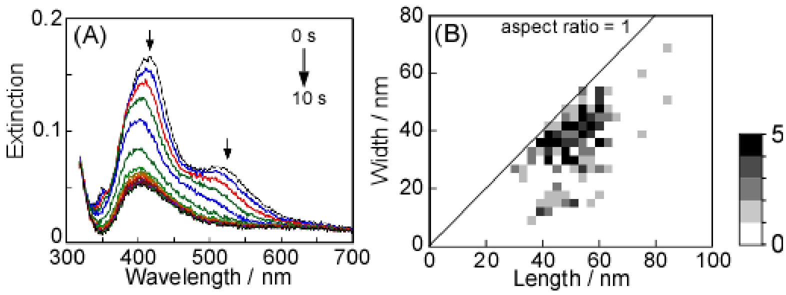

Fig. 1 Fig. 1. (A) Extinction spectral changes observed in the deposited core–shell nanorods under an applied constant potential (0.15 V vs. SCE) in the KCl solution (0.1 M). (B) size distribution of the deposited core–shell nanorods after a 10 s electrolysis. The scale bar indicates the frequencies of nanoparticles

Reference

[1] Y. Hamasaki, N. Nakashima, Y. Niidome, *J. Phys. Chem. C* 117(2013)2521.

Novel thiolate-protected gold clusters with sub-2 nm sized and fcc cores: synthesis and optical property

Shinjiro Takano,[1] Seiji Yamazoe,[1,2] Kiichirou Koyasu,[1,2] and Tatsuya Tsukuda[1,2]

[1] *Department of Chemistry, School of Science, The University of Tokyo, Tokyo, Japan*
[2] *Elements Strategy Initiative for Catalysts and Batteries, Kyoto University, Kyoto, Japan*

[Metal clusters exhibit novel structures and properties that cannot be found in the corresponding bulk metal. Thiolate-protected gold (Au:SR) clusters provide an ideal platforms to study the unique geometrical structures and electronic properties [1]. X-ray diffraction studies revealed that Au:SR have Au cores with five-fold symmetry, such as icosahedron or decahedron, especially when their core diameters are smaller than 2 nm. The Au:SR clusters (<2 nm) also have distinct optical absorption bands and exhibit luminescence, reflecting their quantized electronic structures. We herein report the synthesis of new Au:SR clusters with sub-2 nm sized fcc cores and their novel optical absorption bands in the near-IR region.

Small fcc Au:SR clusters were synthesized by a slow reduction method. First, the aqueous-ethanolic solutions of $HAuCl_4$ and 4-(2-mercaptoethyl)benzoic acid (4-MEBA) were mixed. After the pH value of the mixed solution was adjusted to be >12 by addition of KOH (sample **1**) or NaOH (sample **2**), the aqueous solution of $NaBH_4$ was added. Finally, pure Au:4-MEBA clusters were obtained as black powders after the purification by gel filtration chromatography.

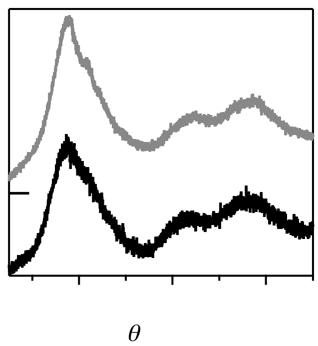

Figure 1. Powder XRD patterns of **1** (black) and **2** (gray). (Cu Kα)

Powder XRD patterns of **1** and **2** (Figure 1) indicated that the Au cores of **1** and **2** have fcc symmetries. Figure 2 shows UV-vis-NIR absorption spectra of **1** and **2**. The spectrum exhibits humps in the UV-vis region and, more surprisingly, peaks in the NIR region (1070 and 1380 nm for **1** and **2**, respectively). To reveal the origin of the NIR region peaks, we conducted a low-temperature UV-vis-NIR absorption measurement of **1**. With decreasing the temperature, the NIR peak was blue shifted as in the case of thiolate-protected $Au_{25}(SR)_{18}$ and $Au_{38}(SR)_{24}$ [2]. This result indicates that the NIR absorption peak is not associated with plasmon resonance absorption, but optical transition between the quantized levels of **1**.

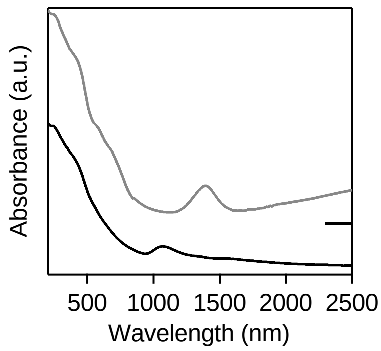

Figure 2. UV-vis-NIR spectra of **1** (black) and **2** (gray).

References
[1] P. Maity, *et al.*, Nanoscale 4 (2012) 4027.
[2] M. S. Devadas, *et al.*, J. Phys. Chem. Lett. 2 (2011) 2752.

Gold ultrathin nanowires and nanorods: First observation of surface plasmon resonance

Ryo Takahata,[1] Seiji Yamazoe,[1,2] Kiichirou Koyasu,[1,2] and Tatsuya Tsukuda[1,2]

[1] *Department of Chemistry, School of Science, The University of Tokyo, Tokyo, Japan*
[2] *ESICB, Kyoto University, Kyoto, Japan*

Gold ultrathin nanowires (Au UNWs) with the diameter of ~1.6 nm and the length of several µm [1] will find applications in various fields by taking advantage of their high flexibility. The aim of this work is to study optical properties of the Au UNWs. To this end, we first prepared Au UNWs and ultrathin nanorods (UNRs) by a method slightly modified with that reported in ref [2]. Typical TEM images of three samples (Figs. 1a–1c) show that they have a common diameter of ~1.7 nm and different average lengths of 370, 40, and 20 nm. These UNWs and UNRs exhibit strong extinction bands in the IR region whose peak positions are redshifted with increase in the length (Figs. 1d–1f). This length-dependent shift of the band positions suggests that they are assignable to a longitudinal mode of surface plasmon resonance (SPR) [3]. In order to confirm this assignment, we aligned the Au UNWs on an aminosilane-coated glass plate and measured their polarized extinction spectra. The extinction in the IR region was enhanced when the incident light was polarized parallel to the longitudinal axis of Au UNWs. This result supports our assignment of the IR band to a longitudinal mode of SPR [4].

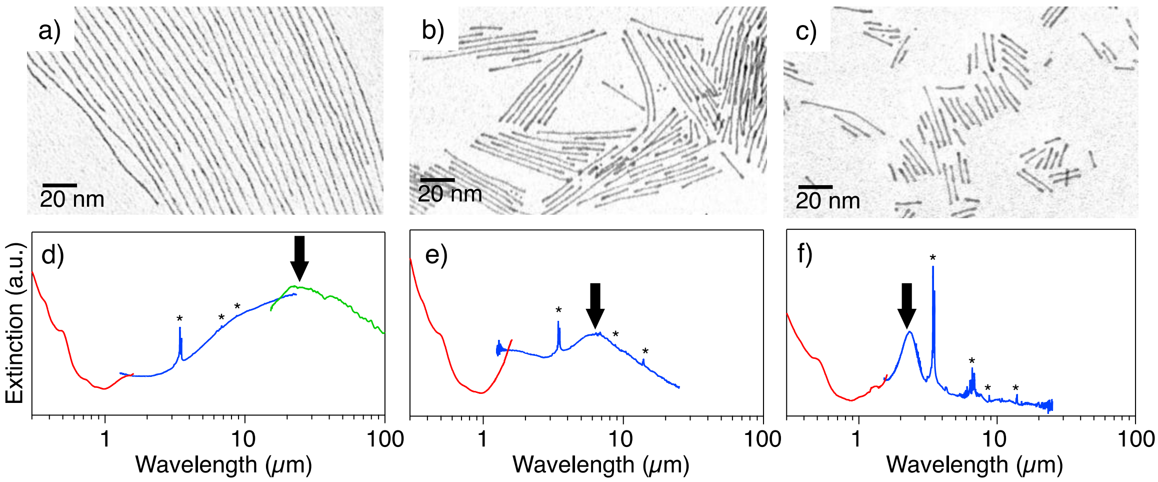

Figure 1. a)–c) Typical TEM images and d)–f) optical extinction spectra of Au UNWs and UNRs with the lengths of 370, 40, and 20 nm, respectively. The asterisks indicate vibrational peaks of OA.

References

[1] A. Halder et al., Adv. Mat. 19 (2007) 1854.

[2] H. Feng, et al., Chem. Commun. (2009) 1984.

[3] X. Lopez-Lozano, et al., Phys. Chem. Chem. Phys. 16 (2014) 1820.

[4] R. Takahata, et al., J. Am. Chem. Soc. 136 (2014) 8489.

Controlled formation of highly luminescent silver clusters in zeolite matrices via high-brilliance soft X-ray irradiation

Didier Grandjean,[1] Eduardo Coutino-Gonzalez,[2] Maarten Roeffaers,[3] Kristina Kvashnina,[4] Eduard Fron,[2] Bert Sels,[3] Johan Hofkens,[2] Peter Lievens[1]

[1]Department of Physics and Astronomy, Laboratory of Solid State Physics and Magnetism, KU Leuven, Celestijnenlaan 200D, B-3001 Leuven, Belgium
[2]Department of Chemistry, KU Leuven, Celestijnenlaan 200F, B-3001 Leuven, Belgium.
[3]Department of Microbial and Molecular Systems, Centre for Surface Chemistry and Catalysis, KU Leuven, Kasteelpark Arenberg 23, B-3001 Leuven, Belgium.
[4]European Synchrotron Radiation Facility (ESRF), CS40220, 38043 Grenoble Cedex 9, France

Oligoatomic (noble) metal clusters feature very peculiar optical and catalytic properties making them very attractive for applications in diverse fields such as plasmonics [1], catalysis [2], and photonics [3]. Template-mediated strategies in which the size and the shape of the metal cluster are controlled by the dimensional restrictions induced by the hard template structure during the cluster formation are nowadays widely used to produce metal clusters with well-defined sizes and shapes. Popular templating host structures include glassy matrices, metal-organic frameworks, and zeolites. Formation of sub-nanometer highly luminescent silver clusters via a thermal and/or a photon-induced approach has been reported in glasses [4] but mostly in zeolite matrices where a clear relationship between the luminescence properties and the size of the Ag-clusters could be demonstrated both in heat-treated [5] and photon-activated [6] Ag-exchanged zeolites.
In parallel to the utilization of different host systems, the development of highly controlled activation procedures appears now crucial for the production of well-defined oligoatomic metal clusters. In this work we explored the formation of silver clusters with very homogeneous luminescence properties under high-brilliance synchrotron soft X-ray controlled irradiation in different zeolite topologies containing sodalite cages [7]. The optical properties of the formed luminescent Ag-clusters were subsequently investigated by employing a combination of stationary and time-resolved spectroscopic techniques and systematically compared to heat and photo-activated samples with the same composition. Compared to conventional heat-treatment, activation of silver zeolites with X-rays provides a more tightly controllable spatial production of silver clusters with very homogeneous luminescent properties at much faster time scales.

Reference(s)

[1] K.G.M. Laurier, M. Poets, F. Vermortele et al., Chem. Commun. 48 (2012) 1559.
[2] K. Shimizu, K. Sawabe and A. Satsuma, Catal. Sci. Technol. 1 (2011) 331.
[3] A. Royon, K. Bourhis, M. Bellec et al., Adv. Mater. 22 (2010) 5282.
[4] K. Bourhis, A. Royon, G. Papon et al., Mater. Res. Bull. 48 (2013) 1637.
[5] G. De Cremer, E. Coutino-Gonzalez, M. Roeffaers et al., J. Am. Chem. Soc. 131 (2009) 3049.
[6] G. De Cremer, Y. Antoku, M.B.J. Roeffaers et al., Angew. Chem. Int. Ed. 47 (2008) 2813.
[7] E. Coutino-Gonzalez, D. Grandjean, M. Roeffaers et al., Chem. Commun. 50 (2014) 1350.

One-step Synthesis and Characterization of Benzenthiol Derivative-protected Gold Clusters

Takuya Ishida,[1] Yukina Takahashi,[2] Hiroaki Okamura,[3] Junichi Kurawaki,[3] and Sunao Yamada[2]

[1] *Department of Materials Physics and Chemistry, Kyushu University, Fukuoka, Japan*
[2] *Department of Applied Chemistry, Kyushu University, Fukuoka, Japan*
[3] *Department of Chemistry and Bioscience, Kagoshima University, Kagoshima, Japan*

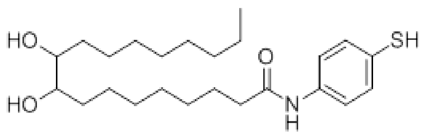

Figure 1. Formula of BD1.

It is known that gold clusters (AuCs) consisting of a few atoms exhibit unique character. It has been reported that AuCs show molecule-like transition due to the discrete energy levels according to the simple relation $E_{Fermi}/N^{1/3}$, predicted by the spherical Jellium model[1]. There are numerous reports for the use of organic thiols as capping and functionalizing agents for AuCs. Although these synthetic approaches of functionalized AuCs have been proposed, the methods have required multistep process and reagents such as reducing and capping agents. In order to utilize AuCs for nanoscale devices, establishment of the simple synthesis methods of functionalized AuCs is needed.

The benzenethiol derivative (BD1) (Fig. 1) was used as a reductive stabilizer for the formation of AuCs. The BD1 is a model compound to develop a new one-step synthesis method of functionalized AuCs. We could synthesize AuCs by just mixing aliquots of ethanol solution of BD1 and $HAuCl_4$.

The absorption edge and emission maxima excited at 355 nm were observed at ~350 nm and ~460 nm, respectively (Fig. 2). ^{1}H-NMR spectrum of BD1-protected AuCs exhibited the lower magnetic field shift of the proton of the benzene than that of the free BD1. It should be associated with an Au-S interaction. The organic-soluble photoluminescent BD1-protected AuCs was assigned to $Au_9(BD1)_6$ mainly by optical spectroscopy and MALDI-TOF-mass.

Reference

[1] J. Zheng, P. R. Nicovich, R. M. Dickson, Annu. Rev. Phys. Chem. 58 (**2007)** 409.

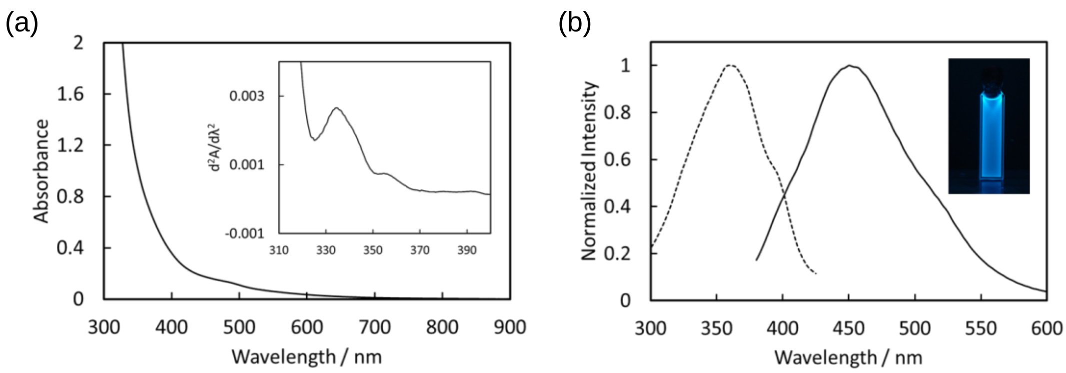

Figure 2. (a) The UV-vis and the secondary differentiation (inset) spectra of BD1-potected AuCs. (b) Excitation (dashed) and emission (solid) spectra of the AuCs. Inset shows emission under UV irradiation (365 nm).

Ultrafast Strong Field Ionization of Small Metal Clusters

Dennis Dieleman, Valeriy Chernyy, Theo Rasing, Andrei Kirilyuk

Institute for Molecules and Materials, Radboud University, Nijmegen, The Netherlands

In this work we investigate the interaction of strong (~1e15 W/cm^2) and short (40 fs) laser pulses with transition metal (Fe, Co, CoRh, CoAu) and lanthanide (Pr, Ho) clusters. For low laser intensities the electrical field that is generated by the light can be treated as a small perturbation to the clusters using standard perturbation theory. When we increase the intensity of the laser however, these electrical fields become of the same or larger strength, than the Coulomb forces that hold matter together. This means the field can no longer be treated as a small perturbation, which opens the way for a whole new range of interesting phenomena.

For example, in a cluster, interaction with an intense laser pulse can ionize the electrons of its constituent atoms almost instantaneously. This so called inner ionization can create a nanoplasma of quasi-free electrons inside the cluster, which has been shown to influence the ionization rate of small metal clusters [1] and be the precursor to phenomena like Coulomb explosion and XUV radiation [2].

We have measured the laser intensity dependency on the ionization rates of small metal clusters, varying the intensity by about 6 orders of magnitude (1e9 – 1e15 W/cm^2). This wide range gives us the possibility to explore the transition region between moderate fields, where multi-photon effects dominate the ionization, and strong fields where mostly the laser field strength influences the ionization dynamics.

For Fe_NO_M, Co_NAu_M, Co_NRh_M, Ho_NO_M and Pr_NO_M clusters, with N ~ 1-10 and O ~ 0-3 we have determined the ionization energy (E_i) using two different models. For the low field multi-photon region we find a good estimation of E_i using the fact that the rate of ionization is equal to the amount of photons necessary for ionization. In the strong field region we use the Barrier Suppression Intensity as measure for E_i, which basically relates the field strength of the laser needed to suppress the coulomb barrier, to E_i. For both models we find good agreement with literature in the case of Fe and Pr. Which shows that this method can also be applied for the doped cobalt clusters, for which E_i was not yet measured before.

Finally we study the influence of the pulse width (40 fs – 5 ps) on the ionization rate and find a stronger dependence on pulse width for CoRh than for Ho and Pr clusters. For Fe clusters we see clear signs of Coulomb explosions even at unexpected moderate intensities when going to shorter pulses.

References:

[1] Smits, M., de Lange, C., Stolow, A., & Rayner, D., Phys. Rev. Lett., 93(20), (2004), 203402.

[2] Fennel, T., Meiwes-Broer, K.-H., Tiggesbäumker, J., Reinhard, P.-G., Dinh, P. M., & Suraud, E. Reviews of Modern Physics, 82(2), (2010) 1793–1842

Monocarbon cationic cluster synthesis from methane-nitrogen mixtures embedded in He nanodroplets and their calculated binding energies

Iogann Tolbatov[1,2], Sylwia Ptasinska[1,2] and Daniel M. Chipman[1]

[1]*Radiation Laboratory, University of Notre Dame, Notre Dame, IN 46556, USA*
[2]*Department of Physics, University of Notre Dame, Notre Dame, IN 46556, USA*

Helium nanodroplets are a unique tool for assembly and study of reactions in various molecular complexes due to their superfluidity at low temperatures and the high ability to be doped. In our study, processes related to molecule and cluster formation in irradiated gaseous methane-nitrogen mixtures in helium droplets are investigated. The molecular structures formed from N2/CH4 mixtures of different concentrations were trapped with the help of an ultracold environment of helium nanodroplets. A beam of low-energy electrons (70 eV) was used for the irradiation. Afterwards, the results of irradiation were analyzed by the TOF mass spectrometer.
From the experiment, it was deduced that all the monocarbon clusters studied are most likely to be formed in the range of 5%–30% of methane in the mixture. A variety of clusters and molecules were observed with the mass to charge ratio up to 80 Da. The synthesized structures were analyzed by quantum chemical calculations using the CCSD(T)/6-311G(2d,p)// CCSD/6-311G(2d,p) method.

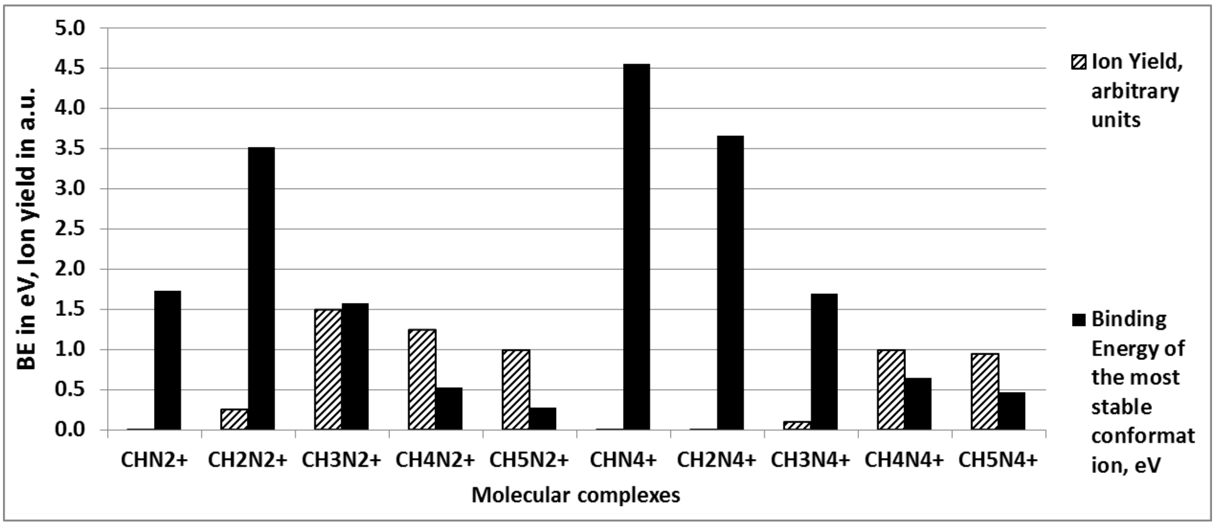

Fig. 1 Ion yield and binding energy values of monocarbon molecular complexes

A summary of the resulting products and their ion yields is shown in Fig.1. Molecular complexes CHN2+, CHN4+, and CH2N2+ exhibit a strong energetical favorability towards C=C-N ring formation. Molecule CH3N2+ has the greatest ion yield and a rather high binding energy of 1.57 eV. Otherwise there is little correlation between the ion yields and the associated binding energies, indicating that kinetic control is more important than thermodynamic control for forming the clusters in most cases.

Genuinely amorphous carbon produced from explosive nano acetylide

Ken Judai,[1] Naoyuki Iguchi,[1] and Yoshikiyo Hatakeyama[1]

[1] *Department of Physics, College of Humanities and Sciences, Nihon University, Tokyo, Japan*

Copper acetylide and silver acetylide are famous as explosive compounds. However, when the explosive crystals are downsized into nanoscale, the explosive nature will be eliminated by much lower thermal conductance preventing the crystals from explosive chain reactions. This nano less-explosive character can be applied to new noble carbon material production.

Generally amorphous carbon is prepared by exposing organic compounds to high temperature for carbonization. The high temperature for carbonization affects the crystallization to graphite partially. In this new method, the carbonization reaction can proceed with lower annealing temperature because of chemical reactive nature of copper acetylide, and genuinely amorphous carbon materials can be prepared.

The following figure shows the Raman spectrum of new carbon materials prepared by lower temperature carbonization of copper acetylide nano compounds and acid treatment for removal of copper element. The peak around 1600 cm^{-1} assigned to G-band was observed in a similar feature to the typical carbon materials, and the peak about 1380 cm^{-1} assigned to D-band as well. However, the spectrum in this method showed extremely broader peaks than those of the typical carbon materials, and the G-band and the D-band were deeply overlapped. This suggests the genuinely amorphous state of carbon

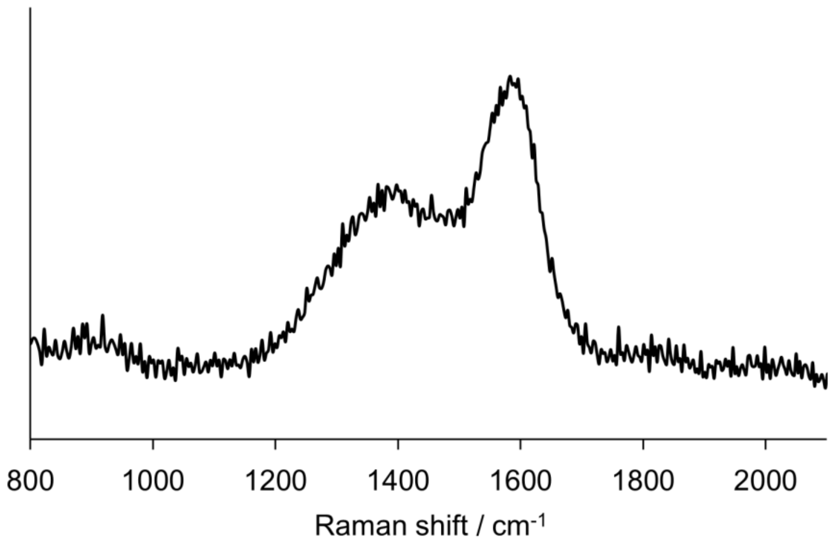

Figure: Raman spectrum of genuinely amorphous carbon. Copper acetylide nano materials could be carbonized at a temperature of 200°C.

Evaluation of the ratio of metal/semiconductive single-wall carbon nanotubes separated in two immiscible aqueous solution phases by utilizing Raman spectroscopy

Shinzo Suzuki,[1] Naoki Kanazawa,[1] Akira Ono,[2] and Yohji Achiba,[3]

[1] *Department of Physics, Kyoto Sangyo University, Kyoto, Japan*
[2] *Department of Engineering, Kanagawa University, Kanagawa, Japan*
[3] *Department of Chemistry, Tokyo Metropolitan University,Tokyo, Japan*

In 2013, C.Y. Khripin et al. reported about spontaneous partition of single-wall carbon nanotubes (SWNTs) in polymer-modified aqueous solution phases [1], where metal/semiconductive SWNTs of large diameter (> 1.2 nm) are shown to be easily separated in two immiscible aqueous solution phases, i.e., polyethylene glycol (PEG) and dextran (DX) aqueous solution. In this presentation, Raman spectroscopy technique was applied to each aqueous solution phase, in order to evaluate the ratio of metal / semiconductive SWNTs by changing excitation photon energy (532 nm and 633 nm).

Briefly, mono-dispersed sodium cholate (SC) solution (2wt%) of SWNTs produced by arc-burning of Ni/Y-carbon composite rod in helium atmosphere was utilized for two immiscible aqueous solution, following the recipe by C.Y. Khripin et al. [1]. After recognizing that PEG sand DX solution phases show different colors because of the difference in the ratio of metal/semi-conductive SWNTs, Raman spectra of each phases were obtained by different excitation photon energy (532 nm and 633 nm). Typical example of Raman spectra (G-band region) for PEG and DX solution phase by excitation photon energy (532 nm and 633 nm) were shown in Figures 1 and 2, respectively. It was clearly shown that the ratio of semiconductive SWNTs to metallic ones was higher in PEG solution phase than that in DX solution phase.

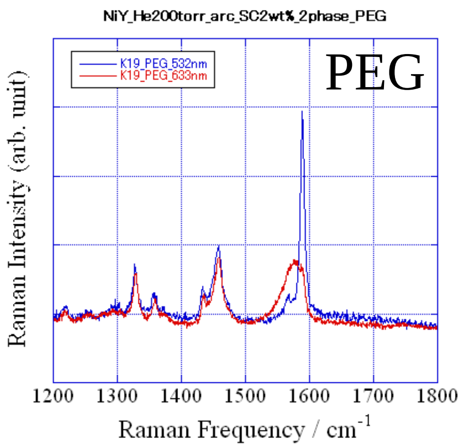

Figure 1.

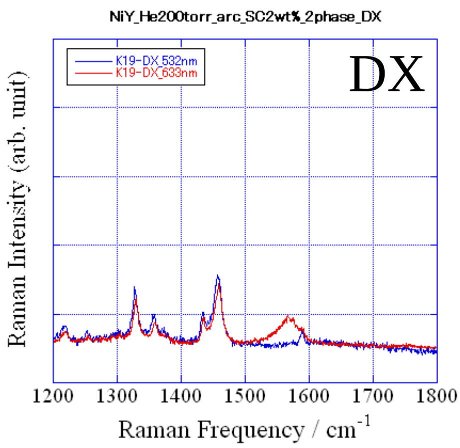

Figure 2.

Reference

[1] C.Y. Khripin et al., *J. Am. Chem. Soc.*, **135**, 6822-6825(2013).

Growth of single-wall carbon nanotubes on the porous glass (PG) sheet by using ACCVD technique

Shinzo Suzuki,[1] Kyohei Nagao,[1] Yosuke Ito, [1]
Nobuaki Ito, [2] Hiroshi Nagasawa, [3] and Yohji Achiba[4]

[1] *Department of Physics, Kyoto Sangyo University, Kyoto, Japan*
[2] *Center for Nano Materials and Technology, JAIST, Ishikawa, Japan*
[3] *Nano-support Co. Ltd., Kanagawa, Japan*
[4] *Department of Chemistry, Tokyo Metropolitan University, Tokyo, Japan*

ACCVD technique has been widely used for the growth of single-wall carbon nanotube (SWNT), because that the ambient temperature for the formation of SWNTs is relatively low (typically, less than 800°C), and the purity of SWNTs in as-grown material is considered to be better than those obtained by other technique, e.g. arc-burning procedure.
Aoki et al., reported in 2005, about the formation of SWNTs in the porous glass (PG) material by using ACCVD technique [1], where a kind of metal particles (e.g. Co particles) were deposited on the PG material before ethanol as carbon source was introduced for making SWNTs in the material. The advantage of using PG material is that, it is very easy to make any kind of shape (rod, sheet.., etc.) made of PG, which implies that the as-grown PG-SWNT complex material itself can also be applied for e.g., optical or electronic devices.
In this presentation, PG-sheets having different pore size (10nm, 30nm, 50nm, and 100nm, respectively) were prepared and tested for SWNT growth by using ACCVD technique. After optimizing the condition for SWNT growth, Raman spectroscopy and SEM technique were applied for the obtained SWNT-PG complex material, in order to characterize the purity and the diameter distribution of SWNTs grown on each PG-sheet.

Reference

[1] Y. Aoki, S. Suzuki, S.Okubo, H. Kataura, H. Nagasawa, and Y. Achiba, *Chem. Lett.*, **34**, 562(2005).

Analysis of the products of single-walled carbon nanotube growth with the aid of density functional theory calculations

[1]Arne Rosén*, [2]Yunguo Li, [4]J. Andreas Larsson, [3]Hamid Reza Barzebar and [3]Thomas Wågberg

[1]Professor em, Department of Physics, University of Gothenburg, SE-412 96 Gothenburg Sweden
[2]Department of Materials Science, Royal Institute of Technology, SE-100 44 Stockholm, Sweden
[3]Department of Physics, Umeå University, SE-901 87 Umeå, Sweden
[4]Applied Physics, Division of Materials Science, Department of Engineering Sciences and Mathematics, Luleå University of Technology, SE-971 87 Luleå, Sweden

1. We report use of a dip-coating method to prepare catalyst particles (mixture of iron and cobalt) with a controlled diameter distribution on silicon wafer substrates by changing the solution concentration and withdrawal velocity [1].The size and distribution of the prepared catalyst particles were analyzed by atomic force microscopy. Carbon nanotubes were grown by chemical vapor deposition, CVD, on the substrates with the prepared catalyst particles. By decreasing the particle size, the growth of carbon nanotubes can be tuned from few walled carbon nanotubes, with homogeneous diameters, to highly pure single walled carbon nanotubes, SWNT. Analysis of the Raman radial breathing mode, showed a relatively broad diameter distribution (0.8-1.4 nm) of single walled carbon nanotubes, SWNT, with different chiralities. By changing the size and composition of the catalyst particles but maintain the growth parameters, the chiralities of SWNT were reduced to mainly four different types: (12,1), (12.0), (8,5) and (7,5) of which quantity is 70 % of all the nanotubes.

2**. A deeper understanding of the growth mechanism of** nanotubes by the CVD is usually done using a modified version of the established vapor-liquid-solid (VLS) method for production of nanowires. For successful growth the catalytic metal particles should be able to: (i) decompose the feed-stock gas, (ii) form graphitic caps at their surface and (iii) stabilize of the growing open end to maintain the hollow structure. Recently criterion (iii) was identified and shown to be fulfilled using Density Functional Theory, DFT, calculations [2,3],when the metal-carbon bond is strong enough to make the dissociation of the catalytic particle and the SWNT unfavorable. Too week metal-carbon bond cannot stabilize the open CNT end. For investigation of the relative stability of hydrogen terminated SWNTs fragments of varying diameter and chirality we have performed electronic structure DFT calculations. Our calculations for tube segments of (n+m) = 9 - 13 tubes show that there is no telling if armchair/armchair-like or zigzag/zigzag-like tubes are the most stable within a series. However, the most stable tubes in the series from our calculations are the ones most frequently seen when characterizing the products of SWNT growth.

Reference(s)

[1] H. R. Barzegar et al, J. Phys. Chem. **C116**,12232 (2012)
[2] F. Ding, P. Larsson, J. A. Larsson, R. Ahuja, H. Duan, A. Rosén, K. Bolton, Nano Lett. **8** (2008) 463.
[3] J. D. Baran, W. Kołodziejczyk, P. Larsson, R. Ahuja, J. A. Larsson, Theor. Chem. Acc. **131**,1270 (2012)

Bonding and Spin-polarized Transport of Co Atomic Chain on Graphene with Topological Line Defects

Cheng-huan Jiang,[1, 2] Gui-xian Ge,[1] Jian-guo Wan[1*], and Guang-hou Wang

[1] *National Laboratory of Solid State Microstructures, and Department of Physics, Nanjing University, Nanjing 210093, China*

[2] *School of media technology, Communication University, Nanjing, China*

Graphene is regarded as a potential material for future spintronics due to its extremely long mean-free path and large spin relaxation time.[1] Transition metals (TMs) adsorbed on pristine graphene exhibit high local magnetic moment,[2] however, TMs have relatively weak bonding with graphene and easily diffuse with low barrier.[3] Recently, it is reported that the '5-5-8' extended line defect (ELD) can be produced on graphene in a controllable way.[4] In this work, based on the first-principle calculations we focus on the investigation of a hybrid system consisting of cobalt atomic chain on graphene with 5-5-8 ELDs. Our results show that the hybrid system has a relatively large binding energy (~0.7 eV/Co) and a high diffusion barrier (~1.2 eV) of Co atoms on graphene, indicating that the Co chain is stable on the system (Figure (a)). Moreover, we find that the interaction between the aggregates comprised of eight Co atoms can generate stable ferromagnetic coupling. Further calculations based on the non-equilibrium Green's function method show that the system exhibits spin-dependent current-voltage (I-V) behaviors with current polarization of ~30% at 0.4 V (Figure (b)). Such unique spin-polarized transport property suggests that the present system may be served as a building block for future spintronic devices.

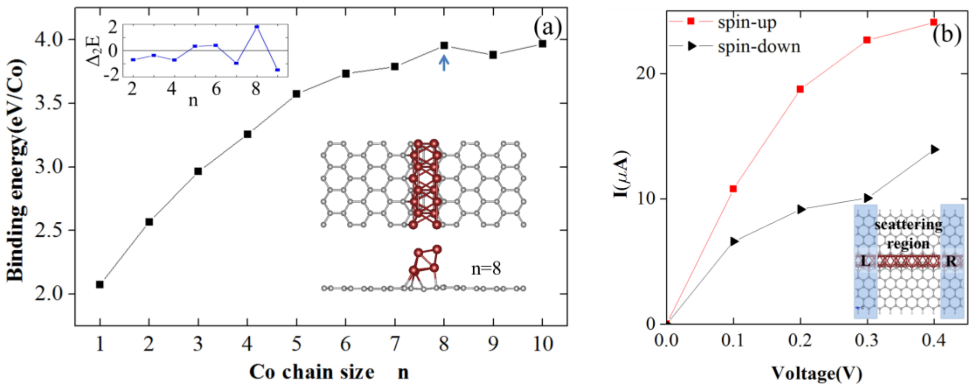

Figure. (a) Binding energy per Co atom as a function of the Co chain size (n). The insets are second difference $\Delta_2E(n)$ as a function of n. (b) Spin-dependent I-V curves for the hybrid system.

References
[1] X. Du, I. Skachko, A. Barker, and E. Y. Andrei, Nature Nanotechnology 3 (2008) 491.
[2] I. Zanella, S. B. Fagan, R. Mota, and A.Fazzio, J. Phys. Chem. C 112 (2008) 9163.
[3] O. V. Yazyev, A. Pasquarello, Phys. Rev. B 82 (2010) 045407.
[4] J. H. Chen, G. Autes, N. Alem, F. Gargiulo, A. Gautam, M. Linck, C. Kisielowski, O. V. Yazyev, S. G. Louie, and A. Zettl, Phys. Rev. B 89 (2014) 121407(R).

Metallic sp^2 carbon nanomaterials with octagons showing high density of states at the Fermi level: A first principles study

Yusuke Noda, Shota Ono, and Kaoru Ohno

Department of Physics, Graduate School of Engineering, Yokohama National University, Yokohama, Kanagawa, 240-8501, Japan

Carbon-based nanomaterials are expected to be useful for wide variety of applications. Since the successful synthesis of monolayer graphene [1], much attention has been paid to its electronic properties, in particular massless Dirac fermion-like behavior in the vicinity of the Fermi level due to the existence of the Dirac cone. This property leads to high electron mobility appropriate for developing carbon-based electronic devices. However, this property is not suitable for new materials alternative to precious metals because the density of states (DOS) at the Fermi level is exactly zero. Exhibiting a high DOS at the Fermi level is a very important characteristic of precious metals such as platinum and palladium [2-4]. If one could additionally introduce a high DOS in graphene, it could find a wide range of applications such as for high-carrier-density, catalytic, superconducting, thermoelectric, ferromagnetic, and other functional materials.

We investigated electronic states of various sp^2 carbon nanomaterials [one-dimensional peanut-shaped fullerene polymers [5] and corrugated graphene systems (see Fig.1)] using density functional calculations. We found that the presence of "isolated" octagons (surrounded by pentagons and hexagons, not adjoined to any heptagon and other octagon) in a unit cell brings about the simultaneous occurrence of flat and dispersive bands, and the flat band leads to extremely high DOS, quite similar to the electronic state of precious metals [6]. Such defects will provide a fertile playground for physics, chemistry, and technological applications of new carbon-based nanomaterials.

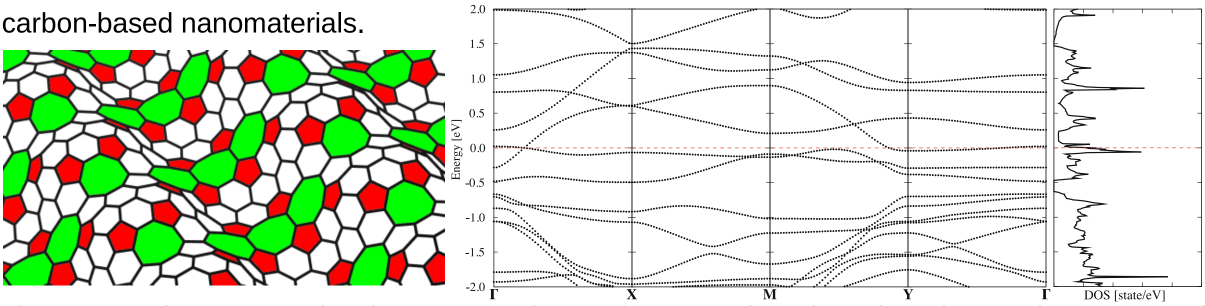

Fig.1 Geometrical structure, band structure, and DOS of corrugated graphene (Fermi energy is set at 0.0 eV)

References

[1] K. S. Novoselov, A. K. Geim, S. V. Morozov, D. Jiang, M. I. Katsnelson, I. V. Grigorieva, S. V. Dubonos and A. A. Firsov, Nature **438** (2005) 197.

[2] O. K. Andersen, Phys. Rev. B **2** (1970) 883.

[3] H. Chen, N. E. Brener and J. Callaway, Phys. Rev. B **40** (1989) 1443.

[4] V. Theileis and H. Bross, Phys. Rev. B **62** (2000) 13338.

[5] J. Onoe, T. Ito, H. Shima, H. Yoshioka, and S. Kimura, Europhys. Lett. **98** (2012) 27001.

[6] Y. Noda, S. Ono, and K. Ohno, Phys. Chem. Chem. Phys. **16** (2014) 7102.

Simultaneous formation of fullerenes and polyynes by laser ablation in the gas phase at room temperature

Hitomi Endo,[1] Yuki Taguchi,[1] Yurika Abe,[1]
Tomonari Wakabayashi,[2] Takeshi Kodama,[1] Yohji Achiba,[1] and Haruo Shiromaru[1]

[1] *Department of Chemistry, Tokyo Metropolitan University, Hachioji, Japan*
[2] *Department of Chemistry, Kinki University, Higashi-Osaka, Japan*

Carbon clusters formed by laser ablation of graphite are generally grouped into linear chains, hollow cages, and rings, of which the former two are isolated as polyynes and fullerenes, respectively. These are usually produced under far different conditions from each other; laser ablation in an organic solvent for polyynes and laser ablation in a high-temperature rare-gas environment for fullerenes. Recently, we found that polyynes and fullerenes are co-produced by laser ablation of graphite in Ar gas flow [1]. In the present study, we examined the effect of propane as a hydrogen source mixed in the Ar gas. Total gas flow rate was 100 mL/min with various propane flow rates from 0 to 1 mL/min (0 to 1% propane). Laser ablation was performed at room temperature in a glass tube with a cone-shaped exit for gas and the ablation products were carried into cooled hydrocarbons at the bottom of a glass bottle. The product molecules were separated by HPLC with an eluent of hexane, and analyzed by UV-Vis absorption.

A HPLC-UV two dimensional spectrum of a typical product solution prepared by laser ablation in 1% propane is shown in Fig. 1, where the characteristic UV bands of C_8H_2, $C_{10}H_2$, $C_{12}H_2$, and C_{60} are clearly observed at 227 nm, 252 nm, 276 nm, and 257 nm, respectively. Fullerene formation was confirmed also for laser ablation in 0 - 0.25% propane. The laser ablation conditions for fullerene formation have so far been extensively studied and high-temperature rare gas is considered to be indispensable. The fullerene formation at room temperature is therefore most likely due to local heating of the glass tube by laser irradiation. The yield of polyynes strongly depends on the propane concentration. The ablation in 0.25% propane enhances the yield significantly.

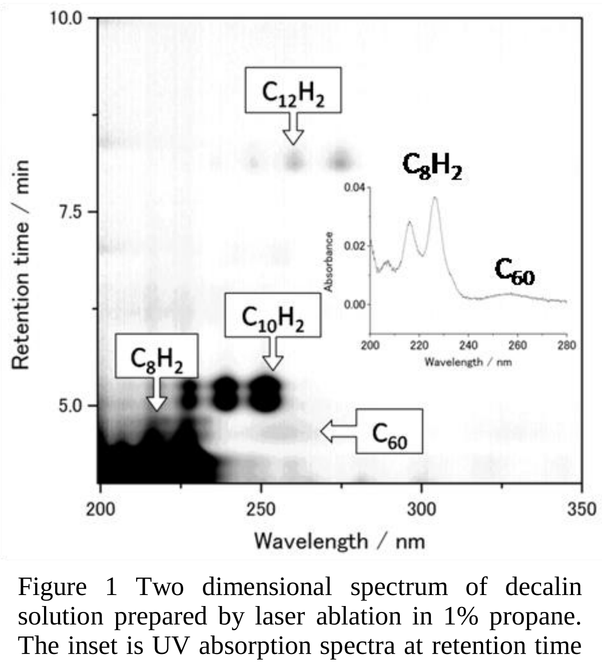

Figure 1 Two dimensional spectrum of decalin solution prepared by laser ablation in 1% propane. The inset is UV absorption spectra at retention time 4.6 min.

Reference

[1] Y. Abe et al., The 46th Fullerene-Nanotubes-Graphene General Symposium (2014) 141.

Pressure dependence of production of carbon nanotubes by High-temperature Pulsed-arc Discharge

Hayato Kikuchi,[1] Atsushi Shimaya,[1] Hiroki Koizumi,[1] Ryota Jinnouchi,[1] Katsuhide Terada,[2] Toshiki Sugai[1]

[1] *Department of Chemistry, Toho University, Funabashi, Japan*
[2] *Faculty of Pharmaceutical Sciences, Toho University, Funabashi, Japan*

A high-temperature pulsed-arc discharge (HTPAD) has been developed to produce carbon nanotubes (CNTs). The system utilizes width controlled pulsed-arc discharge for the vaporization of electrodes in a temperature controlled ambient gas. With those width and temperature controls, novel materials have been produced such as high-quality double wall carbon nanotubes [1]. Since the CNT production of laser and arc related methods are dominated by the gas pressure [2,3], here we present the pressure dependence of HTPAD up to 5 atm to investigate the processes. The standard steady arc discharge is rarely performed in such high pressures [3].

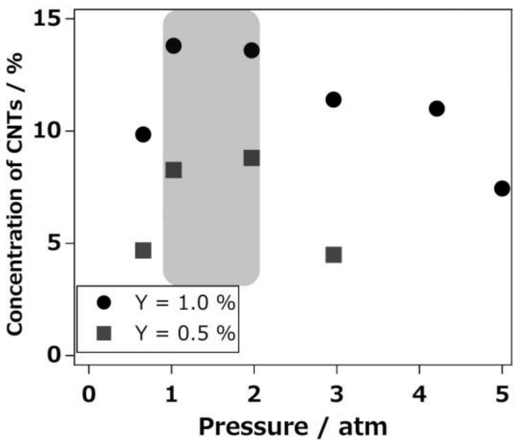

Fig. 1 Pressure Dependence of CNT concentrations obtained by TGA

The details of HTPAD described in elsewhere [1]. Electrodes made of graphite containing catalytic metals (Ni/Y 4.2/0.5 and 4.2/1.0 at. %:Toyo Tanso Co. Ltd.) were vaporized by the pulsed-arc discharges (0.6 ms, 50Hz, and 100 A) and were converted into CNTs in the high-temperature (1250 ℃) and a wide pressure range of Ar (0.2-5 atm). The products were characterized by Raman spectroscopy with excitation laser of 633 nm, TGA, and TEM.

Figure 1 shows the pressure dependence of concentration of CNTs obtained by TGA. The optimal pressure is 1.5 atm in every characterization method. The analyses on the optimal pressure of various conditions such as gas species and temperature have shown that the production processes are mainly dominated by cooling and condensation processes [3]. Our optimal condition of 1.5 atm is exactly corresponding to those obtained by the analyses, which is marked as a shaded area in Fig. 1. The agreement shows that the cooling processes are also crucial for HTPAD even though there are so many differences in vaporization processes.

References

[1] T. Sugai *et al.*, Nano Lett. 3 (2003) 769.
[2] O. Jost, A. A. Gorbunov, J. Möller, W. Pompe, X. Liu, P. Georgi, L. Dunsch, M. S. Golden, and J. Fink, J. Phys. Chem. B 106 (2002) 2875.
[3] Y. Saito, Y. Tani, and A. Kasuya, J. Phys. Chem. B 104 (2000) 2495.

Ligand exchange reactions on transition metal oxo clusters and applications in materials chemistry

Johannes Kreutzer, Ulrich Schubert

Institute of Materials Chemistry, Vienna University of Technology, Vienna, Austria

Transition metal oxo clusters find increasing interest in material science as nanosized building blocks, especially for inorganic-organic hybrid materials. Clusters with polymerizable ligands attached to the cluster surface can act as co-monomers in polymer synthesis. Thereby the inorganic moiety is incorporated in a polymer matrix by covalent bonding. Numerous transition metal oxo clusters with polymerizable ligands were synthesized and used to obtain polymers with tailored properties.

Most of the clusters used as co-monomers so far have a high number of polymerizable groups of the same kind on their surface, resulting in highly crosslinked polymers. Ligand exchange on transition metal oxo clusters is one way to control the ratio of functionalized and non-functionalized ligands and can lead to less crosslinked polymers. Furthermore it is possible to obtain clusters with more than one functional group in the ligand sphere in an easy-to-adjust ratio by ligand exchange reactions.

In this work we will present a detailed NMR study of exchange reactions on carboxylate substituted Zr/Ti oxo clusters with different carboxylic acids. We will show that ligand exchange on the cluster proceeds under retention of the cluster core also in cases where all ligands have been exchanged. Steric and electronic effects of the incoming ligand towards exchange reactions will be discussed. Scrambling reactions between clusters with two different types of ligands are an additional way to easily adjust the ligand composition of transition metal oxo clusters. Complementary applications of ligand exchange reactions in material science will be presented. Polymer properties such as glass transition temper

ature and storage modulus as well as mechanical properties of the polymer can be changed gradually by controlling the ligand sphere of transition metal oxo clusters.

Extending the Sizes and Charge States of Polyanionic Metal Clusters

Steffi Bandelow,[1] Franklin Martinez,[1,2] Gerrit Marx,[1] Lutz Schweikhard,[1] and Albert Vass[1]

[1] *Institute of Physics, Ernst-Moritz-Arndt University Greifswald, Germany*
[2] *present address: Institute of Physics, University of Rostock, Germany*

The ClusterTrap setup [1] combines several ion-storage devices for a variety of experimental studies on metal clusters including collision-induced dissociation, (delayed) photodissociation, further ionization to higher positive or negative charge states by electron impact or electron attachment, respectively. All selection, preparation and interaction steps can be performed on extended time scales up to several seconds. The unique arrangement of two linear radiofrequency quadrupole (RFQ) ion traps (Paul traps) and an ion-cyclotron-resonance trap (ICR or Penning trap) allows one to dedicate them with respect to specific functions and optimizations.

In particular, one Paul trap is used for the accumulation of cluster ions from a pulsed laser-vaporization source and preselection of the cluster size. In the second Paul trap, electrons can be attached at well-defined energies by use of a “digital” (i.e. rectangular) RF trapping potential [2]. This allows one to study for the first time the energy dependence of electron attachment to polyanionic metal clusters and to determine the heights of their repulsive Coulomb barriers. With a recent replacement of the superconducting magnet, the field strength was increased from B = 5 T to 12 T. Thus, the electron attachment in the ICR trap was extended to (negative) charge states as high as z = -6 for gold and z = -10 for aluminum clusters, respectively. The yields of the charge states measured as a function of reaction time confirm a sequential electron-attachment process.

Next, we will study polyanion decay induced by laser light. The studies will be performed with respect to cluster size, charge state and chemical element as well as laser intensity and photon energy, and also regarding possible delays between photo-interaction and electron detachment or cluster dissociation. Furthermore, it is planned to use multi-reflection time-of-flight mass spectrometry, recently further developed by us for precision measurements in nuclear physics [3], for high-resolution separation of the (relatively large) polyanionic cluster, and to combine ion-trap techniques of polyanion production with their investigation by photo-electron spectroscopy.

[1] L. Schweikhard *et al.*, Eur. Phys. J. D 9 (1999) 15; F. Martinez *et al.*, Eur. Phys. J. D 63 (2011) 255; F. Martinez *et al.*, Int. J. Mass Spectrom. 365-366 (2014) 266.
[2] S. Bandelow *et al.*, Int. J. Mass Spectrom. 336 (2013) 47 and 353 (2013) 49.
[3] R.N. Wolf *et al.*, Int. J. Mass Spectrom. 349-350 (2013) 123; F. Wienholtz *et al.*, Nature 498 (2013) 346.

Surface immobilization of gas-phase-synthesized nanoclusters toward construction of nanoelectronics

Masato Nakaya,[1,2] Takeshi Iwasa,[1,2] Hironori Tsunoyama,[1,2]
Toyoaki Eguchi,[1,2] and Atsushi Nakajima[1,2,3]

[1]*Nakajima Designer Nanocluster Assembly Project, JST, Kawasaki,* Japan
[2]*Department of Chemistry, Keio University, Yokohama, Japan*
[3]*Keio Institute of Pure and Applied Sciences (KiPAS), Keio University, Yokohama, Japan*

Constructing nanoelectronics from nanocluster building blocks is one of the most attractive challenges in nanocluster science, since it has been actively demonstrated that various functional nanoclusters can be created in gas phase and their physicochemical properties are controllable by changing their size, compositions, and charge states. In this study, we have created ultrathin metal/molecule and acceptor/donor junctions using the gas-phase-synthesized nanoclusters.

The metal/molecule junctions were formed by depositing size-selected Ag nanocluster cations (Ag_n^+; n = 7, 13, and 55) onto few-layer C_{60} films and were investigated by scanning tunneling microscopy and spectroscopy (STM/STS) [1]. The Ag_n are stably immobilized without marked disintegration on the C_{60} films and can densely cover the surface (Figure 1). In addition, charged carriers can be precisely injected into the topmost C_{60} layers via the Ag_n. These results indicate that the atomically abrupt interface can be formed between the Ag_n and C_{60} films. This is attractive toward realizing high performance devices composed of metal/molecule/metal junctions, because, in the conventional sandwich junctions constructed by depositing metal atoms onto molecular films, undesirable modification of the molecular films generally occurs by penetration of the metal atoms. Furthermore, barrier heights for the carrier injection at the Ag_n/C_{60} interface can be controlled depending on the cluster size and deposition conditions.

We have also deposited the tantalum-atom-encapsulated Si_{16} cage cations ($Ta@Si_{16}^+$) from gas phase where they behave as superatoms with rare-gas-like features. It has been found that the $Ta@Si_{16}$ are densely immobilized onto C_{60} films while maintaining the cage shape, large energy gap of ~2.1 eV, and high thermal durability similar to those in gas phase. In contrast, the $Ta@Si_{16}^+$ are destabilized on bare and oligothiophene-terminated metallic surfaces. STS and theoretical results indicate that positive charge is retained in the surface-immobilized $Ta@Si_{16}$ by forming the charge transfer complex ($Ta@Si_{16}^+$-C_{60}^-).

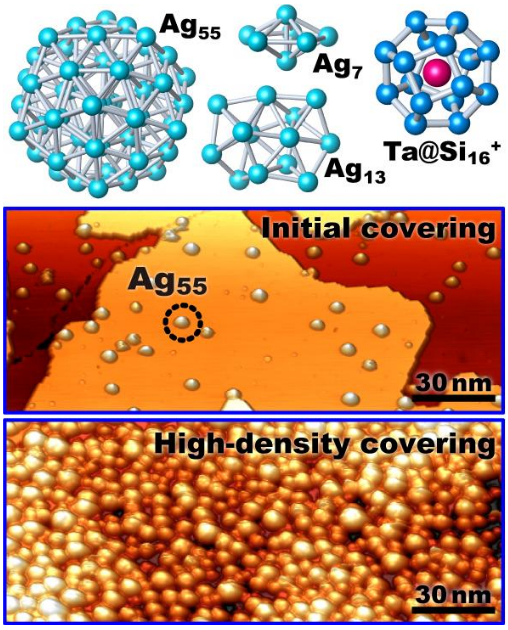

Figure 1. C_{60} thin films (upper) sparsely and (lower) densely covered with Ag_{55}

Reference
[1] M. Nakaya, T. Iwasa, H. Tsunoyama,T. Eguchi, A. Nakajima, Adv. Funct. Mater. 24(2014)1202.

Generation of small and stable Si nanoparticles using a liquid jet co-deposition method

Gediminas Galinis[1], Oliver Youle[1], Hanieh Yazdanfar[1], Mike J. McNally[1], Mumin M. Koç[1], Gauthier Torricelli[1], Mark Watkins[1], Klaus von Haeften[1].

[1] *University of Leicester, Department of Physics & Astronomy, Leicester, LE1 7RH, United Kingdom*

Small and stable nanoparticles are particularly interesting due to their exotic physical and optical properties. These nanoparticles are applicable in opto-electronics [1] and may be used as biosensors [2]. The methods currently available in industry to generate nanoparticles lack an ability to prepare small (<5nm) and stable nanoparticles in liquids without further stabilization by surfactants. We present a novel method to deposit sputtered semiconductor and metal atoms on the surface of a liquid jet *in vacuo* and subsequent growth into stable and small clusters without surfactants. This method is capable of generating large quantities (ml) of nanoparticle-solvent mixtures within few minutes.

The presentation will focus on the generation and characterization of Si nanoparticles, whose stability and sizes were determined by UV-Vis, XPS and AFM measurements. In the UV-Vis spectra we identified a fingerprint of Si clusters; this peak showed a distinct intensity correlation to the deposition rate of Si atoms sputtered from the Si target. Furthermore, time-resolved UV-Vis spectra showed stabilization of Si nanoparticles within a 30 min interval. The sizes of nanostructures were determined by drop-casting nanoparticle colloids on the surface of HOPG, allowing the solvent to evaporate and subsequently probing the heights of residue nanoparticle layers with AFM. A size of 1 nm nanoparticles has been thus demonstrated. Further support for the presence of Si nanoparticles and their size was obtained from XPS measurements: the magnitude of Si-peak-shift suggested structures of a size of 1 to 2 nm [3].

References

[1] K. M. Noone, and S. David Ginger, Acs Nano 3.2 (2009): 261-265.

[2] G. Wang, et al., Optics communications 281.7 (2008): 1765-1770.

[3] M. Vogel, et al., Physical Review B 85.19 (2012): 195454.

Enhanced quantum coherence in graphene by Pd cluster deposition and its zero-temperature saturation

Fengqi Song, Junhao Han, Yuyuan Qin and Guanghou Wang

Department of Physics and National Lab of Solid State Microstructures,Nanjing University, 210093, Nanjing, China

Surface absorption of functional atoms is believed to implement the quantum spin/anomalous hall state. A problem arises that the surface absorption will simultaneously induce additional electronic scattering while introducing the required functionalities. Such scatterings may suppress the coherence of the Dirac Fermions and subsequently disable these desired quantum states. Here we report the increase of the dephasing lengths of the graphene sheet after the deposition of Pd nanoclusters [1] as demonstrated by weak localizations. The dephasing lengths are found to reach some saturated values with the decreasing temperatures, essentially the zero-temperature decoherence. Detailed analysis is carried out on the temperature-dependent and saturated decoherence periods. Our data agree well with the predication of Golubev and Zaikin, where such zero-temperature decoherence is mainly induced by local fluctuations of the electrical fields near disorders. The competition between the surface scattering and electrical field screening leads to the final improvement of quantum coherence. We propose the priority of using the nanoclusters that less scattering is introduced while seeking the same control of the electronic interference through absorbing the same quantity of atoms.

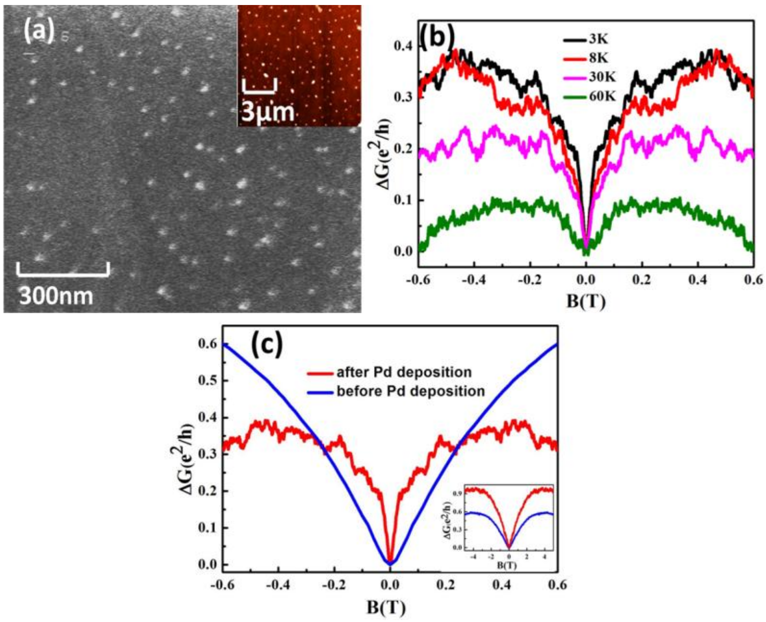

Figure. (a) The SEM image of the graphene sheet after the cluster deposition. (b) The relative magnetic conductance ΔG(B) plotted against the perpendicular fields B at various temperatures. (c) Focusing on the WL cusp at low temperatures. The two curves are the MR curves measured at 2K, before deposition (blue) and 3K, after deposition (red) respectively. The cusp becomes much sharper after the absorption of the Pd clusters, clearly indicating the improvement of the electronic coherence.

The hydrogen Bonded Networks in Hydrated Halogen Anions

Chiaki Ishibashi,[1] Suehiro Iwata,[2] Kaoru Onoe[1] and Hidenori Matsuzawa[1]

[1] *Department of Engineering, Chiba Institute of Technology, Narashino, Japan*
[2] *Department of Chemistry, Keio University, Yokohama, Japan*

Recently we have developed the ab initio theoretical procedure based on the Locally Projected Molecular Orbital Perturbation Theory (LPMO PT), and applied it for the analysis of the water clusters $(H_2O)_n$ (n≦25) and their hydrogen bonded networks [1,2]. The present study is the extension to the hydrated halogen anions $X^-(H_2O)_n$ (n=1-7) clusters.

Various isomers of the $X^-(H_2O)_n$ (n=1-7) cluster are determined with the MP2 method with aug-cc-pvdz basis set. Some of them have the similar geometric structures in literature, and the calculated binding energies are in good agreement with the reported values. The LPMO PT allows us to evaluate the charge-transfer (E_{CT}) and dispersion (E_{Disp}) terms for every pair of water-X^- and water-water. In the earlier papers [1,2], the strong correlations between the E_{CT} and E_{Disp} and between E_{CT} and the hydrogen bond length are found. The correlations are dependent on the types of water molecules involved.

The similar correlations are found also for the halogen-water and water-water hydrogen bonds in $X^-(H_2O)_n$. Figure 1 shows the correlation between the bond length $R_{X\text{-}O}$ of halogen and water vs. E_{CT} and E_{Disp} in the $Cl^-(H_2O)_n$ (n=3-7) cluster is shown. In the figure each water is classified by D*n*A*m*. For instance, water molecule of D0A2Cl has a Cl･･･H and two O･･･HO bonds but no hydrogen bond to the water molecule. Figure 1 shows that the D0A2Cl water molecule is most strongly interacted with Cl anion, because this water molecule is more positively charged by accepting two HO bonds, or by electron-donating to the neighboring molecules. On the other hands, the weakest X^-...H_2O hydrogen bond of water molecule is of D1A0Cl type. Figure 2 is the similar correlation between $R_{O\text{-}O}$ of hydrogen-bonded pair of water molecules vs. E_{CT} and E_{Disp} in the $Cl^-(H_2O)_n$. As was found in the pure water clusters [1,2], the D1A2→D2A1 pairs are the strongest among various pairs of the hydrogen bonds. In the D1A2→D2A1 bond pair, the hydrogen donor water of D1A2 is strongly positive charged, and the hydrogen acceptor water of D2A1 is less positive than the other types of water molecules.

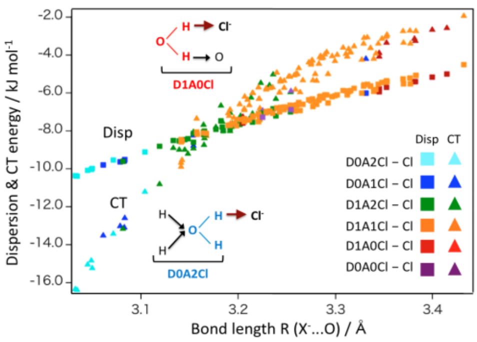

Figure 1. The correlation between the bond length $R_{X\text{-}O}$ of halogen and water vs. E_{CT} and E_{Disp} in the $Cl^-(H_2O)_n$ (n=3-7) cluster

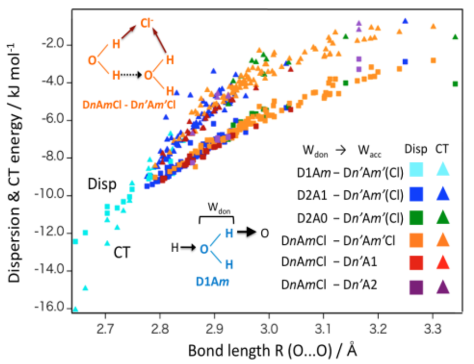

Figure 2. The correlation between the bond length $R_{O\text{-}O}$ of water and water vs. E_{CT} and E_{Disp} in the $Cl^-(H_2O)_n$ (n=3-7) cluster

References
[1] Iwata, Phys. Chem. Chem. Phys. 16 (2014) 11310
[2] Iwata, Bandyopadhyay, Xantheas, J. Phys. Chem. A 117(2013) 6641

Formation of regular polyicosahedral structure during growth of large Lennard-Jones clusters from their global minimum

Wieslaw Polak

Department of Applied Physics, Lublin University of Technology, Lublin, Poland

Monte Carlo simulations of growth of Lennard-Jones (LJ) clusters were carried out for reduced temperature $T^* = 0.35$ and seed clusters having the following structures and sizes: ideal icosahedral (N = 561, 923), icosahedral with empty core (N = 850), and decahedral (N = 823) reported as global minima by Xiang et al. [1]. After thermal equilibration, all these clusters were grown using the cluster growth model [2] in 15 simulation runs up to $N \approx 3300$ by attachments of randomly-moving atoms from supersaturated vapour of atom concentration $n^* = 0.001$.

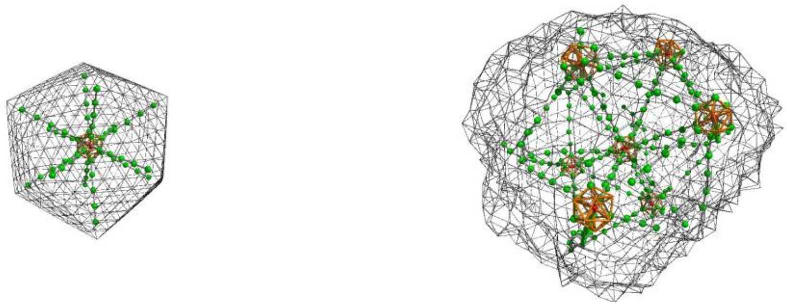

Linear dh chains and icosahedral units inside: (left) seed of N = 923, (right) final r-PIC cluster of $N \approx 3300$.

Structural analysis and visualisation showed that internal structure (see Fig. above) of the equilibrated clusters practically did not change showing only existence of some dislocated atoms on the cluster surface without any surface reconstruction. In all cases the growth leads to formation of regular polyicosahedral structure (r-PIC) in accordance with recent results [3]. Neighbouring local icosahedral units in the internal structure of the growing clusters are connected by decahedral (dh) linear chains of length typically equal to the distance of vertex atoms from cluster center in case of icosahedral clusters. This means that newly-added atoms attain positions transforming the surface layer to hexagonal close-packed (hcp) monolayer characteristic for anti-Mackay packing [4]. Kinetic process in the form of creation of dh chain at a contact of two such hcp monolayers is responsible for formation of the r-PIC structure.

References

[1] Y. Xiang, L. Cheng, W. Cai and X. Shao, J. Phys. Chem. A 108 (2004) 9516.
[2] W. Polak, Phys. Rev. B 71 (2005) 235413.
[3] W. Polak, J. Crystal Growth 401C (2014), http://dx.doi.org/10.1016/j.jcrysgro.2014.01.017.
[4] J.P.K. Doye, D.J. Wales, Z. Phys. D 40, (1997) 466–468.

Structures and dielectric properties of neutral lead clusters

D.A. Götz,[1] A. Shayeghi,[1] R.L. Johnston[2], P. Schwerdtfeger[3], and R. Schäfer[1]

[1] *Eduard-Zintl-Institut für Anorganische und Physikalische Chemie, Technische Universität Darmstadt, Alarich-Weiss-Straße 8, 64287 Darmstadt*

[2] *School of Chemistry, University of Birmingham, Edgbaston, Birmingham B15 2TT, United Kingdom*

[3] Centre for Theoretical Chemistry and Physics, The New Zealand Institute for Advanced Study, Massey University (Albany), Bob Tindall Bldg., 0745 Auckland, New Zealand

Electric molecular beam deflection experiments are an established method for resolving the structures of neutral group 14 clusters [1]. For this purpose deflection profiles are modeled using structures and dielectric properties from quantum chemical calculations and compared to experimental data. Promising Pb_N (N=7-18) structures are located using the unbiased Birmingham Cluster Genetic Algorithm in combination with density functional theory [2]. Lowest lying structures are further relaxed utilizing two-component density functional theory taking spin-orbit effects into account. Simulated beam profiles allow a structural assignment for the most clusters in the examined range. Neutral lead clusters adopt mainly spherical geometries and resemble the structures of lead cluster cations apart from Pb_{10}. Inclusion of spin-orbit effects appears crucial for a correct interpretation of the experimental data [3]. Experiments for clusters with more than 18 atoms reveal strong dipole moments for Pb_{31} and Pb_{36} and a significantly enhanced polarizability for Pb_{25}. This points towards unusual geometries for certain cluster sizes although a structural assignment based on our approach has not been possible yet. Polarizabilities of clusters with more than 45 atoms are in good agreement with a metallic sphere model taking an electron spill-out into account.

References

[1] D.A. Götz, S. Heiles, R.L. Johnston, and R. Schäfer J. Chem. Phys. 138 (2012) 186101.

[2] S. Heiles, A.J. Logsdail, R. Schäfer, and R.L. Johnston Nanoscale 4 (2012) 1109.

[3] D.A. Götz, A. Shayeghi, R.L. Johnston, P. Schwerdtfeger and R. Schäfer J. Chem. Phys. 140, 164313 (2014)

Fabrication of Ag cluster by a novel laser ablation of nanocolloid target

Teppei Nishi, Yusuke Akimoto, Shuji Kajiya, Kosuke Kitazumi, Naoko Takahashi, and Yoshihide Watanabe

[1] *TOYOTA CENTRAL R&D LABS., INC. Aichi, Japan*

We have developed a novel laser ablation method at air-suspension interface for monodisperse single nano-sized particle generation in liquid [1]. In this method, the plasma density induced by laser irradiation is estimated to be low due to the small confined effect of solvent. The collision probability of excited species produced by laser ablation is small. In our previous study, micro-sized particles was agitated in a measuring flask filled with pure water by a magnetic stirrer. Pulsed laser irradiation can induce the fragmentation of target particles agitated in water. It would be expected that much smaller particles such as sub nano-sized clusters can be fabricated using smaller target particles. In this paper, we demonstrate a novel method for fabrication of sub nano-sized Ag cluster by laser ablation at air-suspension interface using Ag nanocolloid target.

Ag nanocolloid target was prepared by laser ablation of Ag powder target precipitated in the bottom of a piriform flask filled with pure water [2]. Second harmonic light from Nd:YAG laser system (532 nm, 400 mJ/pulse, 10 Hz) was irradiated through the bottom of a piriform flask for 60 minutes. Then, 200 mL of Ag nanocolloid was agitated in a measuring flask by a magnetic stirrer. Second harmonic light from Nd:YAG laser system (800 mJ/pulse) was focused onto the air-suspension interface to induce ablation. After laser irradiation for 120 minutes, clear and colorless colloid could be obtained. The product was analyzed by scanning transmission electron microscopy (STEM), UV-Vis spectrometry, electrospray ionization mass spectrometry (ESI-MS) and X-ray photoelectron spectrometry (XPS).

Ag nanocolloid as target showed the surface plasmon absorption around 400 nm. Ag product colloid after laser ablation at air-suspension interface showed absorption peaks in UV region. It can be considered that target particles were fragmented by laser irradiation, resulting in sub nano-sized cluster formation. In addition, STEM and ESI-MS analyses were carried out to confirm the fragmentation of target particles and fabrication of sub nano-sized particles. These results are coincident with the consideration from the result of UV-Vis spectrometry.

References

[1] T. Nishi, N. Suzuki, N. Takahashi, K. Yano, J. Nanopart Res 15 (2013) 1569.

[2] T. Nishi, H. Sugiyama, N. Suzuki, K. Yano, H. Azuma., J. Photochem. Photobiol. A: Chem 226 (2011) 64.

Solvation Chemistry of Water-Soluble Thiol-Protected Gold Nanocluster Au_{102} from DOSY NMR Spectroscopy and DFT Calculations.

Tanja Lahtinen[1], Kirsi Salorinne[1], Sami Malola[2], Jaakko Koivisto[1] and Hannu Häkkinen[1,2]

[1] *Department of Chemistry, Nanoscience Center, University of Jyväskylä, Finland*
[2] *Department of Physics, Nanoscience Center, University of Jyväskylä, Finland*

Water-soluble, thiolate monolayer-protected gold nanoclusters have several biological applications in microscopy and imaging of biomolecules and bionanoparticles, in drug delivery and in disease targeting [1]. The well-known and characterized water-soluble Au_{102}(*p*MBA)$_{44}$ and Au_{144}(*p*MBA)$_{60}$ clusters are composed of a metal core and a protecting *p*-mercaptobenzoic acid (*p*MBA) ligand layer. However, the clusters become water-soluble only when the carboxylic acid group of the *p*MBA ligand is deprotonated. Hydrodynamic diameter of Au_m(*p*MBA)$_n$ [(m,n) = (102,44) and (144,60)] clusters in aqueous media was determined via DOSY NMR spectroscopy [2]. The apparent size of the same (n,m) cluster depends on the counter ion of the deprotonated *p*MBA ligand as explained by the competing ion-pair strength and hydrogen bonding interactions studied in DFT calculations [3].

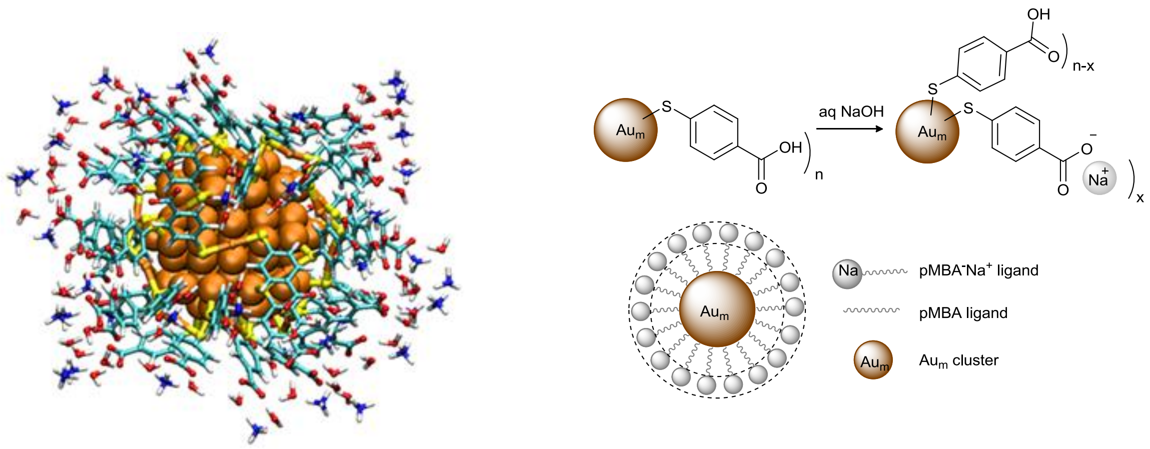

Scheme 1: Left: A model cluster of $Au_{102}(SR)_{44}$ built using computationally relaxed pMBA$^-$ ---$2H_2O$---NH_4^+ complex as a ligand. Right: Schematic presentation of the Au_m(*p*MBA)$_n$ clusters as their sodium salts in aqueous NaOH solution highlighting the effect of sodium counter cation on the hydrodynamic diameter (----) of the cluster.

References

[1] C. J. Ackerson, R. D. Powell and J. F. Hainfeld, Methods Enzymol 48 (2010) 195; V.Marjomäki, T. Lahtinen, M. Martikainen, J. Koivisto, S. Malola, K. Salorinne, M. Pettersson and H. Häkkinen, Proc. Natl. Acad. Sci. USA 111 (2014) 1277.
[2] Y. Cohen, L. Avram and L. Frish, Angew. Chem. Int. Ed. 44 (2005) 520.
[3] K. Salorinne, T. Lahtinen, S. Malola, J. Koivisto and H. Häkkinen, Nanoscale 2014, DOI:10.1039/C4NR01255K.

Size-dependent structures of iron oxide cluster ions studied by ion mobility mass spectrometry

Tatsuya Komukai, Ryoichi Moriyama, Keijiro Ohshimo, and Fuminori Misaizu

Department of Chemistry, Graduate School of Science, Tohoku University, 6-3 Aoba, Aramaki, Aoba-ku, Sendai 980-8578, Japan

Iron oxide clusters were recently studied for the purpose of unveiling microscopic properties of the compounds which are important as semiconductors, magnetic materials, and catalysts. In a previous study on the structures of neutral iron oxide clusters, $(FeO)_n$ [1], stable structures were two-dimensional (2D) rings for $n \le 5$ and three-dimensional (3D) towers for $n \ge 6$. In this study, we have investigated the structures of $(FeO)_n^+$ and $Fe_nO_{n+1}^{+/-}$ cluster ions by ion mobility mass spectrometry (IM-MS) [2].

Iron oxide cluster ions, generated by reactions between iron vapor formed by laser vaporization and mixture gas of O_2/He in supersonic expansion, were injected into an ion-drift cell by a pulsed electric field. The cell was filled with He buffer gas with a pressure of 0.90 Torr. An injected ion reached a constant drift velocity which depends on the collision cross sections between ions and He atoms. Thus we determined the cross section experimentally from the measured arrival time (and the time that the ion spent in the cell).

Fig. 1 shows the arrival time distributions (ATDs) of $(FeO)_n^+$ (n = 4-7) cluster ions. As n increases, the distributions were shifted to longer arrival time. Two Gaussian curves were necessary for fitting of the ATDs for $n \ge 5$. In order to explain these results, we have compared experimental and theoretical collision cross sections of cluster ions. As a result, stable structures of $(FeO)_n^+$ were determined to be 2D rings for $n \le 5$ and 3D towers for $n \ge 6$, as in the previous calculation results on neutrals. Therefore, structural change from 2D to 3D occurs at around n = 6. In addition, 2D sheet-like structural isomers coexist for $n \ge 5$. Therefore, the 2D and 3D structural isomers coexist for n = 6-8. We will also discuss the structures of $Fe_nO_{n+1}^{+/-}$ cluster ions.

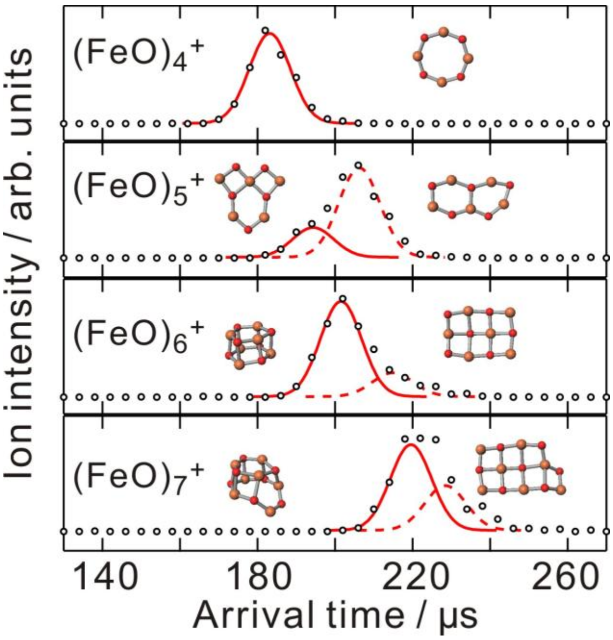

Fig. 1. Arrival time distributions of $(FeO)_n^+$ (n = 4-7). Circles are the observed ion intensities, and the Gaussian curves show component of isomers.

[1] N. O. Jones, B. V. Reddy, F. Rasouli, and S. N. Khanna, Phys. Rev. B 72 (2005) 165411.
[2] K. Ohshimo, T. Komukai, R. Moriyama, and F. Misaizu, J. Phys. Chem. A 118 (2014) 3899.

Fabrication of Rh nanoframes through dissolution of Au cores of Au@Rh core-shell nanorods by the addition of HCl

Yukinori Nakashima,[1] Masashi Hattori,[2] and Masaharu Tsuji[2]

[1] *Department of Applied Science for Electronics and Materials, Kyushu University, Kasuga, Japan*
[2] *Institute for Materials Chemistry and Engineering, Kyushu University, Kasuga, Japan*

Many interesting static and dynamic properties of nanoparticles that cannot be observed in bulk metals have been reported. Among them, nanoparticles of platinum group, such as Pt, Pd, and Rh, were widely used as environmental catalysts for NOx removal. However, nanoparticles of these Pt group are expensive. Therefore, reduction of use of Pt group nanoparticles is expected. Nanoframes having hollow interior structures are expected to have high catalytic activity, because specific surface area of nanoframes is larger than that of normal spherical nanoparticles. In this study, we attempt fabrication of nanoframes of Rh particles using a unique procedure. Rh nanoframes were prepared by synthesis of Au@Rh core-shell nanorods (NRs) followed by the selective etching of Au NR cores by addition of HCl in an aqueous solution.

In the first step Au@Rh core-shell NRs were prepared by heating a mixture of Au NRs, hexadecyl trimethyl ammonium bromide, ascorbic acid, and rhodium chloride in an aqueous solution in an oil bath at 95 ^{o}C for 3 h. TEM and TEM-energy dispersive X-ray spectrometry (EDS) images of products are shown in Figs. 1(a) and 1(c). Results show that Au NR seeds are covered by Rh shells. Rh shells consist of small particles because Rh shells are not formed via layered growth but they are produced via island growth owing to large lattice mismatch between Au and Rh (6.9%).

In the second step, 5 % hydrochloric acid was added to Au@Rh core-shell solution and heated in an oil bath at 95 ^{o}C for 12 h. TEM and TEM-EDS of products are shown in Figs. 1(b) and 1(d). It is clear from Fig. 1(b) that hollow nanoframes are formed. When Au:Rh atomic ratio over this image was evaluated from TEM-EDS image, it was 1 : 9. This suggests that Rh-rich nanoframes were produced in the second step. Rh nanoframes have concave-convex shapes because Rh shells of precursor Au@Rh core-shell nanoparticles consist of small island-type particles. These small Rh particles remain after dissolution of Au NRs and form nanoframe shapes.

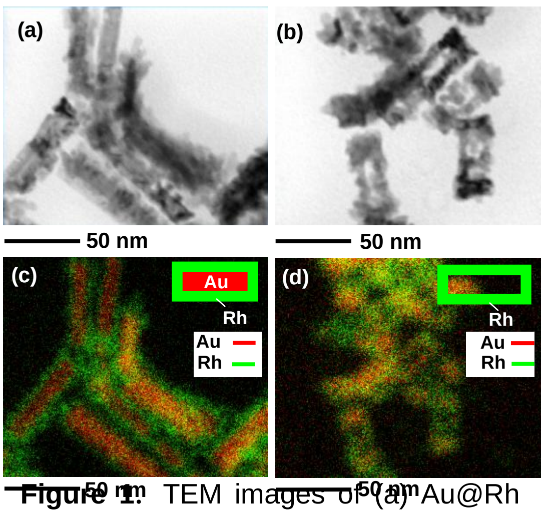

Figure 1. TEM images of (a) Au@Rh NRs and (b) Rh nanoframes. TEM-EDS images of (c) Au@Rh NRs and (d) Rh nanoframes.

Effect of Core Size on Au-Pt Core-Shell Nanoparticles for Oxygen Reduction Reaction

Saki Hirose,[1] Yoshikiyo Hatakeyama,[2] Ken Judai,[2] Takeshi Morita,[1] and Keiko Nishikawa[1]

[1]*Graduate School of Advanced Integration Science, Chiba University, Chiba, Japan*
[2]*College of Humanities and Sciences, Nihon University, Tokyo, Japan*

Au-Pt core-shell nanoparticles are attractive materials for reduction of the Pt usage. The core-shell nanoparticles show the higher catalytic activities for oxygen reduction reaction (ORR) compared to commercial Pt/C.[1] It is also reported that the particles with small Au-cores have higher durability than with large cores.[2] Method of regulation of the catalytic activity by the core-size will be applied to other combination of metals and wide reaction system. Four groups of Au nanoparticles (AuNPs) were prepared for the present study.

The AuNPs were synthesized in an ionic liquid by sputter deposition of Au.[3] The sizes of AuNPs were controlled by temperature of the ionic liquid.[4] Four groups of AuNPs with different sizes were synthesized in 1-butyl-3-methylimidazolium tetrafluoroborate ([C_4mim]BF_4, Fig. 1). The AuNPs-supported carbon blacks (Au/CB) were obtained by mixing AuNPs containing ionic liquids with CB. Pt shells were formed by spontaneous reduction of K_2PtCl_4 on the surface of AuNPs (Au-Pt/CB).[5]

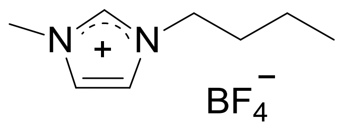

Fig. 1 Chemical structure of [C_4mim]BF_4.

The effect of Pt-shell formation in size of the nanoparticles was investigated by small-angle X-ray scattering (SAXS). The catalytic activities were characterized by electrochemical measurements. Fig. 2 shows the size distribution of Au/CB and Au-Pt/CB. The size slightly increased after the formation of Pt shells. It is thought that increase of the size is caused by reduction and deposition of Pt onto the surface of AuNPs. The same tendency was observed for other Au-Pt/CBs with different core sizes. Hydrogen adsorption-desorption waves are confirmed by cyclic voltammetry after Pt shell formation. In addition to the results, we will discuss ORR activity of Au-Pt/CB in $HClO_4$ aq.

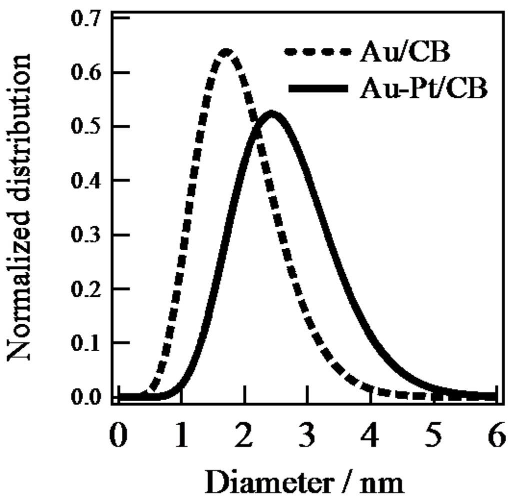

Fig. 2 The size distribution of the formed nanoparticles.

References

[1] X. Li, J. Liu, W. He, Q. Huang, and H. Yang, *J. Colloid. Interf. Sci.*, **344**, (2010) 132.

[2] Inaba et al., *ECS Transactions*, **33**, 1, (2010) 231.

[3] Torimoto et al., *Appl. Phys. Lett.*, **89**, (2006) 243117.

[4] Y. Hatakeyama, S. Takahashi, and K. Nishikawa, *J. Phys. Chem. C*, **114**, (2010) 11098 .

[5] Tsuji et al., The 218th ECS Meeting, Abstract #858 (2010)

Melting of Weakly-Bound Systems by Monte Carlo Simulations – Applications to Mercury and Argon under High Pressure

Elke Pahl,[1] Jonas Wiebke[1], Peter Schwerdtfeger[1]and Florent Calvo[2]

[1] *Centre of Theoretical Chemistry and Physics, Institute for Natural and Mathematical Sciences and The New Zealand Institute for Advanced Study, Massey University Auckland*

[2] *ILM, UMR 5306, 43 Bd du 11 Novembre 1918, 69622 Villeurbanne Cedex*

Our goal is to understand the melting of weakly-bound systems based on parallel tempering Monte Carlo (MC) simulations which are based on highly accurate *ab initio* models for the interaction energy of the *N*-atomic system. I will present results 1) on the explanation of the exceptionally low melting temperature of mercury, Hg [1] and 2) on high-pressure melting of Argon up to pressures of 100 GPa [2].

Mercury is the only elemental metal liquid at room temperature, a fact that puzzled chemists for a long time. We were able to show that this melting point depression is caused by an interplay of scalar-relativistic and complicated many-body effects. Herefore, the many-body effects were described in an efficient way within the so-called diatomics-in-molecules (DIM) formalism [3] and a non-relativistic version of the DIM model was developed [4]. Both models were updated by using highly accurate, *ab initio* ground and excited potential curves of the Hg dimer [5]. While the results for small clusters are not following a well-defined trend with increasing cluster size, we get very convincing results for the extended system - within the relativistic model, the experimental melting temperature as well as the density is very well reproduced. And a comparison with the non-relativistic results proves without doubt the impact of relativity: Without relativistic effects mercury would melt more than 100°C higher than observed and would not be liquid at room temperature [1]!

For the high-pressure melting studies our MC code has been extended from canonical ensembles to isobaric, isothermal ensembles. Results for the melting of solid Argon under high pressures of 1-100 GPa are found to be very accurate and probably exceeding experimental accuracy [2], after effects of ‘super-heating’ in the simulations are accounted for.

References

[1] F.Calvo, E.Pahl, M.Wormit, P.Schwerdtfeger, Angew.Chem.Int.Ed. 17 (2013) 7583–7585.

[2] J.Wiebke, E.Pahl, P. Schwerdtfeger, Angew. Chem. Int. Ed. 52 (2013), 13202-13205.

[3] H. Kitamura, Chem. Phys. 325 (2006) 207–219.

[4] F. Calvo, E. Pahl, P. Schwerdtfeger, F. Spiegelman, J. Chem. Theory Comput. 8 (2012) 639–648.

[5] E. Pahl, D. Figgen, C. Thierfelder, K. A. Peterson, F. Calvo, P. Schwerdtfeger, J. Chem. Phys. 132 (2010)

Design of Three-shell Icosahedral Matryoshka Clusters $A@B_{12}@A_{20}$ (A = Sn, Pb; B = Mg, Zn, Cd, Mn) Including a New Type of Magnetic Superatoms

Xiaoming Huang [1], Jijun Zhao [*1,2], Yan Su [1], Zhongfang Chen [3], R. Bruce King [*4]

[1] Key Laboratory of Materials Modification by Laser, Ion and Electron Beams (Dalian University of Technology), Ministry of Education, Dalian 116024, China.

[2] Beijing Computational Science Research Center, Beijing 100089, China.

[3] Department of Chemistry, Institute for Functional Nanomaterials, University of Puerto Rico, San Juan, PR 00923, USA.

[4] Department of Chemistry and Center for Computational Chemistry, University of Georgia, Athens, Georgia, USA.

We propose a series of icosahedral matryoshka clusters of $A@B_{12}@A_{20}$ (A = Sn, Pb; B = Mg, Zn, Cd), which are thermodynamically and chemically stable with large HOMO-LUMO gaps (1.29 to 1.54 eV) and low formation energies (0.06 to 0.21 eV/atom). A global minimum search using a genetic algorithm and density functional theory calculations confirms that such three-shell onion-like structures are the ground states for these $A_{21}B_{12}$ binary clusters. All of these icosahedral matryoshka clusters, including two previously found ones, i.e., $[As@Ni_{12}@As_{20}]^{3-}$ and $[Sn@Cu_{12}@Sn_{20}]^{12-}$, follow the 108-electron rule, which originates from the high I_h symmetry and consequently the splitting of superatom orbitals of high angular momentum (1H and 1I). More interestingly, two magnetic matryoshka clusters, i.e., $Sn@Mn_{12}@Sn_{20}$ and $Pb@Mn_{12}@Pb_{20}$, are designed, which combine a large magnetic moment of 28 μ_B, a moderate HOMO-LUMO gap, and weak inter-cluster interaction energy, making them ideal building blocks in novel magnetic materials and devices.

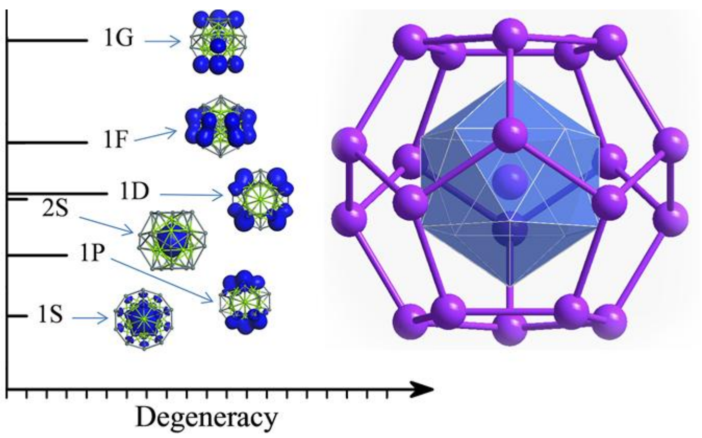

Structures, electronic and magnetic properties of $Fe_2Ge_n^-$ and $Cr_2Ge_n^-$ (n=3-12) clusters from DFT calculations and photoelectron spectra

Xiaoqing Liang[1], Xiaoming Huang[1], Jijun Zhao[1*], Hongguang Xu[2], Weijun Zheng[2]

[1]*State Key Laboratory of Materials Modification by Laser, Electron, and Ion Beams, Dalian University of Technology, Ministry of Education, Dalian 116024, China*
[2]*Beijing National Laboratory for Molecular Science, State Key Laboratory of Molecular Reaction Dynamics, Institute of Chemistry, Chinese Academy of Sciences, Beijing 100190, China*

Transition metal doped semiconductor clusters (such as silicon and germanium clusters) have been focus of intensive studies during the last decade. Until now, most efforts have devoted to semiconductor clusters doped with single transition metal atom. Combining spin-polarized density functional theory (DFT) and photoelectron spectroscopy, the growth behavior, electronic and magnetic properties of $Fe_2Ge_n^-$ and $Cr_2Ge_n^-$ (n=3-12) clusters have been investigated. A genetic algorithm incorporated with DFT optimization has been employed to globally search the ground state configurations. The theoretical photoelectron spectra are in good agreement with our experimental ones. In the lowest-energy structures, one Fe or Cr atom tends to stay in the interior site from n=8. The local magnetic moments on the two Fe atoms in $Fe_2Ge_n^-$ clusters exhibit ferromagnetic ordering. In contrast, the spin moments on two Cr atoms in Cr_2Ge_n clusters show antiferromagnetism or ferrimagnetism. Interestingly, the magnetic moments of two Fe atoms and Cr atoms do not change sensitively with cluster size.

Geometric, electronic, and magnetic structure of Fe_xO_y clusters

Remko Logemann,[1] Gilles de Wijs,[1] Mikhail Katsnelson[1] and Andrei Kirilyuk[1]

[1] *Institute for Molecules and Materials, Radboud University Nijmegen, Nijmegen, The Netherlands*

Atomic clusters are a promising model system to study the emergence of bulk physical properties at the nanoscale and below. For example for transition metal oxides, the photoelectron spectra of $Fe_xO_y^-$ clusters have been used to model the chemisorption of oxygen on iron [1]. Furthermore the *magic* $Fe_{13}O_8$ was extensively studied as a model system to understand the iron oxide interaction [2]. In addition to these studies, we propose Fe_xO_y as a model system to study the fundamental magnetic interactions. As a starting point, a detailed understanding of the relation between the geometry and electronic structure of these clusters is required.

Here we combine Density Functional Theory (DFT) calculations with infrared vibration spectroscopy data [3] to understand the structural, electronic and magnetic properties of gas-phase $Fe_xO_y^{+/0}$ clusters. First, possible geometric structures were identified using a genetic algorithm. They were further geometrically optimized for all magnetic states using the hybrid B3LYP functional [4]. For the lowest-energy structures the vibration spectra are calculated. For unambiguous identification of the cluster structures these were compared with the experimentally measured resonant dissociation spectra of the cluster-messenger [3].

The magnetic structures of $Fe_xO_y^{+/0}$ clusters contain both pure antiferromagnets as well as ferrimagnets where a magnetic moment is present due to the odd number of Fe atoms. The electronic structure of these clusters is compared with calculations on bulk magnetite. In the latter, both Fe^{2+} and Fe^{3+} atoms are present so that the valence state of Fe in the clusters is also considered and compared to the bulk. It turns out Fe_3O_4, Fe_4O_6 are monovalent, whereas Fe_4O_5 and Fe_5O_7 have mixed valence states. Note that the calculations of the magnetic configurations were done both with the B3LYP functional mentioned above, and with the GGA+U approach [5]. The parameter U was derived by comparing the calculated electronic structures, and happened to be of the same order as for the bulk iron oxides.

References

[1] L.S. Wang, H. Wu, and S.R. Desai, Phys. Rev. Lett. **76**, 4853 (1996)

[2] Q. Wang, Q. Sun, M. Sakurai, J.Z. Yu, B.L. Gu, K. Sumiyama, and Y. Kawazoe, Phys. Rev. B **59**, 12672 (1999)

[3] A. Kirilyuk, A. Fielicke, K. Demyk, G. von Helden, G. Meijer, and Th. Rasing, Phys. Rev. B **82**, 020405(R) (2010)

[4] A.D. Becke, J. Chem. Phys. **98**, 5648 (1993)

[5] A.I. Liechtenstein, V.I. Anisimov, and J. Zaanen, Phys. Rev. B **52**, R5467 (1995).

Redispersibility of Solid State Cysteine-Capped CdSe Nanoparticles Depending on pH Values of These Aqueous Solution

Takuya Kurihara, Yasuto Noda, and K. Takegoshi

Division of Chemistry, Graduate School of Science, Kyoto University, Kyoto, Japan

It is important for studies and applications of nanoparticles (NPs) synthesized in solvents to keep their properties after solidification. In this study, we show that the redispersibility of powder cysteine-capped CdSe NPs (CdSe-Cys) depends on pH values of CdSe-Cys aq. in solidifying, and elucidate the dependency by using solid state NMR.

Powder CdSe-Cys were synthesized by means of a method to be presented elsewhere in the conference by the authors. Then they were redispersed into cysteine aq. with pH 11 and 9 and solidified by adding acetone as antisolvent. Each powder is referred below as CdSe-11 and -9. CdSe-11 showed water redispersibility, while CdSe-9 could not be redispersed well.

Figure 1 shows $^{13}C\{^1H\}$ CP/MAS NMR spectra of CdSe-11 (a) and CdSe-9 (b). The peaks shown in Fig.1(a) are assigned as follows : the peak at 33 ppm is ^{13}C bonding to sulfur, at 54~59 ppm are bonding to amine, and at 181 ppm is of carboxy group. While in Fig.1(b), the peak at 181 ppm is fairly week, and a new peak appears at 174 ppm. Abraham et al. reported a ^{13}C solid state NMR peak of carboxy groups of cysteines forming COO^--NH_3^+ ion complex between ligand- and free-cysteines at 173 ppm[1,2]. The pH 9, adjusted in solidifying CdSe-9, is lower than pKa_{NH2} 10.8 of cysteine, thus many amines become NH_3^+ and they are likely to form ionic bonds with COO^- by solidification. Thus this peak would be assigned as ^{13}C of carboxy group of cysteine forming the same ionic bonds between ligand-cysteines and ligand- and/or free-cysteines. Therefore, the reason why CdSe-9 cannot redisperse should be the formation of ionic bonds between cysteines which disturb hydration.

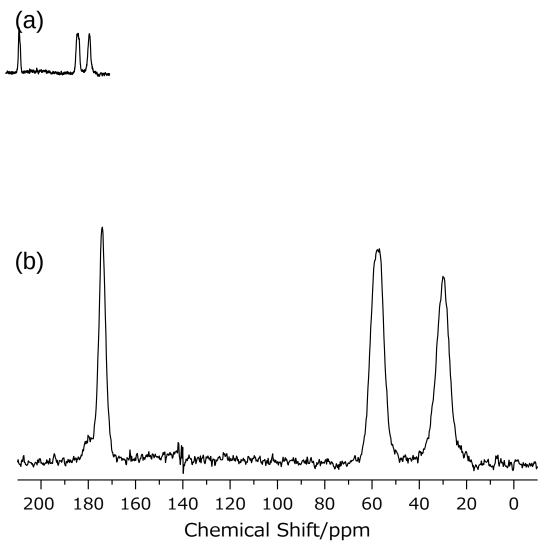

Figure 1 ^{13}C NMR spectra of (a) CdSe-11 and (b) CdSe-9, measured with a 1 ms contact time.

References

[1] A. Abraham et al., J. Phys. Chem. C, 114 (2010), 18109.
[2] A. Abraham et al., J. Phys. Chem. B, 116 (2012), 7771.

This work is supported by JSPS KAKENHI Grant Number 25888009.

Structural Stability in icosahedral Ni-Zr-Nb ternary clusters

Nobuhisa Fujima,[1] Toshiharu Hoshino,[1] and Mikio Fukuhara [2]

[1] *Department of Electronics & Material Science, Shizuoka University, Hamamatsu, Japan*
[2] *New Industry Creation Hatchery Center, Tohoku University, Sendai, Japan*

Interesting electronic transport phenomena, superior (ballistic) conducting and superconducting transport, and electric current-induced voltage (Coulomb) oscillation, have been observed in Ni-Zr-Nb-H amorphous alloys, $((Ni_{0.6}Nb_{0.4})_{1-x}Zr_x)_{100-y}\ H_y$ ($0.3 \leq x \leq 0.5$, $0 \leq y \leq 20$). Local atomic structures (icosahedral clusters and their surroundings) in the alloys play an important role in generation of these phenomena.

We optimize the atomic structures of icosahedral $Ni_4Zr_6Nb_3$ clusters by the first principles calculation, with twenty energetically inequivalent initial atomic positions, where a Ni tetrahedron is includes as a core cluster.[1] Figure 1 shows the total energies of the twenty optimized clusters as a function of Nb-Ni coordination number and two optimized structures with the maximal (1) and minimal (2) energies. We find that all the optimized clusters remain in the (distorted) icosahedral structures as shown in the two examples, and that the total energy almost linearly depends on the Nb-Ni coordination number. These results suggest that the Nb atoms and their clustering isolated from Ni atoms stabilize the icosahedral structure and prevent the local structure from crystallizing to other phases (fcc-like ordered phase etc.).

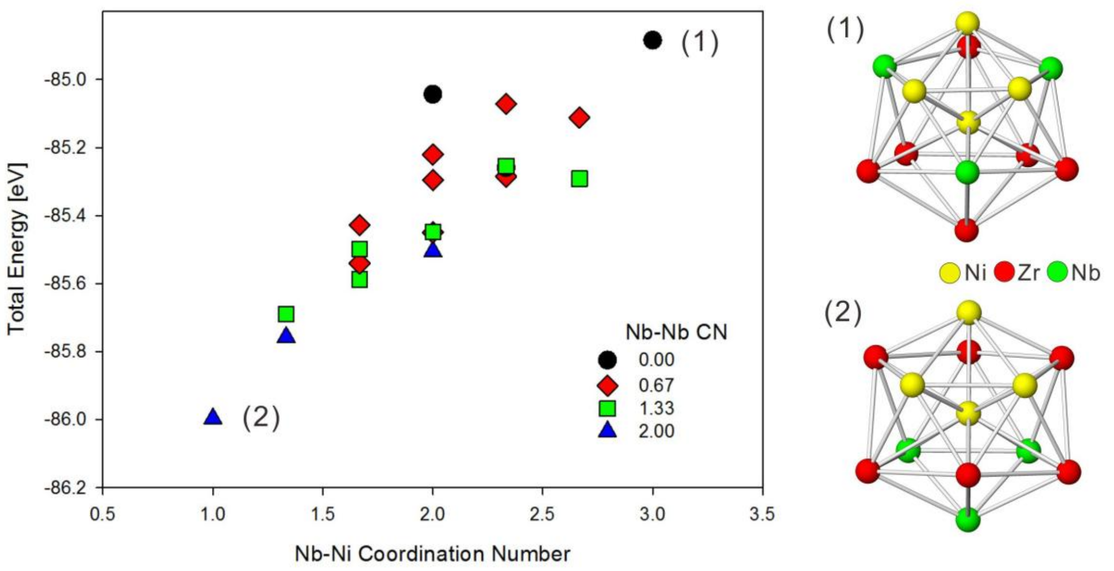

Fig.1 Nb-Ni coordination number dependence in total energy of $Ni_4Zr_6Nb_3$ icosahedral clusters and optimized structures of two clusters (1) and (2).

Reference

[1] N. Fujima, T. Hoshino, and M. Fukuhara, J. Appl. Phys. 114 (2013) 063501.

Synthesis of Porphyrin-face Coordinated Au Clusters and Their Interfacial Interaction

Masanori Sakamoto,[1,2] Daichi Eguchi,[1] and Toshiharu Teranishi[1]

[1] *Institute for Chemical Research, Kyoto University, Japan*
[2] *PRESTO-JST, Japan*

For the organic molecules/Au clusters (AuCs) composites system, interfacial interaction between Au and π-conjugated molecule is an important subject from the viewpoint of scientific interest as well as the application for nanoelectronic devices. In the present research, we synthesized AuC face-coordinated by porphyrin derivatives and investigated their interfacial interactions.

We synthesized porphyrin derivatives contain four acetylthio groups (*i.e.*, binding sites to the AuC) facing the same direction toward the porphyrin ring (SC_nP, n = 0 ~ 2) (Fig.1) [1],[2]. This led to a face-on configuration for the porphyrin on the AuCs through quadridentate coordination. The SC_0P binding sites are directly connected to the *meso*-substituted phenyl groups while SC_1P and SC_2P contain methylene spacers (*i.e.*, distances between the porphyrin ring and the sulfur atoms were ~2.6, ~3.4 and 4.85 Å for SC_0P, SC_1P and SC_2P, respectively). The structure of the porphyrin-coordinated AuC was characterized by atomic resolution high-angle annular dark field scanning transmission electron microscopy, MALDI-TOF-MS, and inductively coupled plasma atomic emission spectroscopy. The interaction between the porphyrin and the AuCs was investigated by UV-vis-NIR and transient absorption (TA) measurements. Interestingly, UV-vis-NIR spectra indicated the strong interfacial interaction between porphyrin and AuC depending on the distance between porphyrin and AuC (Fig.1b). TA measurement revealed the exciplex formation between AuC and porphyrin ring (Fig.1c)[2].

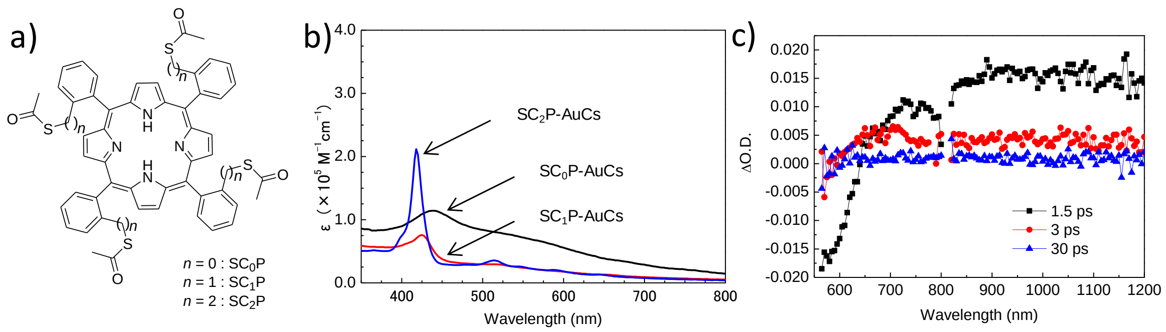

Fig.1 a) structure of porphyrin derivatives ((SC_nP, n = 0 ~ 2)), b) UV-vis-NIR absorption spectra of SC_nP-coodinated AuC, c) TA spectra of SC_0P-coodinated AuC.

References

[1] M. Sakamoto, D. Tanaka, H. Tsunoyama, T. Tsukuda, Y. Minagawa, and Y. Majima, T. Teranishi, J. Am. Chem. Soc. 134 (2012) 816.

[2] D. Tanaka, Y. Inuta, M. Sakamoto, A. Furube, M. Haruta, Y.-G. So, K. Kimoto, I. Hamada, and T. Teranishi, *Chem. Sci.* 5 (2014) 2007.

Origin of Magic Stability for Aluminum-Boron Binary Nanoclusters

Tomomi Nagase,[1] Shoichiro Suga,[1] Hironori Tsunoyama,[1,2] and Atsushi Nakajima[1,2]

[1]*Department of Chemistry, Keio University, Japan*
[2]*Nakajima Designer Nanocluster Assembly Project, JST-ERATO, Japan*

The physical and chemical properties of nanoclusters (NCs), which differ from the bulk, are unique and highly size dependent.[1] Based on extensive experimental and theoretical studies of aluminum (Al) NC anions,[2-7] Al_{13}^- and Al_{23}^- NC anions show superior stability toward etching reaction by molecular oxygen attributable to their closed electronic structures. It has been suggested from electronic structure that doping of boron (B) atoms to Al NC anions enhances the stability of Al-B binary NC anions by replacement of interior Al atoms with smaller B atoms with keeping their total valence electrons.[8] In contrast to extensive studies for small Al and Al-B NCs (smaller than 23-mer), studies for larger magic NCs have been still limited probably because of difficulty in the generation of such NCs by a laser vaporization method, although larger magic numbers have been proposed.[3] In the present study, we have investigated the magic number and composition of Al-B binary NC anions ($Al_nB_m^-$) larger than 23-mer by a magnetron type NC source combined with reaction toward molecular oxygen. We have found that all of NCs with n+m=37 showed the locally maximized stability irrespective of different numbers of B atoms (m=0-6), whereas magic compositions (n/m) appeared for 13- and 23-mer NCs as $Al_{12}B_1^-$ and $Al_{21}B_2^-$. The result suggests that the origin of stability changes from concerted electronic-geometric factors for 13 and 23-mer to the electronic shell closing for 37-mer.

Al-B binary NCs were generated by magnetron sputtering-gas condensation apparatus.[9] At downstream of the NC source, NC ions were reacted with oxygen molecules (O_2) introduced as effusive beam perpendicular to the NC beam. The reactivity of individual NCs was analyzed by quantitative comparison of mass spectra before and after the O_2 exposure; the reaction with O_2 decreased the intensity of NC ions without the formation of oxygen adducts, Al_nO^- and $Al_nO_2^-$.

The series of $Al_nB_m^-$ [(n,m), 5<n<50, m = 0–6] binary NC anions were observed as smooth distribution without prominent magic numbers at n+m=13 and 23 in the mass spectrum without the O_2 introduction. After the reaction with O_2, a series of NC ions with total atoms of 37, (37–m, m) (m=0–6), along with known magic NCs of n+m=13 and 23 were prominently observed. For 13- and 23-mer NCs, the reactivity dramatically increases from (12,1) to (11,2) and (21,2) to (20,3), respectively. In contrast, the intensities of (32,5) and (31,6) were relatively strongly observed than the other neighboring ions, although these ions were overlapped with (34,0) and (33,1) in the mass spectrum, respectively. Note that (34,0) and (33,1) were not strongly observed without the overlapped formation of (n, m)=(32,5) and (31,6) NCs. A spherical harmonic potential[3] predicts electronic stability for 13-, 23-, and 37-mer owing to the electronic shell closing. Therefore, we conclude that the stability of 37-mer results mainly from the electron shell closing, whereas the stabilities of 13- and 23-mer are attributed to both of electronic and geometric factors. In other words, the origin of the stability changes from 23 to 37 atoms; concerted electronic-geometric factors dominates the stability below 23-mer, whereas the electronic factor becomes predominant above 37-mer.

References

[1] R. L. Johnston, "*Atomic & Molecular Clusters*". [2] R.E. Leuchtner *et al.,* J. Chem. Phys. 91 (1989) 2753. [3] X. Li *et al*., Phys. Rev. Lett. 81 (1998) 1909. [4] A. Nakajima *et al.*, Chem. Phys. Lett. 187 (1991) 239. [5] L. Ma *et al.*, J. Chem. Phys. 132 (2010) 104303. [6] T. Iwasa *et al.*, Chem. Phys. Lett. 582 (2013) 100. [7] T. Watanabe *et al.*, J. Chem. Phys. 117 (2013) 6664. [8] H. Kawamata *et al.*, Chem. Phys. Lett. 337 (2001) 255. [9] H. Tsunoyama *et al.*, Chem. Lett. 42 (2013) 857.

Geometrical structures of vanadium oxide cluster ions studied by ion mobility mass spectrometry

Ryoichi Moriyama, Jenna W. J. Wu, Hiroshi Tahara, Keijiro Ohshimo, and Fuminori Misaizu

Department of Chemistry, Graduate School of Science, Tohoku University, 6-3 Aoba, Aramaki, Aoba-ku, Sendai 980-8578, Japan

Neutral and ion structures of vanadium oxide clusters $V_mO_n^{+/0/-}$ have been taken much interest as microscopic models of bulk V_2O_5 catalyst surface. For neutral $(V_2O_5)_{m/2}$ clusters up to m = 24, polyhedron structures were suggested by DFT calculations [1]. The vibrational spectra and photodissociation reactions of small sized cluster ions (m < 10) were also measured, and the results were compared with theoretical predictions [2]. In the present study, collision cross sections (CCSs) of the vanadium oxide cluster ions were measured by ion mobility mass spectrometry. By comparing the experimental CCSs with theoretical ones, geometrical structures were determined.

$V_mO_n^{+/-}$ ions were injected into a drift cell with a pulsed electric field, after generation by laser vaporization with 5 % O_2-mixed He gas in supersonic expansion. In the drift cell, ions collided with He buffer gas under an electrostatic field and reached a constant drift velocity, which depends on the CCS of the ions with He. Experimental CCSs of the ions could be estimated from the time that ions spent in the cell. Theoretical CCSs were independently calculated using the projection approximation method in MOBCAL program, for the structures optimized by B3LYP/6-311+G(d) level.

Most abundant cluster ions were dependent on parity of the number of vanadium atoms m; $(V_2O_5)_{m/2}^+$ for even m and $(VO_2)(V_2O_5)_{(m-1)/2}^+$ for odd m [3]. CCSs of these ions up to m = 60 were measured as shown in Fig.1. Experimental CCSs increase uniformly with cluster size, which follows a rule for three dimensional cluster growth, CCS $\propto$ (mass number)$^{2/3}$. The trend of the calculated CCSs of prism structures for even m up to m = 10 agreed well with experimental data. For odd sized ions (m = 7 and 9), quasi-prism structures were in good agreement with experiment. These quasi-prism structures have one tricoordinated oxygen atom which can also be found in bulk V_2O_5 crystals.

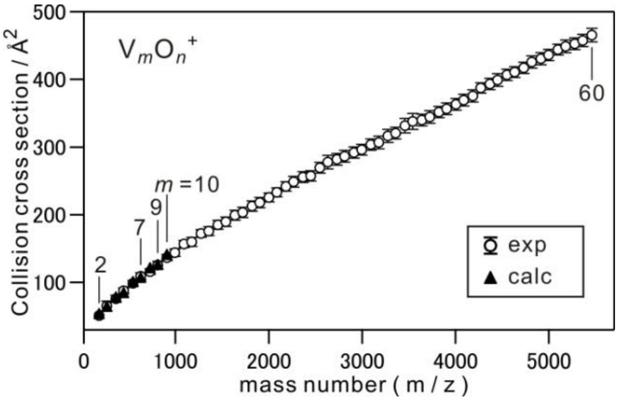

Fig.1 Experimental (m = 2-60) and theoretical (m = 2-10) CCSs of $V_mO_n^+$.

References

[1] S. F. Vyboishchikov, and J. Sauer, J. Phys. Chem. A 105 (2001) 8588.

[2] G. Satambrogio, M. Brümmer, L. Wöste, J. Döbler, M. Sierka, J. Sauer, G. Meijer, and K. R. Asmis, Phys. Chem. Chem. Phys 10 (2008) 3992.

[3] J. W. J. Wu et al., ISSPICXVII. Poster.

Synthesis of stable gold clusters face-coordinated by porphyrin derivatives containing disulfide groups

Daichi Eguchi,[1] Masanori Sakamoto,[1,2] and Toshiharu Teranishi[1]

[1] *Institute for Chemical Research, Kyoto University, Uji, Japan*
[2] *JST-PRESTO, Japan*

Stability of gold clusters (AuCs) is an important aspect for applications, such as catalysis, biosensors, and nanoelectronics. Our groups have recently synthesized the porphyrin face-coordinated AuCs [1,2]. However, the instability of porphyrin face-coordinated AuCs has been an obstacle for applications. In this study, we have synthesized quite stable AuCs coordinated by porphyrin derivatives with disulfide groups and investigated their properties as well as stability.

We synthesized the porphyrin derivative: 5α,10α-bis(2-ethylthiophenyl)-15α,20α-bis (2'-ehylthiophenyl)porphyrinatozinc (Ⅱ) ($ZnSC_2P$-SS, Fig 1). The $ZnSC_2P$-SS contains two disulfide groups facing in the same direction to the porphyrin ring, which bind to the AuCs in a face-coordination fashion. The AuCs coordinated by the $ZnSC_2P$-SS ($ZnSC_2P$-SS-AuCs) were synthesized by the reduction of the Au(Ⅲ) ions in the presence of $ZnSC_2P$-SS. The purification of the obtained $ZnSC_2P$-SS-AuCs was performed by gel permeation chromatography.

The size of the $ZnSC_2P$-SS-AuCs were measured by TEM. $ZnSC_2P$-SS-AuCs have the size of 1.5 ±0.1 nm (Fig. 2), and are thought to possess the platonic hexahedral structure, as shown in Fig. 3 [1]. This result agrees well with the AuCs coordinated by the porphyrin with acetylthio groups, reported in the previous work [1]. $ZnSC_2P$-SS-AuCs showed higher stability than the previous ones in ambient conditions. Furthermore, we will report the electronic, optical, catalytic properties of $ZnSC_2P$-SS-AuCs.

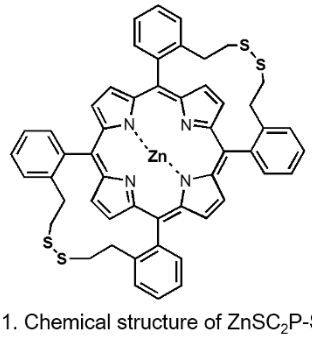

Figure 1. Chemical structure of $ZnSC_2P$-SS.

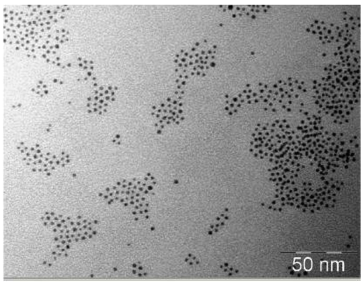

Figure 2. TEM image of $ZnSC_2P$-SS-AuCs.

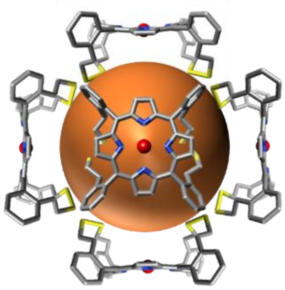

Figure 3. The schematic structure of AuCs coordinated by $ZnSC_2P$-SS.

References

[1] M. Sakamoto, D. Tanaka, H. Tsunoyama, T. Tsukuda, Y. Majima, and T. Teranishi, J. Am. Chem. Soc. vol 134 (2012) 816.

[2] D. Tanaka, Y. Inuta, M. Sakamoto, A. Furube, M. Haruta, Y.-G. So, K. Kimoto, I. Hamada, and T. Teranishi, Chem. Sci. vol 5 (2014) 2007.

Observation of halogen adsorbates on magic numbered gold clusters stabilized by polyvinylpyrrolidone

Setsuka Arii,[1] Satoru Muramatsu,[1] Seiji Yamazoe,[1, 2] Kiichirou Koyasu,[1, 2] and Tatsuya Tsukuda[1, 2]

[1] *Department of Chemistry, School of Science, The University of Tokyo, Tokyo, Japan*
[2] *ESICB, Kyoto University, Kyoto, Japan*

Small (< 3 nm) gold clusters stabilized by polyvinylpyrrolidone (Au:PVP) show size-specific catalysis for aerobic oxidation of alcohols [1]. In contrast to the generally accepted model that bare Au clusters were stabilized by PVP, we observed for the first time a series of halogen adsorbates on Au clusters by MALDI mass spectrometry. We also found that these halides affect the electronic structures and catalysis of Au:PVP.

Au:PVP(X) (X = Cl, Br) with the average diameter of around 1 nm were synthesized by reduction of AuX_4^- in the presence of PVP and deionized by ultrafiltation as previously reported [2]. MALDI mass spectra of Au:PVP(X) were recorded under minimal laser power to suppress laser-induced fragmentation. Halogenated gold clusters $Au_nX_m^-$(X = Cl, Br) with n = 24, 34, 43 were observed as highly abundant species regardless of the halogen (Fig. 1). Interestingly, the numbers of Br adsorbed were larger than those of Cl (Fig. 2).

The effect of halogen adsorbates on the electronic structures of the Au clusters was examined by XPS and XANES. It was demonstrated that Au clusters in Au:PVP(Br) were more negatively charged than those in Au:PVP(Cl). Nevertheless, Au:PVP(Br) showed poorer catalytic activity for alcohol oxidation than Au:PVP(Cl). This result suggests that adsorbed halogens retard the catalysis of Au clusters by steric constraint.

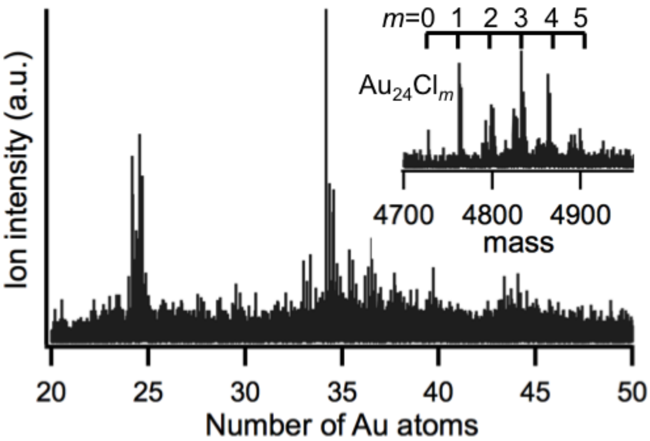

Fig.1 Typical MALDI mass spectra o Au:PVP(Cl)

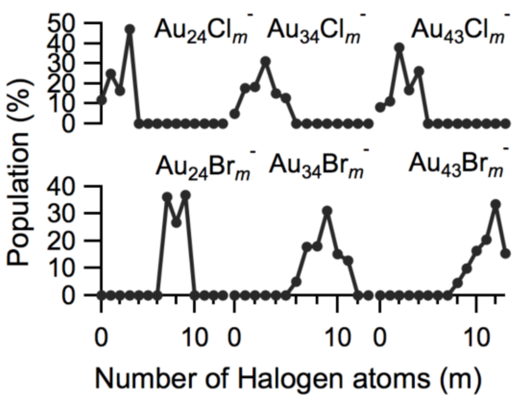

Fig.2 Distribution of number of adsorbed halogen atoms

References

[1] H. Tsunoyama, H. Sakurai, and T. Tsukuda, Chem. Phys. Lett. 429 (2006) 528.

[2] H. Tsunoyama, H. Sakurai, Y. Negishi, and T. Tsukuda, J. Am. Chem. Soc. 127 (2005) 9734.

Secondary ion emission from micro droplets induced by fast ion impacts

Takuya Majima,[1] Tatsuya Nishio,[2] Kensei Kitajima,[2] Yoshiki Oonishi,[2]
Hiroki Ueda,[2] Hidetsugu Tsuchida,[1] and Akio Itoh[1,2]

[1] *Quantum Science and Engineering Center, Kyoto University, Kyoto, Japan*
[2] *Department of Nuclear Engineering, Kyoto University, Kyoto, Japan*

To investigate radiation-induced molecular processes in liquids, we have developed a new experimental system for analyzing secondary ions emitted from micro droplets in MeV-energy ion collisions. Conventional experiments of swift ion interaction with liquid targets were performed under atmospheric pressure because of high vapor pressure of liquid targets. Accordingly, analyzing methods of reaction products is limited to spectroscopic or chemical studies. In this work, we performed fast ion irradiation of liquid droplets in vacuum by employing a droplet beam technique [1]. This allows us to apply mass spectrometric techniques for product ions emitted from droplet surfaces in fast ion impacts.

The experiment was performed at a 2MV tandem type Pelletron accelerator at Quantum Science Engineering Center, Kyoto University. Micro droplets of water and ethanol were injected into a vacuum chamber and crossed with 0.7–2.0 MeV H^+ and 2.0 MeV C^{2+} ion beams from the accelerator. The droplet diameter was estimated to be a range of few μm by analyzing energy loss distributions of H^+ ions after penetrating through the droplets. Positive and negative secondary ions from the droplets in collisions with 2.0 MeV C^{2+} ions were analyzed by a time-of-flight mass spectrometer. Figure 1 shows an example of mass spectra of negative secondary ions from water droplets, exhibiting emission of cluster ions $(H_2O)_nOH^-$ up to about n ~ 15.

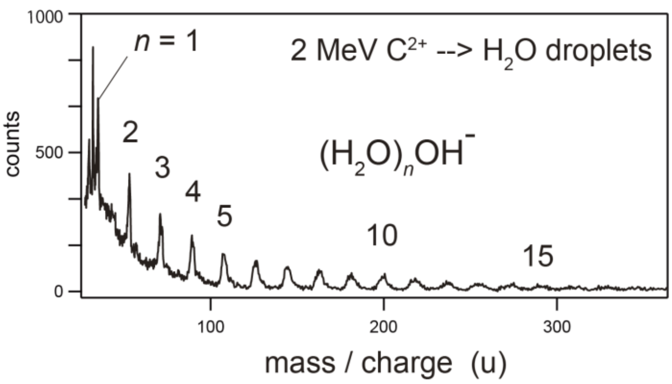

Figure 1. Mass spectrum of negative secondary ions from water droplets induced by 2.0 MeV C^{2+}.

We gratefully acknowledge Dr. J. Kohno for his advice on the liquid droplet technique. One of the authors (T.M.) would like to acknowledge the support of Toyota Physical & Chemical Research Institute Scholars.

Reference

[1] J. Kohno, N. Toyama, T. Kondow, Chem. Phys. Lett. 420 (2006) 146.

Drift time measurements of H_3O^+ hydrate formed by NO^+ injection into drift tube filled with H_2O/buffer gas at low temperatures

Hiroshi Hidaka,[1] Yoichi Nakai,[2] Takao M. Kojima[3], and Naoki Watanabe[1]

[1] *Institute of Low Temperature Science, Hokkaido University, Sapporo 060-0819, Japan*
[2] *RIKEN Nishina Center for Accelerator-Based Science, Wako, Saitama 351-1098, Japan*
[3] *Atomic Physics Laboratory, RIKEN, Wako, Saitama 351-0198, Japan*

H_3O^+ hydrate, $H_3O^+(H_2O)_n$, is known to exist in the terrestrial ionosphere in quantities. As one of the important formation-pathways, $H_3O^+(H_2O)_n$ formation via $NO^+(H_2O)_m$:

$$NO^+(H_2O)_m + H_2O \rightarrow H_3O^+(H_2O)_{m-1} + HONO \ (m=3,4),$$

has been often proposed and indeed studied in flow-tube experiments[1,2]. However, in those experiments, the parent NO^+ ions were produced by conventional electron impact method and thus contained the metastable NO^+. Since the ionization energy to the lowest metastable state of $NO^+(a^3\Sigma^+)$ is 15.66eV[3], H_2O in the ground state having the ionization energy of 12.65 eV can be ionized by the charge exchange with the metastable NO^+ ions. If the charge-exchange reaction occurs, the new formation pathway of $H_3O^+(H_2O)_n$ may open as follows:

$$H_2O + NO^+(a^3\Sigma^+) \rightarrow H_2O^+ + NO,$$

$$H_2O^+ + H_2O \rightarrow H_3O^+ + OH,$$

$$H_3O^+ + H_2O + M \rightarrow H_3O^+(H_2O) + M,$$

$$H_3O^+(H_2O)_{n-1} + H_2O + M \rightarrow H_3O^+(H_2O)_n + M.$$

The above processes are not appropriate in atmospheric environments. Therefore, in order to study the formation pathway of $H_3O^+(H_2O)_n$ via $NO^+(H_2O)_m$ alone, the formation of $H_3O^+(H_2O)_n$ through the charge-exchange reaction must be separated in the experiment.

Using a newly-developed ion drift-tube with selected-ion injection, we tried to separate the contribution of metastable NO^+ on the $H_3O^+(H_2O)_n$ formation. In our experiment, the NO^+ beam including the metastable NO^+ was injected in the H_2O-filled drift-tube and the products of $H_3O^+(H_2O)_n$ were analyzed in the back of the tube. The drift time for the products in the tube provides the information of products' origins. That is, when measuring the drift-time spectrum of $H_3O^+(H_2O)_n$, the spectrum consists of two peaks depending on the different origins, $NO^+(H_2O)_m$ or H_2O^+ from the metastable NO^+.

Reference(s)

[1] N. Eyet, et al., J. Phys. Chem. A 115 (2011) 7582.
[2] F. C. Fehsenfeld et al., J. Chem. Phys. 55 (1971) 2120.
[3] D. L. Albritton, et al., J. Chem. Phys. 71 (1979) 3271.

Solid-state absorption properties and crystal structures of di-alkynylated octanuclear gold clusters

Mizuho Sugiuchi,[1] Naoki Kobayashi,[1] Yukatsu Shichibu,[1,2] and Katsuaki Konishi[1,2]

[1] *Graduate School of Environmental Science, Hokkaido University, Sapporo, Japan*
[2] *Faculty of Environmental Earth Science, Hokkaido University, Sapporo, Japan*

In contrast to conventional monophosphine-ligated gold clusters showing similar optical profiles with each other,[1] we found that diphosphine-ligated gold clusters showed unique prolate geometries and unusual absorptions.[2-4] Among them, octanuclear clusters had some interesting properties such as redox-activated core-shape transformation involving photoluminescence change and selective emission turn-off against Hg (II).[4] Furthermore, di-alkynylations of one of the octanuclear clusters and protonation-responsive chromisms of the pyridylethynyl-substituted clusters in solution were demonstrated.[5] In this work, we synthesized a series of di-alkynylated Au_8 clusters (**2 - 4**). In addition, we examined absorption properties in solid state and crystal structures of the clusters to open new opportunities for solid-state material.

In a typical reaction, a methanol solution of **1**·$(NO_3)_2$ was treated with any one of alkynes in the presence of sodium methoxide and the mixture was stirred for several days (Fig.1). Di-alkynylations of Au_8 clusters (**2 - 4**) after purification were confirmed by electrospray ionization (ESI) mass spectrometry. While broadening of absorptions of **2 - 4** in solid states was observed, overall absorption profiles in liquid states were retained (Fig.2). Though alkynyl groups were found to be situated at *trans* orientation on di-edge-bridged bi-tetrahedral Au_8 structures of **2 - 4** (Fig.1 top left), crystal structure of **2** only showed high symmetry (rhombohedral system) and a honeycomb-like arrangement. Moreover, the unique crystal structure had large solvent accessible void.

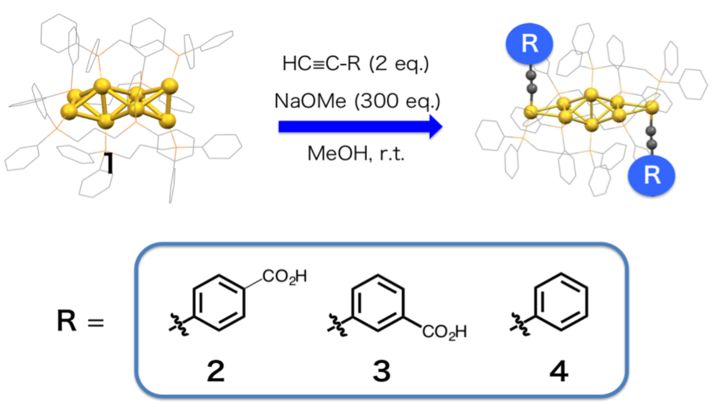

Figure 1. Syntheses of Au_8 clusters (**2 - 4**).

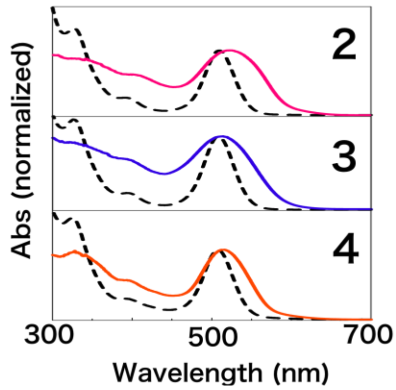

Figure 2. Diffuse reflectance (solid lines) and absorption (dotted lines) spectra of **2 - 4**.

References

[1] K. P. Hall, D. M. P. Mingos, *Prog. Inorg. Chem.* 32 (1984) 237. [2] Y. Shichibu, K. Konishi, *Inorg. Chem.* 52 (2013) 6570. [3] Y. Shichibu, Y. Kamei, K. Konishi, *Chem. Commun.* 48 (2012) 7559. [4] Y. Kamei, Y. Shichibu, K. Konishi, *Angew. Chem. Int. Ed.* 50 (2011) 7442. [5] N. Kobayashi, Y. Kamei, Y. Shichibu, K. Konishi, *J. Am. Chem. Soc.* 135 (2013) 16078.

Helium droplets doped with sulfur and C_{60}

Martina Harnisch,[1] Nikolaus Weinberger,[1] Stephan Denifl,[1] Paul Scheier,[1] Olof Echt[1,2]

[1] *Institut für Ionenphysik und Angewandte Physik, University of Innsbruck, Austria*
[2] *Department of Physics, University of New Hampshire, USA*

Sulfur is the element with the largest number of solid allotropes [1]. S_n molecules containing as many as 10 atoms in various isomeric shapes have been identified in the vapor phase. The ring-shaped S_8 is the dominant species at low temperature but this is not apparent from cationic mass spectra because of strong electron-induced fragmentation.

Fig. 1 displays the relative yield of positively and negatively charged sulfur- and sulfur-C_{60} clusters formed by electron ionization of doped helium droplets. In the absence of C_{60} the most abundant cations (Fig. 1a) have the stoichiometry $(S_8)_m^+$ (integer *m*). Martin [2] has reported a similar pattern but the preference for $(S_8)_m^+$ ions was much less pronounced. The anion spectrum (Fig. 1b), on the other hand, shows strong local minima in the yield for ions of the form $(S_8)_mS^-$. These minima reflect the virtual absence of atomic sulfur in the equilibrium vapor [1]. Conversely, the fact that $(S_8)_m^-$ ions are not as prominent as $(S_8)_m^+$ suggests that electron attachment results in dissociation, too. Indeed, the chain-like structures of S_n^- anions differ strongly from those of neutral S_n which tend to form rings [3].

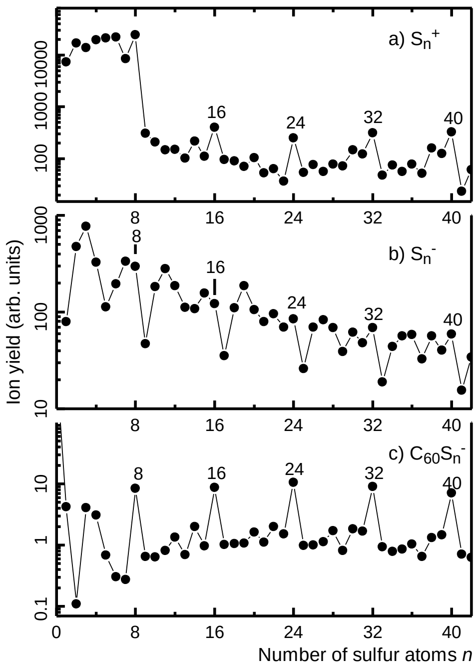

Sulfur-doped microporous carbon materials show promise for energy related applications such as fuel cells, batteries, and hydrogen storage [4]. Fig. 1c displays a negative-ion mass spectrum of helium droplets doped with sulfur and C_{60} (cationic C_{60}-sulfur clusters have already been investigated by Martin and coworkers [5]). A strong preference for ions of the form $C_{60}(S_8)_m^-$ is found; ions of other stoichiometries occur at less than 10 %. Similar distributions are obtained for anions that contain two or more C_{60} molecules.

References

[1] R. Steudel (ed.), *Topics in Current Chemistry* vol. 230 (Springer, 2003).

[2] T. P. Martin, J. Chem. Phys. 81 (1984) 4426.

[3] M. D. Chen, M. L. Liu, L. S. Zheng, Q. E. Zhang, C. T. Au, Chem. Phys. Lett. 350 (2001) 119.

[4] G. M. Zhou, L. C. Yin, D. W. Wang, L. Li, S. F. Pei, I. R. Gentle, F. Li, and H. M. Cheng, ACS Nano 7 (2013) 5367.

[5] F. Tast, N.Malinowski, M. Heinebrodt, I.M.L.Billas, T.P.Martin, J.Chem.Phys. 106 (1997) 9372.

Size- and Isomer-Dependent Reactivity of Nickel Oxide Cluster Ions Studied by Ion Mobility Mass Spectrometry

Keijiro Ohshimo, Shohei Azuma, Tatsuya Komukai, Ryoichi Moriyama, and Fuminori Misaizu

Department of Chemistry, Graduate School of Science, Tohoku University, 6-3 Aoba, Aramaki, Aoba-ku, Sendai 980-8578, Japan

Nickel oxide compounds are widely used as catalysts of valuable reactions such as oxidation of carbon monoxide (CO) [1]. It was recently reported that CO adsorption reactivity on nickel oxide cluster ions is dependent sensitively on the cluster size, for example, the adsorption hardly occurs on $Ni_7O_6^+$ [2]. In this study, we have investigated the structures and reactivities of nickel oxide cluster ions by ion mobility mass spectrometry (IM-MS).

Nickel oxide cluster ions were injected into an ion-drift cell by a pulsed electric field at a given time ($t = t_0$). The cell was filled with He buffer gas with a pressure of 0.80 Torr. After running through the cell, the ions were injected into a time-of-flight mass spectrometer by another pulsed electric fields at a given time later from the first pulse, $t = t_0 + \Delta t$ (Δt : arrival time). We have obtained a collision cross section of an ion from its arrival time distribution (ATD), using kinetic theory of ion transport. We have also observed reactions between the cluster ions with CO by adding 0.5-5 % CO gas to He in the cell.

Figure 1 shows the ATDs of $Ni_nO_{n-1}^+$ (n = 5-9) cluster ions. Observed bands of ATDs gradually shifted to longer arrival time with increasing cluster size. For $Ni_6O_5^+$ and $Ni_7O_6^+$, two Gaussian functions were necessary for the fittings of the ATDs. Thus there are at least two isomers with different collision cross sections for $Ni_6O_5^+$ and $Ni_7O_6^+$ in the present experimental condition. By comparison with our previous IM-MS studies of transition metal oxide clusters [3], these two isomers are assignable to two-dimensional and three-dimensional structures. We will also discuss the rate constants of CO adsorption and subsequent reactions on nickel oxide cluster ions.

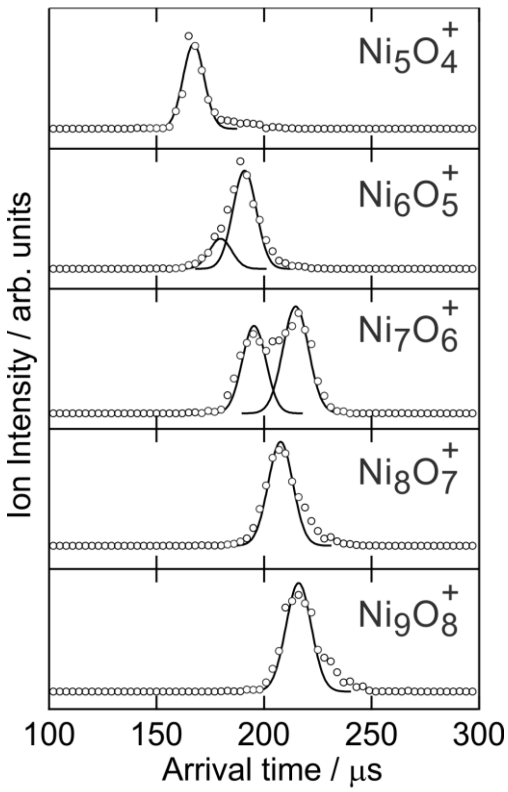

Figure 1. Arrival time distributions of $Ni_nO_{n-1}^+$ cluster ions for n = 5-9. Open circles are the observed ion intensities, and the Gaussian curves show components of isomers.

Reference(s)

[1] P. Konova et al. Chem. Eng. J. 122 (2006) 41.
[2] F. Mafuné et al. J. Phys. Chem. A 117 (2013) 3260.
[3] F. Misaizu et al., Chem. Phys. Lett. 588 (2013) 63; J. Phys. Chem. A, in press.

Protected but Accessible: Oxygen Activation by Calixarene-stabilized Undecagold Cluster

Xi Chen,[1] Hannu Häkkinen[1,2],

[1] *Department of Chemistry, University of Jyväskylä, Jyväskylä, Finland*
[2] *Department of Physics, University of Jyväskylä, Jyväskylä, Finland*

This work was motivated by a recent experiment [1] and presents computational evidence of a novel way to stabilize gold nanoclusters with porous ligand layer facilitating access of small reactant molecules to active metal sites [2]. We have validated that calixarenes can form a protective but porous ligand layer on the surface of a sub-nanometer Au_{11} cluster, while maintaining accessibility to metal sites of the core. Three out of 11 Au atoms (27%) remain accessible to small reactant molecules, and it was shown here that binding and activation of up to three dioxygen molecules per cluster can take place. In fact the calixarene-stabilized Au_{11} cluster discussed here works in a similar way as part of an enzyme protecting the active reaction center from reaction inhibitors but allowing for small molecules to access the reactive metal sites. Our computational results provide strong support for the experiment and predict that this class of stable hybrid metal-organic nanomaterial should be very interesting for catalyzing aerobic oxidations at ambient conditions.

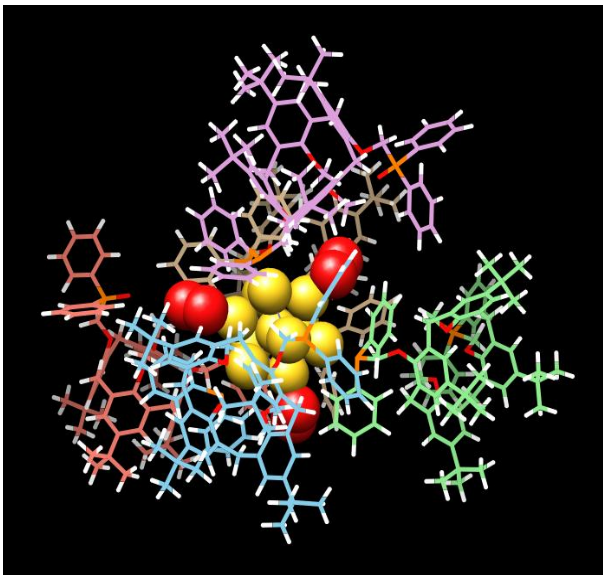

Figure 1: The structure of $Au_{11}L_5(O_2)_3$

Reference(s)

[1] de Silva, N.; Ha, J.-M.; Solovyov, A; Nigra, M. M; Ogino, I.; Yeh, S. W.; Durkin K. A.; Katz, A. Nature Chem. **2010**, 2, 1062.

[2] Chen, X.; Häkkinen, H. J. Am. Chem. Soc. **2013**, 135, 12944.

The origin of the high selectivity and catalytic activity of small ruthenium clusters in the methanation of CO

Sandra M. Lang,[1] Thorsten M. Bernhardt,[2] Marjan Krstić,[2] and Vlasta Bonačić-Koutecký[2,3]

[1] *Institute of Surface Chemistry and Catalysis, University of Ulm, Germany*
[2] *Interdisciplinary Center for Advanced Science and Technology, University of Split, Croatia*
[3] *Department of Chemistry, Humboldt-University Berlin, Germany*

The low temperature polymer electrolyte fuel cell (PEFC) has gained increasing importance for the generation of electrical energy in transportation and decentralized small scale appliances. However, the typically employed hydrogen feed gas usually contains small amounts of CO which can lead to poisoning of the catalyst in the PEFC. One promising approach for CO removal is the catalytic reaction with hydrogen (methanation). At the same time the reaction of CO_2 (also present in the feed gas) with H_2 should be avoided to prevent excessive hydrogen loss. For such *selective* CO methanation very small (< 1 nm) zeolite supported ruthenium particle catalysts have been shown to be very promising materials [1]. However, the origin of the activity and particular selectivity of sub-nanometer ruthenium particles for fuel cell feed gas purification remains an open question.

Toward this goal we employed gas phase ruthenium clusters Ru_n^+ (n = 2 – 6) as model systems and investigated their reactive properties toward molecules contained in typical fuel cell feed gases in an ion trap experiment and via first-principles density functional theory calculations. Three fundamental properties of these clusters are identified which determine the selectivity and catalytic activity [2,3]: (i) high reactivity toward CO in contrast to inertness in the reaction with CO_2; (ii) promotion of cooperatively enhanced H_2 coadsorption and dissociation on pre-formed ruthenium carbonyl clusters, i.e. no CO poisoning occurs; and (iii) the presence of low coordinated Ru-atom sites, which are particularly active for H_2 coadsorption and activation. Furthermore, the theoretical investigations provide mechanistic insight into the CO methanation reaction and discover a reaction route involving the formation of a formyl-type intermediate.

These insights from gas phase studies are for the first time directly compared to results obtained from experimental studies on zeolite supported (sub-)nanometer size ruthenium particle catalysts which have been performed in the group of R. J. Behm (Institute of surface chemistry and catalysis, Ulm University). This comparison shows that free clusters cannot only serve as model systems for mechanistic studies but can also open new routes for the rational design of catalytic materials consisting of intrazeolite anchored small Ru clusters.

References

[1] S. Eckle, M. Augustin, H.-G. Anfang, R. J. Behm, Catal. Today **181** (2012) 40
[2] S. M. Lang, U. Förtig, T. M. Bernhardt, M. Krstić, V. Bonačić-Koutecký, J. Phys. Chem. A (2014) **DOI:** 10.1021/jp501242c
[3] S. M. Lang, T. M. Bernhardt, M. Krstić, V. Bonačić-Koutecký, Angew. Chem. Int. Ed. 53 (2014) 5467

Low-temperature catalytic activity of CO oxidation driven by strong electronic interaction between Pt-Ag bi-element cluster and Si surface

Hisato Yasumatsu[1] and Nobuyuki Fukui[2]

[1] *Cluster Research Laboratory, Toyota Technological Institute,*
In [2] East Tokyo Laboratory, Genesis Research Institute, Inc., Chiba, Japan

We present experimental evidence that low-temperature catalytic activity is derived from strong electronic interaction between a Pt cluster and a Si surface. Temperature-programmed desorption (TPD) measurements [1] in the thermal CO oxidation were repeated for a given cluster sample, Pt_N or Pt_NAg_1 (N=30, 60) [2] bonded to the (111) surface of a Si substrate [3], with systematic change of the reactant amounts adsorbed as shown in Figure 1. The peaks observed in the TPD spectra were deconvoluted so as to obtain probabilities of individual reactions [4]. It was found that this system reveals low-temperature reductive activation of oxygen molecules, which is one of the critical steps in the CO oxidation. Furthermore, doping of only a single Ag atom to the cluster as an electron donor improves this activity.

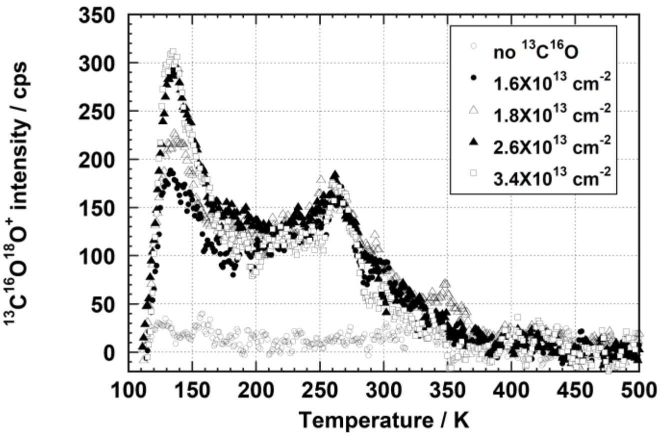

Figure 1. TPD spectra of $^{13}C^{16}O^{18}O$ produced in thermal oxidation of $^{13}C^{16}O$ by $^{18}O_2$ catalyzed on Pt_{30} disks bonded to a Si substrate at the various adsorption amounts of $^{13}C^{16}O$ at the constant $^{18}O_2$ one of 8.5×10^{-11} cm^{-2}.

These high performances are explained in terms of the efficient electron donation to O_2 due to negative charges accumulated at a sub-nano interface between the cluster disk and the silicon substrate surface as a result of strong electronic interaction of them [5]. Namely, clusters promoted by an appropriate environment are expected to become functional materials with a higher performance than conventional bulk and nano materials. The results of this research accelerate approaches to the next step of mass synthesis of functional cluster materials.

References

[1] H. Yasumatsu and N. Fukui, J. Phys. Conf. Ser. 438 (2013) 012004.
[2] H. Yasumatsu, Euro. Phys. J. D 63 (2011) 195.
[3] H. Yasumatsu, T. Hayakawa, S. Koizumi and T. Kondow, J. Chem. Phys. 123 (2005) 124709.
[4] H. Yasumatsu and N. Fukui, submitted to Phys. Chem. Chem. Phys. (2014).
[5] H. Yasumatsu, T. Hayakawa, S. Koizumi and T. Kondow, Chem. Phys. Lett. 487 (2010) 279.

Dynamics of truly monodisperse cluster catalysts under the STM

Y. Fukamori, F. Knoller, M. König, F. Esch, U. Heiz.

Chemie Department, Technische Universität München, Lichtenbergstr. 4, Garching, Germany

In our laboratory, we aim at uncovering the size-specific chemistry of supported clusters for the application in catalysis. By preparing supported clusters with the highest level of control possible, in terms of deposition, substrate and clusters adsorption site, a local probe characterization of isomer structures and single cluster reactivity can be realized, which will be further compared with integral reactivity studies.

In this work, we present an STM ripening study of Pd clusters, produced by our size-selected cluster source (laser ablation and quadrupole mass-selection). The size-selected clusters are soft-landed on highly ordered epitaxial films of graphene and hexagonal boron nitride on Ru(0001) and Rh(111). Moiré moieties formed on such films have been shown to be good candidates for the stabilization of clusters [1].

Our ripening studies show that on substrates with a low cluster-support interaction (e.g. Pd on graphene/Rh(111)) the cluster ripen by a Smoluchowsky type mechanism, whereas on substrates with a higher interaction (e.g. Pd on h-BN/(Rh(111)) Ostwald ripening is the predominant mechanism[2].

In order to get a more defined insight on the processes that lead to the ripening and to quantify the cluster-support interaction, an Atom Tracking device has been implemented and first results are shown.

References

[1] B. Wang, B. Yoon, M. König, Y. Fukamori, F. Esch, U. Heiz, U. Landman, Nano Lett. 12 (2012) 5907-5912.

[2] Y. Fukamori, M. König, B. Yoon, B. Wang, F. Esch, U. Heiz, U. Landman, ChemCatChem 3 (2013) 3330-3341.

Effects of Ir addition on gas-phase and supported Au nanoclusters towards catalytic CO oxidation

Laura Michelle Jiménez-Díaz,[1] and Luis Antonio Pérez[1]

[1] *Instituto de Física, Universidad Nacional Autónoma de México, Apdo. Postal 20-364, Mexico D.F. 01000, Mexico*

Recent studies show that the addition of iridium to Au/TiO_2 catalysts, stabilize them against sintering and improves their catalytic activity for CO oxidation [1]. Furthermore, it has been found that Ir-Au/rutile catalysts have small iridium particles containing gold and having dimensions of the order of 1 nm and, probably, these nanoparticles are responsible for the enhancement of the activity of these catalysts for the CO oxidation [2]. In order to study this phenomenon, we performed density functional calculations of the O_2 adsorption on small bimetallic Au-Ir nanoclusters, with sizes ranging from 4 to 6 atoms, both in gas-phase and supported on TiO_2. Moreover, we also comparatively studied the O_2 dissociation in these systems by using the nudged elastic band method. The results suggest that the addition of Ir to Au clusters can enhance their catalytic activity towards CO oxidation.

This work was supported by PAPIIT-DGAPA-UNAM IN106714. Numerical calculations were performed at Miztli supercomputer of DGTIC-UNAM (Project SC14-1-I-49).

References

[1] A. Gómez-Cortés, G. Díaz, R. Zanella, H. Rodríguez, P. Santiago, J.M. Saniger, J. Phys. Chem. C 113, 9719 (2009).

[2] X. Bokhimi, R. Zanella, C. Angeles-Chavez, J. Phys. Chem. C 114, 14101 (2010)

Theoretical investigation for isomerizaiton of allyl alcohol over Au cluster

Mitsutaka Okumura,[1,2] Kohei Tada,[1] Kohei Sakata,[1] Hiroaki Koga,[2] Takashi Kawakami,[1] and Shusuke Yamanaka[1]

[1] *Department of Chemistry, Graduate School of Science, Osaka University, 1-1 Machikaneyama, Toyonaka, Osaka 560-0043, Japan*
[2] *Elements Strategy Initiative for Catalysts and Batteries (ESICB), Kyoto University, 1-30 Goryoohara, Kyoto 615-8245, Japan*

Transformation of allylic alcohols to saturated carbonyl compounds is one of the interesting reactions for chemical processes. This reaction basically contains a two-step sequential oxidation and reduction. Isomerization of allylic alcohols enables one-step transformation, thus various homogeneous catalysts have been developed over Ru and Rh containing catalysts.
On the other hand, since Haruta et al. invented that gold nanoparticles supported on metal oxides remarkably high catalytic activity for CO oxidation at low temperatures, Au catalysts have attracted growing interest not only in gas phase but also in liquid phase, particularly for the aerobic oxidation of alcohols. Lately, dehydrogenation of alcohol to aldehyde has been achieved even in the absence of O_2. One-pot reactions using hydrogen-borrowing strategy over Au catalysts, in which hydrogen atoms produced by the first step alcohol dehydrogenation are used for the second step reduction, has also emerged. Tokunaga have attempted this strategy to apply for the Au-catalyzed isomerization of allyl alcohol to propanal.
In order to discuss this isomerization of allyl alcohol over Au catalysts, theoretical study was performed using Au_6 cluster, since Au_6 cluster is the smallest cluster that has vertex and edge atoms. From these calculations, it was found that the hydrogen transfer easily proceed on Au clusters and the first dehydrogenation step was the rate deterring step. Additionally, the protonation to the enolate C–C double bond was also suggested by DFT calculations.

Reference

[1] Tamao Ishida, Jun Aimoto, Akiyuki Hamasaki, Hironori Ohashi, Tetsuo Honma, Takushi Yokoyama, Kohei Sakata, Mitsutaka Okumura, and Makoto Tokunaga, Chem. Lett. in press.

Synthesis of Ag@Pd/TiO_2 catalysts in an aqueous solution for the hydrogen generation from decomposition of formic acid at room temperature

Daisuke Shimamoto,[1] Masashi Hattori,[2] Takeshi Daio,[3] and Masaharu Tsuji[1,2]

[1] *Institute for Materials Chemistry and Engineering, Kyushu University, Kasuga, Japan*
[2] *Department of Applied Science for Electronics and Materials, Kyushu University, Kasuga, Japan*
[3] *International Research Center for Hydrogen Energy, Kyushu University, Fukuoka, Japan*

Formic acid (HCOOH) has received a great attention as an in situ source of hydrogen for fuel cells, because it offers high energy density, is non-toxic and can be safely handled in aqueous solution. Although there has been a lack of solid catalysts that are sufficiently active and/or selective for hydrogen production from formic acid at room temperature, Tedsree et al.[1] reported that Ag nanoparticles coated with a thin layer of Pd atoms can significantly enhance the production of H_2 from formic acid at ambient temperature. We have recently studied preparation of Ag-Pd bimetallic nanoparticles supported on TiO_2 nanoparticles under two-step microwave heating in ethylene glycol (EG) with a boiling point of 180 ^oC.[2] Results show that catalytic activity of Ag-Pd particles is enhanced by about 300% in the presence of TiO_2 support. It is reported that catalytic activity Ag@Pd core-shell particles is higher than Ag-Pd alloy particles.[1] Therefore, preparation of Ag@Pd particles with low Ag-Pd alloy components is required for the formation of more active Ag-Pd catalytic system.

In this study, Ag-Pd bimetallic nanocatalysts supported on anatase-type of TiO_2 nanoparticles have been prepared in an aqueous solution under microwave heating at 100 ^oC. At first, anatase-type of TiO_2 nanoparticles with average diameter of 10±2 nm were prepared as a catalytic support by hydrolysis of titanium tetraisopropoxide in *1,5*-pentanediol under microwave (MW) heating. Then TiO_2-supported Ag-Pd bimetallic nanocatalysts were prepared from formic acid using a two-step MW-polyol method for hydrogen production. In the first step, small Ag nanoparticles were prepared under low-power MW heating (150 W). Then in the second step, monodispered TiO_2-supported Ag-Pd bimetallic particles were prepared under higher power MW heating (150 W) for 20 min (Fig. 1). The hydrogen product rate of Ag@Pd/TiO_2 from formic acid at 30 °C was measured to be 28.24 L / h g, which was higher than that of AgPd@Pd/TiO_2 particles prepared in EG (16.00 L / h g). The higher catalytic activity can be explained by suppression of alloying in Ag-Pd particles ($Ag_{96}Pd_4$ based on XRD data.)

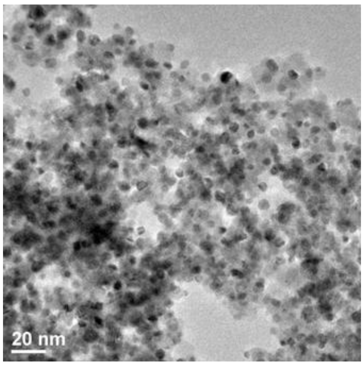

Fig. 1. TEM image of Ag@Pd/TiO_2 catalysts prepared by microwave heating.

References
[1] K. Tedsree, T. Li, S. Jones, C. W. A. Chan et al., Nat. Nanotech., 6 (2011) 302.
[2] M. Hattori, H. Einaga, T. Daio, and M. Tsuji, Nat. Commun., submitted for publication.

Reaction of aluminum cluster cations with a mixture of O_2 and H_2O gases: Formation of hydrated-alumina clusters

Masashi Arakawa, Kei Kohara, and Akira Terasaki

Department of Chemistry, Kyushu University, Fukuoka, Japan

Aluminum is known as a reactive metal as we can imagine from the fact that it is readily oxidized by O_2 and/or H_2O in the air to form a passive surface. Reduction of H_2O by aluminum, for example, is one of the efficient ways to produce H_2. It is anticipated also that aluminum hydrides are used as hydrogen storage materials. In this regard, clusters are attracting much attention for modeling interactions of metal surfaces with reactants. We have reported that aluminum-cluster cations (Al_N^+) react with a H_2O molecule to form Al_NO^+, which implies H_2 generation [1]. In the present study, we investigated reaction of Al_N^+ toward a mixture of O_2 and H_2O gases to model reactions in natural environments.

In the experiment, Al_N^+ (N = 1–14) were generated by a magnetron-sputter cluster-ion source. They were mass-selected and guided into a reaction cell filled with a buffer He gas containing H_2O and O_2. The ions produced by the reaction of Al_N^+ with H_2O and O_2 were identified by a quadrupole mass analyzer.

Reaction products with a mass of 157 and 175 amu were observed for all the sizes except N = 1. Since only Al^+ was found to be inert, we speculated that these products originate from Al_2^+, which is produced by dissociation of Al_N^+ ($N \geq 3$). By controlling the partial pressures of O_2 and H_2O, reaction intermediates such as Al_2O^+, $Al_2O_3^+$, $Al_2O_4H_3^+$, and $Al_2O_5H_5^+$ were observed, and the prominent products were assigned to be $Al_2O_6H_7^+$ and $Al_2O_7H_9^+$ for 157 and 175 amu, respectively. The chemical composition of these products, $Al_2O_3(H_2O)_nH^+$, is similar to that of hydrated alumina such as boehmite, diaspora, and gibbsite except for the proton. To obtain structural information of these products, we performed collision-induced dissociation experiment of $Al_2O_7H_9^+$ (175 amu) with an Ar gas, where products of 157, 139 and 121 amu were observed. The prominent products of 157 and 175 amu were thus identified as $Al_2O_4H_3(H_2O)_2^+$ and $Al_2O_4H_3(H_2O)_3^+$ with two and three H_2O molecules remaining intact, respectively.

We further investigated formation process of these protonated hydrated-alumina clusters by observing the reaction steps to model reactions of aluminum in natural environments; each reaction intermediate was generated in the cluster source, and reaction with either H_2O or O_2 was examined in a step-by-step manner. It was found that reaction of aluminum with O_2 and H_2O to form alumina, Al_2O_3, at initial steps is followed by successive hydroxylation and hydration reactions.

Reference

[1] M. Arakawa, K. Kohara, T. Ito, and A. Terasaki, Eur. Phys. J. D 67 (2013) 80.

Adsorption and catalytic activation of the molecular oxygen on the metal supported h-BN

Andrey Lyalin,[1] Akira Nakayama,[1,2] Kohei Uosaki,[3] and Tetsuya Taketsugu[1,2]

[1] *Elements Strategy Initiative for Catalysts and Batteries (ESICB), Kyoto University, Kyoto, Japan*
[2] *Department of Chemistry, Faculty of Science, Hokkaido University, Sapporo, Japan*
[3] *Global Research Center for Environment and Energy based on Nanomaterials Science (GREEN), National Institute for Materials Science (NIMS), Tsukuba, Japan*

Adsorption and catalytic activation of the molecular oxygen on the hexagonal boron nitride (h-BN) monolayer supported on Ni(111) and Cu(111) surfaces have been studied theoretically using density functional theory with the gradient-corrected exchange–correlation functional of Wu and Cohen (WC) [1]. It is demonstrated that inert h-BN monolayer can be functionalized by the metal support and become active for O_2 activation [1-3]. It is shown that O_2 adsorbs on h-BN/Ni(111) and h-BN/Cu(111) systems in two configurations, corresponding to the superoxo-like and peroxo-like states of oxygen. It is shown that the metal substrate influences the molecular adsorption and chemical reactions on the supported h-BN surface via the mixing between metal *d* and h-BN *π* bands. Such an effect can open a new way to tune adsorption characteristics of O_2 and reactant molecules on h-BN by the selection of metal substrate.

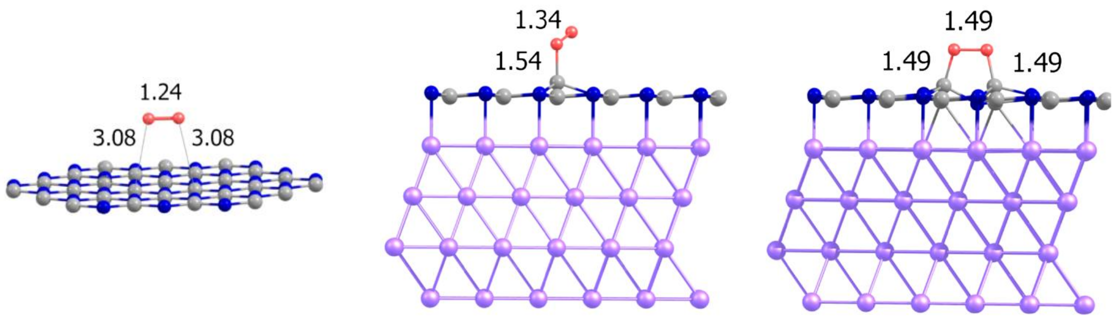

Figure 1. Optimized structure of the molecular oxygen physisorbed on a free h-BN monolayer (left) and chemisorbed on the h-BN/Ni(111) surface in on top (middle) and bridge (right) configurations.

References
[1] A. Lyalin, A. Nakayama, K. Uosaki, and T. Taketsugu, Top. Catal. 57 (2014) 1032.
[2] A. Lyalin, A. Nakayama, K. Uosaki, and T. Taketsugu, J. Phys. Chem. C 117 (2013) 21359.
[3] K. Uosaki, G. Elumalai, H. Noguchi, T. Masuda, A. Lyalin, A. Nakayama, and T. Taketsugu, JACS 136 (2014) 6542.

Reductive Activation of CO_2 by Cobalt Cluster Anions

Akimaro Yanagimachi,[1] Kiichirou Koyasu,[1,2] and Tatsuya Tsukuda[1,2]

[1] *Department of Chemistry, The University of Tokyo, Tokyo, Japan*
[2] *ESICB, Kyoto University, Kyoto, Japan*

Development of catalysts that can activate chemically inert carbon dioxide (CO_2) is desired for its use as a reusable carbon source to establish sustainable society. Conventionally, Lewis base catalysts have been used to activate CO_2 by nucleophilic interaction at the carbon site of CO_2 and subsequent electron transfer [1]. Metal clusters are promising candidates for alternative catalysts, because of their unique unsaturated surface sites and quantized electronic structures. In this study, reaction of cobalt cluster anions (Co_n^-) and CO_2 were studied experimentally and theoretically.
The apparatus used in the present study is composed of four parts: a laser ablation cluster source, a reaction cell, a Wiley–McLaren type time-of-flight mass spectrometer, and a magnetic bottle type photoelectron spectrometer [2]. Briefly, Co_n^- produced by the laser vaporization method was allowed to react with CO_2 under a high pressure of He and the anionic products were analyzed by the TOF mass spectrometer. Photoelectron spectra of Co_n^- and $Co_nCO_2^-$ (n = 5–9) were mesured using the 3rd harmonic of Nd:YAG laser (355 nm). Fig. 1a shows a typical mass spectrum of the cluster anions produced by the laser ablation of a Co rod. The mass peaks of Co_n^- were observed. After the reaction (Fig. 1b), the peak intensities of Co_n^- decreased and the mass peaks assigned to $Co_nCO_2^-$ were newly observed via the following reaction,

$$Co_n^- + CO_2 \rightarrow Co_nCO_2^-.$$

Photoelectron band of Co_n^- at low binding energy region disappeared after the reaction with CO_2. The same trend was observed for all the clusters studied here (n = 5–9). This suggests that electronic charge is transferred from Co_n^- to CO_2.
In order to confirm this interpretation, the geometric and electronic structures of $Co_7CO_2^-$ were studied by DFT calculation at B3LYP/LanL2DZ(Co), 6–311++G*(C, O) level. Fig. 2 shows the optimized structure. CO_2 is bonded to Co_7^- clusters through C and O. The bent structure of CO_2 suggests that it is negatively charged. Mulliken population analysis indicates the electron transfer from Co_7^- to CO_2. These experimental and theoretical results indicate that CO_2 can be activated reductively by Co_n^-.

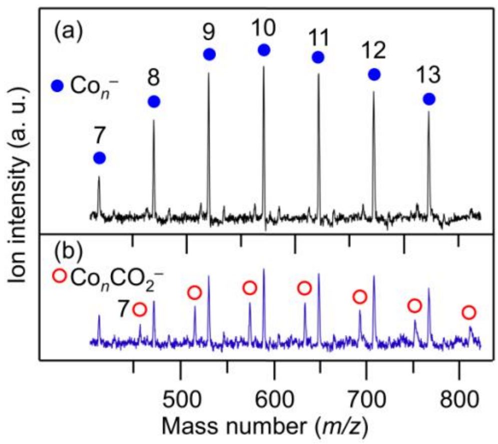

Figure 1. Mass spectra of Co_n^- (a) before and (b) after the reaction with CO_2.

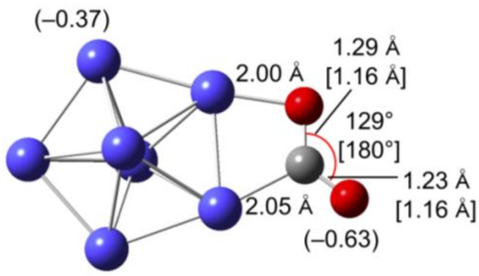

Figure 2. Optimized structure of $Co_7CO_2^-$. The numbers in parenthesis indicate Mulliken charge. Structure parameters of free CO_2 are also shown in brackets.

References
[1] T. Sakakura, J.-C. Choi, and H. Yasuda, Chem. Rev. 107 (2007) 2365.
[2] T. Watanabe, T. Tsukuda, J. Phys. Chem. C 117 (2013) 6664.

Theoretical study on the isomerization of small gold clusters induced by O_2 adsorption

Min Gao,[1] Daisuke Horita,[1] Yuriko Ono,[1] Andrey Lyalin,[2] Satoshi Maeda[1,2] and Tetsuya Taketsugu[1,2]

[1] *Department of Chemistry, Faculty of Science, Hokkaido University, Sapporo, Japan*
[2] *Elements Strategy Initiative for Catalysts and Batteries, Kyoto University, Kyoto, Japan*

Gold clusters possess unique catalytic activity in various oxidation reactions by molecular oxygen [1]. Several mechanisms have been proposed to investigate the origin of high catalytic activity of gold clusters. No matter which route oxidation reactions follow, the adsorption and activation of O_2 molecule on gold clusters are always the key initial step. There are two forms of oxygen adsorption on gold clusters: the superoxo form (η^1–Au_nO_2) with only one O atom bounded to the gold cluster and peroxo form (η^2–Au_nO_2) with O_2 molecule bridging two gold atoms on the cluster surface. Recently, Fielicke *et al*. observed these two adsorption forms for odd-sized gold clusters using analysis of O-O vibrational stretching frequencies [2]. However, the origin of two vibrational fundamentals for Au_nO_2 is still not clear, because one or more isomers of the gold cluster as well as more than one binding geometry of the oxygen molecule on gold cluster can coexist.

In the present work, we applied single-component artificial force induced reaction (SC-AFIR) method [3] to search for the structural transformations upon adsorption of O_2 molecule on gold clusters (Au_3 – Au_{12}). The stable geometrical structures, adsorption energies, vibrational frequencies, and charge transfers from gold clusters to oxygen molecule are investigated to understand the structure dependence on oxygen adsorption. It is demonstrated that oxygen molecule adsorbs on the odd-sized gold clusters either in the peroxo or superoxo forms, but in the case of even-sized gold clusters only peroxo form can exist. The O-O bond length in the η^2–Au_nO_2 form is longer than the one in η^1–Au_nO_2 form, which indicates that O_2 is more activated in the η^2–Au_nO_2 form due to the more excess electron transfer from gold clusters. O_2 molecule adsorbs in the η^1–Au_nO_2 form on the most stable gold clusters, but in the η^2-Au_nO_2 form on the energetically low-lying isomers. Oxygen molecule in the η^2–AuO_2 form is more active. The interaction energies between O_2 and gold cluster in superoxo form are approximately twice as large as the binding energy in peroxo form. Although O_2 molecule prefers to adsorb on the most stable structures in the form of η^1–Au_nO_2, it can be isomerized to η^2–Au_nO_2 with very low barrier. The pathways of isomerization between gold clusters and Au_nO_2 are also compared. More details will be presented in poster session.

References

[1] M. Haruta, T. Kobayashi, H. Sano, and N. Yamada, Chem. Lett. 16 (1987) 405.
[2] A. P. Woodman, G. Meijer, and A. Fielicke, J. Am. Chem. Soc. 135 (2013) 1727.
[3] S. Maeda, T. Taketsugu, and K. Morokuma, J. Comput. Chem. 35 (2014) 166.

Materials Development for Realization of Carbon-Neutral Energy Cycles

Miho Yamauchi,[1]

[1] *International Institute for Carbon-Neutral Energy Research (WPI-I²CNER), Kyushu University, Fukuoka, Japan*

[2] *JST-CREST, Saitama, Japan*

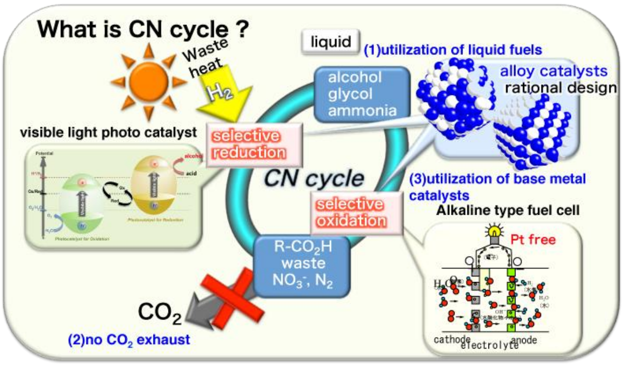

Figure 1. Concept of carbon-neutral energy cycles.

The CO_2 concentration of the atmosphere has been inadvertently increased by consuming finite energy resources of fossil fuels, and increased concerns about climate issues due to CO_2 emissions have spurred the development of alternative and sustainable energy cycle systems. We have proposed novel energy cycles where electrical power is generated by partial oxidation of liquid fuels without CO_2 emission, resulting in CO_2-free power generation, and fuels are regenerated by using renewable energies, and fuels are regenerated from oxidized wastes by using renewable energies,[1] i.e., carbon-neutral (CN) energy cycles.[2] Among a number of energy carrying materials, ethylene glycol (EG) can be cited as a fascinating candidate as it has a high boiling point (197.3 °C) and low vapor pressure (8 Pa at 20 °C). Previous studies have revealed that Pt-based catalysts show the highest selectivity for partial oxidation of EG and mainly produce glycolic acid, i.e., 4-electron oxidation. For the sake of the efficient use of fuels and the suppression of CO_2 concentration in the environment, deeper oxidation of EG without CO_2 emission should be the best desirable process. We herein demonstrate the successful synthesis of a well-mixed Fe-group ternary nanoalloy (NA) catalyst, a carbon supported FeCoNi NA catalyst (FeCoNi/C), that exhibits selective EG electrooxidation to oxalic acid without CO_2 emission in alkaline media, where the NA structure were maintained throughout the catalytic reaction. Furthermore, an alkaline fuel cell fabricated with the FeCoNi/C anode catalyst and a solid oxide electrolyte was found to exhibit power generation from EG without any precious-metal catalysts.[3]

References

[1] M. Yamauchi, R. Abe, T. Tsukuda, K. Kato, M. Takata, J. Am. Chem. Soc., 133, 1150-1152 (2011).

[2] M. Sadakiyo, H. Kasai, K. Kato, M. Takata, M. Yamauchi, J. Am. Chem. Soc., 136, 1702–1705 (2014).

[3] T. Matsumoto, M. Sadakiyo, M. L. Ooi, S. Kitano, T. Yamamoto, S. Matsumura, K. Kato, T. Takeguchi, M. Yamauchi, Scientific Reports, in press.

Adsorption and decomposition of NO on foreign metal-doped copper cluster cations

Shinichi Hirabayashi[1] and Masahiko Ichihashi[2]

[1] *East Tokyo Laboratory, Genesis Research Institute, Inc., Chiba, Japan*
[2] *Cluster Research Laboratory, Toyota Technological Institute, Chiba, Japan*

Doped metal and bimetallic clusters often exhibit different chemical properties from those of single-component metal clusters. Here we demonstrate the results of the investigation of adsorption and reactions of nitric oxide (NO) on foreign metal-doped copper cluster cations, Cu_nX^+ (X = Al, Ti, and Rh), in the gas phase. The Cu_nX^+ clusters are produced by an ion sputtering source, and their reactivity is measured by using a tandem-type mass spectrometer. The NO adsorption cross sections for Cu_nAl^+ show an pronounced even-odd alternation in the region of n = 8−16, where the clusters with odd-numbered n are more reactive than the adjacent ones with even n. This alternation can be understood in terms of the electron pairing. In the reactions of Cu_nTi^+, the reaction cross section tends to increase with increasing cluster size, and most of the doped clusters exhibit significantly larger reaction cross sections than undoped Cu clusters [1]. The results suggest that these doped clusters have relatively large NO adsorption energies. However, the reactivity decreases rapidly above n = 11, and then $Cu_{15}Ti^+$ is totally unreactive toward NO, which can be explained by its stability related to the electronic shell closing [2]. The multiple-collision reactions are also investigated for some reactive clusters, Cu_nAl^+ (n = 9 and 11) and Cu_nTi^+ (n = 7, 9, 11, and 12). These reactions result in the production of the cluster dioxides, which is accompanied by the release of Cu atoms and an N_2 molecule. This observation indicates that the decomposition of NO can proceed via dissociative adsorption on these clusters. Since it is considered that the process of dissociative adsorption involves more than one constituent atom, Cu atoms should act as an active site with the foreign atom. On the other hand, for Cu_nRh^+, the NO adsorption cross sections are mostly smaller than those for reactive Cu_nAl^+ and Cu_nTi^+ clusters, and no clear evidence of NO decomposition is found.

Reference(s)

[1] S. Hirabayashi and M. Ichihashi, J. Phys. Chem. A 118 (2014) 1761.
[2] E. Janssens, S. Neukermans, and P. Lievens, Curr. Opin. Solid State Mater. Sci. 8 (2004) 185.

withdraw

Base catalysis of $[Nb_6O_{19}]^{8-}$ and $[Nb_{10}O_{28}]^{6-}$

Shun Hayashi,[1] Seiji Yamazoe,[1, 2] Kiichirou Koyasu,[1, 2] and Tatsuya Tsukuda[1, 2]

[1] *Department of Chemistry, The University of Tokyo, Tokyo, Japan*
[2] *Elements Strategy Initiative for Catalysts and Batteries, Kyoto University, Kyoto, Japan*

Anionic metal-oxide clusters called polyoxometalates (POMs) with well-defined structures show promise for a variety of applications including catalysts, electronic devices and chromic devices. Recently, it was reported that polyoxotungstate acted as base catalysts for Knoevenagel condensation reactions [1]. It is expected that polyoxoniobates (e.g. $[Nb_6O_{19}]^{8-}$ and $[Nb_{10}O_{28}]^{6-}$) show higher basicity than polyoxotungstates (e.g. $[W_6O_{19}]^{2-}$) because niobium (group V) forms more negatively charged POMs than tungsten (group VI). According to this hypothesis, we studied basic nature of $[Nb_6O_{19}]^{8-}$ and $[Nb_{10}O_{28}]^{6-}$ theoretically and applied them as catalysts for Knoevenagel condensation and CO_2 fixation reactions for the first time.

DFT calculations were conducted for $[Nb_6O_{19}]^{8-}$ and $[Nb_{10}O_{28}]^{6-}$. Natural Bond Orbital analysis indicated that the maximum negative charges of surface oxygen atoms in polyoxoniobates (–0.90 for $[Nb_6O_{19}]^{8-}$ and –0.86 for $[Nb_{10}O_{28}]^{6-}$) were larger than those in polyoxotungstates (e.g. –0.72 for $[W_6O_{19}]^{2-}$). This result suggests that polyoxoniobates possess more basic sites.

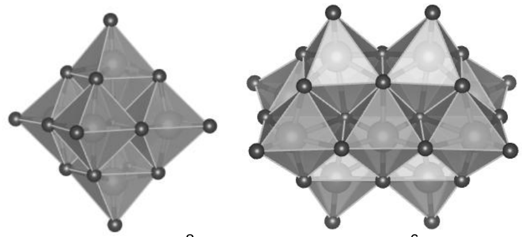

Figure 1: $[Nb_6O_{19}]^{8-}$ (left) and $[Nb_{10}O_{28}]^{6-}$ (right).

$Na_7H[Nb_6O_{19}]\cdot 15H_2O$ and $(TBA)_6[Nb_{10}O_{28}]$ (TBA: tetrabutylammonium) were synthesized according to the methods reported in refs [2, 3]. Then, they were applied to Knoevenagel condensation, a model reaction to evaluate base strengths of catalysts. $Na_7H[Nb_6O_{19}]\cdot 15H_2O$ catalyzed condensation of ethyl cyanoacetate (pKa = 13.1) in heterogeneous system, whereas $(TBA)_6[Nb_{10}O_{28}]$ showed catalytic activity for condensation of 4-methoxybenzyl cyanide (pKa = 23.8) in homogeneous system (Figure 2). We also found that $(TBA)_6[Nb_{10}O_{28}]$ acted as catalysts for fixation of CO_2 (0.1 MPa) with epoxide.

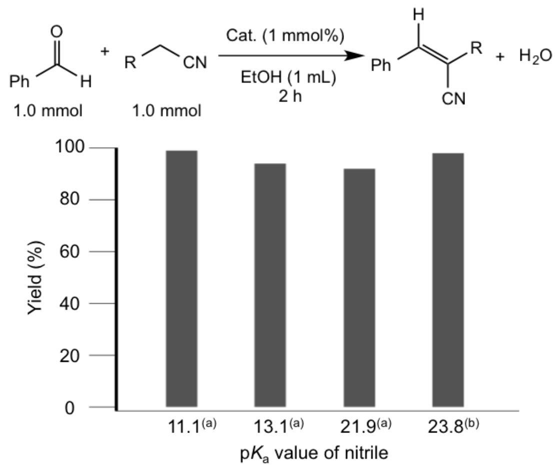

Figure 2: Knoevenagel condensation catalyzed by $TBA_6[Nb_{10}O_{28}]$ for nitriles with various pK_a values (reaction temperature: (a) 30ºC, (b) 80ºC).

Reference(s)

[1] N. Mizuno et al., Chem. Commun. 48 (2012) 8422. [2] S. Yamazoe et al., Chem. Lett. 42 (2013) 380. [3] A. Yagasaki et al., Polyhedron 29 (2010) 2196.

FT-ICR study of chemical reaction of acetonitrile molecules on cobalt clusters

Kazuki Ogasawara,[1] Yuta Tobari,[2] Yoshinori Sato,[1] Makoto Saito,[1] Shohei Chiashi,[1] Toshiki Sugai,[2] and Shigeo Maruyama[1]

[1] *Department of Mechanical Engineering, The University of Tokyo, Tokyo, Japan*
[2] *Department of Chemistry, Toho University, Funabashi, Japan*

The chemical vapor deposition (CVD) method is the most common technique for production of single walled carbon nanotubes (SWNTs). During the CVD process, an SWNT grows from decomposed carbon atoms on a catalytic metal particle fed by molecules such as CO, CH_4 or ethanol at high temperature. Therefore, understanding surface chemical reaction is critically important, however, little is known due to the complexity of these nanoparticles. Recently, Thurakitseree et al. [1] reported that changing the carbon feedstock from pure ethanol to a few % mixture of acetonitrile (CH_3CN) in ethanol during CVD drastically reduces the average diameter of the SWNTs, and this change is reversible and repeatable. It is suggested that the nitrogen atoms in acetonitrile molecules impeded the formation of larger diameter SWNT on the surface of catalytic particles. However, the detailed mechanism of the reaction is also still not clear.

In this study, the chemical reactions of cobalt cluster cation with acetonitrile was observed by Fourier transform ion cyclotron resonance (FT-ICR) mass spectrometer with direct injection laser vaporization cluster beam source [2]. Cobalt clusters were trapped within the FT-ICR cell, subsequently acetonitrile was introduced. Figure 1 shows the typical mass spectrum of the reaction products from Co_{11}^+ clusters. Dotted lines indicate the simple chemisorption of acetonitrile such as $+CH_3CN$ or $+(CH_3CN)_2$. We can also observe the dehydrogenated chemisorption such as $+(CCN)_2$ or $+(CCN)_2(HCCN)$. Figure 2 shows the schematic diagram of the $Co_{11}(CCN)_2^+$ cluster. The drastic cluster size dependence of these reaction such as the change of simple /dehydrogenate chemisorption ratio was observed. The difference of reactivity compared with the ethanol (C_2H_5OH), nitrogen-free molecules, and the cluster size dependence of these reactions will also be discussed.

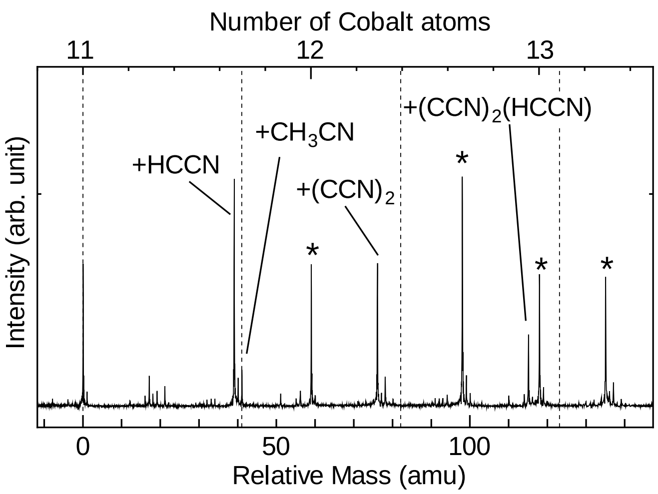

Fig.1 Chemisorption on Co_{11}^+ clusters; ∗ indicates peaks originated from Co_{12}^+ or Co_{13}^+.

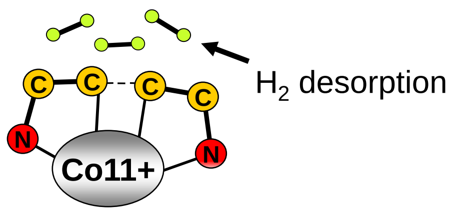

Fig.2 Schematic diagram of $Co_{11}(CCN)_2^+$ cluster.

Reference(s)

[1] T. Thurakitseree, et al., ACS Nano, 7 (2013) 2205.

[2] S. Maruyama, et al., Rev. Sci. Instrum., 61 (1990) 3686.

Gold Nanoparticle-Catalyzed C–H Bond Functionalization for Biaryl Synthesis

Yoshiyuki Mise,[1] Shohei Aikawa,[1] Tamao Ishida,[1,5] Ryota Akebi,[1] Akiyuki Hamasaki,[1] Hironori Ohashi,[2] Tetsuo Honma,[3] Tetsuro Tsuji,[4] Yasushi Yamamoto,[4] Mitsuru Miyasaka,[4] Takushi Yokoyama,[1] Makoto Tokunaga[1]

[1] *Graduate School of Sciences, Kyushu University, Fukuoka, Japan*
[2] *Faculty of Arts and Science, Kyushu University, Fukuoka, Japan*
[3] *Japan Synchrotron Radiation Research Institute (JASRI/SPring-8), Hyogo, Japan*
[4] *UBE Industries Ltd., Yamaguchi, Japan*
[5] *Research Center for Gold Chemistry, Tokyo Metropolitan University, Tokyo, Japan*

Direct transformation of C–H bonds into C–C bonds for synthesizing biaryl compounds has been a great issue in organic chemistry over the decade. Although many kinds of homogeneous metal catalysts, including Ru, Pd, and Au complexes have been developed, heterogeneous metal catalysts are still scarce. Very recently, Au nanoparticles (NPs) supported on TiO_2 has been reported to be catalytically active for C–H/C–H coupling of arenes into biaryls, but to control the regioselectivity of substrates remained challenge. In this work we studied on the C–H/C–H coupling of dimethyl phthalate (DMP) to produce tetramethyl biphenyltetracarboxylate (S-DM/A-DM) over supported Au NPs, and found that Au catalysts can produce S-DM with excellent regioselectivity. As shown in Table 1, Au catalysts showed higher catalytic activity than Pd catalysts. Among the catalysts tested, Au/Co_3O_4 and Au/ZrO_2 exhibited the highest activity (entries 4 and 5). In addition, Au catalysts showed excellent regioselectivity to S-DM without the addition of ligands. After optimization of reaction conditions for Au/ZrO_2, the dimer yield increased up to 73% with excellent selectivity (entry 6). We confirmed that homogeneous Au complex, $Au(OAc)_3$ was inactive under our conditions (entry 7), and Co_3O_4 without Au did not catalyze this reaction (entry 8), suggesting that Au(0) NPs are the catalytically active species.

Table 1. Oxidative coupling of DMP.[a)]

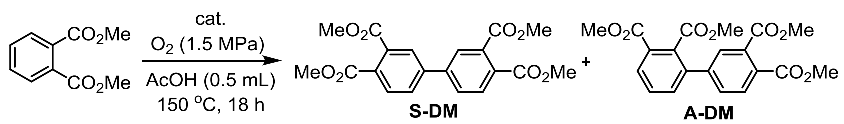

Entry	Catalyst	Conv. (%)	Dimer Yield (%)	S/(S+A) (%)
1	PdO/Co_3O_4	7	1	0
2	Au/TiO_2	45	27	85
3	Au/MnO_2	39	20	95
4	Au/Co_3O_4	49	48	94
5[b)]	Au/ZrO_2	66	51	88
6[c)]	Au/ZrO_2	88	73	95
7	$Au(OAc)_3$	0	0	0
8	Co_3O_4	0	0	0

a) Conditions: DMP (1 mmol), catalyst (metal 4 mol%), AcOH (0.5 mL), O_2 (1.5 MPa), 150 °C, 18 h. b) O_2 (1.8 MPa). c) O_2 (1.8 MPa), 120 °C, 96 h.

Gas Phase Modeling of the Catalytically Active Centers in Iron Sulfur Proteins

Heiko Heim, Thorsten M. Bernhardt, Sandra M. Lang

[1] *Institute of Surface Chemistry and Catalysis, University of Ulm, Germany*

Small iron-sulfur (FeS-)clusters are often considered as the active reaction centers of the most common naturally occurring proteins (FeS-proteins) and are thus of fundamental importance for all living organisms. Apart from their role as electron transfer medium in biochemical redox reactions, FeS-clusters are especially important as biocatalysts in numerous pivotal processes [1]. In particular, the mild reaction conditions and the ability of such biocatalysts to activate molecular nitrogen renders them ideal materials for a "green", i.e. environmentally friendly and sustainable, catalysis. Thus, the investigation of the catalytic mechanisms in enzyme reactions is not only of particular importance for a basic understanding of the functionalities of life; enzymes as biocatalysts also represent ideal systems to learn from nature and to use this knowledge for the development of new catalytically active and selective materials.

Toward this goal we aim to mimic the active centers of FeS-proteins in form of gas phase clusters. In a first step these clusters have been prepared in a CORDIS sputter source [2] by sputtering of binary targets pressed from iron and sulfur powder. However, iron and in particular iron powder easily oxidizes at air which should lead to a considerable amount of oxygen in the target and thus in the produced clusters. To unambiguously assign the mass peaks in the produced cluster distribution and to gain insight into the degree of a possible oxygen contamination of the targets, a series of different targets have been produced and the formation and stability of iron oxide and iron sulfur clusters has been investigated in detail

In a second step some FeS-cluster cations $(FeS)_n^+$ (n = 2, 4) have been mass-selected from the produced cluster distribution and their reactivity towards N_2, H_2, and mixtures thereof have been investigated in an ion trap experiment [3]. Temperature dependent product distributions in conjunction with kinetic data provide detailed insight into the reaction mechanism as well as the energetics of the reaction between $(FeS)_n^+$ and N_2 and H_2, respectively, as well as a potential ammonia synthesis reaction.

Reference(s)

[1] H. Beinert, R. H. Holm, E. Münck, Science **277** (1997) 653

[2] R. Keller, F. Nöhmeier, P. Spädtke, M. H. Schönenberg, Vacuum **34** (1984) 31

[3] T. M. Bernhardt, Int. J. Mass Spectrom. **243** (2005) 1

Thermal stability and reactivity with CO molecules of cerium oxide and gold-appended cerium oxide clusters

Toshiaki Nagata, Ken Miyajima, and Fumitaka Mafuné

Department of Basic Science, School of Arts and Sciences, The University of Tokyo, Tokyo, Japan

Cerium oxide (CeO_2, ceria) is widely used for automotive three-way catalysts that convert harmful exhaust gases including NO_x, CO, and small hydrocarbons into N_2, CO_2, and H_2O. Ceria is also used as a support of catalysts; one of the most important supported materials is nanosized gold [1]. In this work, we studied thermal stability and reactivity with CO molecules of cerium oxide and gold-appended cerium oxide cationic clusters ($Au_mCe_nO_{2n+x}^+$; m = 0–2, n = 3–7, x = −1–+2) in the gas phase using a newly developed post-heating method [2].

The clusters were prepared by laser ablation of rod-shaped CeO_2 and Au targets using focused second harmonic of Nd:YAG pulse laser in the presence of oxygen diluted in helium. The generated clusters were introduced into a reaction gas cell filled with CO diluted in helium, followed by passing in a temperature controlled heating tube (post-heating). Then the clusters were introduced into a vacuum and detected by a time-of-flight mass spectrometer.

Figure 1 shows the abundance distributions of generated $Au_mCe_nO_{2n+x}^+$ clusters at room temperature and after heating up to 573 K. Figure 2 shows the cluster ion intensities as functions of temperature in the heating tube. In a high temperature, oxygen-excess clusters released O_2 molecules and turned to be compositions of $Ce_nO_{2n+x}^+$ (x = −1, 0) and $Au_mCe_nO_{2n+x}^+$ (m = 1, 2; x = 0, +1), which are considered to be the stable stoichiometry. The activation energies (E_a) of O_2 releasing were estimated from the temperature dependence based on Arrhenius equation.

We observed CO oxidation and CO adsorption reactions on cerium oxide clusters, although only CO adsorption was observed on gold-appended cerium oxide clusters. There is significant size dependence in reactivity with CO. The CO attached clusters released CO molecules by the post-heating. The E_a of CO releasing processes were estimated in the same way as O_2 releasing.

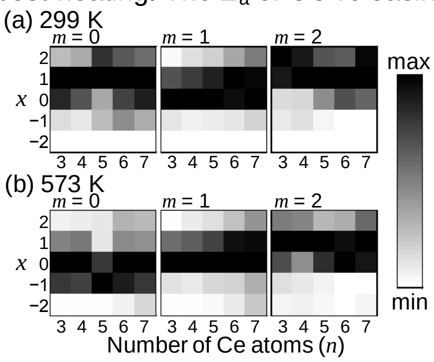

Figure 1. Intensities of $Au_mCe_nO_{2n+x}^+$ at (a) r.t. and (b) 573 K.

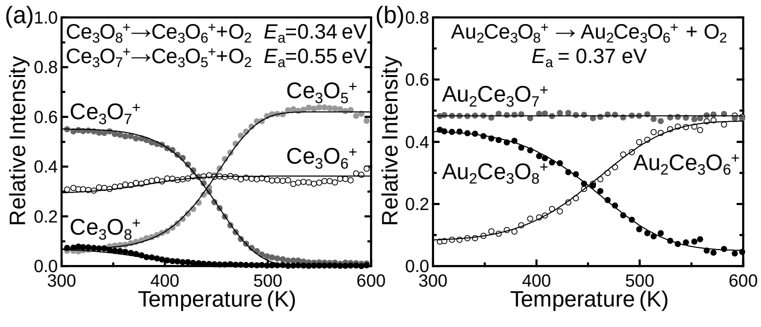

Figure 2. Relative intensities of (a) $Ce_3O_{5–8}^+$ and (b) $Au_2Ce_3O_{6–8}^+$ as functions of heating temperature.

References

[1] M. Haruta, Catal. Today 36 (1997) 153.

[2] K. Morita, K. Sakuma, K. Miyajima, and F. Mafuné, J. Phys. Chem. A 117 (2013) 10145.

Enhancement of photocatalytic activity of TiO_2 nanoparticles by addition of Ag nanoparticles

Mari Yonemura, Naoki Nishida, Hideki Tanaka

Department of Applied Chemistry, Chuo University, Tokyo, Japan

TiO_2 nanoparticles have drawn much attentions because of their photocatalytic activity. However, the photocatalytic performance of traditional TiO_2 nanoparticles is restricted due to lack of absorption for visible light. In this study, we examined to load Ag nanoparticles, which have strong absorption of visible light, onto the TiO_2 nanoparticles and measured the visible-light photoactivity of TiO_2 nanoparticles by addition of Ag nanoparticles.

Ag nanoparticles were produced by gas aggregation method heated at 1100 ^{o}C with N_2 gas flow at 2.0 slm, and were directly sprayed on TiO_2 nanoparticles. The sample thus prepared was immersed to azobenzene methanol solution, and were irradiated for 4 hours by visible light. Supernatant of the obtained solution was analyzed by UV-vis spectroscopy.

Figure 1 shows the absorption spectrum for the sample before and after irradiation. The dominant peak at ～316 nm was attributed to azobenzene. The absorption for this peak was drastically decreased for the after-irradiation sample. Since the azobenzene molecule is known to be stable for visible-light irradiation, this decrease is considered to be caused by photocatalytic activity of the present sample. In addition, the degradation rate for the sample (39 %) was higher than that for the pristine TiO_2 nanoparticles (23 %) . This indicates that addition of Ag nanoparticles effectively improve the photocatalytic activity of TiO_2 nanoparticles.

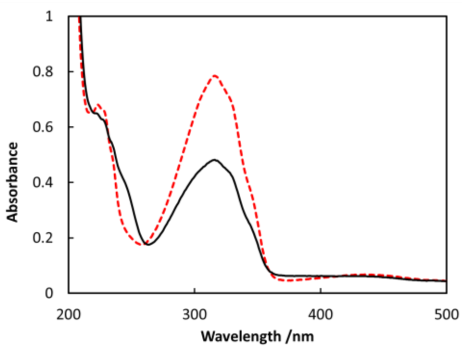

Figure 1. The absorption spectrum for the sample before (red dashed line) and after (black solid line) visible light irradiation for 4 hours.

Towards the Creation of Functionalized Metal Nanoclusters and Highly Active Photocatalytic Materials Using Thiolate-Protected Magic Gold Clusters

Yuichi Negishi

Department of Applied Chemistry, Faculty of Science and Photocatalysis International Research Center, Tokyo University of Science, 1-3 Kagurazaka, Shinjuku-ku, Tokyo 162-8601 Japan.

Advances in developments in nanotechnology have encouraged the creation of highly functionalized nanomaterials. Because of their nanoscale size (< 2 nm), thiolate-protected gold clusters ($Au_n(SR)_m$) exhibit size-specific physical and chemical properties not observed in bulk metals. Therefore, they have attracted attention as functional units or building blocks in nanotechnology. The highly stable, magic $Au_n(SR)_m$ clusters possess great potential as new nanomaterials. We are studying the following subjects related to magic $Au_n(SR)_m$ clusters: (1) establishing methods to enhance their functionality, (2) developing high-resolution separation methods and (3) utilizing the clusters as active sites in photocatalytic materials. Through these studies, we aim to create highly functional metal nanoclusters and apply them as highly active photocatalytic materials. The results of our efforts to date are summarized in this presentation.

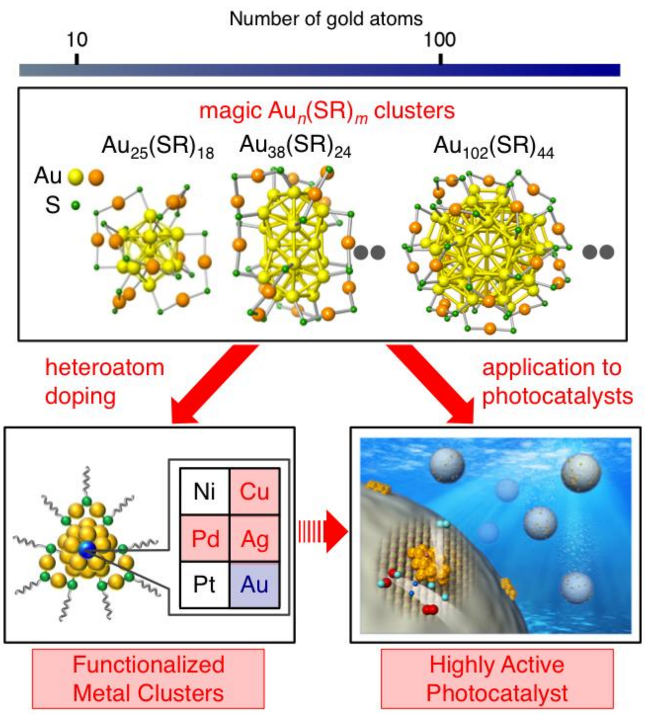

Figure 1. Our study towards the creation of functionalized metal nanoclusters and highly active photocatalytic materials.

Formation and structural analysis of composite of Ag nanoplates with TiO_2 nanoparticles

Hiroki Nanjyo, Ken Iwai, Naoya Kinoshita, Naoki Nishida, and Hideki Tanaka

Department of Applied Chemistry, Chuo University, Tokyo, Japan

Ag triangular nanoplates have attracted much attention owing to their unique geometric structure and optical properties which indicate that they have the potential for use in various applications. These unique points are known to be complementary to each other since their optical properties are induced by surface plasmon resonances that originate from their structure. On the other hand, TiO_2 nanoparticles have been commercialized for the purposes of self-cleaning walls in houses, toilets, interior walls in tunnels, etc. In principal, TiO_2 nanoparticles have been much attention as photocatalytic materials. In this study, we have demonstrated the composition of Ag nanoplates with TiO_2 nanoparticles that combines the best of both and investigate their structure.

Ag triangular nanoplates were synthesized by photoreduction of $AgNO_3$ with PVP (polyvinylpyrrolidon) [1]. The obtained nanoplates were mixed with TiO_2 aqueous solution. The structure of obtained sample was analyzed by scanning transmission electron microscope (STEM). In addition, optical property of obtained solution was analyzed by optical spectroscopy.

The triangular nanoplates and spherical nanoparticles were observed by STEM image. The average diameters of triangular nanoplates and spherical nanoparticles were ~ 100 nm and ~ 35 nm respectively. The spherical nanoparticles were expected TiO_2 nanoparticles from these sizes. On the other hand, triangular nanoplates were expected Ag triangular nanoplates from these shapes. Furthermore, extinction spectrum of the obtained solution exhibited two peaks at ~ 350 nm and ~ 700 nm. The peak at ~ 350 nm is ascribed to the TiO_2. This indicated that the obtained sample were contained TiO_2 nanoparticles. In addition, the peak at ~ 700 nm is characteristic signal for Ag triangular nanoplates [1]. This indicated that the obtained sample were contained Ag triangular nanoplates.

Reference

[1] H. Murayama, N. Hashimoto and H. Tanaka, Chem. Phys. Lett 482 (2009) 291.

Instantaneous cooling of metal clusters by collision with rare gas clusters – Incorporation mechanism of a cobalt cluster ion into an argon cluster

[1]Hideho Odaka, [2]Masahiko Ichihashi

[1] *East Tokyo Laboratory, Genesis Research Institute, Inc., Ichikawa, Japan*
[2] *Cluster Research Laboratory, Toyota Technological Institute, Ichikawa, Japan*

Cryogenic cooling has a huge advantage for spectroscopic measurements with high resolution, and therefore the structural difference of reacting molecules can be distinguished, which are dissociatively or molecularly adsorbed on metal clusters. Especially, instantaneous cooling has been achieved by incorporation of these metal clusters into a helium cluster to suspend chemical reactions at the beginning or an intermediate state. Thus far, a small metal cluster has been formed in a helium cluster by sequential pick-up of metal atoms, the size of which has been clearly identified by IR spectroscopy because of the advantage of few isomers. To simplify the measured spectra, we developed a novel method that a size-selected metal cluster ion is incorporated into a rare gas cluster by merging two cluster beams. We formed cluster complexes from cobalt cluster ions and argon clusters, and discuss the incorporation mechanism in this presentation.

Cobalt cluster ions were produced by laser ablation and their translational energy spread was reduced by the collision with helium buffer gas in a gas cell. The cluster ions, size-selected by a quadrupole mass selector (QMS), were deflected into an octupole ion guide for merging collision (IG_{col}) by a quadrupole ion bender. Neutral argon clusters were produced by supersonic expansion from a pulse valve with the stagnation pressure of 20 bar and the pulse width of 250 μs. The argon cluster beam was overlapped and merged with the cobalt cluster ion beam in the IG_{col} at a low relative velocity (V_{rel}). Formed cluster complexes were analyzed by another QMS.

Size distribution of complex ions, $Co_2^+Ar_n$, formed by the collision of Co_2^+ with Ar_N is shown in Fig. 1. The maximum number of argon atoms attached on Co_2^+ is expected to be more than 30. The intensity of product ions decreases with n monotonically, but more gradually at V_{rel} = 0.6 km s^{-1} than V_{rel} = 1.3 km s^{-1}, and almost levels off above n ~ 25. $Co_2^+Ar_n$ is considered to be formed via the sequential evaporation of argon atoms from $Co_2^+Ar_N$ for relaxation of excess internal energy as follows;

$$Co_2^+ + Ar_N \rightarrow Co_2^+Ar_N \rightarrow Co_2^+Ar_n + (N - n)\ Ar. \quad (1)$$

The size distribution of reactant Ar_N is supposed to follow a log-normal distribution [1], and then the size distributions of product $Co_2^+Ar_n$ calculated reproduce those experimentally obtained very well as shown in Fig. 1. The relative velocity of 0.6 km s^{-1} corresponds to the collision energy of 0.2 eV, and the average number of evaporated Ar atoms from $Co_2^+Ar_N$ is estimated to be three.

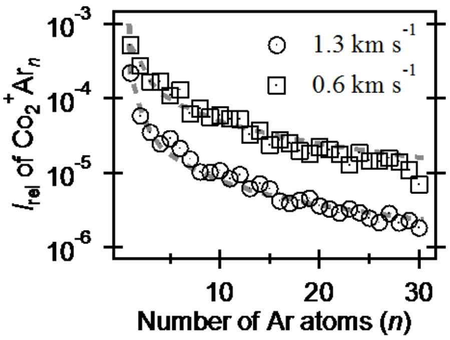

Fig. 1. Size distributions of $Co_2^+Ar_n$. Intensities were normalized to unreacted Co_2^+. The broken lines are fitting curves.

Reference

[1] J. Harms, J.P. Toennies, and F. Dalfovo, Phys. Rev. B **58** (1998) 3341.

Surface oxide luminescence of Silicon nanoclusters

Hanieh Yazdanfar[1], Gediminas Galinis[1], Mike J. McNally[1], Mumin. M. Koç[1], Oliver Youle[1], Gauthier Torricelli[1], Mark Watkins[1], Klaus von Haeften[1].

[1] *Department of Physics and Astronomy, University of Leicester, UK*

Fluorescent silicon nanoclusters are of considerable interest, both as means of studying the fundamental properties of silicon, the most important technological material of our age, but also for their many possible applications. Luminescent clusters of silicon have applications in optoelectronic devices [1] and lasers [2], as well as for biological labels [3] and sensors [4], it's low toxicity giving it an advantage over other light emitting materials.

Silicon nanocluster solutions have been produced by deposition of atomic silicon on a liquid jet in vacuum. XPS analysis confirms that the silicon is present in a high oxidation state and that the clusters are extremely oxygen rich, and FTIR shows the presence of bonds linked to SiO, SiO2 and SiO3 [5,6]. Clusters show a solvent sensitive fluorescence band at 350 – 420 nm and solvent transfer is fully reversible between ethanol and water. The solvent exchange suggests that fluorescence originates from the solvent / cluster-surface interface. These observations and other work in the field suggests the fluorescence emerges from oxygen rich surface states [6].

Reference(s)

[1] K. M. Noone, D. S. Ginger, ACS Nano, 3 (2009) 261 – 265
[2] L. Canham, Nature, 408 (2000)
[3] Y. He, Y. Su, X. Yang, Z. Kang, T. Xu, R. Zhang, C. Fan, S. Lee, J. Am. Chem. Soc, 131 (2009) 4434-4438
[4] G. Wang, S. Yau, K. Mantey, M. H. Nayfeh, Optics Communications, 281 (2008) 1765 – 1770
[5] B. Tremblay, P. Roy, L. Manceron, M. E. Alikhani, D. Roy, J. Chem. Phys, 104 (1996) 2773
[6] X. Yang, X. L. Wu, S. H. Li, H, Li, T. Qiu, Y.M. Yang, P. K. Chu and G. G. Siu, App. Phys. Lett. 86 (2005) 201906.

Autoionization in cluster Coulomb explosion studied by magnetic time-of-flight ion imaging

C. Schaal, R. Irsig, S. Skruszewicz, J. Tiggesbäumker, and K.-H. Meiwes-Broer

Institut für Physik, Universität Rostock, Universitätsplatz 3, D-18051 Rostock, Germany

The Coulomb explosion of small argon clusters exposed to intense ultrashort optical laser pulses is studied by energy-momentum spectroscopy. A position sensitive multi-channel plate delay-line detector is incorporated to record the temporal and spatial signals of all ionic species entering the magnetic field region. From the ion energies and momentums, charge state selective kinetic energy distributions have been extracted. The rapidly expanding highly charged ion cloud shows signatures of autoionization of Rydberg-like matter, see Fig. 1. The spectrometer extends our current instrumentation to study intense laser-cluster interactions and in principle allows for the analysis of cluster Coulomb explosions on a single shot basis.

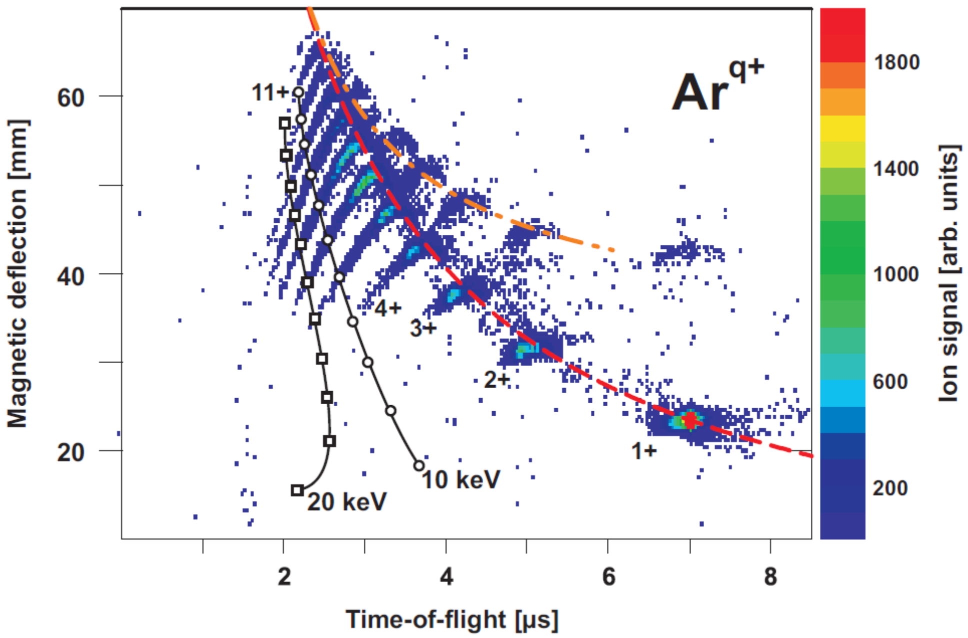

Figure 1: Magnetic deflection time-of-flight imaging spectrum of the Coulomb explosion of argon clusters (N=1000) exposed to intense femtosecond laser pulses (τ_L = 110 fs, I_L = 2.3×10^{15} W/cm^{-2}, double pulse delay Δt = 500 fs).

AUTHOR INDEX

List of Sponsors

日本万国博覧会記念基金	:	The Japan World Exposition 1970 Commemorative Fund
徳山科学技術振興財団	:	TOKUYAMA SCIENCE FOUNDATION
アイシン精機株式会社	:	AISIN SEIKI Co., Ltd.
株式会社アイリン真空	:	AILIN VACUUM CO.,LTD.
アドキャップバキュームテクノロジー株式会社	:	ADCAP VACUUM TECHNOLOGY Co., Ltd.
株式会社アールバキュームラボ	:	R Vacuum Lab Co., Ltd.
イムラ・アメリカ	:	IMRA America, Inc.
九州計測器株式会社	:	Kyushu Keisokki Co., Ltd.
株式会社コンポン研究所	:	Genesis Research Institute, Inc.
三洋貿易株式会社	:	SANYO TRADING Co., Ltd.
シュプリンガー・ジャパン株式会社	:	Springer Japan KK
スペクトラ・フィジックス株式会社	:	Spectra-Physics K.K.
正晃株式会社	:	SEIKO CO., LTD.
誠南工業株式会社	:	seinan indusutries Co., Ltd
TANAKAホールディングス株式会社	:	TANAKA HOLDINGS Co., Ltd.
株式会社デンソー	:	DENSO CORPORATION
株式会社東京インスツルメンツ	:	Tokyo Instruments, Inc.
株式会社トヤマ	:	TOYAMA Co., Ltd.
トヨタ自動車株式会社	:	Toyota Motor Corporation
株式会社豊田自動織機	:	Toyota Industries Corporation
日本ナショナルインスツルメンツ株式会社	:	National Instruments Japan
ブロンコスト・ジャパン株式会社	:	Bronkhorst Japan K.K.
福岡観光コンベンションビューロー	:	Fukuoka Convention & Visitors Bureau
九州大学	:	Kyushu University

助成　日本万国博覧会記念基金
Supported by the Japan World Exposition 1970 Commemorative Fund.
この助成金は、日本万国博覧会の収益を基にしています。
公益財団法人　関西・大阪21世紀協会

公益財団法人　徳山科学技術振興財団
TOKUYAMA SCIENCE FOUNDATION

TANAKA

TOYAMA

AISIN
One Team, Best Future

IMRA

DENSO

R Vacuum Lab

ADCAP

TII
株式会社 東京インスツルメンツ
TOKYO INSTRUMENTS, INC.

Bronkhorst®
JAPAN

AILIN VACUUM

QUALITY & HIGH TECHNOLOGY
SEINAN

Springer

NATIONAL INSTRUMENTS™

正晃株式会社

QUALITY & KINDNESS
QK 九州計測器株式会社

FCVB 公益財団法人 福岡観光コンベンションビューロー
Fukuoka Convention & Visitors Bureau

KYUSHU UNIVERSITY